



**HAL**  
open science

**Ataxin-7 SUMOylation and its functional consequences  
in the spinocerebellar ataxia type 7 (SCA7)  
pathophysiology**

Martina Marinello

► **To cite this version:**

Martina Marinello. Ataxin-7 SUMOylation and its functional consequences in the spinocerebellar ataxia type 7 (SCA7) pathophysiology. *Neurons and Cognition [q-bio.NC]*. Université Pierre et Marie Curie - Paris VI, 2014. English. NNT : 2014PA066266 . tel-01374194

**HAL Id: tel-01374194**

**<https://theses.hal.science/tel-01374194>**

Submitted on 3 Nov 2016

**HAL** is a multi-disciplinary open access archive for the deposit and dissemination of scientific research documents, whether they are published or not. The documents may come from teaching and research institutions in France or abroad, or from public or private research centers.

L'archive ouverte pluridisciplinaire **HAL**, est destinée au dépôt et à la diffusion de documents scientifiques de niveau recherche, publiés ou non, émanant des établissements d'enseignement et de recherche français ou étrangers, des laboratoires publics ou privés.

Université Pierre et Marie Curie

École Doctorale : Cerveau, Cognition, Comportement (ed3c)

INSERM UMR1127/CNRS 7225 – Institut du Cerveau et de la Moelle épinière

**Ataxin-7 SUMOylation and  
its functional consequences in the  
Spinocerebellar Ataxia Type 7 (SCA7)  
pathophysiology**

Presented by Martina Marinello

for the degree of PhD in Neuroscience

Supervised by Dr. Annie Sittler

Defended on September 26<sup>th</sup>, 2014

Thesis Jury :

**Prof. Jean MARIANI**

*President*

**Dr. Didier DEVYS**

*Rapporteur*

**Dr. Dominique LEPRINCE**

*Rapporteur*

**Dr. Jacob SEELER**

*Examiner*

**Dr. Valerie LALLEMAND-BREITENBACH**

*Examiner*

**Prof. Alexis BRICE**

*Examiner*

**Dr. Annie SITTLER**

*Thesis Supervisor*



*“One of the greatest diseases is to be nobody to anybody.”*

*Mother Theresa*



# Summary

The word "ataxia" comes from the Greek, "a taxis" meaning "without order or incoordination". Patients affected by this disease present a lack of balance in their gait and fine movement incoordination. Spinocerebellar ataxia type 7 (SCA7) is a dominantly inherited autosomal disease caused by a CAG (encoding Q) trinucleotide expansion within the coding region of the *SCA7* gene, which is translated into an expanded polyglutamine (polyQ) stretch in the corresponding ataxin-7 protein. In SCA7, cerebellar ataxia is associated with blindness secondary to pigmentary macular dystrophy and retinal degeneration. Recent evidence has suggested that protein context and post-translational modifications influence the neurotoxicity of the polyQ proteins.

In particular, the SUMOylation pathway was proposed to modulate the pathogenesis of several neurodegenerative diseases. This is why we focused on this modification. In 2010 our team identified ataxin-7 as a new SUMO target. Hallmarks of the disease, ataxin-7 positive nuclear inclusions, colocalizing with SUMO1 and SUMO2, were observed in cortex and cerebellar cells. In a SCA7 disease cellular model, our team found that preventing SUMOylation of expanded ataxin-7 leads to higher amounts of SDS-insoluble aggregates. These results demonstrate that SUMOylation influences aggregation of polyQ expanded ataxin-7, which is likely a key event during progression of pathogenesis.

My aim was to investigate about different aspects of this pathway to better understand its role in mutant ataxin-7 nuclear aggregation. In order to identify potential ataxin-7 SUMOylation actors, I analysed the expression and subcellular distribution of proteins that may be implicated in this pathway.

One of the first steps was to identify the enzyme responsible for the transfer of a SUMO protein to the substrate, ataxin-7. This process is usually facilitated by SUMO E3 ligases, which might function as platforms that position the target in a favourable orientation for SUMO transfer. I focused my attention on the enzyme RanBP2, a nucleoporin (Nup358), which my team hypothesized to be the SUMO E3 ligase for ataxin-7, a protein known to shuttle, as it contains three NLS and a NES. The purpose was to investigate whether RanBP2 is responsible for ataxin-7 SUMOylation or if other enzymes could catalyse this reaction. I showed that RanBP2 is the major E3 ligase that adds SUMO-1 to ataxin-7, *in vitro* and in a cellular model, and that silencing RanBP2 renders mutant ataxin-7 more prone to aggregation, thus demonstrating the implication of RanBP2 in SCA7 pathophysiology. RanBP2 may interact directly or indirectly with ataxin-7, as shown by immunoprecipitation.

To first establish that SUMO modification enzymes are present in brain regions affected in SCA7 disease, we quantified expression of SUMO-related genes in mouse cerebellum, striatum and retina using quantitative RT-PCR (qRT-PCR). *Sumo-1* and *Sumo-2* are expressed in wild-type mouse brain at relatively high levels. These data demonstrate that the SUMO machinery is present in relevant brain regions. To determine if SUMO-related genes show expanded repeat SCA7-dependent alterations in expression patterns, each was quantified in *Atxn7<sup>50Q/5Q</sup>* and *Atxn7<sup>100Q/5Q</sup>* mouse cerebellum, striatum and retina at 6 and 12 months. At 6 months, some deregulations begins to occur, and by 12 months, there is a statistically significant impairment in *Sumo-1* and levels in *Atxn7<sup>100Q/5Q</sup>* cerebellum suggesting that *in vivo* SUMO-modifying pathways may be perturbed in SCA7 disease.

Finally I identified that ataxin-7 is also a target for SUMOylation by isoform 2. As already demonstrated for PML, SUMO-2 is able to poly-SUMOylate its partners and operates as a signal for degradation via the proteasomal machinery. I was interested in verifying whether RNF4, a poly-SUMO-specific ubiquitin E3 ligase, played a role in the degradation of SUMOylated ataxin-7 by its recruitment to the proteasome. Indeed, wild-type RNF4 mediates poly-SUMO-2 mutant ataxin-7 degradation and this effect is abolished with a mutant of RNF4. I thus conclude that poly-SUMOylation of mutant ataxin-7 is a signal for RNF4 mediated degradation.

The structural data for the SUMO E3 enzyme RanBP2 in complex with the other components of the SUMO pathway is now available, making possible the structure-based design of specific inhibitors or activators. For this reason, the principal aim of my project was to elucidate the mechanisms regulating ataxin-7 degradation via SUMOylation cascade, including modifying and de-modifying enzymes, to identify the useful target for therapeutic intervention.



# TABLE OF CONTENTS

<b>ABBREVIATIONS</b>	<b>13</b>
<b>1. INTRODUCTION</b>	<b>15</b>
<b>1.1. PROTEIN MISFOLDING AND NEURODEGENERATIVE DISEASE</b>	<b>15</b>
1.1.1. THE BASIC MECHANISM OF PROTEIN FOLDING	16
1.1.2. PROTEIN MISFOLDED AGGREGATES: CAUSE OR CONSEQUENCE? AN ONGOING STORY	17
1.1.3. THERAPEUTIC STRATEGIES	20
<b>1.2. POLYQ DISEASES AS REPEAT EXPANSION DISEASES</b>	<b>22</b>
1.2.1. REPEAT EXPANSION DISEASES	22
1.2.2. POLYGLUTAMINE DISEASE: GENETIC CHARACTERISTICS	26
1.2.3. PATHOGENESIS OF POLYGLUTAMINE DISEASES	30
1.2.4. CELLULAR PROTECTIVE MECHANISMS	31
1.2.5. MECHANISM FOR CLEARANCE OF POLYGLUTAMINE AGGREGATES: THE UPS AND AUTOPHAGY	33
1.2.6. DIFFERENCES IN TOXICITY IN THE CENTRAL NERVOUS SYSTEM AND PERIPHERY: THE IMPORTANCE OF THE CONTEXT	38
1.2.7. POST-TRANSLATIONAL MODIFICATION ON POLYQ DISEASE	39
<b>1.3. SPINOCEREBELLAR ATAXIA TYPE 7 (SCA7)</b>	<b>42</b>
1.3.1. ANATOMOPATHOLOGY	42
1.3.2. GENETICS ASPECTS IN SCA7	43
1.3.3. MOLECULAR MECHANISMS	44
<b>1.4. SUMOYLATION</b>	<b>50</b>
1.4.1. THE SUMOYLATION CYCLE	50
1.4.2. SUMO E3 LIGASES	52
1.4.3. SENPs	54
1.4.4. SUMO-INTERACTING MOTIFS	54
<b>1.5. PML</b>	<b>55</b>
1.5.1. PML NUCLEAR BODIES	57
1.5.2. ROLE OF PML IN THE NERVOUS SYSTEM	58
1.5.3. CLASTOSOMES	60
<b>1.6. RNF4 – E3 UBIQUITIN LIGASE</b>	<b>63</b>
1.6.1. RNF4 RING DOMAIN IS SUFFICIENT FOR UBIQUITYLATION ACTIVITY.	65
1.6.2. THE GUARDIANS OF THE NUCLEUS: PML, SUMO AND RNF4	66

<b>2. AIMS OF THIS WORK</b>	<b>69</b>
<b>3. RESULTS</b>	<b>71</b>
<b>3.1. IDENTIFICATION OF A NEW INTERACTION BETWEEN ATAXIN-7 AND SUMO-2</b>	<b>71</b>
3.1.1. ATAXIN-7 IS MODIFIED BY BOTH SUMO-1 AND SUMO-2	71
3.1.2. ENDOGENOUS ATAXIN-7 IS A TARGET OF SUMO-1 AND SUMO-2	74
3.1.3. RANBP2 IS THE MAIN SUMO E3 LIGASE FOR MODIFICATION OF ATAXIN-7 BY SUMO-1.	77
3.1.4. ENDOGENOUS RANBP2 CO-IMMUNOPRECIPITATES WITH ENDOGENOUS ATXN7.	83
3.1.5. SUMO E3 LIGASE SILENCING ENHANCES MUTANT ATAXIN-7 AGGREGATION	84
3.1.6. ATAXIN-7 IS SUMOYLATED BY RANBP2 <i>IN VITRO</i> : A VALIDATION THAT IT IS A CANDIDATE ATAXIN-7 SUMO E3 LIGASE.	87
3.1.7. ATAXIN-7 CONTAINS MOTIFS FOR NON-COVALENT BINDING TO SUMO	87
<b>3.2. DOES PML SUMOYLATION AFFECT MUTANT ATAXIN-7 AGGREGATION OR DEGRADATION?</b>	<b>90</b>
3.2.1. RNF4 ATTENUATES THE PROPENSITY OF ATAXIN-7 TO AGGREGATE	95
<b>3.3. SUMO PATHWAY DEREGLATION IN SCA7 KI MICE</b>	<b>104</b>
3.3.1. DEREGLATION OF PIAS AND SUMO IN SCA7 MOUSE BRAIN	104
<b>3.4. SUMO PATHWAY COMPONENTS DETECTED IN THE CEREBELLUM OF A SCA7 PATIENT</b>	<b>115</b>
<b>4. MATERIALS &amp; METHODS</b>	<b>117</b>
<b>4.1. PLASMIDS AND SITE-DIRECTED MUTAGENESIS</b>	<b>117</b>
<b>4.2. RNA INTERFERENCE</b>	<b>117</b>
<b>4.3. PRIMARY ANTIBODIES</b>	<b>118</b>
<b>4.4. CELL CULTURE</b>	<b>118</b>
<b>4.5. ANIMALS</b>	<b>119</b>
<b>4.6. <i>IN VITRO</i> SUMOYLATION AND <i>IN VITRO</i> BINDING ASSAY</b>	<b>119</b>
<b>4.7. PROTEIN EXTRACTION AND WESTERN BLOT ANALYSIS</b>	<b>120</b>
<b>4.8. IMMUNOPRECIPITATION</b>	<b>121</b>
<b>4.9. PROXIMITY LIGATION ASSAY (PLA) – DUOLINK® <i>IN SITU</i></b>	<b>122</b>
<b>4.10. FILTER RETARDATION ASSAY</b>	<b>123</b>
<b>4.11. RNA PURIFICATION AND REAL-TIME QUANTITATIVE PCR</b>	<b>124</b>
<b>4.12. IMMUNOFLUORESCENCE</b>	<b>124</b>
<b>4.13. HUMAN POST-MORTEM BRAIN</b>	<b>126</b>
<b>4.14. IMMUNOHISTOCHEMICAL ANALYSIS</b>	<b>126</b>
<b>5. DISCUSSION</b>	<b>129</b>
<b>5.1. SUMOYLATION AS REGULATOR OF TOXIC ATXN7 PROTEIN IN SCA7 DISEASE</b>	<b>130</b>

5.1.1. SCIENTIFIC BACKGROUND	130
5.1.2. CONTRIBUTION AND CONTEXTUALISATION OF THIS WORK	132
<b>5.2. RANBP2 AS A MAJOR SUMO E3 LIGASE OF ATAXIN-7 FOR SUMO-1 CONJUGATION.</b>	<b>135</b>
5.2.1. SCIENTIFIC BACKGROUND	135
5.2.2. CONTRIBUTION AND CONTEXTUALISATION OF THIS WORK	136
5.2.3. FUTURE RESEARCH PERSPECTIVES	139
<b>5.3. PML IV SUMOYLATION: A ROLE IN EXPANDED ATAXIN-7 DEGRADATION?</b>	<b>140</b>
5.3.1. SCIENTIFIC BACKGROUND	140
5.3.2. CONTRIBUTION AND CONTEXTUALISATION OF THIS WORK	140
5.3.3. FUTURE RESEARCH PERSPECTIVES	142
<b>5.4. THE ROLE OF RNF4 IN ATXN7 DEGRADATION</b>	<b>142</b>
5.4.1. SCIENTIFIC BACKGROUND	142
5.4.2. CONTRIBUTION AND CONTEXTUALISATION OF THIS WORK	142
<b>5.5. SUMO ENZYMES AND PROTEINS DEREGULATION IN SCA7 KI MOUSE MODEL</b>	<b>144</b>
5.5.1. SCIENTIFIC BACKGROUND	144
5.5.2. CONTRIBUTION AND CONTEXTUALISATION OF THIS WORK	144
5.5.3. FUTURE PERSPECTIVE	147
<b>5.6. SUMO-1 AND RANBP2 ACCUMULATION IN THE BRAIN OF SCA7 PATIENTS</b>	<b>147</b>
5.6.1. SCIENTIFIC BACKGROUND	147
5.6.2. CONTRIBUTION AND CONTEXTUALISATION OF THIS WORK	148
5.6.3. FUTURE PERSPECTIVE	148
<b>6. CONCLUSIONS</b>	<b>151</b>
<b>BIBLIOGRAPHY</b>	<b>153</b>



# TABLE OF FIGURES

FIGURE 1 – NEURODEGENERATIVE DISEASES CHARACTERISTIC LESIONS .....	19
FIGURE 2 - HYPOTHETICAL SEVERAL-STEP PATHWAY OF PROTEIN AGGREGATION.....	21
FIGURE 3 - GENIC LOCATION OF DISEASE-ASSOCIATED REPEATS.....	24
FIGURE 4 - SCHEMATIC REPRESENTATION OF PATHOLOGICAL THRESHOLD, PREMUTATION AND COMPLETE MUTATION.....	28
FIGURE 5 - RELATIONSHIP BETWEEN AGE AT ONSET AND CAG REPEAT LENGTH FOR POLYGLUTAMINE DISORDERS .....	29
FIGURE 6 - A SCHEMATIC ILLUSTRATION OF PROTEIN QUALITY CONTROL IN THE CELL.....	32
FIGURE 7 - ATAXIN-7 ROLE INTO STAGA COMPLEX AND ITS CONSEQUENCES DUE TO EXPANDED POLYQ MUTATION .....	46
FIGURE 8 - MODEL OF POTENTIAL MECHANISMS BY WHICH POLYQ-EXPANDED ATAXIN-7 INDUCES TOXICITY IN ROD PHOTORECEPTORS .....	47
FIGURE 9 - THE SUMOYLATION PATHWAY .....	51
FIGURE 10 - THE RANBP2/RANGAP1*SUMO1/UBC9 COMPLEX IS A MULTISUBUNIT SUMO E3 LIGASE .....	53
FIGURE 11 - THE PML GENE AND PROTEIN ISOFORM .....	56
FIGURE 12 - A MODEL OF PML-NB FORMATION .....	58
FIGURE 13 - THE ROLE OF PML IN THE NERVOUS SYSTEM.....	60
FIGURE 14 - MODEL OF RNF4 ACTIVATION BY POLYSUMO CHAINS.....	65
FIGURE 15 RECOGNITION AND CLEARANCE OF MISFOLDED PROTEIN BY THE CONCERTED ACTION OF PML, SUMO, AND RNF4.....	67
FIGURE 16 – ATAXIN-7 IS MODIFIED BY SUMO-1 AND SUMO-2: SUMO-2 ATTENUATES THE PROPENSITY OF EXPANDED POLYQ ATAXIN-7 TO AGGREGATE.....	72
FIGURE 17 - ENDOGENOUS ATAXIN-7 IS A SUMO-1 AND SUMO-2 TARGET IN MCF7 CELLS AS SHOWN BY IMMUNOPRECIPITATION.....	76
FIGURE 18 – IDENTIFICATION OF A MAJOR SUMO E3 LIGASE FOR ATAXIN-7 MODIFICATION ..	79
FIGURE 19 - SUMOYLATION OF ATAXIN-7 BY RANBP2 .....	80
FIGURE 20 - RANBP2 $\Delta$ FG FRAGMENT BUT NOT RANBP2 $\Delta$ FG WITH A MUTATION IN THE IR1 MOTIF CAUSES EFFICIENT SUMO-1 -MEDIATED DEGRADATION OF ATAXIN-7 AGGREGATES.....	82
FIGURE 21 - ENDOGENOUS ATAXIN-7 AND RANBP2 ARE IN A COMPLEX IN MCF7 CELLS.....	84
FIGURE 22 - PIAS AND RANBP2 SILENCING ENHANCE MUTANT ATAXIN-7 AGGREGATION.....	86
FIGURE 23 - ATAXIN-7 IS EFFICIENTLY SUMOYLATED <i>IN VITRO</i> BY FREE RANBP2 AND BY THE RANBP2/RANGAP1*SUMO1/UBC9 COMPLEX. ATAXIN-7 ALSO INTERACTS WITH SUMO-1 AND SUMO-2.....	88
FIGURE 24 - SUMO-DEFICIENT PML IS STILL ABLE TO PARTIALLY COLOCALIZE WITH MUTANT ATAXIN-7 .....	91

FIGURE 25 - SUMO-DEFICIENT PML DEGRADES MUTANT ATAXIN-7 AGGREGATES.....	94
FIGURE 26 - RNF4 OVEREXPRESSION IN THE PRESENCE OF SUMO-2 LEADS TO A DECREASE IN MUTANT ATAXIN-7 AGGREGATES .....	96
FIGURE 27 - PROTEASOME INHIBITION ABOLISHES MUTANT ATAXIN-7 DEGRADATION BY RNF4 .....	100
FIGURE 28 - PROTEASOME INHIBITION BY HIGH CONCENTRATION OF MG132 AND LACTACYSTIN DID NOT IMPAIR MUTANT ATAXIN-7 DEGRADATION BY OVEREXPRESSED RNF4 .....	102
FIGURE 29 - DEGRADATION OF MUTANT ATAXIN-7 IN THE PRESENCE OF PML IV OR RNF4...	103
FIGURE 30 - DOWNREGULATION OF SUMO-1 AND SUMO-2 MRNA IN <i>ATXN7<sup>100Q/5Q</sup></i> KI MICE.....	106
FIGURE 31 - QRT-PCR ANALYSIS OF SUMO-MODIFYING PROTEINS AND ENZYMES IN STRIATUM AND RETINA OF WILD-TYPE COMPARED TO <i>ATXN7<sup>100Q/5Q</sup></i> KI MICE .....	107
FIGURE 32 - DEREGULATION OF SUMO-MODIFYING PROTEINS AND ENZYMES EXPRESSION IN <i>ATXN7<sup>100Q/5Q</sup></i> KI MOUSE MODEL AT A LATE STAGE OF DISEASE .....	109
FIGURE 33 - CO-LOCALISATION OF SUMO-1 AND ATAXIN-7 IN THE CEREBELLUM OF <i>ATXN7<sup>100Q/5Q</sup></i> KI MICE.....	111
FIGURE 34 - SUMO-1 AND SUMO-2 IN NUCLEAR DOTS IN <i>ATXN7<sup>100Q/5Q</sup></i> KI MICE.....	113
FIGURE 35 - RANBP2 STAINING INCREASES IN THE <i>ATXN7<sup>100Q/5Q</sup></i> KI MOUSE .....	114
FIGURE 36 - SUMO-1 AND RANBP2 ACCUMULATE ABNORMALLY IN THE CEREBELLUM OF A SCA7 PATIENT.....	116

## Abbreviations

AD: Alzheimer Disease

ALS: Amyotrophic Lateral Sclerosis

Bp: Base pair

CNS: Central Nervous System

CRX: Cone Rode homeoboX

DM: Myotonic Dystrophy

ER: Endoplasmic Reticulum

GFP: Green Fluorescent Protein

HA: HemAgglutinin

HAT: Histone Acetyl Transferase

HD: Huntington Disease

HDAC: Histone De-ACetylase

HSP: Heat Shock Protein

IHC: Immuno Histo Chemistry

KI: Knock-In

MT: Microtubule

NB: Nuclear Bodies

NES: Nuclear Export Signal

NII: Neuronal Intranuclear Inclusions

NLS: Nuclear Localisation Signal

PD: Parkinson Disease

PIAS: Protein Inhibitor of Activated Stat

PML: Promyelocytic leukemia protein

Q: glutamine

qRT-PCR: quantitative Reverse Transcription Polymerase Chain Reaction

RNF: Ring Finger protein

ROS: Reactive Oxygen Species

SBMA: Spinal and Bulbar Muscular Atrophy

SCA: Spino-Cerebellar Ataxia

SIM: Sumo Interacting Motif

STAGA: SPT3/TAF9/GCN5 acetyltransferase complex

SUMO: Small Ubiquitin-like Modifier

TFTC: Tata-binding protein-free TAF-containing complex

# 1. Introduction

## 1.1. Protein misfolding and neurodegenerative disease

Neurodegenerative diseases are some of the most debilitating disorders, affecting reasoning, feelings, cognition, memory and motion alike. Despite important differences in their clinical manifestations, neurodegenerative disorders share some common features such as when they appear, usually not before the 4<sup>th</sup>-5<sup>th</sup> decade or later in life. Typical shared characteristics are the extensive neuronal loss, synaptic abnormalities, and the presence of cerebral deposits of misfolded protein aggregates. These deposits are the typical signatures of neurodegenerative diseases and, although the main protein component is different in each disease, they have similar morphological, structural, and staining characteristics.

In each neurodegenerative disease, the distribution and composition of protein aggregates are different (Soto, 2003). For example, in Alzheimer's disease (AD), there are two types of protein deposits: amyloid- $\beta$  and tau. Amyloid plaques are extracellular deposits in the brain parenchyma and around the cerebral vessel walls. Their main component is a 40- or 42-residue peptide termed *amyloid- $\beta$  protein* (A $\beta$ ) (Glennner and Wong, 2012). Tangles are the second type of deposits in AD. They are located in the cytoplasm of degenerating neurons and comprise aggregates of hyperphosphorylated tau protein (Grundke-Iqbal et al., 1986).

Likewise, in patients with Parkinson's disease (PD), Lewy bodies are observed in the cytoplasm of neurons of the *substantia nigra* in the brain. The major constituents of these aggregates are fragments of a protein named  *$\alpha$ -synuclein*. In patients with Huntington's disease, intranuclear deposits of a polyglutamine-rich version of huntingtin protein are a typical feature of the brain. In amyotrophic lateral sclerosis (ALS), patients present aggregates mainly composed of superoxide dismutase in the cell bodies and axons of motor neurons (Soto, 2003).

Genetic studies support the causal role of protein misfolding in neurodegenerative diseases. “Mutations in the genes encoding the protein component of fibrillar aggregates are associated with the inherited forms of all neurodegenerative diseases. Mutations in the respective fibrillar proteins have been found in AD, PD, ALS and HD and related polyglutamine disorders”. Significant evidence coming from biochemical, genetic, and neuropathological studies support the involvement of protein misfolding and aggregation in the pathology of neurodegenerative diseases (Soto, 2003). Moreover, the presence of abnormal aggregates usually occurs in the brain regions most damaged by the disease, even though they can be found in other brain regions that are less affected or even completely unaffected. Mutations in the gene encoding the misfolded protein produce inherited forms of the disease, which usually have an earlier onset and more severe phenotype than the sporadic forms (Bucciantini et al., 2002). Transgenic animals expressing the human mutant gene for the misfolded protein develop some of the typical neuropathological and clinical characteristics of the human disease (Price et al., 2000). As we will see later, protein misfolding plays a pivotal role also in Spinocerebellar Ataxia type 7 (SCA7).

### 1.1.1. The basic mechanism of protein folding

Protein folding is the main mechanism through which an unstructured sequence of amino acids assumes a fully functional three-dimensional structure. This core mechanism is necessary to correctly select and regulate biochemical processes, including the trafficking of molecules to specific cellular locations and cellular growth and differentiation. Only correctly folded proteins have long-term stability in cellular environments and are able to interact selectively with their natural partners. It is then not surprising that the failure of proteins to fold correctly, or to remain correctly folded, is the origin of a wide variety of pathological conditions (Dobson, 2003) (Dobson, 2002).

Native states of proteins almost always correspond to the structures that are most thermodynamically stable under physiological conditions. In particular, it is now clear that the folding process does not involve a series of mandatory steps between specific partly folded states, but rather a stochastic search of trial and error among

the many conformations accessible to a polypeptide chain (Dobson et al., 1998) (Wolynes et al., 1995).

The inherent fluctuations in the structure of an unfolded (or partially folded) polypeptide chain let the residues that are widely separated in the amino-acid sequence to come into contact with each other. Since native-like interactions between residues are more stable and persistent, the polypeptide chain is able to find its lowest-energy structure through the trial-and-error process. Natural selection has enabled proteins to evolve so that they are able to fold rapidly and efficiently.

A key question is how does the correct fold emerge? The structural transitions taking place during *in vitro* folding can be investigated in detail by a variety of techniques, ranging from optical methods to NMR spectroscopy, some of which can now even be used to follow the behaviour of single molecules (Dobson, 2003). The results of many studies (Vendruscolo et al., 2003) (Fersht, 2000) (Lindorff-Larsen et al., 2004) suggest that the fundamental mechanism of protein folding involves interactions among of a relatively small number of residues to form a folding nucleus and that the remainder of the structure rapidly condenses around it.

### 1.1.2. Protein misfolded aggregates: cause or consequence? An ongoing story

Protein misfolding and aggregation are undoubtedly associated with neurodegenerative diseases, but the mechanism by which misfolded aggregates produce synaptic dysfunction and neuronal death is unknown. The initial dominating belief was that large amyloid-like protein deposits were the species responsible for brain damage. However, results of histopathological, biochemical, and cell biology studies (Haass and Selkoe, 2007) has challenged the idea that deposited aggregates are toxic. Neuropathological analysis of the brains of patients with PD or AD has shown that neurons containing Lewy bodies or neurofibrillary tangles seem healthier than neighboring cells in morphological and biochemical analyses (Bondareff et al., 1989). In a mouse model of Alzheimer's disease, cerebral damage and clinical symptoms have been detected before protein aggregates form (Moechars et al., 1999). In addition, in cellular models of Huntington's disease, it was first asserted, in 1998, that aggregates were not deleterious, because

intranuclear inclusions containing ubiquitinated mutant huntingtin formed before apoptosis was initiated (Saudou et al., 1998). In a mouse model of spinocerebellar ataxia type 1 (SCA1), it was shown that mice expressing ataxin1-82Q with a mutated NLS did not develop the disease, demonstrating that nuclear localization is critical for pathogenesis (Klement et al., 1998). Even more interesting, a new transgenic mouse expressing a mutant ataxin-1 unable to self-associate due to the deletion of the self-association region of ataxin-1 did not show ataxin-1-like nuclear aggregation, but developed Purkinje cell pathology and ataxia. The formation of nuclear aggregates of ataxin-1 is thus not required for the initiation of pathogenesis (Klement et al., 1998). In order to better determine, in a Huntington's disease model in striatal cells, whether inclusion bodies are pathogenic, incidental or a beneficial attempt to adapt, the team of Steve Finkbeiner at UCSF developed an automated microscope that returns to precisely the same neuron after arbitrary intervals. They showed that many neurons died without forming an inclusion body and, surprisingly, that inclusion body formation predicted improved survival and led to decreased levels of mutant huntingtin elsewhere in neurons. Inclusion body formation proposed to act as an adaptive response to toxic mutant huntingtin (Arrasate et al., 2004).

This evidence indicates that inclusion body formation might be a protective response of the cell against misfolded proteins and promotes the idea that neurons have developed both cellular and molecular mechanisms to deal with aggregated and misfolded proteins. Nonetheless, some cell culture studies found that inclusions could actually be cytoprotective. Saudou and collaborators developed a cell model of HD that recapitulated the polyglutamine- and cell type-specific cytotoxicity observed in human patients. While cell death was specific to striatal cells in this model, aggregation could be detected in both striatal and hippocampal (unaffected in HD) cells and did not correlate with cell death. Furthermore, expressing a dominant negative form of an ubiquitin-conjugating enzyme was able to dramatically reduce aggregation, but increased cytotoxicity. This led the authors to conclude that inclusions could be protective for the cell (Saudou et al., 1998).

Increasing evidence also suggests that inclusion bodies might represent an end-stage manifestation of a multistep aggregation process (Ignatova et al., 2007). Early

events before the formation of inclusion bodies might cause toxicity. Possible toxic agents include abnormal monomers of the disease proteins, or small assemblies of abnormal aggregated protein, which are termed oligomers or protofibrils.

The early prefibrillar aggregates associated with stages of oligomerization, are highly damaging to the cells, in contrast with mature fibrils deposited in the brain, which are usually relatively benign (Caughey and Lansbury, 2003) (Ross and Poirier, 2004) (Ross and Poirier, 2005) (Figure 1). Consequently, the most accepted hypothesis is that the process of misfolding and early stages of oligomerization are in fact responsible for neurodegeneration (Glabe and Kaye, 2006) (Haass and Selkoe, 2007) (Lansbury and Lashuel, 2006).

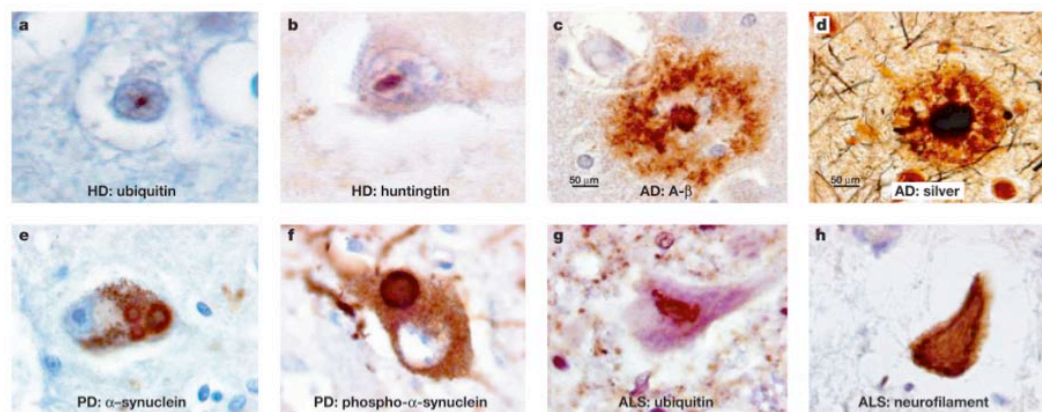


**Figure 1 – Neurodegenerative diseases characteristic lesions**

Characteristic neurodegenerative disease neuropathological lesions involve deposition of abnormal proteins, which can be intranuclear, cytoplasmic or extracellular. All are labeled with antibodies (except d), as indicated. (a) HD, intranuclear inclusion labeled for ubiquitin (cerebral cortex) (b) HD, intranuclear inclusion labeled for huntingtin (cerebral cortex). (c) AD, neuritic plaque labeled for AB (cerebral cortex). (d) AD, neuritic plaque, silver stained (Hirano method). (e) PD, Lewy bodies labeled for alpha-synuclein (fine granular brwn label in this and the next panel represent neuromelanin) (substantia nigra). (f) PD, Lewy bodies labeled for phosphorylated alpha-synuclein (substantia nigra). (g), ALS, cytoplasmic skein of neurofilaments labeled with ubiquitin (medulla oblongata). (h) AL, cytoplasmic skein of neurofilaments labeled with neurofilament (medulla oblongata) (Roos and Poirier, 2004).

This hypothesis could explain why the presence of inclusion bodies correlates poorly with other markers of neurodegeneration, or with ante-mortem clinical features. This lack of correlation is most apparent in the polyglutamine diseases. In HD, for example, inclusions bodies are present in the cells of the striatum, which undergoes massive degeneration, but are more dense in the cerebral cortex, which undergoes only moderate degeneration (Gutkunst et al., 1999). Moreover, striatal inclusion bodies are most prevalent in large interneurons, which are spared in HD,

rather than in medium spiny neurons, which are selectively lost in the disease (Kuemmerle et al., 1999). In SCA7 as well, nuclear inclusions are not restricted to regions affected by the disease. They were most frequent in neurons of the inferior olive (a prominent oval structure in the medulla oblongata, the lower portion of the brainstem), severely affected in SCA7, but could also be observed at high frequency in brain regions not known to be harmed, such as the supramarginal gyrus (a portion of the parietal lobe), and the insula (a portion of the cerebral cortex folded deep within the brain) (Holmberg et al., 1998). In the cerebellum, another region with extensive neuronal loss, so few Purkinje cells remained that accurate estimation of the frequency of inclusions was impossible (Holmberg et al., 1998). These studies suggested that the presence of mutant protein inclusions may not be able to fully explain the toxicity seen in human patients and mouse models of polyglutamine diseases and they do not distinguish whether inclusions could be slightly toxic entities or passive benign formations.

### 1.1.3. Therapeutic strategies

The cell has developed mechanisms to defend itself against misfolded and aggregated proteins. The first line of defence involves the many molecular chaperones that aid the normal folding and the refolding of abnormal conformations back to the native state (McClellan and Frydman, 2001). If these fail, abnormal proteins can be targeted for degradation by covalent attachment of polyubiquitin followed by targeting to the proteasome and degradation (Goldberg, 2003). The presence of ubiquitin, chaperones and proteasome components in inclusion bodies seems to represent cellular defences overwhelmed by the excessive aggregation within cells.

Two possible therapeutic strategies would consist in enhancing the cellular defence mechanisms or in stimulating the proteasome activity. For example our team discovered that mutant ataxin-7 nuclear inclusions colocalize with proteasome components, in a subnuclear structure called clastosomes, which are nuclear bodies specialized in UPS-mediated degradation (Janer et al., 2006). Drugs such as interferon beta enables up-regulation of the expression of PML (Promyelocytic leukemia protein), a component of PML bodies, and most importantly for

neurodegenerative diseases, interferon beta was able to cross the blood-brain barrier. Our team showed how interferon beta treatment improved the clearance of insoluble mutant ataxin-7 in the cerebellum and other brain regions in the SCA7<sup>266Q/5Q</sup> knock-in mouse model. The number and size of ataxin-7 nuclear inclusions in cerebellar Purkinje cells, specifically affected in SCA7, was notably reduced by 30% after 7 weeks of treatment, in this particularly severe mouse model of SCA7. This therapeutic strategy also ameliorated significantly the pathological ataxic locomotor phenotype in the SCA7<sup>266Q/5Q</sup> knock-in mouse model (Chort et al., 2013).

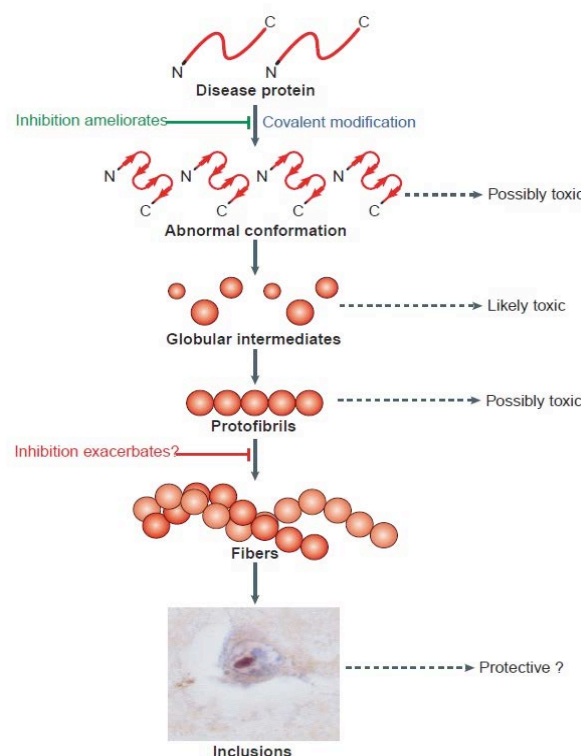


**Figure 2 - Hypothetical several-step pathway of protein aggregation**

Flowchart for therapeutic intervention in a hypothetical several-step pathway of protein aggregates (Ross and Poirier, 2004).

One potential danger of inhibiting a single step in a several-step aggregation pathway is that accumulation of a toxic intermediate could increase toxicity (Figure 2). Nevertheless, even if not all compounds have beneficial effects, they may prove to be powerful probes that will help elucidate the protein-misfolding pathway. Other therapeutic interventions might directly reduce the level of abnormal protein within the cell, for instance using RNA interference (McBride et al., 2011) (Ramachandran et al., 2014), although its delivery would have to overcome the formidable barriers to

entry across the blood-brain barrier and access to neurons in the relevant region of the brain.

These approaches could ideally be applied to all neurodegenerative diseases. A great hope in this area is thus that the development of understanding and therapy for one disease may have implications for the others.

## 1.2. PolyQ diseases as repeat expansion diseases

### 1.2.1. Repeat expansion diseases

A new type of human genetic disease mutation was discovered more than 22 years ago: the expansion of a repeated microsatellite sequence. It was quite unexpectedly that, in 1991, two totally unrelated diseases, the X-linked disorders fragile X mental retardation syndrome (FMR1) and spinal and bulbar muscular atrophy (SBMA), were reported to result from expansion of a repeated sequence (Verkerk et al., 1991), (LaSpada et al., 1991). We now recognize SBMA as the first member of a subcategory of repeat expansion disorders, known as "CAG/polyglutamine" repeat diseases. Concerning the fragile-X syndrome, further work indicated that the CGG repeat expansion in FMR1 is located in the 5' UTR. The expansion reduces expression of FMR1 by promoting DNA hypermethylation at the promoter (Jin et al., 2004).

Since these seminal discoveries, more than 25 repeat expansion mutations have been identified (Table 1). Repeat expansion diseases include some of the most common inherited diseases, such as Huntington's disease (HD) and myotonic dystrophy. Twenty of the repeat diseases, either principally or exclusively affecting the neuroaxis (the axial part of the central nervous system, composed of the spinal cord, rhombencephalon, mesencephalon, and diencephalon), are degenerative disorders. Almost all of these inherited neurological disorders are caused by large expanded repeats that are highly unstable (also called dynamic mutations). The repeated sequence and its location within the gene are the most useful characteristics to consider for classifying the different repeat disorders. As shown in Table 1, there are many different types of repeats that vary in length and sequence composition. The most frequent are CAG trinucleotide repeats, CTG trinucleotide repeats, and GCG trinucleotide repeats.

Clinical and molecular characteristics of inherited neurological repeat expansion disorders					
Disease	Main clinical features	Causal repeat (gene)	Repeat location	Mechanism or category	Comments
DM1	Muscle weakness, myotonia, cardiac-endocrine-GI disease, MR	CTG ( <i>DM1</i> , also known as <i>DMPK</i> )	3' UTR	RNA GOF	A very common form of muscular dystrophy
DM2	Muscle weakness, myotonia, cardiac-endocrine-GI disease	CTG ( <i>ZNF9</i> , also known as <i>CNBP</i> )	Intron	RNA GOF	A striking phenocopy of DM1
DRPLA	Seizures, choreoathetosis, ataxia, cognitive decline	CAG ( <i>ATN1</i> )	Coding region	Polyglutamine GOF	Very rare, most patients are in Japan
FMR1	MR, facial dysmorphism, autism	CGG ( <i>FMR1</i> )	5' UTR	Hypermethylation of promoter, LOF	Most common inherited MR
FMR2	MR, hyperactivity	GCC ( <i>FMR2</i> )	5' UTR	LOF	Needs to be ruled out in X-linked MR
FRDA	Ataxia, sensory loss, weakness, diabetes mellitus, cardiomyopathy	GAA ( <i>FXN</i> )	Intron	LOF, phenocopy of mitochondrial disease	Most common inherited ataxia in Caucasian ethnicity
FXTAS	Ataxia, intention tremor, parkinsonism	CGG ( <i>FMR1</i> )	5' UTR	RNA GOF	Pre-mutation carriers only
HD	Chorea, dystonia, cognitive decline, psychiatric disease	CAG ( <i>HTT</i> )	Coding region	Polyglutamine GOF	One of the most common inherited diseases in humans
HDL2	Chorea, dystonia, cognitive decline	CTG ( <i>JPH3</i> )	3' UTR, coding region	RNA GOF, poly-amino acid GOF and/or LOF?	A striking phenocopy of HD
Myoclonic epilepsy of Unverricht and Lundborg	Photosensitive myoclonus, tonic-clonic seizures, cerebellar degeneration	CCCCGCCCGCGG ( <i>CSTB</i> )	Promoter	LOF	Rare autosomal recessive disorder found in Finland and N. Africa
OPMD	Eyelid weakness, dysphagia, proximal limb weakness	CCG ( <i>PABPN1</i> )	Coding region	Polyalanine GOF	Modest expansion causes disease
SBMA	Proximal limb weakness, lower motor neuron disease	CAG ( <i>AR</i> )	Coding region	Polyglutamine GOF	Phenotype includes LOF androgen insensitivity
SCA1	Ataxia, dysarthria, spasticity, ophthalmoplegia	CAG ( <i>ATXN1</i> )	Coding region	Polyglutamine GOF	Accounts for 6% of all dominant ataxia
SCA2	Ataxia, slow eye movement, hyporeflexia, motor disease, occasional parkinsonism	CAG ( <i>ATXN2</i> )	Coding region	Polyglutamine GOF	<i>ATXN2</i> protein may not reside in the nucleus
SCA3	Ataxia, dystonia, lower motor neuron disease	CAG ( <i>ATXN3</i> )	Coding region	Polyglutamine GOF	Most common dominant ataxia
SCA6	Ataxia, dysarthria, sensory loss, occasionally episodic	CAG ( <i>CACNA1A</i> )	Coding region	Polyglutamine GOF	Causal gene encodes a subunit of a P/Q-type Ca <sup>2+</sup> channel
SCA7	Ataxia, dysarthria, cone-rod dystrophy retinal disease	CAG ( <i>ATXN7</i> )	Coding region	Polyglutamine GOF	Clinically distinct as patients have retinal disease
SCA8	Ataxia, dysarthria, nystagmus, spasticity	CTG/CAG ( <i>ATXN8</i> )	Untranslated RNA, coding region	RNA GOF and polyglutamine GOF	Many cases of reduced penetrance
SCA10	Ataxia, dysarthria, seizures, dysphagia	ATTCT ( <i>ATXN10</i> )	Intron	RNA GOF?	Huge repeats; only Mexican ancestry?
SCA12	Tremor, ataxia, spasticity, dementia	CAG ( <i>PPP2R2B</i> )	Promoter, 5' UTR?	Unknown	Causal gene encodes a phosphatase
SCA17	Ataxia, dementia, chorea, seizures, dystonia	CAG ( <i>TBP</i> )	Coding region	Polyglutamine GOF	Causal gene encodes a common transcription factor ( <i>TBP</i> )
Syndromic/non-syndromic X-linked mental retardation	MR alone, with seizures or with dysarthria and dystonia	CGG ( <i>ARX</i> )	Coding region	Probably LOF	Associated with West syndrome or Partington syndrome

**Table 1 - Molecular features of unstable repeat expansion disorders**

AR, androgen receptor; ARX, aristaless-related homeobox; ATN1, atrophin 1; ATXN, ataxin; CACNA1A, voltage-dependent P/Q-type calcium channel subunit  $\alpha$ -1A; CSTB, cystatin B; DM, myotonic dystrophy; DMPK, DRPLA, dentatorubral-pallidoluysian atrophy; FMR1, fragile X mental retardation syndrome; FMR2, fragile X E mental retardation; FRDA, Friedreich's ataxia; FXN, frataxin; FXTAS, fragile X tremor ataxia syndrome; GI, gastrointestinal; GOF, gain of function; HD, Huntington's disease; HDL2, Huntington's disease-like 2; HTT, huntingtin; JPH3, junctophilin 3; LOF, loss of function; MR, mental retardation; OPMD, oculopharyngeal muscular dystrophy; PABPN1, poly(A)-binding protein, nuclear 1; PPP2R2B, protein phosphatase 2 regulatory subunit B,  $\beta$  isoform; SBMA, spinal and bulbar muscular atrophy; SCA, spinocerebellar ataxia; TBP, TATA box-binding protein; ZNF9, zinc finger 9 (La Spada and Taylor, 2010).



one (HD), and perhaps a greater number of these disorders, may principally involve a simultaneous dominant-negative partial loss of the normal function of the disease protein. The next class of disorders are a much more disparate group of repeat disorders called “loss of function repeat disorders”. These disorders include different repeats that vary in sequence composition and gene location, but share a final common pathway of disease pathogenesis: a loss of function of the disease gene. This group includes various classic trinucleotide repeat disorders such as the two fragile X syndromes of mental retardation (FRAXA and FRAXE) (Sutherland and Baker, 1992) (Allingham-Hawkins and Ray, 1995) and Friedreich’s ataxia (Campuzano et al., 1996); but also encompasses the dodecamer repeat expansion in progressive myoclonic epilepsy type 1 (Lehesjoki, 2002), and possibly the CAG repeat expansion in Huntington’s disease like-2 (HDL2) gene (Margolis et al., 2001), (Stevanin et al., 2003). The third group of repeat diseases involves the production of toxic RNA species: this category of repeat diseases is thus called the RNA gain of function disorders. Included among these disorders are two closely related forms of DM, the common and classic myotonic dystrophy type 1 (DM1) (Bundey et al., 1970) and its uncommon phenocopy, myotonic dystrophy type 2 (DM2) (Udd et al., 2003). Another member of this group is the recently described fragile X tremor-ataxia syndrome (FXTAS) in male premutation carriers (a male of female who has between 55-200 CGG repeats in the Fragile X (FMR1) gene; the full mutation is defined as over 200 CGG repeats): an example of two different disease pathways operating upon the same expanded repeat mutation based upon size range differences (Jacquemont et al., 2003). One form of spinocerebellar ataxia (SCA8) has also been placed into this category: Daughters and co-authors showed that CUG-repeat transcripts expressed from the SCA8 locus form RNA foci in specific neurons in SCA8 patients and mouse brains. In fact the presence of the CTG expansion leads to nuclear retention of the mutant transcript, and at the cellular level, this retention is manifested by the formation of ribonuclear inclusions called RNA foci. Also for Huntington’s disease-like 2 (HDL2) it was proposed that RNA toxicity may contribute to the pathogenesis: RNA foci resembling DM1 (myotonic dystrophy type 1) foci were detected in neurons in HDL2 cortex and other brain regions (Rudnicki et al., 2007). The genetic defect in DM1 is the expansion of a CTG repeat tract in the 3’ untranslated region of a protein kinase gene, *DMPK*. The pathogenic *DMPK*

transcripts do not enter into the speckles suggesting that their export is blocked at an early step in nucleoplasmic transport. The muscleblind-like 1 (MBNL1) proteins, implicated in pre-mRNA alternative splicing regulation (Ho et al., 2004), were found to bind these expanded CUG repeats and to colocalize with nuclear foci of CUGexp-RNAs in DM1 cells (Miller et al., 2000).

The last class of repeat disease are the GCG-polyalanine disorders that are grouped together because all involve short GCG repeat tracts falling within the coding regions of unrelated genes that become expanded to moderately sized GCG repeats. With the exception of oculopharyngeal muscular dystrophy, all are developmental malformation syndromes, and while gain-of-function polyalanine toxicity has been proposed for a number of these disorders, loss of function due to the polyalanine expansion seems more likely for other diseases. Finally, a number of repeat disorders including spinocerebellar ataxia type 10 (SCA10), spinocerebellar ataxia type 12 (SCA12) currently defy classification because very little is known about their molecular basis. In the next chapter we will focus on the first class of repeat expansion diseases, which includes SCA7.

### 1.2.2. Polyglutamine disease: genetic characteristics

The polyglutamine diseases are a family of nine genetically-similar progressive, neurodegenerative diseases that includes Huntington's Disease (HD), Spinal and Bulbar Muscular Atrophy (SBMA), Dentatorubral-pallidoluytian atrophy (DRPLA), and the spinocerebellar ataxia (SCA) types 1, 2, 3, 6, 7 and 17 (Table 2). These diseases arise from the expansion of an unstable CAG triplet repeat within the coding region of a given gene. This results in the expansion of a glutamine stretch in the protein, which renders the host protein toxic mainly through gain-of-function mechanisms. Although the disease-causing proteins are expressed widely in the CNS, specific populations of neurons are vulnerable in each disease, resulting in characteristic patterns of neurodegeneration and clinical features. Nonetheless, these diseases share some similarities including progressive neurodegeneration in a disease-specific subset of neurons and the presence of insoluble protein aggregates.

The polyglutamine diseases have a striking genotype-phenotype correlation. Furthermore, the length of the CAG repeat has a strong positive correlation with the

age of the individual at onset of disease (Orr, 2001). It was described that the expanded polyglutamine protein has a toxic function related to neurons in a length-dependent manner regardless of the function of each gene (La Spada et al., 1994) (Orr, 2001) (Christie et al., 2014).

Disease	Mutation/ repeat unit	Gene name (protein product)	Putative function	Normal repeat length	Pathogenic repeat length
SCA1	(CAG) <sub>n</sub>	SCA1 (ataxin 1)	Transcription	6–39	40–82
SCA2	(CAG) <sub>n</sub>	SCA2 (ataxin 2)	RNA metabolism	15–24	32–200
SCA3 (MJD)	(CAG) <sub>n</sub>	SCA3 (ataxin 3)	De-ubiquitylating activity	13–36	61–84
SCA6	(CAG) <sub>n</sub>	CACNA1A (CACNA1 <sub>A</sub> )	P/Q-type α1A calcium channel subunit	4–20	20–29
SCA7	(CAG) <sub>n</sub>	SCA7 (ataxin 7)	Transcription	4–35	37–306
SCA17	(CAG) <sub>n</sub>	SCA17 (TBP)	Transcription	25–42	47–63
DRPLA	(CAG) <sub>n</sub>	DRPLA (atrophin 1)	Transcription	7–34	49–88
SBMA	(CAG) <sub>n</sub>	AR (androgen receptor)	Steroid-hormone receptor	9–36	38–62
HD	(CAG) <sub>n</sub>	HD (huntingtin)	Signalling, transport, transcription	11–34	40–121

**Table 2 - PolyQ diseases table summary (Gatchel and Zoghbi, 2005)**

### *Pathological Threshold*

In each gene responsible for a trinucleotide expansion disease, non-affected individuals have two normal sized alleles. The number of repeats is polymorphic in the general population and everyone has his own number of triplets. An allele is called normal when it presents a number of repeats under a specific threshold, different for each gene. On the other hand, the allele is called pathogenic or mutant when the number of repeats exceeds this pathogenic limit, after which it triggers the disease pathology.

Starting from a precise number of repeats and due to mechanisms that we will discuss later, repeats expansions become unstable and are inclined to increase in size. Thus, in addition to the normal alleles, we observe in some healthy individuals intermediate-sized alleles at the origin of *de novo* mutations in the next generation. This is also the case for the spinocerebellar ataxia type 7 (SCA7). In this disorder, the trinucleotide repeat (CAG)<sub>n</sub> encodes for polyglutamine (polyQ) and the normal alleles contain from 4 to 35 triplets (the majority of individuals have 10 to 12 repeats, whereas pathogenic alleles have 37 or more repeats). However, there is an intermediate group of alleles, containing from 28 to 35 repeats, for which there is a

risk of instability and thus occurrence of mutation in the offspring (Stevanin et al., 1998). The notion of an intermediate allele is even more pronounced in non-coding triplet expansion diseases, in which the number of repeats is higher and the instability is greater. This is the reason why they were not called intermediate alleles but directly pre-mutations (Figure 4). One example is the fragile-X syndrome caused by the (CGG)<sub>n</sub> expansion. In fragile-X syndrome, the normal allele possesses from 6 to 50 repeats, the premutation range is 50-200 and the pathogenic range from 230 to more than 1000 CGGs.

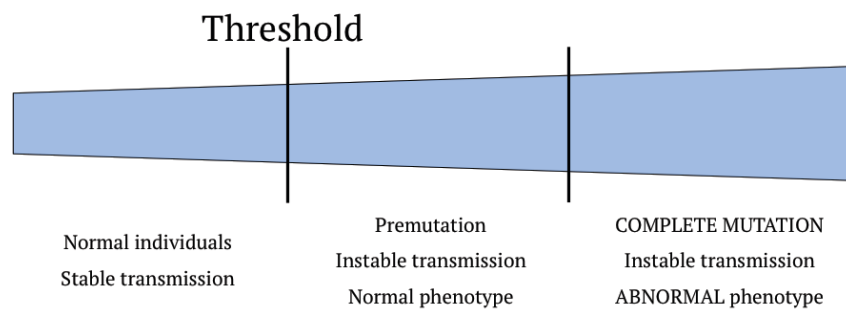


**Figure 4 - Schematic representation of pathological threshold, premutation and complete mutation**

### *Correlation between the number of repeats, disease onset and severity*

There is a correlation between the number of repetitions in the pathogenic allele and disease severity (David et al., 1998) (Gusella and MacDonald, 2000) (Stevanin et al., 2000): a higher number of repeat leads to earlier onset of disease and faster progression (Figure 5). This explains the clinical heterogeneity encountered in triplet-expansion diseases that are relatively mild and very severe infantile forms of the same disease. However, given a constant number of repeats, strong individual variations in the age at onset of symptoms can be observed. Due to instability, pathogenic allele size differs among patients, even in the same family. The use of this correlation to predict the age at onset of the disease, especially during a pre-symptomatic diagnosis, is then inappropriate. The number of repeats accounts in fact only for 50 to 75% of the variability in the age at onset, suggesting that other genetic or environmental factors may modulate the severity of the disease (Stevanin et al., 2000).

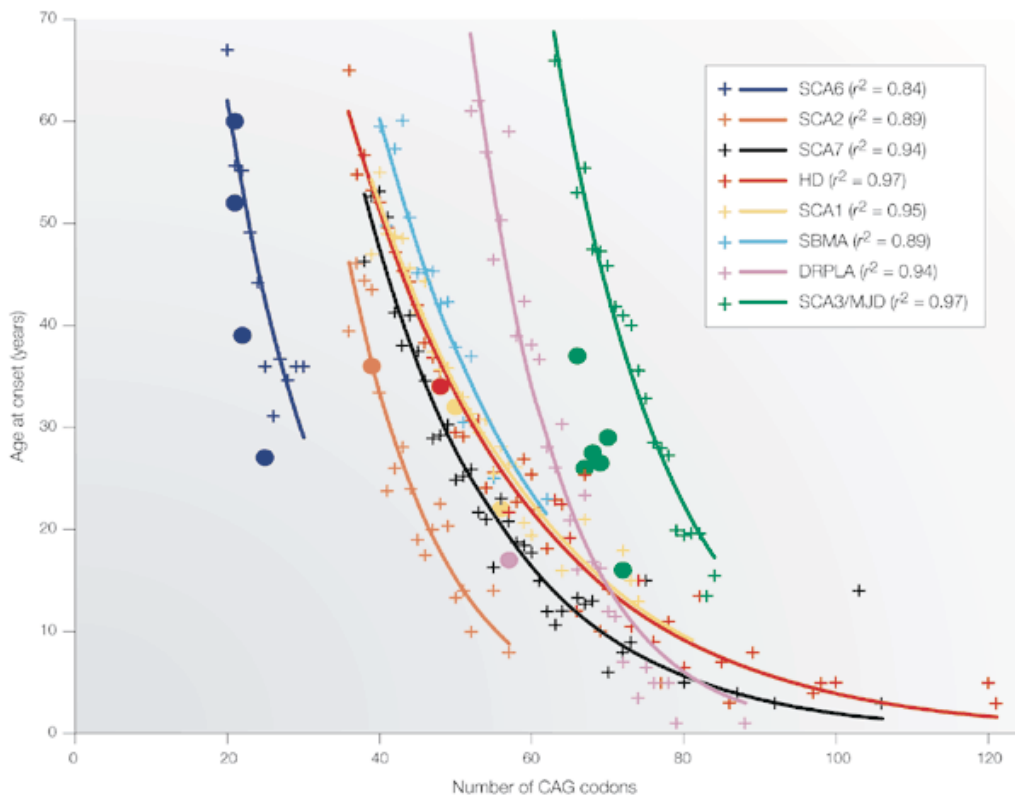


**Figure 5 - Relationship between age at onset and CAG repeat length for polyglutamine disorders**  
 Filled circles represent the onset age of homozygous patients with respect to the greatest expansion (Gusella and MacDonald, 2000).

### *Mechanisms at the origin of the instability*

In all triplet expansion diseases, the number of repeats evolves over successive generations: this is why they are called dynamic mutations. Most often they increase in size, while they rarely decrease. The instability is usually observed in mammals and especially in humans (Hardy and Orr, 2006) (Rubinsztein et al., 1995). This instability could result from the formation of secondary DNA structures by the repeats during replication and results in a shift of the DNA polymerase (Marquis Gacy et al., 1995) (Pearson et al., 2005). In fact, small repeats, which cannot form such structures are more stable. Moreover, interruption of the expansion seems to confer greater stability to large normal alleles. Two mechanisms could explain the expansion of normal alleles into pathological alleles: first, a loss of interruptions that would make these alleles unstable; or second, an expansion from uninterrupted large normal alleles. The fact that instability is greater in humans seems to represent an accelerated evolutionary mechanism due to the appearance or loss of a specific genetic factor or a transition threshold beyond which the cellular machinery is overwhelmed.

### *Germline mosaicism and genetic anticipation*

The mechanisms that we have just described are responsible for significant germline mosaicism, usually in the father (Pearson et al., 2005). The large number of cell divisions in spermatogenesis increases the probability of accumulating replication errors and explains the wide variety of sizes of mutated alleles observed in the patient's sperm. In comparison, oogenesis implicates only a limited number of divisions that stop early during embryogenesis, whereas spermatogenesis continues during the entire patients' life. This explains why the number of repeats tends to increase over successive generations, and the significant paternal contribution (Table 3). Among all polyglutamine diseases, SCA7 has the most pronounced instability (Stevanin et al., 2000). Furthermore, the size of transmitted expansions increases with age during paternal transmission in many mouse models (Mangiarini et al., 1997) (Savouret, 2003) and patients (Goldberg et al., 1993) (Stevanin et al., 2000). Expansion instability, the resulting germline mosaicism and the correlation between the number of repeats and disease severity, are responsible for dynamic-mutation diseases characterized by the genetic anticipation: the appearance of earlier and more severe symptoms in successive generations of an affected family.

	<i>Gender of the transmitting parent</i>	
	<i>Male</i>	<i>Female</i>
<i>SCA1</i>	+2.0 (-2 to +8, n=16)	+0.2 (-1 to +1, n=5)
<i>SCA2</i>	+3.5 (-8 to +17, n=33)	+1.7 (-4 to +8, n=23)
<i>SCA3/MJD</i>	+0.9 (-3 to +5, n=26)	+0.6 (-8 to +3, n=34)
<i>SCA7</i>	+12.1 (0 to +85, n=34)	+4.8 (-6 to +18, n=34)
<i>DRPLA</i>	+7.0 (0 to +28, n=33)	+0.3 (-4 to +4, n=9)
<i>SBMA</i>	+1.8 (-2 to +5, n=11)	+0.2 (-4 to +2, n=20)
<i>HD</i>	+6.1 (-4 to +74, n=156)	+0.6 (-4 to +16, n=160)

**Table 3 - Comparison of CAG repeat instability in polyQ diseases**

Comparison of CAG repeat instability during transmission to progeny at loci SCA1, SCA3, SCA2, SCA7, DRPLA, SBMA and HD (Stevanin et al., 2000)

### 1.2.3. Pathogenesis of polyglutamine diseases

A proteolytic cleavage appears to initiate most polyglutamine diseases by generating a toxic fragment. The expanded polyglutamine tract then allows the transition into a distinct conformation that may cause toxicity in several ways. For example, the peptide may exert toxicity as a monomer or it may self-associate to form toxic oligomers. The oligomers can assemble into larger aggregated species and ultimately

to be deposited in macromolecular intracellular inclusions. The principal toxic effects of the incorrectly folded protein may include alterations in different cellular pathways. They include: i) misfolding of the disease protein resulting in altered function (Todi et al., 2007), ii) deleterious protein interactions engaged in by the mutant protein (Bennett et al., 2005), iii) formation of toxic oligomeric complexes; iv) transcriptional dysregulation (Palhan et al., 2005) (McMahon et al., 2005), v) mitochondrial dysfunction resulting in impaired bioenergetics and oxidative stress (Lin and Beal, 2006), vi) impaired axonal transport (Caviston et al., 2007), vii) aberrant neuronal signaling including excitotoxicity, viii) cellular protein homeostasis impairment (Tang et al., 2005), and ix) RNA toxicity (Li et al., 2008)

#### 1.2.4. Cellular protective mechanisms

The tendency of proteins to aggregate has made it necessary for cells to evolve several defence mechanisms against misfolded or abnormal proteins (Figure 6).

The first defence is provided by molecular chaperones, many of which have been identified as heat shock proteins (Hsp). These molecules can refold abnormal proteins and render them non-toxic. Cell transfection studies have shown that molecular chaperones can increase the solubility of mutant polyglutamine proteins (Muchowski et al., 2000) (Sittler et al., 2001) and suppress mutant polyglutamine-mediated neuronal toxicity *in vitro* (Miller et al., 2005) and in invertebrate models *in vivo* (Chan et al., 2000), although the effects of molecular chaperone overexpression in mouse models have been variable. The enhancement of the HSP70 chaperone activity increased the protection against neurodegeneration and improved motor function in a SCA1 mouse model (Cummings et al., 2001); on the contrary, in a transgenic SCA7 mouse model, co-expression of HSP70 with its co-factor HDJ2 did not prevent either neuronal toxicity or aggregate formation (Helmlinger et al., 2004a).

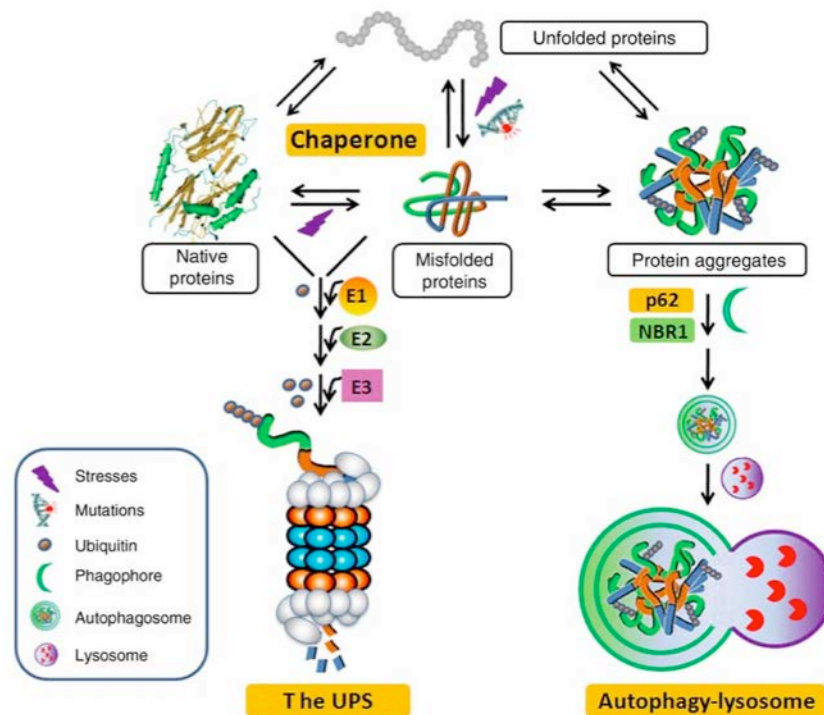


**Figure 6 - A schematic illustration of Protein Quality Control in the cell**

A schematic illustration of PQC in the cell. Chaperones facilitate the folding of nascent polypeptides and the unfolding/refolding of misfolded proteins, prevent the misfolded proteins from aggregating, and escort terminally misfolded proteins for degradation by the UPS. The UPS degrades both misfolded/damaged proteins and most unneeded native proteins in the cell. This process involves two steps: first, covalent attachment of ubiquitin to a target protein by a cascade of chemical reactions catalysed by the ubiquitin-activating enzyme (E1), ubiquitin-conjugating enzymes (E2), and ubiquitin ligase (E3); and then the degradation of the target protein by the proteasome. The autophagy-lysosomal pathway participates in PQC by helping remove protein aggregates formed by the misfolded proteins that have escaped from the surveillance of chaperones and the UPS. Protein aggregates or defective organelles are first segregated by an isolated double membrane (phagophore) to form autophagosomes, which later fuse with lysosomes to form autophagolysosomes, where the segregated content is degraded by lysosomal hydrolases. The legend for symbols used is shown in the box at the lower left (Su and Wang, 2009).

A second important cellular defence against misfolded proteins involves degradation by the proteasome. The proteasome is a complex molecular machine that can unfold proteins and process them to short peptide fragments in an interior space that contains proteolytic enzymes. Proteins are typically targeted for proteasomal degradation by ubiquitylation, although other mechanisms of targeting are also possible, including targeting by the chaperone protein CHIP.

A third defence mechanism involves autophagy, which has several variants, including macroautophagy, microautophagy and chaperone-mediated autophagy. These lysosome-mediated pathways can degrade soluble cytoplasmic proteins, especially those that do not undergo rapid turnover. Chaperone-mediated autophagy

involves the delivery of proteins that contain a consensus motif to transporters in the lysosomal membrane by a chaperone and co-chaperone complex. Autophagy can also be involved in the degradation of proteins with mutant polyglutamine repeats, as it was shown for huntingtin (Thompson et al., 2009) (Heng et al., 2010), ataxin-3 (Menzies et al., 2010) and ataxin-7 (Yu et al., 2013), also by our team (Alves et al., 2014). Proteasomes and autophagy are also involved in the normal turnover of proteins.

### 1.2.5. Mechanism for clearance of polyglutamine aggregates: the UPS and autophagy

The degradation of misfolded proteins involves two main pathways in eukaryotic cells: the ubiquitin-proteasome system (UPS) and autophagy. In contrast to autophagy, UPS is highly specific. In mammalian cells, about a thousand E3-ubiquitin ligase enzymes are responsible for the specific detection and binding of their substrates, which include misfolded proteins and short half-life regulatory proteins. In this process, the 76 amino acid protein ubiquitin is conjugated to a lysine residue on the degradation-bound substrate via the concerted actions of three enzymes: an activating enzyme (E1), a conjugating enzyme (E2), and a ligase (E3). Through this pathway, soluble, short-lived proteins are targeted to the 26S proteasome, a multisubunit protease (Pickart, 2001). The proteasome consists of a 20S central core complex and two 19S lid complexes. The barrel-shaped central complex comprises four stacked rings. The two identical outer rings are each made up of seven  $\alpha$ -subunits (termed  $\alpha$  1–7), and the two identical inner rings each consisting of seven  $\beta$ -subunits (termed  $\beta$  1–7). The proteolytic activity resides in three active subunits:  $\beta$ 1,  $\beta$ 2 and  $\beta$ 5, that have caspase-like activity to cleave behind acidic residues, trypsin-like activity to cleave after basic residues, and chymotrypsin-like activity to cleave behind hydrophobic residues, respectively. The two 19S lid complexes that bind to both sides of the central complex restrict the access to the proteolytic sites. Subunits of these 19S regulatory lid complexes bind to ubiquitin chains on substrates, release the ubiquitin chains, and allow the substrate to enter the central proteolytic complex. Proteasomal degradation of target substrates results in short polypeptides that are released into the cytoplasm or the nucleus, where they are then further processed by peptidases for antigen presentation or degraded into

amino acids. In polyglutamine diseases intracellular aggregates recruit components of the UPS. While it is commonly thought that proteasomes are irreversibly sequestered into these aggregates, leading to impairment of the UPS (Bennett et al., 2005), the data on proteasomal impairment in Huntington's disease and in SCA7 are contradictory. For example for Huntington, it was described an inhibition of UPS function in both early and late stage in HD patients' cerebellum, cortex, substantia nigra and caudate-putamen brain regions (Seo et al., 2004). Moreover, altered proteasomal function was associated with disruption of the mitochondrial membrane potential (Jana et al., 2001). M. Rechsteiner' team proposed, based on *in vitro* data, that the proteasome activator REGgamma could contribute to UPS impairment in polyglutamine diseases by suppressing the proteasomal catalytic sites responsible for cleaving Gln-Gln bonds (Li and Rechsteiner, 2001). Capping of proteasomes could potentially 'clog' the proteasome by pathogenic polyglutamines. Surprisingly, in the 13-week-old Huntigton R6/2 mouse model developed by G. Bates, a collaborative study with M. Rechsteiner described that proteasomal chymotrypsin-like activity, increased compared to non-R6/2, irrespective of REGgamma levels. Assays of 26S proteasome activity in mouse brain extracts revealed no difference in the proteolytic activity of R6/2 or REGgamma genotypes. The authors concluded that overall proteasome function is not impaired by trapped mutant polyglutamine in R6/2 mice (Bett et al., 2006).

Others authors showed that accumulation of ubiquitin conjugates in a R6/2 mouse model occurs without global ubiquitin/proteasome impairment (Maynard et al., 2009). Moreover, in a conditional HD94Q mouse model, which express an inducible chimeric mouse/human httQ94<sup>(exon1)</sup>, an earlier reported UPS impairment could not be detected, but an increase in both trypsin- and chymotrypsin-like activity was observed. This was similar to the increase in activities observed in cells expressing so-called immunoproteasome, induced upon treatment with IFN gamma. The labelling of immunoproteasome subunits indeed confirmed the presence of immunoproteasome in brains of HD mice (Díaz-Hernández et al., 2003). The same debate also concerns SCA7. In 2001, Matilla demonstrated the association of ataxin-7 with the proteasome subunit S4 of the 19S regulatory complex: these results suggested a role for S4 and ubiquitin-mediated proteasomal degradation in the

molecular pathogenesis of SCA7 (Matilla et al., 2001). But four years later, the impairment of UPS was excluded as a necessary step for polyglutamine neuropathology (Bowman et al., 2005).

How can these apparently contrasting findings in proteasome activity be explained? *In vitro* experiments did not show any impairment when proteasomes were incubated with isolated mutant htt aggregates and, although proteasomes were associated with aggregates, the cells still contained a large fraction of proteasomes that were not associated (Bennett et al., 2005) (Díaz-Hernández et al., 2006). This evidence, coupled with the observation that proteasomal impairment can already occur before aggregate formation, argues against a sequestration model. Moreover, improved survival of neurons with inclusion bodies was again demonstrated in the striatal cell model observed by automated fluorescence microscopy developed by Steven Finkbeiner (Arrasate et al., 2004). To determine proteasome activity in these cells, coexpression of the short-lived UPS reporter, mRFP, with mutant GFP-htt exon1 coincided with less proteasomal impairment (Mitra et al., 2009). Intriguingly, inclusion body-containing cells showed a significant decrease in proteasome activity just before inclusion bodies were formed. This suggests that inclusion body formation might be a protective mechanism to sequester toxic mutant htt species that would otherwise impair the UPS.

To summarize, impairment of the proteasome remains contradictory. It is unknown whether proteasomes are "good guys" because they can efficiently degrade nuclear mutant polyglutamine fragments, or "bad guys" because they generate toxic, aggregation-prone polyQ peptides, or even "ugly" guys when they become clogged and impaired by the polyQ fragments (Schipper-Krom et al., 2012). In all cases, modification of proteasome activity could stimulate clearance and prevent aggregation and toxicity of the polyQ fragments in related disorders. Introduction of activators, exchanging catalytic subunits or even using specific compounds that modulate proteasome activity, might improve the proteolytic cleavage of polyQ proteins, making the proteasome an interesting therapeutic target (Schipper-Krom et al., 2012).

The UPS and autophagy have long been regarded as two separate cellular pathways with distinct functions. It was previously thought that autophagy predominantly

degraded long half-life proteins and that the clearance of the short-lived proteins would not be affected by this pathway. However, recent findings suggest that the two systems communicate, at least under certain circumstances, and might even have compensatory functions in some cases. Short lived proteins normally degraded by the UPS can be indeed degraded by autophagy under various growth conditions, as for example serum deprivation (Fuertes et al., 2003a) (Li, 2006) and long-lived proteins can also be degraded by the UPS (Fuertes et al., 2003b). It is now clear that a number of proteins can be degraded by both autophagy and the proteasome (Webb et al., 2003). A perfect example is ataxin-7, which is a target for both the proteasome and autophagy (Alves et al., 2014) (Yu et al., 2012). In a SCA7 transgenic mouse model, using an antibody specific for LC3, immunostaining of cerebellum demonstrated an increase in LC3-positive structures in Purkinje cells (Mookerjee et al., 2009). Our team demonstrated that in a SCA7 knock-in (KI) mouse model, mutant ataxin-7 accumulated in inclusions immunoreactive for the autophagy-associated proteins mTOR, beclin-1, p62 and ubiquitin. Atypical accumulations of the autophagosome/lysosome markers LC3, LAMP-1, LAMP-2 and cathepsin-D were also found in the cerebellum of the SCA7 KI mice (Alves et al., 2014). Furthermore, mutations that interfere with the proteasomal degradation of a protein may increase the dependency of such proteins on autophagy for their degradation, as this will then become the default clearance route (Wong and Cuervo, 2010). This is especially true for mutated proteins with an increased tendency to aggregate: oligomeric and higher-order structures become inaccessible to the narrow proteasome barrel. This seems to be the case for most of mutant polyQ protein; ataxin-7 (Alves et al., 2014), huntingtin (Ravikumar et al., 2003) and ataxin-3 (Menzies et al., 2010) (Nascimento-Ferreira et al., 2011) have been shown to be targeted via the autophagic degradation pathway.

Numerous studies in yeast and mammalian cells, including primary neurons, have reported that proteasome inhibition leads to the upregulation of autophagy (Ding et al., 2003) (Ding et al., 2007) (Rideout et al., 2004). The converse does not occur. Inhibition of autophagy leads, in fact, to impaired degradation of substrates destined for the proteasome (Korolchuk et al., 2009). This is dependent on the ubiquitin-binding protein p62, which is an autophagy substrate that accumulates in

autophagy-deficient cells (Bjørkøy et al., 2005). The resulting elevated levels of p62 appear to compromise the UPS by delaying the delivery of ubiquitinated substrates to the proteasome and sequestering them away from other ubiquitin-binding proteins (for example, p97). Prolonged inhibition of autophagy would therefore also result in reduced flux through UPS. This may be relevant to the interpretation of studies examining the effects of autophagy knockout in various tissues, since some of the effects may be secondary consequences of a compromised UPS (for example, p53 elevation and apoptosis) (MacLaren et al., 2001).

A growing amount of data has recently drawn attention to p62 and its possible role in connecting autophagy with the UPS. P62, also called sequestosome1 SQSTM1, is cleared by both the UPS and autophagy (Komatsu et al., 2007); it is commonly detected in ubiquitin-containing protein aggregates associated with various neurodegenerative diseases (Bjørkøy et al., 2005) (Kuusisto et al., 2001) (Nagaoka et al., 2004), in particular polyQ diseases such as SCA3 (Nascimento-Ferreira et al., 2011), Huntington (Heng et al., 2010) and, as we demonstrated, SCA7 (Alves et al., 2014). P62 polymerizes via its NH<sub>2</sub>-terminal PB1 domain and binds to polyubiquitin chains via its COOH-terminal UBA domain. *In vitro* GST-pulldown data revealed that p62 interacts with LC3, and it has been suggested that this may facilitate the autophagic clearance of ubiquitin-positive protein aggregates (Pankiv et al., 2007). The strongest support for this hypothesis comes from studies using an artificially ubiquitinated peroxisomal integral membrane protein, where it was demonstrated that a single ubiquitin molecule is sufficient as a degradation signal for autophagy, in contrast to the tetra-ubiquitin chain that is necessary to signal for the degradation of proteasome clients (Kim et al., 2008). Unfortunately, definitive data supporting this mechanism for the clearance of endogenous proteins are still missing. P62 is unlikely to be necessary for the clearance of most autophagic substrates, as there does not appear to be a defect in bulk autophagy in p62 knockout mice (Komatsu et al., 2007).

### 1.2.6. Differences in toxicity in the central nervous system and periphery: the importance of the context

Regardless of the widespread expression of many polyglutamine disease proteins in non-neural cell types, the selective vulnerability of the CNS is a main feature of polyglutamine diseases. However, there is a striking divergence in clinical phenotypes among the polyglutamine diseases: neurologists can easily distinguish the movement disorder of HD from the weakness in SBMA or the ataxia in SCA1. The disease-specific features reflect selective loss of different neurons populations. Despite a wide expression within the CNS, polyglutamine expansion in huntingtin selectively affects striatal neurons and cortical neurons, whereas the same genetic mutation in the androgen receptor (or in ataxin-7) targets respectively motor neurons or Purkinje neurons. On the basis of these observations, it was predicted that features other than polyglutamine and unique to each disease protein must influence pathogenesis (La Spada and Taylor, 2003). Recent advances support this prediction and highlight the importance of the host protein context in polyglutamine disease pathogenesis and in determining cell-type specificity.

The problem of cell-type specificity is not only relevant to the polyglutamine diseases; indeed, the question exists for other major neurodegenerative disorders, including Alzheimer's disease, Parkinson's disease, and ALS. While the toxic effects of polyglutamine expansion are cell-type- or protein context-dependent, an increasing amount of evidence suggests that we can modulate these effects by posttranslational modification. For example, lysine modification by a small ubiquitin-like protein (SUMO-1) or acetylation has been shown to modulate protein accumulation and toxicity in HD (Steffan et al., 2004), SCA1 (Riley et al., 2005), DRPLA (Terashima et al., 2002) and SBMA (Chan et al., 2002). More recently our team demonstrated how SUMOylation attenuates the aggregation propensity and cellular toxicity of polyglutamine expanded ataxin-7 (Janer et al., 2010). Dissecting the role of post-translational modifications in polyQ disease can shed light into the mechanisms of polyQ neurodegeneration and could ultimately help in developing novel therapeutic strategies to counteract disease progression and manifestations.

### 1.2.7. Post-translational modification on polyQ disease

One of the most intriguing aspects of polyQ disease is that unique populations of neurons are affected in each disorder, despite the widespread and overlapping distribution of the disease-causing proteins in the central nervous system. The molecular bases for neuronal specificity are unknown. But recent evidence has suggested that protein context and post-translational modifications influence the neurotoxicity of the polyQ proteins. In the next paragraph we will analyse two aspects of the effect of post-translational modifications on polyQ toxicity: their general effect on cell homeostasis and their specific effect on the polyQ proteins.

#### *Phosphorylation*

Phosphorylation, a highly regulated post-translational modification that regulates protein localization, turnover and function, can be initiated in neurons by neurotrophin and growth factor signalling and is propagated by kinase cascades. Among the growth factors, insulin-like growth factor 1 (IGF-1) possesses remarkable neuroprotective properties (Trejo et al., 2004). Binding of neurotrophic factors and IGF-1 to their receptors activates two major signalling pathways: the mitogen-activated protein kinase (MAPK) and the phosphatidyl-inositol 3-kinase/Akt pathways. Alterations in neurotropic or growth factor signalling are associated with several neurodegenerative conditions such as spinal and bulbar muscular atrophy (SBMA) (Sopher et al., 2004) and Huntington's disease (HD) (Colin et al., 2005). Although dysfunction of these signalling pathways is not likely to be the primary cause of neurodegeneration in polyQ diseases, it may contribute to disease progression and manifestation. PolyQ huntingtin (htt), androgen receptor (AR) and ataxin-1 are substrate for Akt. Of remarkable importance is that phosphorylation by Akt has different consequences on these polyQ proteins. Phosphorylation of polyQ htt at serine 421 by Akt results in the decreased formation of nuclear inclusions and reduced toxicity in cultured striatal neurons (Humbert et al., 2002) and in a rodent model of HD (Pardo et al., 2006). This phosphorylation is reduced in the cortex and striatum of mouse model of HD (Warby et al., 2005). If phosphorylation of polyQ and AR protects against toxicity, phosphorylation of ataxin-1 by Akt has opposite effects. Phosphorylation of ataxin 1 at serine 776 increases interactions with the molecular chaperone 14-3-3 and results in increased protein stabilization and

formation of neuronal inclusions (Chen et al., 2003). In fly models of spinocerebellar ataxia type 1 (SCA1), activation of the phosphatidylinositol 3-kinase/Akt pathway can worsen the eye degeneration associated with the expression of mutant ataxin-1. In mouse model of SCA1, substitution of serine 776 with alanine, a non-phosphorylatable residue, reduces the accumulation of the protein in nuclear inclusions and decreases the toxic properties of the expanded polyQ protein (Emamian et al., 2003).

### Acetylation

The covalent binding of an acetyl group to lysine residues is a reversible reaction catalyzed by histone acetyltransferase (HAT) enzymes, such as CREB-binding protein (CBP); histone deacetylase (HDAC) enzymes are responsible to its remove. The major targets of acetylation are histones and transcription factors such as AR. Histone and transcription factor acetylation leads to transcriptional activation of specific genes. The disruption of the delicate equilibrium between HAT and HDAC activities results in reduced expression of vital genes in HD (Sadri-Vakili et al., 2007). For example, CBP is an acetyltransferase, the activity of which is altered in polyQ disease. In fact, the polyQ protein/CBP interaction causes loss of CBP function by decreasing its availability. Moreover, the interaction of polyQ htt, atrophin 1, ataxin 3 or AR with CBP sequesters CBP into inclusions, thereby decreasing the amount of soluble CBP (McC Campbell et al., 2000) (Nucifora et al., 2001) and enhancing its ubiquitylation and degradation through the proteasome (Jiang et al., 2003). On the contrary, the overexpression of CBP protects neurons against the toxicity of expanded polyQ (McC Campbell et al., 2000) (Taylor et al., 2003). In ataxin-7, lysine 257 (K257), a highly conserved residue near the D266 caspase cleavage site, was acetylated, identifying it as an important modulator of fragment accumulation *in vitro* and *in vivo*. Modification of ataxin-7 K257 by acetylation promotes accumulation of the fragment, whereas unmodified ataxin-7 is degraded (Mookerjee et al., 2009). Our team had identified simultaneously lysine K257 as a target for SUMOylation and its implication in ataxin-7 toxicity and aggregation (Janer et al., 2010).

### Ubiquitylation

Ubiquitylation plays an important role in polyQ disease: it reduces polyQ toxicity by enhancing protein degradation. For instance, the overexpression of the ubiquitin ligase E4B increases ataxin 3 ubiquitylation, reduces the accumulation of insoluble species and suppresses neurodegeneration in a fly model of SCA3 (Matsumoto et al., 2004). Overexpression of the ubiquitin ligase C-terminus of Hsp70-interacting protein (CHIP) reduces the aggregation and toxicities of polyQ ataxin-3 and htt (Jana et al., 2001), AR (Adachi et al., 2007) and ataxin-1 (Al-Ramahi et al., 2006). Overexpression of the E3 enzyme parkin enhances ataxin-3 ubiquitylation, degradation and reduces its toxicity (Tsai et al., 2003). Normal ataxin-3 is a poly-ubiquitin-binding protein the overexpression of which reduces the accumulation of various polyQ proteins and suppresses neurodegeneration *in vivo* (Warrick et al., 2005). Importantly, the ubiquitin-associated activity of ataxin-3 is required to protect against neurodegeneration. In contrast, ubiquitylation can also enhance toxicity: for example, inhibition of the E2 enzyme Hip2 reduces the accumulation of insoluble fragments of polyQ htt (de Pril et al., 2007). Moreover, CHIP was shown to enhance the ubiquitylation of polyQ ataxin-1, leading to a reduction in solubility and increased accumulation in insoluble aggregates (Choi et al., 2007).

### SUMOylation

The covalent and reversible attachment of SUMO (small ubiquitin-related modifier) proteins to the side chain of target protein lysine residues is referred to as SUMOylation. One consensus sequence motif for SUMOylation is  $\Psi$  KX[D/E], where C is a hydrophobic residue, K is the acceptor lysine, X is any amino acid and D/E is an aspartate or glutamate. SUMO co-localizes with neuronal inclusions in autopsy brain and cell models of dentatorubral pallidoluysian atrophy (DRPLA) (Terashima et al., 2002), HD (Steffan et al., 2004) and SCA7 (Janer et al., 2010). Interestingly, the amount of SUMOylated proteins is increased in autopsy brain tissues of DRPLA, SCA1, SCA3, HD and SCA7 patients (personal contribution in this manuscript) and in mouse models of SCA1, suggesting that SUMO modification contributes to neurodegeneration in polyQ disease (Ueda et al., 2002) (Table 4).

Disease	Substrate	Modified residue	Functional impact
Polyglutamine diseases			
HD	Huntingtin	K6, K10, K15	Negative regulation of Htt97Q aggregation when fused to SUMO; sumoylation increases nuclear targeting and transcriptional repression
SBMA	Androgen receptor	K385, K518	Attenuates polyglutamine-mediated aggregation
SCA type 1	Ataxin-1	Multiple sites	Mutant ataxin-1-82Q is sumoylated to a lesser extent than WT
SCA type 7	Ataxin-7	K257	Negative regulation of mutant ataxin-7 aggregation
SCAN1	TDP1	K111	Proper sub-nuclear targeting
DRPLA	Atrophin 1		Co-expression of SUMO1 and atrophin with expanded poly-glutamine stretches increases its nuclear aggregation

**Table 4 - SUMOylation in polyQ diseases (Krumova and Weishaupt, 2013)**

An even more intriguing aspect of the genetic interaction between SUMOylation and polyQ disease emerges from the finding that polyQ proteins, including htt (Steffan et al., 2004), AR (Poukka et al., 2000), ataxin-1 (Riley et al., 2005) and ataxin-7 (Janer et al., 2010) are direct targets for SUMOylation. SUMO modification of the polyQ proteins is important for their toxicity and it may influence neurodegeneration by different mechanisms. For example, SUMOylation attenuates the aggregation propensity and cellular toxicity of the polyglutamine expanded ataxin-7 (Janer et al., 2010). Moreover, enhanced htt SUMOylation increases the stabilization of the protein, possibly due to competition with ubiquitylation at the same lysine residues, and reduces aggregation of polyQ htt (Steffan et al., 2004). In contrast, loss of SUMOylation in polyQ htt reduces neurodegeneration (Steffan et al., 2004) but increased mutant ataxin-7 aggregates (Janer et al., 2010).

### 1.3. Spinocerebellar Ataxia type 7 (SCA7)

#### 1.3.1. Anatomopathology

SCA7 is a rather unique disease from a clinical and neuropathological point of view because it is the only polyQ disease in which the cerebellum and retina are both affected, sometimes leading to blindness (Enevoldson et al., 1994).

Symptoms in patients usually start with a cerebellar disease, which is characterized by ataxia and disorders of balance movement and speech. Other neurological

disorders such as dysarthria, dysphagia, hearing loss and abnormal eye movements often accompany this cerebellar syndrome. It also affects the corticospinal tract, inducing exaggerated osteo-tendon reflexes and spasticity.

In patients characterised by a large repeat expansion, the disease appears already during childhood and in a very severe form. In this case, we also observe a broader phenotype including affected non-neuronal tissues, as for example the heart (Benton et al., 1998) (David et al., 1998) (Johansson et al., 1998) (Whitney et al., 2007). Most frequently, SCA7 patients present atrophy of the cerebellum, pons, dentate nucleus of the inferior olive, the subthalamic nucleus and spinocerebellar and pyramidal tracts (Martin et al., 1999) (Michalik et al., 2003).

Patients also have significant loss of Purkinje cells in the cerebellum, whereas the granular layer is relatively spared. They also have massive neuronal loss in the inferior olive, some nuclei of cranial nerves (III, IV and XIII) and the basal ganglia including the substantia nigra (Martin et al., 1999). Other important characteristics are a hypomyelination of the optic nerve and gliosis in the geniculate bodies and visual cortex (David et al., 1998) (Martin et al., 1994).

### 1.3.2. Genetics aspects in SCA7

From a genetic point of view, normal *SCA7* alleles contain a number of repeats varying from 4 to 35 pure CAGs (75% of population has 10 repetitions), whereas pathogenic alleles contain more than 35 repeats (Benomar et al., 1994) (Benton et al., 1998) (David et al., 1998) (Del-Favero et al., 1998) (Gouw et al., 1998) (Moseley et al., 1998).

SCA7 is the most unstable polyQ disease. Patients can in fact possess up to 306 repetitions (Benton et al., 1998). When the allele contains an intermediate number of repetitions (28 to 35), it can increase in the number and lead to *de novo* mutations in the next generation (Stevanin et al., 1998). This is typical of polyQ diseases, as explained in the previous sections. Another phenomenon, called anticipation, is extremely significant in SCA7; the largest additive expansion transmitted by a father and to his son was 263 repeats (Benton et al., 1998). Although paternal transmission is associated with larger expansions, the disease is most often transmitted by maternal DNA (Monckton et al., 1999). This suggests that the paternal transmission

probably leads to death at the embryonic state or to a default during the fertilization step.

The *SCA7* gene occupies a special place in our laboratory since 1997 when it was cloned with J.L Mandel's group in Strasbourg (David et al., 1997). It encodes the ataxin-7 protein, which is composed by 892 amino acids and is ubiquitously expressed, primarily in the heart, placenta, skeletal muscle and pancreas. In the CNS, ataxin-7 transcript levels are higher in the cerebellum (David et al., 1997). At the cellular level, ataxin-7 is found in the nucleus and is associated with the nuclear matrix (David et al., 1997) (Kaytor et al., 1999). It is also found in the cytoplasm of cells in several other brain regions (Cancel et al., 2000) (Holmberg et al., 1998).

A very recent paper also reports that cytoplasmic ataxin-7 is a microtubule (MT)-associating and (MT)-stabilizing protein. This association with MTs was observed for both wild type and mutant ataxin-7 (Nakamura et al., 2012). Three NLS (Nuclear Localisation Signals) (Chen et al., 2004) (Kaytor et al., 1999) and one NES (Nuclear Export Signal) (Taylor et al., 2006) control the nuclear and cytoplasmic localisation of this shuttling protein. The polyQ expansion appears to inhibit the NES function, which might explain the nuclear accumulation of the protein in patients affected by the disease. Protein cleavage might also regulate translocation: an N-terminal fragment excluding the NES has been described in mouse models and in patients (Garden et al., 2002) (Young et al., 2007) (Yvert et al., 2000).

The ataxin-7 protein has cleavage sites for caspase 7 at amino acids 266 and 344: they seem able to regulate the location and toxicity of this protein (Young et al., 2007). In particular, non-cleavable mutant ataxin-7 translocates into the nucleus where it aggregates and is less toxic than the cleavable form.

### 1.3.3. Molecular mechanisms

By combining profile-based sequence analysis with genome-wide functional data in model organisms, Scheel and co-authors found that ataxin-7 is orthologous to the open reading frame Ygl066c in Sgf73, a yeast protein of *Saccharomyces cerevisiae* (Scheel et al., 2003). The study suggested that Ygl066c was a component of the SAGA (*SPT/Ada/Gcn5 acetylase*) histone acetyltransferase complex. This study also

suggested that the finding had implications for disease pathogenesis, since it provided a direct connection between SCA7 and histone acetylation.

In 2004, it was confirmed that ataxin-7 belongs to the SAGA-like complexes TFIIIC (*TATA-binding protein-free TAF-containing complex*) and STAGA (*SPT3/TAF9/GCN5 acetyltransferase complex*), which are transcriptional coactivators. Both complexes are involved in the histone acetylation, DNA repair and pre-mRNA splicing (Helmlinger et al., 2004b). These complexes are the link between transcription factors bound to DNA and RNA polymerase II (Blazek et al., 2005) (Timmers and Tora, 2005). The same authors also described the existence of a new zinc-binding domain between amino acids 330 and 401 in ataxin-7. This area is responsible for the interaction of ataxin-7 with the TFIIIC complex and STAGA; the latter contains the GCN5 protein with histone acetyl-transferase activity (HAT). In that study, the polyQ expansion did not change the composition of the complex and ataxin-7 incorporation (Helmlinger et al., 2004b).

In 2005, two studies completed this work (McMahon et al., 2005) (Palhan et al., 2005). The first confirmed that SGF73 belongs to SAGA-like complexes via observations on a yeast model. SGF73 in the complex is essential for its organization and HAT activity. This study found that wild type or mutated human ataxin-7 are capable of binding without Sgf73 and that it is usually incorporated in the yeast complex. However, whereas the incorporation of GCN5 was detected, as expected, the presence of the polyQ expansion affected the HAT activity of the complex containing the mutated ataxin-7. The observed consequence was a decrease in the recruitment of regulatory subunits, such as Ada2, Ada3 and TAF12 (McMahon et al., 2005). This first study therefore suggested that the polyQ expansion disrupts the normal function of ataxin-7 and the complex it belongs to. This dysfunctional complex could subsequently act in a dominant and negative fashion and be recruited to promoters in the same way as the wild type complex. However, it can also have different effects on histone acetylation and transcriptional regulation.

The second study confirmed that polyQ repeats do not modify the incorporation of ataxin-7 or any other protein, in the complex (Palhan et al., 2005). This work was carried out in stable transfected HEK293 cells. It demonstrated that ataxin-7 stabilizes the STAGA complex and that it directly interacts with GCN5. In this case,

when ataxin-7 binds to GCN5 and to the transcription factor CRX (Cone Rod homeobox), it allows STAGA recruitment to the gene promoters expressed in CRX-regulated photoreceptors by inducing their activation. It was then demonstrated that mutant ataxin-7 decreases the incorporation of HAT regulatory proteins such as SPT3, Ada2b and TAF12, into the STAGA complex. This complex is thus usually recruited to promoters, but its HAT activity decreases, leading to a CRX-dependent inhibition of gene transcription by a dominant negative effect (Palhan et al., 2005) (Figure 7).

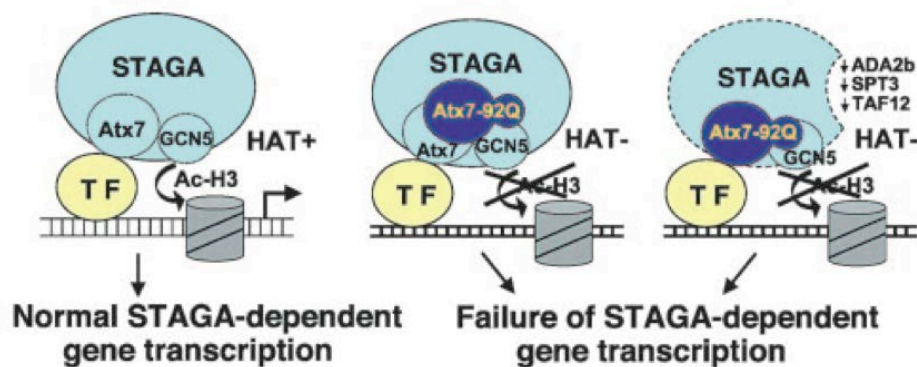


**Figure 7 - Ataxin-7 role into STAGA complex and its consequences due to expanded polyQ mutation**

Models indicating (i) normal function of WT ataxin-7 (Atx7), as an integral GCN5-interacting subunit of STAGA, in facilitating STAGA recruitment and GCN5-mediated histone H3 acetylation through interactions with a promoter-bound transcription factor (TF) such as CRX (*Left*), and (ii) dominant-negative inhibition of GCN5 function (histone acetylation) within promoter-bound STAGA by poly(Q)-expanded ataxin-7 (Atx7-92Q) after interactions with WT ataxin-7-containing STAGA (*Center*) or after incorporation into STAGA in place of WT ataxin-7 resulting in reduced incorporation of ADA2b, SPT3, and TAF12 (*Right*) (Palhan et al., 2005).

A study based on the analysis of the SCA7 mouse retina, however, contradicts these observations (Helmlinger et al., 2006). The reason why the retina was chosen is because this is where anomalies in transcription cause photoreceptor dysfunction (Helmlinger et al., 2006). The composition of the purified complex from the retina of SCA7 mice is identical to that in healthy mice, although it contains mutated ataxin-7. Its HAT activity on free histones or nucleosomes is equal to that of the complex in wild type mice. In SCA7 mice, this complex is nevertheless recruited in an unusual way to some specific gene promoters, leading to histone H3 hyperacetylation. In agreement with these results, the chromatin structure appears deeply perturbed. In the retina, whereas control photoreceptors have a large central region of heterochromatin and a thin border of peripheral euchromatin, in photoreceptor

from SCA7 mouse, nuclei are enlarged and heterochromatin is condensed. Surprisingly, in this case, gene hyperacetylation leads to a decrease in transcription. To account for this observation, the authors proposed the following model. They suggested that deregulation of the function of the complex increases recruitment to specific photoreceptor gene promoters, leading to hyperacetylation, chromatin decondensation and an increase in the volume of the nucleus. This increase in volume would then lead to a secondary dilution of transcription factors, explaining the decrease in the transcription of specific genes that are usually highly expressed in photoreceptors (Figure 8).

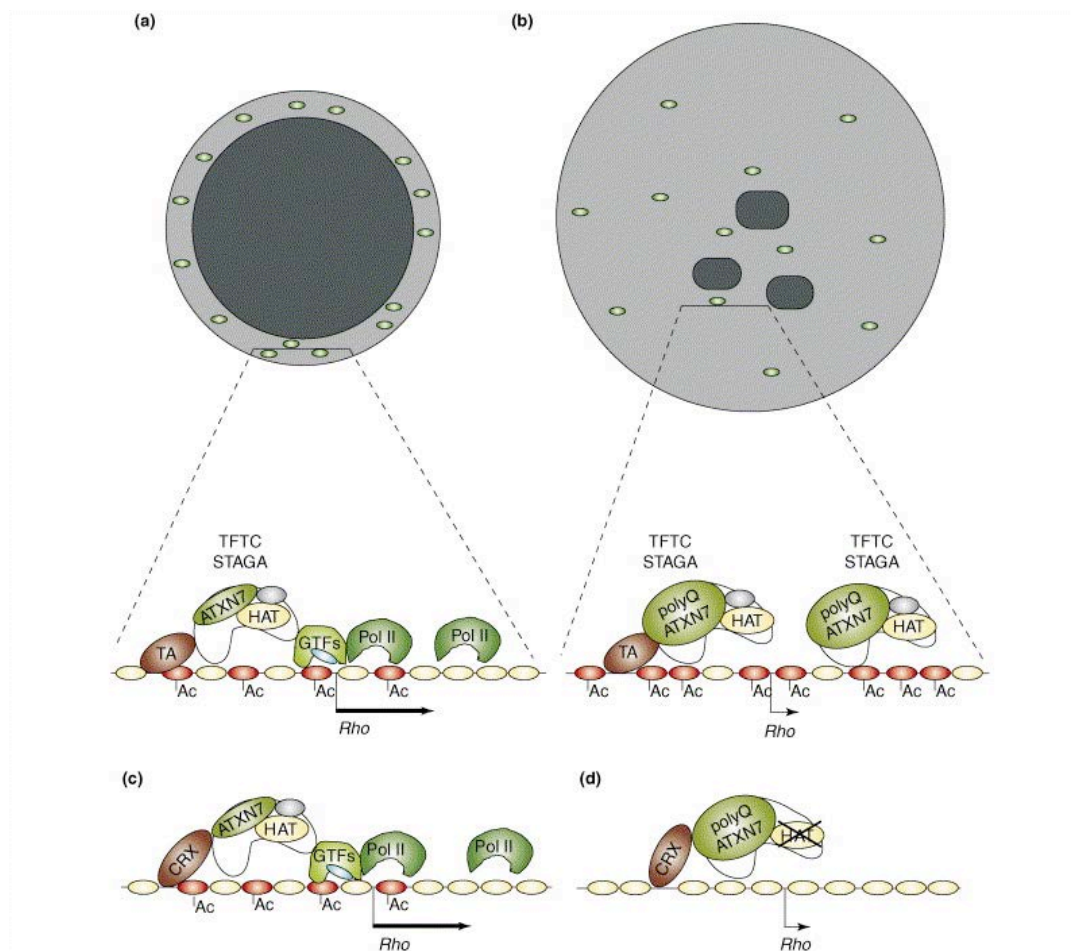


**Figure 8 - Model of potential mechanisms by which polyQ-expanded ataxin-7 induces toxicity in rod photoreceptors**

Model of the potential mechanisms by which polyQ-expanded ataxin-7 induces toxicity in rod photoreceptors. (a) In normal rod photoreceptor nuclei, strongly expressed genes are localized in the small peripheral compartment of euchromatin (light gray) whereas non-expressed and housekeeping genes are found in the large central region of heterochromatin (dark gray). The concentration of specific and general transcription factors (green ovals) in euchromatin leads to strong and restricted expression of rod-specific genes such as rhodopsin (Rho). TFTC/STAGA complexes, which contain normal ataxin-7, act as coactivators for transcriptional activators (TA) of these genes. (b) In SCA7

retina, polyQ-expanded ataxin-7 induces a severe decondensation of heterochromatin that increases rod nuclear volume and perturbs the normal gene compartmentalization seen in rod photoreceptors. Dilution of transcription factors primarily affects expression of genes strongly expressed in this cell type. Incorporation of polyQ-expanded ataxin-7 (polyQ-ataxin-7) in TFTC/STAGA complexes does not modify the subunit composition or the HAT activity of these complexes but leads to deregulation of TFTC/STAGA recruitment over large genomic regions, thereby inducing histone H3 hyperacetylation, chromatin decondensation and dilution of the transcriptional machinery over the increased nuclear volume. (c,d) An alternative model proposed by Pahlan et al. in which TFTC/STAGA is recruited at the promoters of rod-specific genes through direct interaction between CRX and ATXN7 (c). Incorporation of polyQ-ataxin-7 in TFTC/STAGA decreases the recruitment of other subunits (ADA2b, SPT3 and TAF12: gray ovals) thereby leading to reduced HAT activity of these complexes (d). Acetylated nucleosomes are shown as orange ovals and unacetylated nucleosomes as yellow ovals. GTFs: general transcription factors; Pol II: RNA polymerase II (Helmlinger et al., 2006b).

The contradictions between the results obtained in these three studies probably come from differences in the used models. The *in vivo* study seems the most convincing and the most coherent because it integrates the results obtained in different SCA7 mouse models. Ataxin-7 seems to play an important role in the transcriptional regulation. It would now be interesting to elucidate its precise function in the complex and identify the genes controlled by TFTC/STAGA. The SAGA-like complex indeed regulates about 10% of the yeast genome, and most of the genes are activated by a stress response.

To gain further insight into the importance of SAGA and GCN5, a recent study examined the effects of GCN5 mutations on mice bearing polyQ-ataxin-7 (Chen et al., 2012). In this study, they introduced single copies of either a *Gcn5* hypomorphic allele (*Gcn5<sup>fn/+</sup>*), or a deletion allele (*Gcn5<sup>Δ/+</sup>*), into *Atxn7<sup>100Q/5Q</sup>* or *Atxn7<sup>100Q/100Q</sup>* mice. The resulting reduction of GCN5 expression of around 50% was performed to investigate the consequences in hetero- and homozygous SCA7 KI mice model. Partial loss of GCN5 function accelerates neuronal dysfunction and pathogenesis in the two major neurological phenotypes of SCA7 mice. However, the complete deletion of GCN5 in normal Purkinje cells, which are the most affected neuronal cell in SCA7, was not sufficient to induce severe ataxia in the presence of wild-type ataxin-7. These data demonstrate that loss of GCN5 function can contribute to SCA7, further indicating that polyQ-ataxin-7-interacting proteins in SAGA are important for the development of the disease (Chen et al., 2012).

Two other studies on the transcriptome in two different SCA7 mouse models support the hypothesis of ataxin-7 involvements in the regulation of transcription. In 2006,

a transcriptome study on R7E mouse retina, a model overexpressing mutant ataxin-7 (90Q) only in photoreceptors, showed a very strong decrease in the expression of genes essential for retinal photoreceptor function. It also highlighted how photoreceptors expressing polyQ expansion proteins progressively lose their differentiation features due to transcriptional alterations of mature photoreceptor genes compared to the wild type retina (Abou-Sleymane et al., 2006). More recently, a transcriptome analysis of the cerebellum was performed in another SCA7 mouse model overexpressing mutant ataxin-7 (52Q). In this study realized after the appearance of the first symptoms, the team described the repression of certain genes expressed in mouse cerebellum. These genes are known to be involved in various phenomena ranging from the regulation of glutamatergic neurotransmission to myelinisation (Chou et al., 2010).

Transcriptional deregulation in polyglutamine diseases has also been associated with changes in the state of acetylation due to alteration of the HAT activity of member complexes (McCullough and Grant, 2010) or by a direct interaction of ataxin-7 with histone deacetylases (HDACs), in particular HDAC3 (Tsai et al., 2004) (Evert et al., 2006). A very recent paper showed that HDAC3 enhances the post-translational modifications and the stability of ataxin-7, with evidence that ataxin-7 and HDAC3 are colocalized and interact physically. Their association enhances cellular toxicity in a polyQ-dependent manner. The same studies also detected an increased level of HDAC3 in SCA7 mice, as well as altered levels of lysine acetylation and deacetylase activity in the brain of SCA7 transgenic mice, indicating that the association between HDAC3 and ataxin-7 may be a pathological feature of the disease (Duncan et al., 2013).

Interestingly, the scientific literature does not contain documented studies of the implications of ataxin-7 polyglutamine expansions on the function of the SAGA complex deubiquitination module (USP22). It is easy to imagine that disruption of SAGA complex HAT activity would be sufficient to cause the deregulation of a large number of genes by itself. However, it is difficult to ignore the potential for the additional alteration of deubiquitination activity, given that several studies confirm that ataxin-7 plays a role in the anchoring of the functional deubiquitination activity to the greater SAGA complex (Lang et al., 2011).

Further studies are necessary to elucidate whether polyglutamine expansions in ataxin-7 alter the deubiquitination activity of the SAGA complex and whether it affects the regulation of SAGA-dependent genes. A better understanding of the molecular mechanisms underlying SCA7 pathology will facilitate the development of effective treatments for SCA7 and other polyglutamine-expansion disorders.

## 1.4. SUMOylation

Post-translational modification with the small ubiquitin-related modifier (SUMO) was shown to regulate a vast variety of proteins in many pathways. The key to SUMO's role as a molecular switch is the reversible nature of the modification it induces. SUMO-specific enzymes attach to SUMO in an ATP-dependent enzymatic cascade that resemble ubiquitylation (Komander and Rape, 2012). Since at least some SUMO proteins can themselves serve as targets for SUMOylation, chains may be formed in consecutive steps (poly-SUMOylation). Dedicated SUMO-specific proteases reverse the modification by stimulating hydrolysis of the isopeptide bond (Drag and Salvesen, 2008) (Hickey et al., 2012). Most targets seem to undergo rapid cycles of SUMOylation and de-SUMOylation, often resulting in a very low steady-state level of the modified species. In 2010, our team identified ataxin-7 as a SUMO target protein and SUMOylation as a post-translational modification that attenuated aggregation propensity and cellular toxicity of polyglutamine-expanded ataxin-7 (Janer et al., 2010). On the basis of these findings, we have continued to investigate the influence of these post-translational modifications of ataxin-7. In the next section, we will describe the scientific and experimental background of SUMOylation, as an introduction to the work presented in this thesis.

### 1.4.1. The SUMOylation cycle

SUMOylation regulates many aspects of normal protein function, including subcellular localization, protein partnering and transcription factor transactivation (Yeh, 2009) (Geiss-Friedlander and Melchior, 2007) (Zhao, 2007). Cells express three major SUMO paralogs: SUMO-1, SUMO-2 and SUMO-3; SUMO-2 and SUMO-3 resemble each other more than to SUMO-1. A gene encoding SUMO-4 has been described, however it remains unclear whether SUMO-4 is processed or conjugated to cellular proteins (Guo et al., 2004).

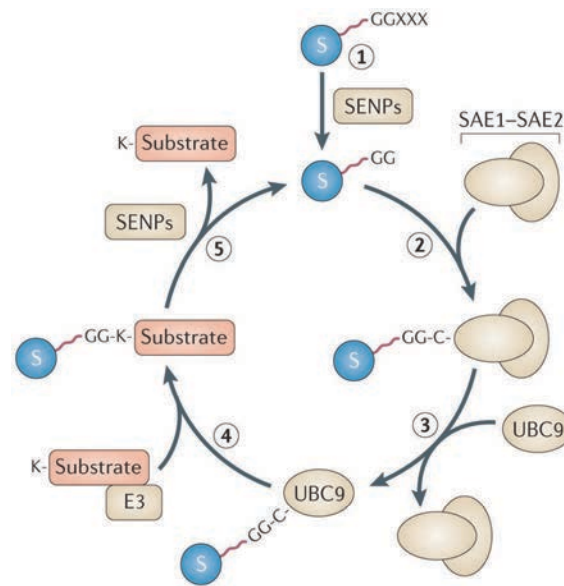


**Figure 9 - The SUMOylation pathway**

The translated small ubiquitin-like modifier (SUMO; denoted S in the figure) precursor is processed into its mature form by the action of SUMO-specific proteases (SENPs), which cleave the SUMO carboxyl terminus to reveal a Gly-Gly motif (step 1). This motif is essential for all subsequent steps of the SUMO cycle and mediates the direct linkage of SUMO to each enzyme and target molecule. Mature SUMO is activated by and covalently linked to a catalytic Cys in the SUMO-activating enzyme 1 (SAE1)–SAE2 heterodimer (E1 enzyme) (step 2). Activated SUMO is transferred to the catalytic Cys of the SUMO-conjugating enzyme UBC9 (E2 enzyme) (step 3). UBC9 catalyses the conjugation of SUMO to Lys residues in target proteins, either independently of or in concert with a SUMO E3 ligase, both of which determine target and Lys specificity (step 4). SENPs can cleave SUMO from target substrates (deconjugation), thus releasing an unmodified target and free SUMO (which can re-enter the sumoylation cycle) (step 5). (Everett et al., 2013)

Like ubiquitin, attachment of SUMO to proteins involves a series of enzymatic steps. In the first step, the SUMO protein is cleaved by the SUMO-specific carboxyl-terminal hydrolase activity of a sentrin-specific protease (SENPs); the enzyme cleaves the SUMO protein to produce a carboxyl-terminal diglycine motif. The mature SUMO protein is covalently attached via a thioester bond to a cysteine in the SUMO-activating enzyme subunit 2 (SAE2) of the heterodimeric SUMO E1. This activates enzymes in an ATP-dependent reaction (Desterro et al., 1999) (Okuma et al., 1999). SUMO is then transferred from the E1 to Ubc9, the SUMO E2 enzyme, which then attaches the SUMO to a lysine in the target protein that is often found within the consensus sequence  $\Psi$ KXE ( $\Psi$  represents hydrophobic amino acids) (Johnson and Blobel, 1997) (Rodriguez et al., 2001). SUMO E3 proteins stimulate protein SUMOylation by associating it with both Ubc9 and substrate to increase the efficiency of the modification reaction (Geiss-Friedlander and Melchior, 2007). The SUMO E3 proteins identified so far include members of the protein inhibitor of

activated STAT (PIAS) family of proteins (PIAS1, PIAS3, PIAS  $\alpha$  and PIAS  $\gamma$ ) (Kahyo et al., 2001) (Takahashi et al., 2001), the polycomb protein 2 (Pc2) (Kagey et al., 2003), and Ran-binding protein 2 (RanBP2) (Pichler et al., 2002). SUMO groups are removed from proteins by the action of enzymes called SENPs, six of which exist in human cells (Mukhopadhyay and Dasso, 2007). SENP1 and SENP2 are able to remove all three SUMO polypeptides from modified proteins, whereas the other SENPs seem to be selective for SUMO-2 and SUMO-3. SENP1 and SENP2 also function as the C-terminal hydrolases described earlier. They catalyse the removal of short stretches of C-terminal residues from the SUMO proteins, which must occur before they can be conjugated to target proteins (Figure 9).

#### 1.4.2. SUMO E3 ligases

E3 ligases catalyse the transfer of ubiquitin or ubiquitin-related proteins from an E2 enzyme to a target lysine residue. Several structural studies on SUMO, but also on RING-type ubiquitin E3 ligases, provide insight into their function (Plechanovová et al., 2012a) (Reverter and Lima, 2005). E3 ligases mediate or stabilize the interaction of the target with the charged E2, and they lock the flexible Ubl~E2 thioester bond in an orientation that is favourable for nucleophilic attack by the target lysine. The largest family of SUMO E3 ligases is a group of SP-RING-containing proteins. Six members have been identified in humans so far: the protein inhibitor of activated STAT (PIAS) proteins, PIAS1, PIAS2 and its isoforms PIAS $\alpha$  and PIAS $\beta$ , PIAS3, PIAS  $\gamma$  and Nse2/Mms21 (Andrews et al., 2005). The SP-RING domain is required for Ubc9 interaction and flanking regions mediate the interaction with SUMO and specific targets. PIAS proteins are best known for their roles in transcriptional regulation. Many of these functions can be attributed to their E3 ligase activity, but others seem to depend on non-covalent interactions with SUMOylated proteins (Rytinki et al., 2009). A unifying theme among the SUMO E3 ligases is their ability to interact non-covalently with SUMO proteins via their SUMO Interacting motifs (SIMs), which appear to be required for the activity of select SUMO E3 ligases (Masclé et al., 2013).

An unrelated E3 ligase is the 358-kDa nucleoporin and Ran-binding protein 2: RanBP2, also known as Nup358 (Pichler et al., 2002). Its vertebrate-specific E3 ligase

region, which is natively unfolded, does not show any obvious homology to other known SUMO or ubiquitin E3 ligases. It is characterized by two 50 amino acid internal repeats (IR1 and IR2, which are 43% identical) separated by a 20 amino acid linker (M) (Figure 10). Both IR1 and IR2 can bind to Ubc9, and can catalyse sumoylation of model substrates *in vitro*. However, IR2 has significantly lower affinity for Ubc9 than IR1, and is much less effective in SUMOylation (Pichler et al., 2002) (Tatham et al., 2005). In addition, the RanBP2 E3 ligase region also has two SUMO binding sites: after IR1 in the direction of the N-terminal is a noncovalent SUMO-interaction motif (SIM), a short hydrophobic stretch flanked by acid residues (Kerscher, 2007). No SIM motif has been identified in M and IR2, but Tatham and coworkers (Tatham et al., 2005) found that M-IR2 interacts with SUMO-1 in pull-down assays.

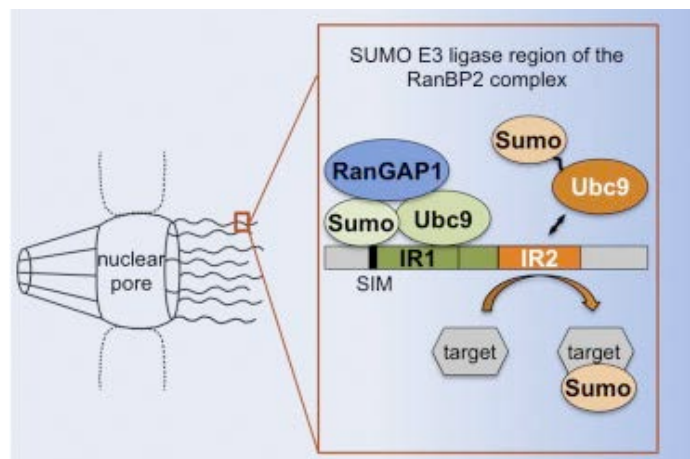


**Figure 10 - The RanBP2/RanGAP1\*SUMO1/Ubc9 complex is a multisubunit SUMO E3 ligase (Werner et al., 2012)**

*In vitro* activity requires only one of two closely spaced amino acid repeat regions that can both bind to Ubc9 and SUMO (Tatham et al., 2005). *In vivo*, however, RanBP2, SUMOylated RanGAP1, and Ubc9 form a stable isopeptidase-resistant complex that represents the functional and physiologically relevant multisubunits E3 ligase, named RanBP2/RanGAP\*SUMO1/Ubc9 complex (Werner et al., 2012). Intriguingly, this complex should interact with many proteins because binding sites for nuclear transport receptors and the GTPase Ran flank the E3 ligase core. These transport factors and their cargos could serve as SUMO targets during nucleocytoplasmic transport or mitosis, events in which RanBP2 E3 ligase activity

seems to be most relevant (Hamada et al., 2011). Several teams also showed how RanBP2 preferentially conjugates with SUMO-1 rather than SUMO-2 (Saitoh and Hinchey, 2000) (Hecker et al., 2006).

### 1.4.3. SENPs

The family of proteases that catalyse small ubiquitin-related modifier (SUMO) processing and deconjugation includes two ubiquitin-like protein-specific proteases in yeast (Ulp1 and Ulp2) and six sentrin-specific proteases (SENPs) in humans (SENP1-3 and SENP5-7).

SENPs can be divided into three families. The first family consists of SENP1 and SENP2, which have broad specificity for the three mammalian SUMOs (SUMO1–3). However, SENP1 displays a slight preference for processing SUMO1, whereas SENP2 couples better with SUMO2. The second family includes SENP3 and SENP5, which favour SUMO2/3 as substrates and are localized in the nucleolus. The third family contains SENP6 and SENP7, which have an additional loop inserted in the catalytic domain and also appear to preferentially deconjugate SUMO2/3 and SUMO chains. From an evolutionary standpoint, SENP1–3 and SENP5 are more closely related to Ulp1, whereas SENP6 and SENP7 are related to Ulp2 (Yeh, 2009).

Family members differ in their subcellular localization and can undergo changes in localization in a cell cycle-dependent manner (Gareau and Lima, 2010). SENP2 is located in the nuclear pore complex, whereas SENP1, SENP6 and SENP7 are present in the nucleoplasm and SENP3 and SENP5 are observed in the nucleolus.

### 1.4.4. SUMO-interacting motifs

A SUMO-interacting motif (SIM) is a short element sequence (less than 10 amino acids), that potentially includes phosphorylated amino acids; it is found in many proteins and interacts with a specific surface groove in small ubiquitin-like modifiers (SUMO) (Kerscher, 2007). Although the properties of all SIMs are similar, consensus sequences for given SUMO paralogues are only now beginning to emerge (Namanja et al., 2012). Most SIMs that have been identified so far have two important elements: a core of 3-4 hydrophobic residues (usually Val or Ile) and a nearby acidic region, which can be Glu or Asp side chains or phosphorylated Ser or Thr residues.

The hydrophobic residues of the SIM bind to the  $\beta 2$  strand of SUMO and extend the  $\beta$ -sheet of the  $\beta$ -grasp fold. The acidic residues bind a nearby basic patch on the SUMO surface, thereby reinforcing the interaction and orientation of the SIM (parallel or antiparallel to the  $\beta 2$  strand) (Song et al., 2005) (Hecker et al., 2006). Although the SIM is the best-studied motif that binds SUMO, a variant SUMO-binding motif has recently been described (Danielsen et al., 2012), and others are likely to be discovered in the future.

### 1.5. PML

The promyelocytic leukemia protein (PML) is a member of the tripartite motif (TRIM) family of proteins, which contain an N-terminal RBCC region, consisting of a RING domain, one or two B boxes (for PML), and a coiled-coil (CC) motif, followed by a variable C-terminal region. Many members of this family are ubiquitin ligases that generate subcellular structures through autoassembly (Reymond et al., 2001)(Meroni and Diez-Roux, 2005) (Figure 11).

SUMO was the first identified partner of PML in a two-hybrid screen (Boddy et al., 1996). PML directly interacts with Ubc9 (Duprez et al., 1999) and may be SUMOylated on three lysine residues: K65 in the RING domain, K160 in the B1 box and K490 in the coiled coil region. Moreover PML SUMOylation at K160 is essential for PML ability to recruit nuclear partners into NBs (Lallemand-Breitenbach et al., 2001). In addition, the SUMOylation state or the presence of a SUMO Interacting Motif (SIM) in partner proteins were proposed to be the major signals driving their recruitment into NBs (Lin et al., 2006) (Cho et al., 2009). Pandolfis team investigated the mechanisms of PML nuclear body formation (Shen et al., 2006), using *Pml*<sup>-/-</sup> mouse cells, because functional PML NBs can only be reconstituted by introducing wild-type (WT) not SUMOylation-deficient PML (Ishov et al., 1999) (Lallemand-Breitenbach et al., 2001). Thus, PMLs with the three lysines/K mutated into arginine/R were transfected into *Pml*<sup>-/-</sup> MEFs (mouse embryonic fibroblasts) with or without GFP-SUMO-1. Immunoprecipitation with anti GFP showed that PML mutated at 3K was still efficiently pulled down, implying that there is another non-covalent interaction between PML and SUMO. PML thus retained a SUMO binding domain that is independent of its SUMOylation sites. Another study has indeed

identified a SUMO-binding consensus sequence, VVVI (Song et al., 2004), in PML at amino acids 508-511. Mutation or deletion of this SUMO-interacting motif (SIM) in the 3K mutant abolished the ability of PML to bind GFP-SUMO-1. The sequence VVVI in PML was finally identified as the SIM required for non-covalent SUMO-1 binding (Shen et al., 2006).

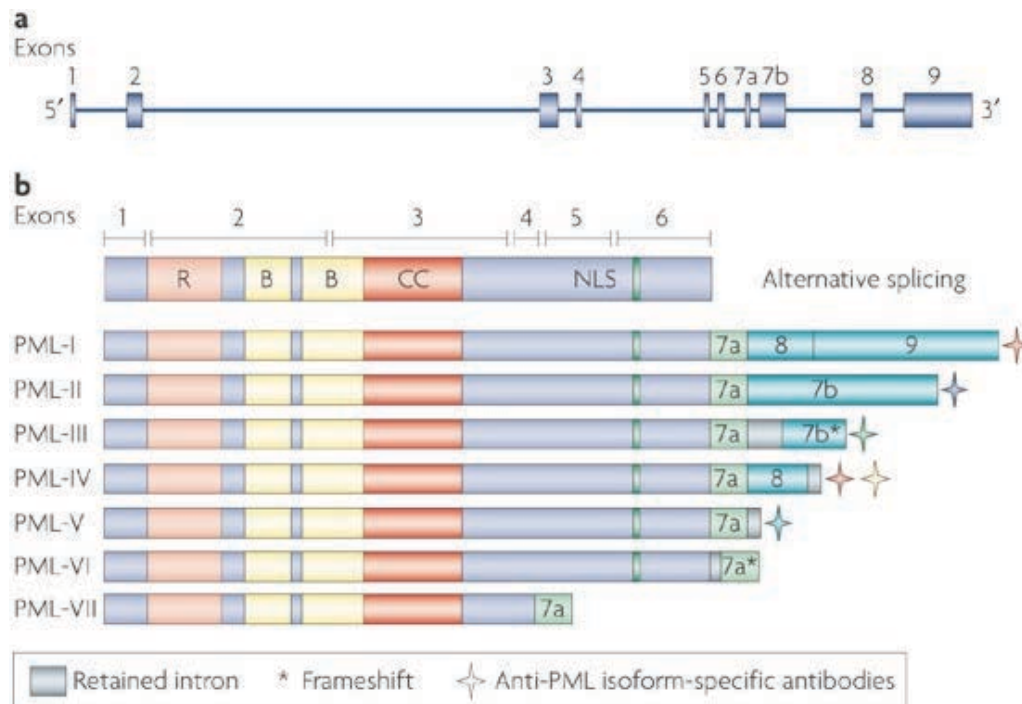


**Figure 11 - The PML gene and protein isoform**

The human promyelocytic leukaemia (*PML*) gene is located on chromosome 15q22. It spans ~53,000 bases and contains nine exons (see figure). Alternative splicing of C - terminal exons leads to the generation of several PML isoforms, some of which partially retain intronic sequences. Most PML isoforms show a predominantly nuclear localization because exon 6 contains a nuclear localization signal (NLS). However, alternative splicing of exons 4, 5 and 6 has been reported for many isoforms, making it possible that all PML isoforms exist in a cytoplasmic form. Indeed, cytoplasmic PML aggregates are often detected in some cell lines, although this does not necessarily reflect the expression of cytoplasmic PML as overexpressed nuclear PML can also show some cytoplasmic staining. All PML isoforms contain the first three exons, which encode the RBCC/TRIM motif. This is a tripartite structure that contains a zinc - finger called the RING motif (R), two additional zinc - finger motifs (B-boxes; B) and a coiled-coil domain (CC). The RBCC motif promotes homo - multimerization and the formation of macromolecular complexes. Variable C - terminal sequences in PML isoforms might create different binding interfaces and functional specificity. This has indeed been described for some isoforms: PML - IV induces premature senescence through p53 binding, promotes Myc destabilization and cellular differentiation and binds to and induces PU.1 - mediated transcription; PML - I binds the transcription factor AML1 to enhance AML1 - induced transcription; and PML - III interacts with the centrosome. Additionally, a cytoplasmic isoform of PML has been shown to regulate transforming growth factor -  $\beta$  signalling. Recently, isoform - specific PML antibodies (stars in the figure indicate different antibodies) have been generated, which will be of great use in exploring the function of specific PML isoforms as well as the structure of PML nuclear bodies (Bernardi and Pandolfi, 2007).

The same authors provided evidence that the mutation in the RING sequence (PMLcs) reduced its SUMO binding ability. Their data suggest, but do not prove, that the PML RING domain can also mediate SUMO binding. It is possible that the subtle structural changes caused by mutation of the RING domain may result in reduced SUMO binding. However, the authors also demonstrated that the PML RING-domain mutants fold properly and can dimerize with wild type PML, forming heterodimers. However, the PML RING domain is required for PML SUMOylation by SUMO-1, since mutation of the PML RING domain drastically decreases PML SUMOylation.

All these studies propose that the SUMO binding motif (SIM) contributes to interactions between PML and other SUMOylated proteins *in vivo*; the SUMO binding ability of the PML RING domain would mediate enzymatic activity such as the PML auto-SUMOylation or the SUMOylation of other proteins. Since the RING domain is essential for the activity of a class of SUMO E3 ligases (Seeler and Dejean, 2003), and since only PML with GFP-SUMO1 were overexpressed in *Pml*<sup>-/-</sup> MEFs, the authors speculated that PML acts as a SUMO E3 ligase that catalyzes self-SUMOylation (Shen et al., 2006). This is in agreement with a study in yeast showing that the PML RING domain was essential for PML self SUMOylation (Quimby et al., 2006).

### 1.5.1. PML Nuclear Bodies

The PML protein is the key organizer of PML Nuclear Bodies (NBs). PML NBs are implicated in multiple cellular process including virus-defence, apoptosis, and senescence. The nuclear structures are strongly associated with the SUMOylation process (Van Damme et al., 2010).

In mitosis, PML is found in aggregates or foci resulting from de-SUMOylation, subsequent disassembly of the PML NBs (Everett et al., 1999) and PML dimerization/multimerization mediated by its RBCC motif (Jensen et al., 2001). During interphase, once PML is SUMOylated, its SUMO binding motif (SIM) can mediate interactions with nearby SUMOylated PML molecules, hence allowing the formation of orderly PML networks (Figure 12). A large number of proteins, discovered to be associated with the PML NBs, are also SUMOylated or contain SUMO binding motifs. In particular, Daxx contains also a SIM (Lin et al., 2006) and Daxx SUMOylation is required to form mature NBs. It was proposed that many

SUMO-modified proteins are recruited to the PML networks to form higher-order protein structures such as the PML NB through non-covalent interactions mediated by covalently bound SUMO and SUMO binding motifs present in PML and other NB components (Shen et al., 2006).

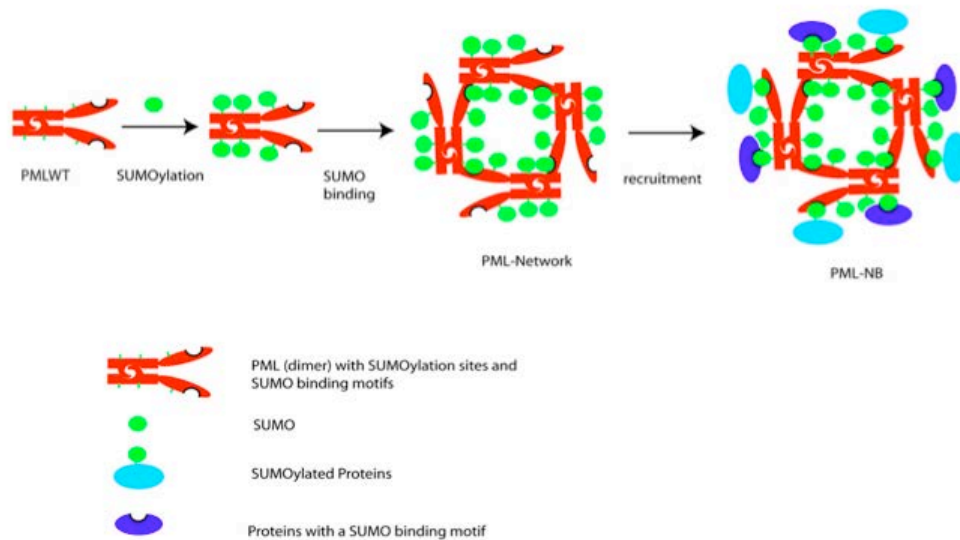


**Figure 12 - A model of PML-NB formation**

In mitosis, deSUMOylation of PML causes disassembly of PML-NBs. As a result, PML is in aggregate mediated by its RBCC motif (shown as a dimer). In interphase, PML is SUMOylated. Subsequently, the noncovalent interactions between two PML molecules mediated both by SUMO binding motif and RBCC motif promote the growth of concentrated PML networks, in which nuclear body proteins that are SUMOylated and/or contain SUMO binding motifs will be recruited through SUMO moieties and SUMO binding motifs that are amply provided by PML. Although, based on this model, it is not clear how the electron-dense core material in the center of the PML NB is packaged during the NB biogenesis (not shown in the model), it is likely that PML SUMOylation is associated with the packaging process and that the diameter of the NB is determined by the volume of the core material. Red rods, PML dimers; green circles, SUMO; light blue circle joined to green circle, SUMOylated proteins; and dark blue circle with indentation, proteins containing a SUMO binding motif (Shen et al., 2006).

### 1.5.2. Role of PML in the Nervous System

PML expression at the transcript level in the postnatal mouse brain is very low (Gray et al., 2004). In the developing brain, on the contrary, it is highly enriched in germinal areas (Regad et al., 2009). These include the ventricular zone of the neocortex, the hippocampus, and the cerebellum. In these regions, PML accumulates in both the nucleoplasm and PML-NB. Isoforms localized in the cytoplasm are not expressed in the developing brain, and only nuclear isoform 1 and 2 are readily detected. PML expression was absent from postmitotic cells in developing cortex, cerebellum, and hippocampus (Regad et al., 2009), with the exception of Purkinje

neurons. In adult mouse brains, PML becomes re-expressed in the cortex and hippocampus. PML is expressed in the adult human brain, in neurons of the substantia nigra (Woulfe et al., 2004) (Woulfe et al., 2007), supraoptic area (Villagra et al., 2006) and sensory ganglia (Villagr a et al., 2004). It is also highly expressed in terminally differentiated Purkinje cells, which are the cell type mostly affected in SCA. In particular, PML-NBs are often associated with intranuclear inclusions in both normal and pathological conditions. Early reports showed that PML is associated in cells with nuclear aggregates formed by mutant ataxin-1 (Klement et al., 1998a), ataxin-3 (Chai et al., 1999), and ataxin-7 (Kaytor et al., 1999). This association was later confirmed in samples from patients, for example, in SCA1 (Dovey et al., 2004) and also SCA7 (Takahashi et al., 2002). In normal control cases, ataxin-7 was found in cell bodies and in nuclei; neurons contained several (5-15) small PML-immunoreactive dots, which correspond to NBs. In SCA7 patients' brain, PML-positive NIIs were larger than normal NBs (> 1.0  $\mu\text{m}$ ). This could result from the accumulation of ataxin-7 and other proteins in the NBs (Takahashi et al., 2002). PML-immunopositive structures with a maximum size of 3.7  $\mu\text{m}$  were also detected in SCA2, SCA3, SCA7, SCA17 and DRPLA (Takahashi et al., 2003). Tissue from frontotemporal dementia patients contained ubiquitin nuclear inclusions associated with PML-NBs (Mackenzie et al., 2006). Colocalization with Marinesco bodies, another form of intranuclear inclusions, was also reported in non-degenerative conditions (Kumada et al., 2002). What then is the role of PML in intranuclear inclusions in neurodegenerative diseases?

PML-positive inclusions contain ubiquitin and in some cases proteasome subunits, thus suggesting that aberrant proteasomal function causes these aggregates. Alternatively, they could represent active sites of proteasomal degradation (Figure 13), as we showed in SCA7 and other polyglutamine disorders (Janer et al., 2006). In chapter 1.2.5, we presented the ongoing debate on whether inclusions positively or negatively affect the proteasome and, more generally, if alterations of the proteasome contribute to neurodegeneration in polyQ-associated diseases. A recent report has described a mechanism underlying PML and PML-NB degradation by the proteasome, which is dependent on an elevation of ROS levels leading to the formation of disulfide bonds and ubiquitin-dependent breakdown (Jeanne et al.,

2010) (Zhang et al., 2010). Cellular redox control is one of the potential mechanisms underlying the pathogenesis of polyQ-associated diseases (Imarisio et al., 2008), thus suggesting that formation of PML inclusions in dysfunctional neurons could be related to changes in ROS levels accompanied by impaired proteasomal functions.

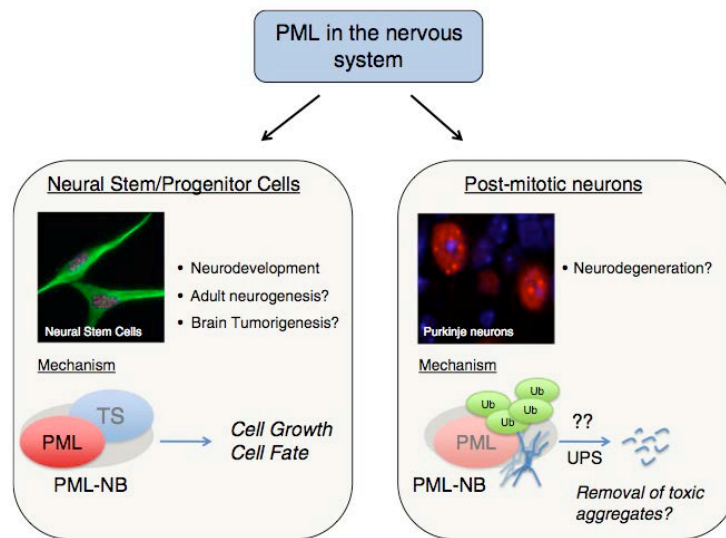


**Figure 13 - The role of PML in the Nervous System**

Within neural stem/progenitor cells NPC, PML interacts with and regulates other tumor suppressors (TS), thus mediating vital NPC functions such as proliferation. Within post-mitotic neurons, PML has been found associated with intranuclear inclusions of neurodegenerative diseases, suggesting it may play an important role in mediating degradation of aberrant proteins by the proteasome (Salomoni and Beth-Henderson, 2011).

More recently, PML NB was shown to regulate oxidative stress-responsive SUMOylation through cooperation between PML, Ubc9, and RNF4. In particular, NB biogenesis was shown to involve two distinct steps: an initial oxidation-sensitive PML multimerization and, subsequently, a polarized SIM-SUMO-dependent recruitment of partner proteins. PML NBs act as a cellular sensor, which aggregates upon oxidative stress, and globally enhances sensitivity to SUMOylation and other post-translational modifications, most likely of NB partners (Sahin et al., 2014).

### 1.5.3. Clastosomes

Clastosomes, a subset of PML bodies, contain components of the UPS and were suggested to be possible sites for protein degradation in the nucleus (Lafarga et al., 2002). They appear to be transient structures that assemble when proteolysis is highly active in the nucleus but disappear when the proteasome is inhibited (Lafarga et al., 2002). Our team has shown that clastosomes, and specifically PML isoform IV,

are actively involved in the clearance of mutant ataxin-7, via a recruitment of ataxin-7 into newly formed PML IV bodies, as demonstrated by time-lapse photography in a cellular model in which PML IV was overexpressed (Janer et al., 2006). Soluble mutant ataxin-7 is thus directed towards a structure, the clastosome enriched in proteasomes, in which mutant ataxin-7 can be degraded. As a consequence, insoluble SDS resistant intranuclear inclusions are also cleared. Interaction between ataxin-7 and PML IV was demonstrated by co-immunoprecipitation. We showed that PML III isoform was not able to degrade mutant ataxin-7, and the PML bodies obtained by expression of PML III did not colocalize with accumulated ataxin-7 aggregates in the nucleus, thus demonstrating the isoform-specificity of clastosomes. Using different doses of cadmium chloride to alter the amount of endogenous PML bodies in cells expressing mutant ataxin-7, we demonstrated that aggregation of mutant ataxin-7 was dependent on the absence or presence of PML bodies, as shown by filter assay, suggesting that endogenous clastosomes are indeed involved in the degradation of mutant ataxin-7. Finally because  $\beta$ -IFN was reported to up-regulate the expression of PML (Regad and Chelbi-Alix, 2001), we investigated its effect on the PML-dependent degradation of mutant ataxin-7.  $\beta$ -IFN treatment led to the formation of large, strongly immunoreactive PML bodies that colocalized with mutant ataxin-7. Accordingly, degradation of overexpressed mutant ataxin-7 or normal ataxin-7 was observed; interestingly, the level of endogenous ataxin-7 was unaffected. This latter result suggested that  $\beta$ -IFN might have therapeutic value (Janer et al., 2006).

To follow-up on this study, the next step was to investigate whether interferon beta is similarly protective in a preclinical model of SCA7, the SCA7<sup>266Q/5Q</sup> knock-in mouse (Yoo et al., 2003). Endogenous interferon beta was detected in the wild-type mice, but its expression was significantly higher in the SCA7 knock-in mice, indicating that expression of mutant ataxin-7 itself induces expression of the cytokine, perhaps as a defensive response to the disease state. Interferon beta, administered intraperitoneally three times a week in the knock-in mice, was internalized with its receptor in Purkinje cells. These results show that exogenous interferon beta crosses the blood-brain barrier in treated mice and upregulates the expression of its receptor, a known interferon-responsive gene. To determine whether interferon beta

treatment had a deleterious effect on Purkinje cell morphology, we also analysed sections of the cerebellum with an antibody against the Purkinje cell marker calbindin. We did not detect any difference in cell morphology between interferon beta and MSA-treated mice. There was also no reactive gliosis in the interferon-treated SCA7 KI mice compared to MSA-treated controls, as shown by the labelling of the astrocyte marker glial fibrillary acidic protein (GFAP) and the macrophage/microglia marker Iba1. The treatment reduced neuronal intranuclear inclusions composed by insoluble mutant ataxin-7, the hallmark of the disease. The decrease in mutant ataxin-7 was related to increased PML protein expression and the formation of PML protein nuclear bodies by interferon beta treatment. Immunohistochemical analysis of cerebellar section with an antibody against PML revealed an increase in PML immunoreactivity in the molecular, Purkinje cell and granule cell layers of the cerebellum, notably in the nuclei, in interferon beta-treated mice compared with the MSA-treated animals. The performance of the SCA7<sup>266Q/5Q</sup> knock-in mice was significantly improved on two behavioural tests sensitive to cerebellar function: the Locotronic<sup>®</sup> Locomotor Test and the Beam Walking Test. Quite importantly, interferon beta induces PML-dependent protein degradation, which is the physiological mechanism involved in clearance of the mutant protein in SCA7. This decreases the burden of the mutant protein in Purkinje and other cells and improves cerebellum-related motor function. Although, this is probably not the only effect of the cytokine, the treatment might be effective in patients with SCA7, alone or in conjunction with other treatments aimed at preventing accumulation of the mutant protein or enhancing its degradation, such as the substances cited above or gene silencing techniques, all of which were active against polyglutamine proteins (Chort et al., 2013).

The ability of PML to modulate the degradation of mutant proteins, for example by enhancing its transcription, suggests it plays a protective role against neurodegeneration. As a result, PML loss in neurodegeneration-prone animal models should result in aggravation of the phenotype. In this regard, a very recent paper shows how PML deficiency exacerbates behavioural and pathological phenotypes in the BO5 mouse model of SCA1 (Guo et al., 2014). PML deficiency or *Atxn1* 82Q transgene expression alone was insufficient to cause motor defects at 7

weeks of age. But interestingly, performance on the Rotarod of *Pml*<sup>-/-</sup>: *Atxn1tg*<sup>-/-</sup> mice was severely impaired compared to either *PML*<sup>+/+</sup>: *Atxn1tg*<sup>-/-</sup> or *Pml*<sup>-/-</sup> mice. Moreover, a PML deficiency significantly increased the number of aggregate-containing Purkinje cells in Atxn1 82Q transgenic mice (Guo et al., 2014). These results suggest that endogenous PML plays a role in preventing the accumulation of misfolded proteins in SCA1 animals and in suppressing the progression of this neurodegenerative disease.

## 1.6. RNF4 – E3 Ubiquitin ligase

The 2004 Nobel Prize in Chemistry was awarded to Avram Hershko, Aaron Ciechanover and Irwin Rose for the discovery of the functions of a small (76-residue), ubiquitous, eukaryotic cellular protein that was given the name **ubiquitin**. These laureates, along with others, found that ubiquitin is covalently attached to target proteins to signal their subsequent degradation by a multicompartimentalized protease called the 26S proteasome (Glickman and Ciechanover, 2002).

Ubiquitin is activated in an ATP-dependent manner by an ubiquitin-activating enzyme known as an enzyme-1 (E1), and it is transferred to an ubiquitin-conjugating enzyme (E2). The latter, with the help of an ubiquitin-protein ligase (E3), specifically attaches ubiquitin to a target protein through the ε-amino group of a lysine residue. The ubiquitin chain is lengthened by the E2 and E3, sometimes with the help of an accessory factor (E4) (Koegl et al., 1999), to at least four sequentially attached ubiquitins, which is sufficient to allow the ubiquitylated target protein to be recognized and degraded by the 26S proteasome. Finally, there is a mechanism of considerable physiological and pathological importance, in which deubiquitylating enzymes can remove ubiquitins.

There are two broad classes of ubiquitin E3 ligases: ‘homologous to E6-AP C terminus’ (HECT) ligases and ‘really interesting new gene’ (RING) ligases (Deshaies and Joazeiro, 2009). HECT-type ubiquitin E3 ligases contain a catalytic cysteine residue that forms a thioester intermediate with ubiquitin before the final transfer. RING E3 ligases do not form a covalent intermediate, but catalyze direct transfer of ubiquitin from the E2~Ub thioester to a substrate. RING proteins contain a

conserved arrangement of cysteine and histidine residues that coordinate two zinc atoms and cross-brace the folded structure.

SUMO-targeted ubiquitin ligases (STUbLs) are a conserved family of proteins that target SUMO-modified proteins for ubiquitylation (Perry et al., 2008) (Uzunova et al., 2007), as typified by RING finger protein 4 (RNF4) in mammals. STUbLs contain multiple SUMO-interaction motifs (SIMs) allowing them to specifically recognize poly-SUMO chains (Song et al., 2004) (Hecker et al., 2006) (Song et al., 2005) and a RING domain. SIMs are short peptide motifs that can be classified as SIMa, SIMb or SIMr according to their exact amino acid sequence (Keusekotten et al., 2014). Structurally the SIM motif was shown to adopt a short  $\beta$  strand structure that inserts into a hydrophobic groove formed between a  $\beta$  strand and an  $\alpha$  helix in SUMO (Song et al., 2005). In a number of proteins, including components of PML nuclear bodies, like PML itself, Sp100 or the E3 SUMO ligase PIAS1, it appears that a stretch of negatively charged amino acids flanking the hydrophobic core of the SIM enhances their affinity for SUMO (Hecker et al., 2006). One function of SUMO-targeted ubiquitin ligases or ubiquitin ligases (E3) is to mediate their target degradation by the proteasome.

To date the most studied STUbL is probably RNF4. It possesses both ubiquitin E3 ligase activity and 4 SIM motifs (Sun et al., 2007) and can itself be SUMOylated and polyubiquitylated. Whereas in yeast (Slx5-Slx8) function as heterodimers, the human homologue RNF4 functions as a homodimer: the RING from the two subunits make contact with a single ubiquitin-charged E2 (Liew et al., 2010) (Plechanovová et al., 2011) (Plechanovová et al., 2012b).

In cells under normal growth conditions SUMO chains are maintained at low levels. During stress responses such as DNA damage, arsenic treatment or heat shock, SUMO chains accumulate and it was predicted that they activate RNF4.

PML was identified as a first physiological substrate of RNF4 : the STUbL promotes ubiquitylation of SUMOylated PML *in vitro* and disrupts PML nuclear bodies (PML-NBs) in cells treated with arsenic trioxide (Weisshaar et al., 2008). In the case of arsenic trioxide treatment, SUMO chains are formed on PML protein present in nuclear bodies, and RNF4 is rapidly recruited to these sites in a SIM-dependent

RING-independent fashion (Tatham et al., 2008) (Lallemand-Breitenbach et al., 2008), (Geoffroy et al., 2010). PolySUMOylated PML is the target of RNF4, which, after dimerization through its RING domain, catalyzes the addition of poly-ubiquitin chains onto PML, which is subsequently degraded via the proteasome.

### 1.6.1. RNF4 RING domain is sufficient for ubiquitylation activity.

The RNF4 C-terminal RING domain is required for ubiquitin E3 ligase activity, whereas four tandem SIMs located in the N-terminal region provide binding specificity for its substrate (Keusekotten et al., 2014), poly-SUMO chains (Figure 14). RNF4 is capable of autoubiquitylation and attaches ubiquitin to its internal lysine residues. The isolated RING domain of RNF4 is active in autoubiquitylation, confirming that the RING domain is sufficient for ubiquitin transfer. However, it was unable to ubiquitylate poly-SUMO2 chains (Plechanovová et al., 2011).

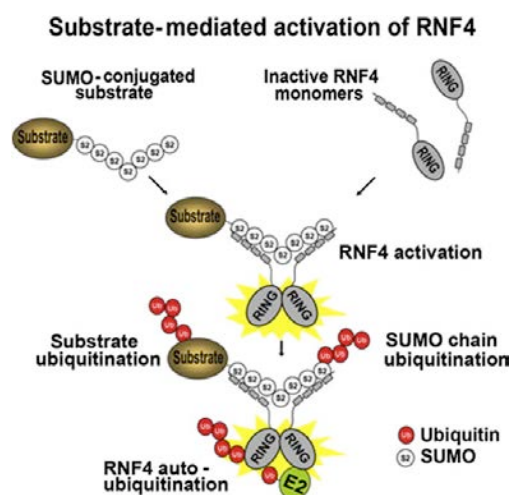


**Figure 14 - Model of RNF4 activation by polySUMO chains**

STUbL RNF4 is predominantly monomeric and inactive in the absence of its poly-SUMO substrate. However, cellular accumulation of SUMO chains serves to recruit monomeric RNF4, creating a locally high concentration that allows the RING dimerization and activation of ubiquitylation activity (Rojas-Fernandez et al., 2014).

In 2010, Tony Hunter's team generated a number of point mutation in different residues to identify features of the RNF4 RING domain (Liew et al., 2010). They identified three residues (Met<sup>140</sup>, Asp<sup>141</sup> and Arg<sup>181</sup>) in the RING domain, which are predicted to contact with the E2 UbCh5b and favour ubiquitylation of target protein. The second set of mutants was focused on understanding the role of the C-terminal residues that they were required for the biological activity of RNF4 (Sun et al., 2007).

Lastly, they also made mutations that are expected to disrupt dimerization, but not affect the C-terminal tail (V161A, V134A/E, I153A/E, S155A/E). Their studies showed that disruption of either E2 recruitment or RING dimerization inactivates the E3-ligase activity of RNF4: analysis of mutant RNF4 proteins suggests that RING dimerization destabilizes the E2-ubiquitin conjugate so that ubiquitin transfer is favoured. Moreover, the C-terminal domain may have another role, because the monomeric mutants that disrupt the dimer interface (but have a wild type C-terminus) retain some, albeit low *in vitro* activity, but those that disrupt the C-terminal residues are inactive (Liew et al., 2010). A full understanding of the role played by the C-terminus is still missing. But this observation is consistent with analysis of the RING domains from MDM2 and MDMX, which showed that mutation of the C-terminal residues disrupted ubiquitylation of the substrate, p53, but not MDM oligomerization (Uldrijan et al., 2007).

#### 1.6.2. The guardians of the nucleus: PML, SUMO and RNF4

Very recently, Guo and co-authors followed the fate of the aggregation-prone mutant polyQ ataxin-1 with 82Q and Htt97Q as well as misfolded model substrates that do not belong to the polyQ type. They presented a clearance pathway for nuclear misfolded protein where PML, SUMO and RNF4 have a very coordinated role. The model presents PML as a SUMO E3 ligase that promotes the attachment of polymeric SUMO chains to the target proteins. SUMO2/SUMO3 chains subsequently serve as a docking site for RNF4, which finally catalyzes misfolded protein degradation by adding a poly-ubiquitin tag, thus marking it for proteasomal degradation (Guo et al., 2014). This is indeed of physiological significance, as in a mouse model for SCA1 in which loss of PML was genetically induced, the neurodegenerative phenotype was more severe.

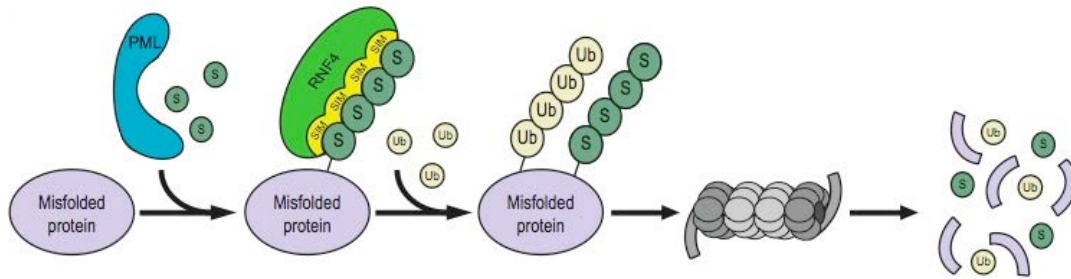


**Figure 15 Recognition and Clearance of Misfolded Protein by the concerted action of PML, SUMO, and RNF4**

Nuclear misfolded proteins are selectively recognized by PML and marked with poly-SUMO2/3 chains. RNF4, which is a SUMO-dependent E3 ubiquitin ligase, binds to the poly-SUMO2/3 chains via tandem SUMO interacting motifs (SIM) and ubiquitylates the protein, which leads to its proteasomal degradation (Gartner and Muller, 2014).

A conceptual question emerges as to the reason why cells use a two-step, SUMO-primed pathway for ubiquitylation and clearance of misfolded proteins rather than triggering their ubiquitylation directly. One might hypothesize that it aims at adding an additional regulatory layer to the protein quality control pathway of damaged proteins in mammalian, but also yeast cells. Conjugation of SUMO-1 and SUMO-2 in their monomeric form may also allow the recruitment of factors that facilitate refolding or disassembly of polyglutamine-containing aggregates. In that case SUMOylation may not necessarily lead to the removal of the protein.

Finally, the additional regulatory layer of protein quality control by the SUMOylation pathway could represent an option for therapeutic intervention: stimulating the attachment of SUMO2/SUMO3 to a misfolded protein should foster its removal (Gärtner and Muller, 2014). It remains a challenging task since, according to the disease, enhanced SUMO-2 modification proves to be beneficial for SCA7 (our work, presented in this manuscript) and SCA1 (Guo et al., 2014), but caused an increase in insoluble mutant huntingtin possibly due to impairment of the downstream clearance machinery (O'Rourke et al., 2013).



## 2. Aims of this work

How does the cell promote degradation of nuclear proteins that accumulate? Our team showed the importance of two molecular pathways: one by SUMOylation, a post-translational modification, which is able to influence ataxin-7 protein aggregation and toxicity. Another is the clearance of mutant ataxin-7 in a subpopulation of PML nuclear bodies, clastosomes, involving the UPS. The two pathways might act together, possibly via SUMO-2, which is known to target proteins for degradation.

Two series of experiments will be presented. The first were performed to increase our knowledge of the impact of SUMOylation, and how it influences the function of the ataxin-7 protein in normal (10Q) and pathological expanded (92Q) proteins. SUMOylation regulates the molecular interactions of the modified proteins leading to changes in solubility or even stability of the respective target proteins. I will show that endogenous ataxin-7 is a target for both SUMO-1 and SUMO-2. I propose that RanBP2 is the main SUMO E3 ligase for ataxin-7, via SUMO-1 the known partner of RanBP2. When SUMO-2 is overexpressed together with RNF4 we will observe a reduction in the concentrations of soluble and insoluble mutant ataxin-7 protein, and thus propose that RNF4 mediates the polyubiquitination and subsequent proteasomal degradation of mutant ataxin-7.

The second series of experiments was performed in *Atn7<sup>100Q/5Q</sup>* knock-in mice. We will evaluate the expression levels of SUMO-1 and 2 and those of enzymes involved in SUMOylation, conjugation and de-sumoylation by quantitative RT-PCR. We will also use immunohistochemistry in a late stage of their disease to correlate SUMO-related gene expression patterns with alterations in protein expression related to presence of mutant ataxin-7. We will conclude that SUMOylation is globally impaired in this SCA7 mouse model compared to wild type littermates, suggesting that this pathway is deregulated *in vivo*.



# 3. Results

## 3.1. Identification of a new interaction between ataxin-7 and SUMO-2

### 3.1.1. Ataxin-7 is modified by both SUMO-1 and SUMO-2

Our team previously demonstrated that full-length normal ataxin-7 is SUMOylated by SUMO-1 on Lys257 in cells overexpressing ATXN7-10Q by mutagenesis of the target lysine (Janer et al., 2010). We also showed by *in vitro* SUMOylation that ATXN7-10Q could be modified by SUMO-2; in addition to unmodified ataxin-7 bands, bands of higher molecular weight were detected on western blot.

To determine whether SUMO-1 or SUMO-2 was attached preferentially to normal or mutant ataxin-7, we examined SUMOylation in HeLa and COS-7 cell models, in which we overexpressed normal ATXN7-10Q and polyQ-expanded ATXN7-92Q, with or without SUMO-1 or SUMO-2.

When ATXN7-10Q and SUMO-1 were co-expressed for 48 hrs, we detected, on western blots of total extracts with an anti-ataxin-7 polyclonal antibody, the presence of a modified band at approximately 120 kDa, corresponding to the 15-20 kDa expected shift due to the addition of SUMO-1 to unmodified ataxin-7 (Figure 16-A). We also observed a decrease in the amount of soluble unmodified ataxin-7 (Figure 16-A, right panel). When ATXN7-10Q and SUMO-2 were co-expressed, the same band shift, corresponding to the addition of one SUMO-2 residue, was observed. In addition, there was a faint band above this modified band, which can be attributed to the conjugation of two SUMO-2 residues. PolySUMOylated bands were technically difficult to detect, probably due to their low abundance. The unmodified ataxin-7 band was more intense in the absence of SUMO-1 than when SUMO-1 was expressed, possibly due to protein degradation in the presence of SUMO-1 or to downregulation of its expression via SUMO-1. Using anti HA antibody we detected free SUMO-1 and free SUMO-2 around 18 kDa. In some other experiments, we

showed that free SUMO-2 is more abundant than free SUMO-1 (Figure 18-B), in agreement with the fact that SUMO-1 is usually conjugated to substrates in cells rather than free in the nucleoplasm (Saitoh and Hinchey, 2000).

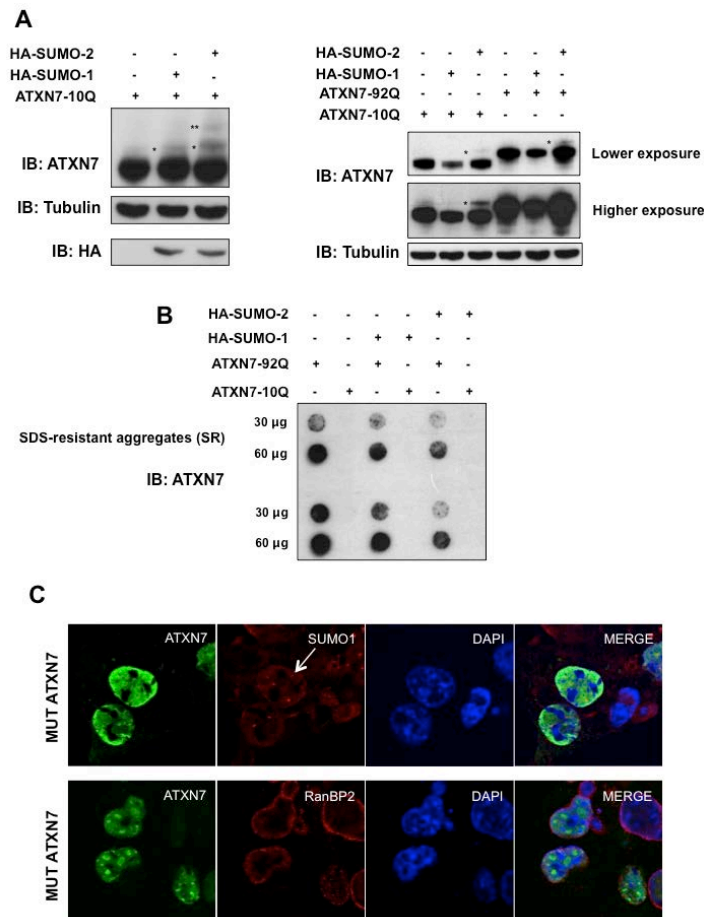


**Figure 16 – Ataxin-7 is modified by SUMO-1 and SUMO-2: SUMO-2 attenuates the propensity of expanded polyQ ataxin-7 to aggregate**

(A) HA-SUMO-1 and HA SUMO-2 were transfected into HeLa (left panel) and COS-7 (right panel) cells in combination with either ATXN7-10Q or ATXN7-92Q. Expression of SUMO-1 and ATXN7-10Q leads to the appearance of a band above unmodified ataxin-7 corresponding to ataxin-7 conjugated with one SUMO-1 residue (\*). Co-expression of SUMO-2 gives rise to 2 bands resulting from conjugation of one (\*) or two (\*\*\*) SUMO residues. Expression of SUMO-2 and ATXN7-92Q led to SUMO-2 conjugation (\*) of mutant ataxin-7; due to the abnormal migration of polyQ-containing proteins, the separation between unmodified and SUMO-2-conjugated ATXN7-92Q is difficult. Total extracts (40 µg) were analysed on 4-12% gels (left panel) and on 4-20% gels (right panel). Tubulin was used as loading control. SUMO-1 and SUMO-2 were detected with anti-HA tag antibody. (B) Filter retardation assay from two experiments are presented, one from lysates in the right panel (A) and a second from another (not shown), to detect SDS-resistant aggregates (SR); 30 and 60 µg of total extract were analysed; ataxin-7 was detected with a polyclonal anti-ataxin-7 antibody. ATXN7-10Q did not form aggregates. ATXN7-92Q aggregation was concentration dependent. SUMO-1-conjugated ataxin-7 aggregated less than polyQ ataxin-7 expressed alone; SUMO-2 had a greater effect. (C) Immunofluorescence of COS-7 cells 40 h after transfection with ATXN7-92Q. Endogenous SUMO-1 and RanBP2 expression were analysed. Mutant ataxin-7 labelling in nuclei was either strong but diffuse (upper panel) or aggregated (lower panel). The number and size of aggregates varied on the amount of ataxin-7 accumulated. Endogenous SUMO-1 labelling was in dots (possibly nuclear bodies) in the nucleus and at the nuclear membrane corresponding to the presence of RanBP2 in complex with RanGAP1. Labelling with anti-RanBP2 antibody (lower panel) showed the characteristic nuclear rim staining of endogenous RanBP2.

When ATXN7-92Q and SUMO-1 were co-expressed, the shift of the SUMO-1-modified band was difficult to separate from the unmodified ATXN7-92Q band, especially as the polyQ species accumulated strongly in cells over 48h. The use of 4-12% gradient gels permitted visualization of both free SUMO species in transfected cells and full-length polyQ-containing ataxin-7 that migrates at 140 kDa. The expression of HA-SUMO-1 and 2 species was verified as above. When SUMO-2 was co-expressed, we detected higher molecular weight bands above the unmodified polyQ-ataxin-7. The smear, in which the bands were detected, corresponded most probably to poly-SUMOylated ataxin-7. The levels of soluble unmodified polyQ-ataxin-7 was slightly reduced by overexpression of SUMO-1, but not by SUMO-2, again indicating that modification of ataxin-7 by these two isoforms are different.

To investigate the potential of SUMO-2 and SUMO-1 to degrade SDS-insoluble ATXN7-92Q aggregates, we analyzed the samples by filter retardation assay, which permits separation of inclusions or aggregates from soluble mutant ataxin-7 by boiling in the presence of SDS and DTT and filtration through a 0.2  $\mu$ m pore cellulose acetate membrane. The retained material, corresponding to SDS-resistant or insoluble ataxin-7, was detected with the anti-ataxin-7 antibody, as for western blots. Using this technique, we observed a decrease in ATXN7-92Q aggregates after overexpression of SUMO-1 for 48h, compared to cells transfected only with mutant ataxin-7 and an empty vector (pcDNA3). In the presence of SUMO-2, a much stronger decrease by 50% in poly-Q-containing aggregates was observed (Figure 16-B) compared to mutant ataxin-7 expression alone.

These results show that SUMO-2 conjugation to ataxin-7 reduces its aggregation to a greater extent than SUMO-1. We have demonstrated in cell models that mutant ataxin-7 modification by SUMO-2, a stress-responsive modification pathway not previously investigated for SCA7, regulates the accumulation of insoluble mutant ataxin-7.

To analyse the sub-cellular localization of mutant ataxin-7 and endogenous SUMO-1, we seeded COS7 on cover slips and transfected them with ATXN7-92Q to subsequently perform immunofluorescence. Two pattern of staining were observed (Figure 16-C): in the upper panel, a strong but rather uniform nuclear staining was present before the formation of aggregates of mutant ataxin-7. On the contrary in

the lower panel, three cells in which aggregates had formed can be seen: ataxin-7 staining was in the nucleus but there were additional dots with more intense staining by the ataxin-7 antibody. The presence of these nuclear inclusions confirms that mutant ataxin7 is able to aggregate in the nucleus. The number and size of aggregates varies depending upon the amount of ataxin-7 accumulated in each cell. The staining pattern of endogenous SUMO-1 was also nuclear with a few intense dots. It was also present around the nuclear rim; this was expected since highly SUMOylated RanGAP and RanBP2, a SUMO E3 ligase, are a part of the nuclear pore complex at the nuclear rim. The SUMO-1-positive dots may correspond to nuclear bodies. The lower panel shows the characteristic staining of RanBP2 at the nuclear rim: the SUMOylation pathway, in fact, is implicated in the shuttling of target proteins from the cytoplasm to the nucleus (Kirsh et al., 2002)(Salinas et al., 2004).

### 3.1.2. Endogenous ataxin-7 is a target of SUMO-1 and SUMO-2

Usually only a small fraction, up to 2-3% of a given protein in the cellular pool is SUMOylated at steady state (Hay, 2005). Consequently, SUMOylated targets are difficult to detect, especially when the unmodified proteins are present in low abundance. Furthermore, SUMOylation is easily lost during nondenaturing lysis, because SUMO isopeptidases remain highly active in many buffer conditions. The group of Frauke Melchior recently developed a method for the specific enrichment of endogenous SUMO-1 and SUMO-2/3-modified proteins based on denaturing lysis of biological material, immunoprecipitation with monoclonal antibodies recognizing SUMO-1 or SUMO-2/3, and specific elution of SUMO targets (Barysch et al., 2014). We used this technique to gain insight into the regulation and role of SUMOylation of endogenous ataxin-7. We undertook a denaturing immunoprecipitation in MCF7 cells to examine endogenously SUMOylated ataxin-7. This method allows the enrichment of endogenous SUMO targets. The experiments were performed in MCF7 cells as they contain higher levels of endogenous ataxin-7 than COS-7 or HeLa cells. The experiment was performed in the laboratory of F. Melchior. We processed MCF7 lysates further by fragmenting DNA by sonication and reducing disulfide bonds by boiling the sample in DTT followed by dilution in RIPA buffer conditions ensures that the initial SDS concentration does not interfere with the SUMO immunoprecipitation. To immunoprecipitate SUMOylated ataxin-7, we incubated

the input material with antibody-coupled beads at 4°C overnight then eluted SUMO conjugates with an excess of epitope-spanning peptides to ensure specificity: one pre-elution step (incubation without peptide) followed by two-elution steps (incubation with epitope-spanning peptide). To facilitate detection of endogenous ataxin-7, we precipitated the eluted protein with trichloroacetic acid (TCA) precipitation.

The results presented in Figure 17-A show that after elution with a peptide competing with SUMO-2 we detected the presence of a band slightly above the band corresponding to unmodified endogenous ataxin-7, with a polyclonal antibody raised against ataxin-7. The absence of this band in the control IP, and its intensity in the SUMO-2 eluate, strongly suggests that endogenous ataxin-7 is modified by SUMO-2. Similarly, we detected a less intense band after elution with a peptide competing for SUMO-1. Thus endogenous ataxin-7 is a target for both SUMO-1 and SUMO-2, with a preference for SUMO-2 because SUMO-2-conjugated beads captured more ataxin-7. SUMOylated RanGAP1, well known SUMO-1 target was used as a positive control for the immunoprecipitation. This result is coherent with the results of the above-described experiments showing that overexpressed ataxin-7 is preferentially modified by isoform 2 of SUMO.

While performing the SUMO immunoprecipitation experiments, we performed SUMO controls blots of samples termed “input”, “flow-through”, “pre-elution wash” and “eluate” to verify the successful completion of the protocol. These experiments confirmed that SUMO-1 and -2 were present in the control blot; in addition a band corresponding to SUMOylated RanGAP1 was detected in the immunoblot revealed with SUMO-1 (Figure 17-A).

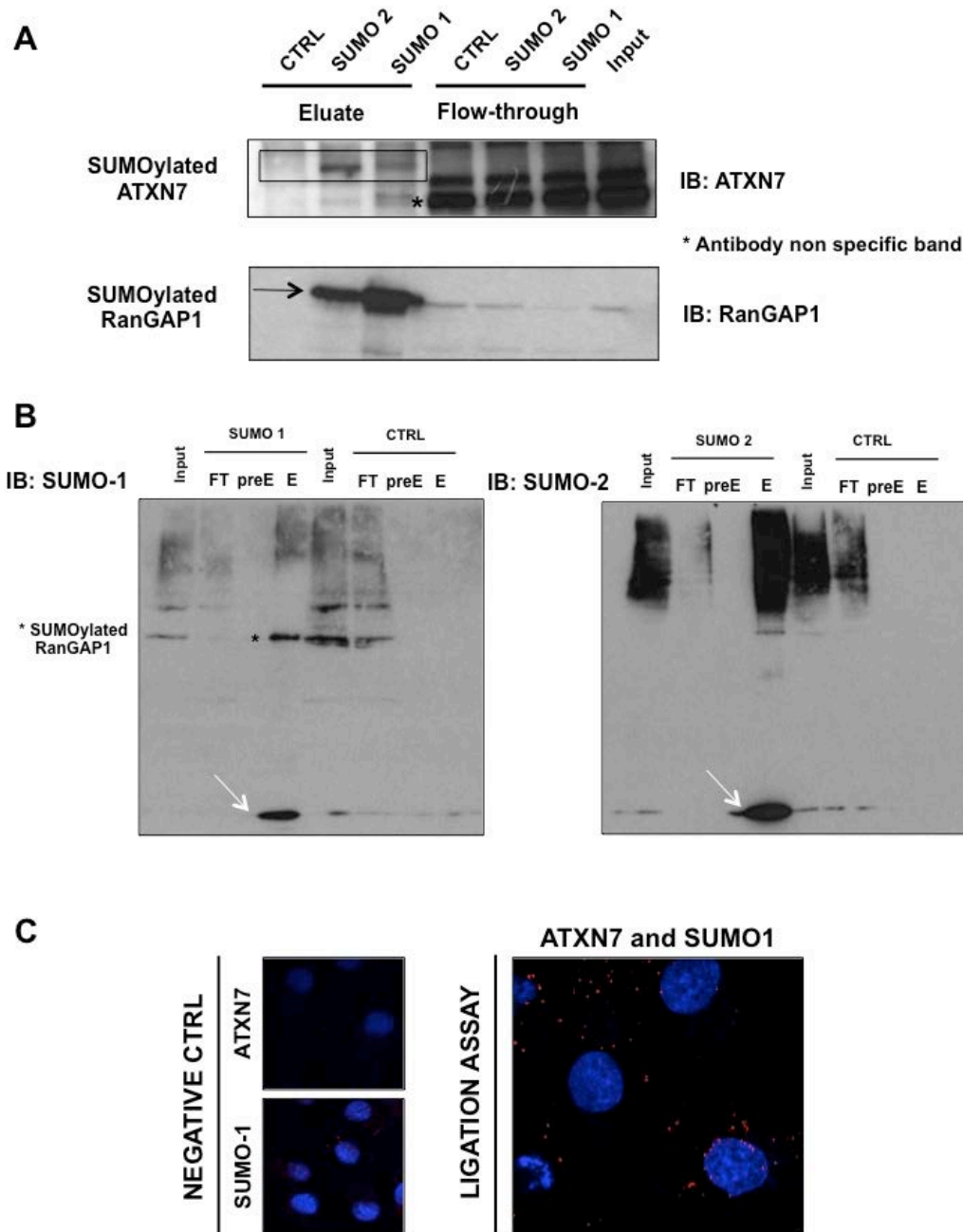


**Figure 17 - Endogenous ataxin-7 is a SUMO-1 and SUMO-2 target in MCF7 cells as shown by immunoprecipitation**

(A) Immunoblots of ataxin-7 and RanGAP1 showing the SUMOylation of ataxin-7 and RanGAP1 immunoprecipitated by antibodies against SUMO-1 (ab 21C7) and SUMO-2 (ab 8A2) and eluted with epitope-containing peptides or control peptides; IgG is the negative control; RanGAP1 immunoprecipitation is the positive control; SUMO-modified ataxin-7 is boxed. (B) Positive controls for SUMO immunoprecipitation: arrows indicate eluted free SUMO-1, free SUMO-2 and SUMOylated RanGAP1. CTRL, control; FT, flow-through; preE, pre-elution wash; E, eluate. IB, immunoblot. Asterisk (\*) non-specific band. (C) Proximity ligation assay (PLA) to show proximity (<40 nm) between endogenous SUMO-1 and ataxin-7 (red dots) performed with monoclonal anti-1C1 (ataxin-7) and polyclonal anti-SUMO-1 antibodies. Secondary antibodies were labelled with specific oligonucleotides that were hybridized, ligated, amplified before detection. Red fluorescent dots attest that SUMO-1 and ataxin-7 are very close or interact; red dots along the nuclear membrane show endogenous ataxin-7 modified by SUMO-1 or interacting with another SUMO-1-positive protein, such as RanGAP1, a partner of RanBP2 in the nuclear complex. Negative controls: anti-1C1 or anti-SUMO-1 alone do not generate a signal.

To confirm that endogenous ataxin-7 is indeed SUMOylated, we investigated the modification of ataxin-7 by proximity ligation assay (PLA). Also known as Duolink *in situ*, this technique is based on a pair of oligonucleotide labeled secondary antibodies (PLA probes) that generates a signal only when the two PLA probes are bound in close proximity (< 40 nm). The signal from each detected pair of PLA probes is visualized as an individual red fluorescent spot. As shown in Figure 17-C, endogenous ataxin-7 and endogenous SUMO-1 were recognized by their respective antibodies: the close proximity of these two proteins leads to an interaction between DNA strands and amplification of the DNA by a polymerase. The red fluorescent spots confirm the interaction between these two proteins; particularly noteworthy is the presence of positive red dots around the nuclear membrane. This result reinforces our hypothesis that ataxin-7 is SUMOylated at the nuclear rim by RanBP2 that we suggest to be the major SUMO E3 ligase for ataxin-7. To properly evaluate our results, we included negative controls by omission of ataxin-7 or SUMO-1 antibodies, respectively. In absence of one primary antibody, the two PLA probes will not be able to bind together. The negative controls show that the red fluorescent spots that we detected are due to a real proximity between endogenous ataxin-7 and SUMO-1. Thus endogenous ataxin-7 is either modified by SUMO-1, or interacts with another protein that is SUMO-1 positive, like RanGAP, which is known to interact with RanBP2.

### 3.1.3. RanBP2 is the main SUMO E3 ligase for modification of ataxin-7 by SUMO-1.

Potential interactions between ataxin-7 and an E3 SUMO ligase were first investigated by *in vitro* SUMOylation assay in the presence of recombinant enzymes. The obtained results suggested that RanBP2 was a major candidate for conjugation of SUMO to ataxin-7 (Janer et al., 2010). RanBP2 is a protein that is part of the nuclear pore complex and has been implicated in protein shuttling from cytoplasm to nucleus associated with SUMOylation of target proteins (Kirsh et al., 2002). Other SUMO E3 ligase could also be implicated in the modification of ataxin-7: the PIAS (Protein Inhibitor of Activated Stat) proteins that can act as SUMO E3 ligases. To test the implication of PIAS in ataxin-7 SUMOylation and evaluate each PIAS protein for its ability to enhance SUMOylation of ataxin-7, we overexpressed ATXN7-92Q in presence of six different constructs for the known SUMO E3 ligases (5 for different

PIAS and RanBP2) in combination with alternative expression of SUMO-1 and SUMO-2. We tested PIAS1, PIAS $\alpha$ , PIAS $\beta$ , PIAS3 and PIAS4 and compared their effect on western blots and on filter assays. As described in section 3.1.1, we show that SUMO-1 overexpression leads to a slight reduction of mutant soluble ataxin-7 (Figure 18-B lane 2 compared to lane 1) and a strong decrease of aggregated SDS insoluble protein (Figure 18-A). On western blots, PIAS1 slightly enhanced the modification of ATXN7-92Q with SUMO-1 overexpression (Figure 18-B lane 3 asterisk). But the major effect, which was easily detected on western blots, was the increase in ataxin-7 poly-SUMOylation by SUMO-2 (Figure 18-B, lanes 8-13 compared to lane 1, single asterisk for mono-SUMOylation and double asterisk for poly-SUMOylation); this modification also correlated with a reduction of SDS-insoluble ATXN7-92Q (Figure 18-A). In particular, the degradation of the aggregates seems to be dependent on co-expression of SUMO-1 or -2 combined with the different SUMO E3 ligases. For example, PIAS $\alpha$  seems to be more prone to catalyze the modification of ataxin-7 when supported by SUMO-1 (Figure 18-A); on the contrary, PIAS3 and 4, in presence of SUMO isoform 2, massively degrades ataxin-7 aggregates (Figure 18-A). Because the PIAS proteins are regulators of transcription, like SUMO, and can act as coactivators and corepressors in addition to their E3 ligase activity, a myc-actin construct under CMV-based promoter was cotransfected to account for transcriptional effects. The corresponding fusion protein, used as control, was detected by an anti c-myc antibody (Figure 18-B). An anti-HA antibody detected free SUMO-1, known to be less abundant than free SUMO-2. An anti-T7 antibody detected the overexpressed PIAS that were tagged with T7.

We tested directly the action of RanBP2 only with SUMO-1, because it has a greater affinity for SUMO-1 than for SUMO-2 (Hecker et al., 2006). We expressed a fragment of RanBP2, delta FG ( $\Delta$ FG, aa 2553-2838), that contains the E3 ligase catalytic activity (Werner et al., 2012), since full-length RanBP2, a 358 kDa protein, cannot be efficiently expressed due to its large size. The effects of RanBP2 expression on the degradation of ataxin-7 aggregates in the presence of SUMO-1 were more important than those of the other SUMO E3 ligases tested. We obtained a reduction by 87% of mutant protein aggregates when both RanBP2 and SUMO-1 were expressed, relative

to the expression of ATXN7-92Q alone or coexpressed with RanBP2 alone (Figure 18-A).

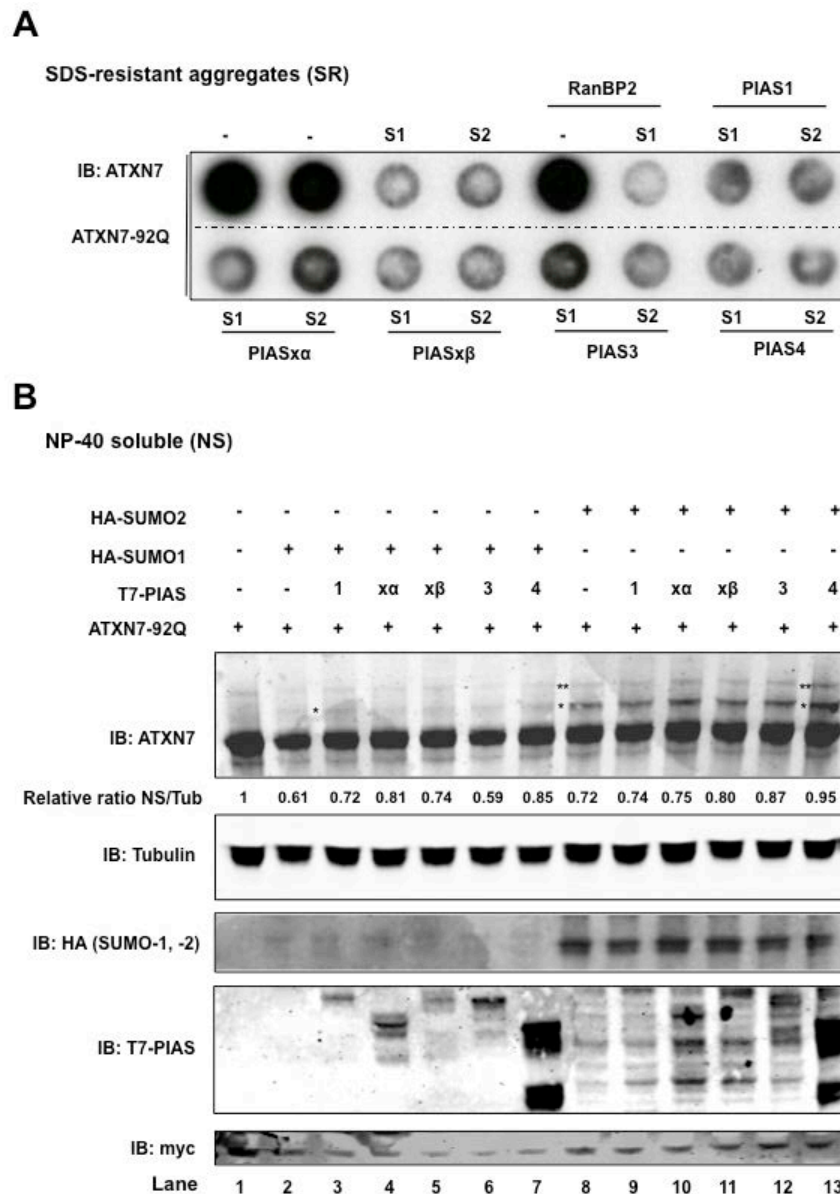


**Figure 18 – Identification of a major SUMO E3 ligase for ataxin-7 modification**

(A) Filter retardation assay. In COS7 cells, co-expression of ATXN7-92Q and SUMO-1 or SUMO-2 with candidate SUMO E3 ligases: PIAS1, PIAS $\alpha$ , PIAS $\beta$ , PIAS3, PIAS4 and a fragment of RanBP2 (aa 2553-2838) that contains the E3 catalytic activity. ATXN7-92Q was expressed in all samples. SUMO-1 or SUMO-2 overexpression decreased aggregation of mutant ataxin-7 by around 76% and 70%, respectively, compared to aggregation level of ATXN7-92Q expression alone. RanBP2 co-expressed with SUMO-1 decreased aggregation by 87%; PIAS1 co-expressed with SUMO-1 by 65%; PIAS $\alpha$  and SUMO-2 by 45%. S1, SUMO-1; S2, SUMO-2. (B) Western blot analysis. ATXN7-92Q co-expressed with SUMO-1 or SUMO-2 and different PIAS isoforms. SUMO-1 in combination with PIAS1 reduced soluble ataxin-7 by 28% (lane 3) and PIAS4 by 15% (lane 7). SUMO-2 increases the mono (\*) and poly-SUMOylation (\*\*) of ataxin-7; addition of PIAS4 increased by 173% the level of modified ataxin-7 (lane 13, \* mono-SUMO). To control for transcriptional effects of PIAS, one tenth of a myc-actin construct under CMV-based promoter was co-transfected. SUMO-1 (less abundant than SUMO-2) was detected with an anti-HA tag antibody; PIAS was detected with the anti-T7 antibody. Relative ratios of NS ataxin-7 versus tubulin are indicated.

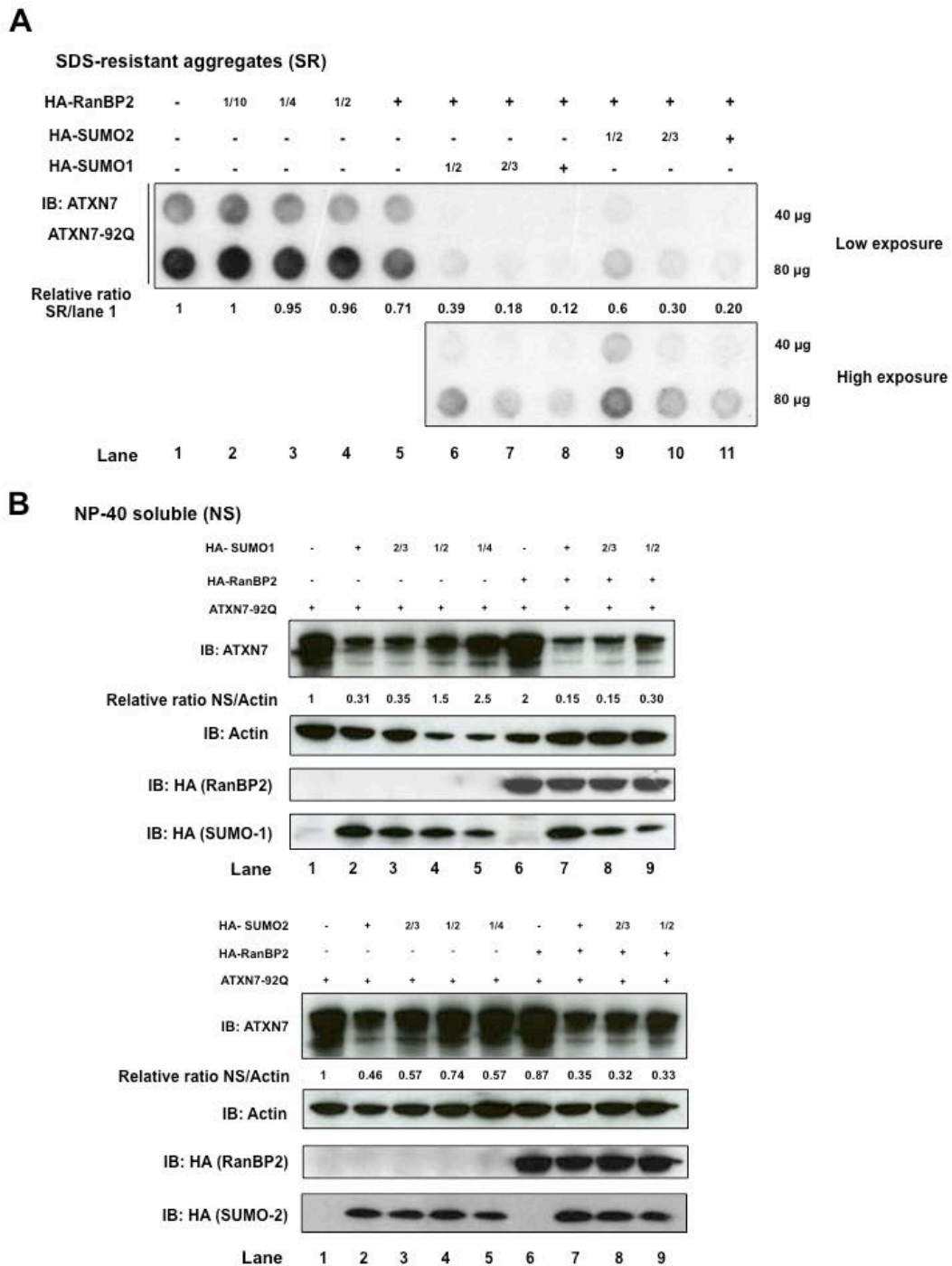


**Figure 19 - SUMOylation of ataxin-7 by RanBP2**

ATXN7-92Q (1 µg per well) was co-expressed in COS7 cells with different concentrations of plasmids expressing RanBP2, SUMO-1 and SUMO-2. (A) Filter retardation assay. Increased SUMO-1 expression reduced SDS-resistant aggregates (SR) more (lane 6-8) than SUMO-2 (lane 9-11). Forty and 80 µg of total protein extracts were applied to the filter. Ataxin-7 was detected with an anti ataxin-7 antibody (rabbit). Relative ratios of SR ataxin-7 versus lane 1 are indicated (B) Western blot analysis. Amounts of plasmids are as in (A). The catalytic fragment of RanBP2 and free SUMO-1 and 2 were detected with an anti-HA antibody. Actin was the loading control. Upper panel: SUMO-1 titration showed a decrease in soluble ataxin-7 by 69% (lane 2) due to both transcriptional repression and protein degradation. RanBP2 caused additional degradation of soluble ataxin-7 by 85% (lane 7). Bottom panel: SUMO-2 caused less degradation than SUMO-1 by 56% (lane 2); co-expression with RanBP2 had a slightly greater effect (decreased by 65%, lane 7). Relative ratios of NS ataxin-7 versus actin are indicated.

To further investigate the role of RanBP2 as the major SUMO E3 ligase of ataxin-7, SUMO isoforms were titrated with and without overexpression of the enzyme to confirm its preferential interaction with SUMO-1 in ataxin-7 modification. First, in the absence of SUMO expression, RanBP2 had a small but dose-dependent effect on ataxin-7 aggregates (Figure 19-A, lanes 1 to 5) that can be explained by the presence of endogenous SUMO-1. Increased amounts of overexpressed SUMO-1 (from  $\frac{1}{4}$ ,  $\frac{1}{2}$ ,  $\frac{2}{3}$  to 1) reduced soluble ataxin-7 (Figure 19-B, upper panel, lanes 2-5) and the insoluble aggregates (Figure 19-A, lanes 6-8): this effect was increased by the addition of RanBP2 (Figure 19-A, lanes 6-8 and -B, upper panel, lanes 6-9 compared to lanes 2-5). On the contrary, SUMO-2 overexpression reduced the level of soluble mutant ataxin-7 less than SUMO-1 (bottom panel in Figure 19-B, lanes 1-5). However co-expression of SUMO-2 and RanBP2 slightly reduced soluble mutant ataxin-7 (Figure 19-B lower panel, lanes 7-9), but strongly reduced ataxin-7 aggregates (Figure 19-A, lanes 9-11). Together our results suggest that RanBP2 is the major SUMO E3 ligase for modification of ataxin-7 by SUMO isoform 1; SUMO-1 is a known partner of RanBP2. However, in this overexpression model, RanBP2 and SUMO-2 also seem to target mutant ataxin-7.

We also tested the effects of a RanBP2 plasmid coding for the same fragment ( $\Delta$ FG) used in the above-described experiment but with a mutation that inactivated its SUMO E3 ligase activity (L2651A/L2653A/F2658A). In COS7 cells, we overexpressed ATXN7-10Q or -92Q and SUMO-1, with or without wild type or mutant RanBP2 $\Delta$ FG. By western blot, we confirmed the expression of the two RanBP2 constructs using an anti-HA antibody. Soluble ATXN7-92Q accumulated more than its ATXN7-10Q counterpart, which always has a more rapid turnover in cells, as seen on the western blot. Overexpression of SUMO-1 and RanBP2 decreased the level of ATXN7-10Q (Figure 20-A, lane 10 compared to lane 7 and to lane 8), again suggesting that RanBP2 acts in concert with SUMO-1 on its target ataxin-7. Mutant RanBP2 did not have the same effect (Figure 20-A, lane 12). Neither did RanBP2 WT in the absence of SUMO-1 (Figure 20-A, lane 9).

A small decrease in the amount of soluble ATXN7-92Q was observed when RanBP2 was coexpressed with SUMO-1 (Figure 20-A, lane 4 compared to lane 1). When extracts of cells co-transfected with wild type or mutant RanBP2 and ATXN7-92Q

were examined by filter retardation assay, the reduction of mutant ataxin-7 aggregates was much stronger when the wild type form of RanBP2 fragment was expressed. As to why the mutant fragment was active, it is possible that when the IR1 motif is inactivated, the IR2 motif is able to be cryptically activated (Andreas Werner, personal communication).

We conclude that in an overexpression system, the RanBP2 fragment containing the SUMO-1 E3 ligase activity is able to mimic SUMOylation of normal and mutant ataxin-7. Thus, mutant ataxin-7 is probably more efficiently or rapidly modified by SUMO-1 and aggregates much less than if only SUMO-1 is expressed.

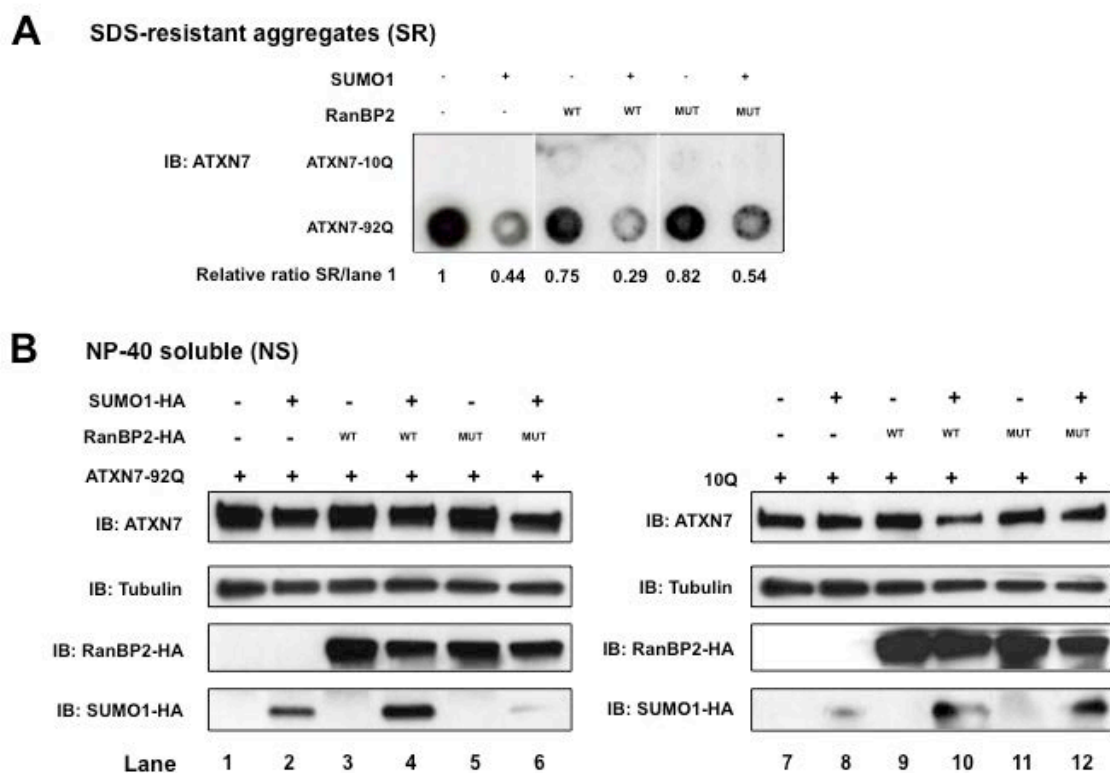


**Figure 20 - RanBP2  $\Delta$  FG fragment but not RanBP2  $\Delta$  FG with a mutation in the IR1 motif causes efficient SUMO-1 -mediated degradation of ataxin-7 aggregates**

ATXN7-92Q was co-expressed, in COS7 cells with SUMO-1 and a fragment of wild-type RanBP2 (RanBP2 $\Delta$ FG with or without a mutation in the IR1 motif that inactivates E3 ligase activity (L2651A/L2653A/F2658A) (MUT). (A) Filter retardation assay. SUMO-1 reduced aggregation by 56%; SUMO-1 and RanBP2 $\Delta$ FG reduced aggregation even more, by 71%; SUMO-1 and mutant RanBP2 $\Delta$ FG reduced it by 46%. Relative ratios of SR ataxin-7 versus ATXN7-92Q overexpression alone (lane 1) are indicated. (B) Western blot of samples in (A). Co-expression of SUMO-1 and ATXN7-92Q (left panel) or ATXN7-10Q (right panel).

### 3.1.4. Endogenous RanBP2 co-immunoprecipitates with endogenous ATXN7.

To avoid the effects of non-physiological conditions, we performed an immunoprecipitation under non-denaturing conditions, as above, to confirm the possible interaction between ataxin-7 and RanBP2 in MCF7 cells.

Since RanBP2 is part of the nuclear pore complex, we used two different extraction buffers to determine the best conditions for isolating this protein from the nuclear membrane and avoid losing it in the pellet after centrifugation. We opted for an extraction buffer containing non-ionic detergents, either NP-40 0.5% or TRITON X-100 0.1% (50 mM Tris pH 7,4; 100 mM NaCl; 2 mM MgCl<sub>2</sub>; 1mM EGTA). Analysis of the input samples confirmed that we were able to extract endogenous RanBP2 protein with the two buffers quite similarly, as well as ataxin-7, which was less abundant. Immunoprecipitation of samples with anti-RanBP2 and anti-ataxin-7 antibodies confirmed the binding of the two proteins. Similar amount of ataxin-7 were immunoprecipitated in both buffers, whereas RanBP2 was more abundant in eluates when immunoprecipitated in NP-40 buffer. Ataxin-7 protein was co-immunoprecipitated when RanBP2 was immunoprecipitated, and vice versa, regardless of the extraction buffer. This suggests that endogenous ataxin-7 interacts with RanBP2 in MCF7 cells. We confirm the specificity of the binding with an immunoprecipitation using an anti-myc antibody: neither ataxin-7 nor RanBP2 were immunoprecipitated. The control using beads without antibodies demonstrated that neither RanBP2 nor ataxin-7 stuck non-specifically to the beads. Using two different buffers we confirm that the interaction of ataxin-7 with RanBP2 is specific.

In 2006 our team published the interaction between ataxin-7 and another SUMO target, PML. Thereafter, other teams suggested that RanBP2 was a candidate SUMO E3 ligase for PML (Saitoh et al., 2006). Our immunoprecipitation experiment confirmed the already described interaction of ataxin-7 with PML. We have now shown that RanBP2 might well be a SUMO E3 ligase for PML. Our immunoprecipitation experiments show that RanBP2 and PML interact, indirectly within a complex, or maybe directly (Figure 21). Finally we conclude that RanBP2 and ataxin-7 interact with each other: our hypothesis is that RanBP2-catalyzed SUMOylation of ataxin-7 confers this interdependence, probably during nuclear import (Figure 21).

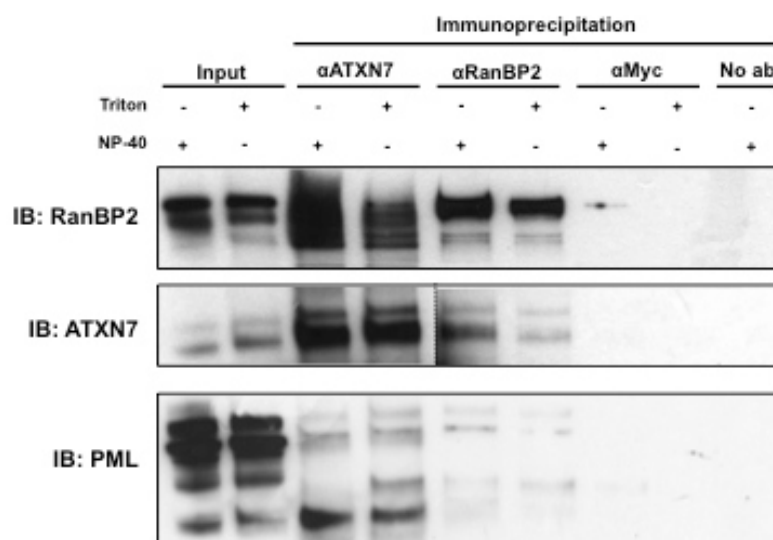


**Figure 21 - Endogenous ataxin-7 and RanBP2 are in a complex in MCF7 cells**

MCF7 cell extracts were subjected to immunoprecipitation with anti-ATXN7, anti-RanBP2 or anti-myc antibodies. Input samples and immunoprecipitated material (IP) were analysed on 4-20% gel; blots were revealed with the indicated antibodies. Samples precipitated with anti ataxin-7 were revealed with the antibody against RanBP2 or *vice versa*. PML in the samples was co-immunoprecipitated with anti ataxin-7 and, to a lesser extent with anti-RanBP2. No ab, control incubated only with beads. Triton: 0.1% in the extraction buffer; NP-40: 0.5% in the extraction buffer. The blot corresponding to immunoprecipitation with anti-ataxin-7 is shown at a shorter exposure to avoid saturation.

### 3.1.5. SUMO E3 ligase silencing enhances mutant ataxin-7 aggregation

The results presented above show the implication of a major SUMO E3 ligase on ataxin-7 modification by SUMO-1: overexpression of RanBP2 in presence of SUMO-1 enhanced mutant ataxin-7 degradation. In order to confirm that this enzyme plays an important role in protein modification, we studied the effect of SUMO E3 ligase depletion on ataxin-7 SUMOylation. We transfected ATXN7-10Q and -92Q in HeLa cells during silencing of the individual PIAS or RanBP2 SUMO E3 enzymes with a pool of four different siRNA for each target gene. The silencing was confirmed at the protein level by western blot using specific antibodies against PIAS1, or PIAS2, PIAS3, PIAS4 or RanBP2. The analysis was performed 60 hours after administration of the siRNA onto cells. In (Figure 22-A, middle panel), we show that in the presence of a pool of control "Non-Target" siRNA we detect each PIAS and RanBP2 at their endogenous levels. After individual silencing of each target, the corresponding proteins are no longer detected, thus confirming efficient knockdown of the PIAS and RanBP2. Since ATXN7-10Q protein levels are lower than those of ATXN7-92Q, which accumulates, we analysed samples transfected with ATXN7-10Q to determine

the effect of SUMO E3 ligase silencing on SUMOylation of ataxin-7 (Figure 22-B). A long exposure of the western blot is shown to visualize the reduction of the modified bands after silencing. There is a clear decrease in the SUMOylation of ataxin-7 after silencing of SUMO E3 enzymes: in particular, we detected an important decrease of SUMOylation after RanBP2 and PIAS4 (Figure 22-B) silencing. If RanBP2 is silenced, other PIAS may take over the role of the major SUMO E3 ligase for ataxin-7. We are still able to detect some modification of ataxin-7 after RanBP2 and PIAS4 silencing. As PIAS and RanBP2 may be both contribute to SUMOylation, we never observed a total absence of ataxin-7 SUMOylation, but we did see a very strong effect (loss of bands migrating above ataxin-7) after PIAS4 or RanBP2 silencing.

We next investigated the influence of silencing each PIAS or RanBP2 on mutant ataxin-7 aggregation by filter retardation assay. Compared to cells treated with non-target siRNA, we observed an increase in ataxin-7 aggregates when we prevented SUMO E3 ligase expression (Figure 22-B). This was true for all PIAS. The greatest aggregation was observed after RanBP2 silencing, again indicating that it could play a specific role in the fate of mutant ataxin-7 via SUMOylation.

Finally we wanted also to confirm RanBP2 depletion by immunofluorescence (Figure 22-C). As expected, endogenous RanBP2 was stained around the nuclear rim when we used “Non-target” siRNA (siCTRL). Interestingly, in some cells, endogenous ataxin-7 staining was also detected at the nuclear rim colocalized with RanBP2, supporting the notion that the two proteins may interact during shuttling of ataxin-7 from the cytoplasm to the nucleus. In the presence of siRNA that targeted RanBP2, we were not able to detect cells reporting nuclear rim staining of ataxin-7. We reasoned that the silencing of RanBP2 had a negative effect on the localization of endogenous ataxin-7 at the nuclear-rim. This would be in agreement with our hypothesis that ataxin-7 is SUMOylated via RanBP2 at the nuclear membrane.

Together our experiments demonstrate that PIAS4 and RanBP2 are involved in the SUMOylation of normal and mutant ataxin-7. The silencing of these E3 SUMO ligases leads to increased aggregation of mutant ataxin-7 in the cells. RanBP2 could be the major E3 SUMO-1 ligase acting at the nuclear pore, coupling SUMO-1 modification of ataxin-7 to its entry into the nucleus.

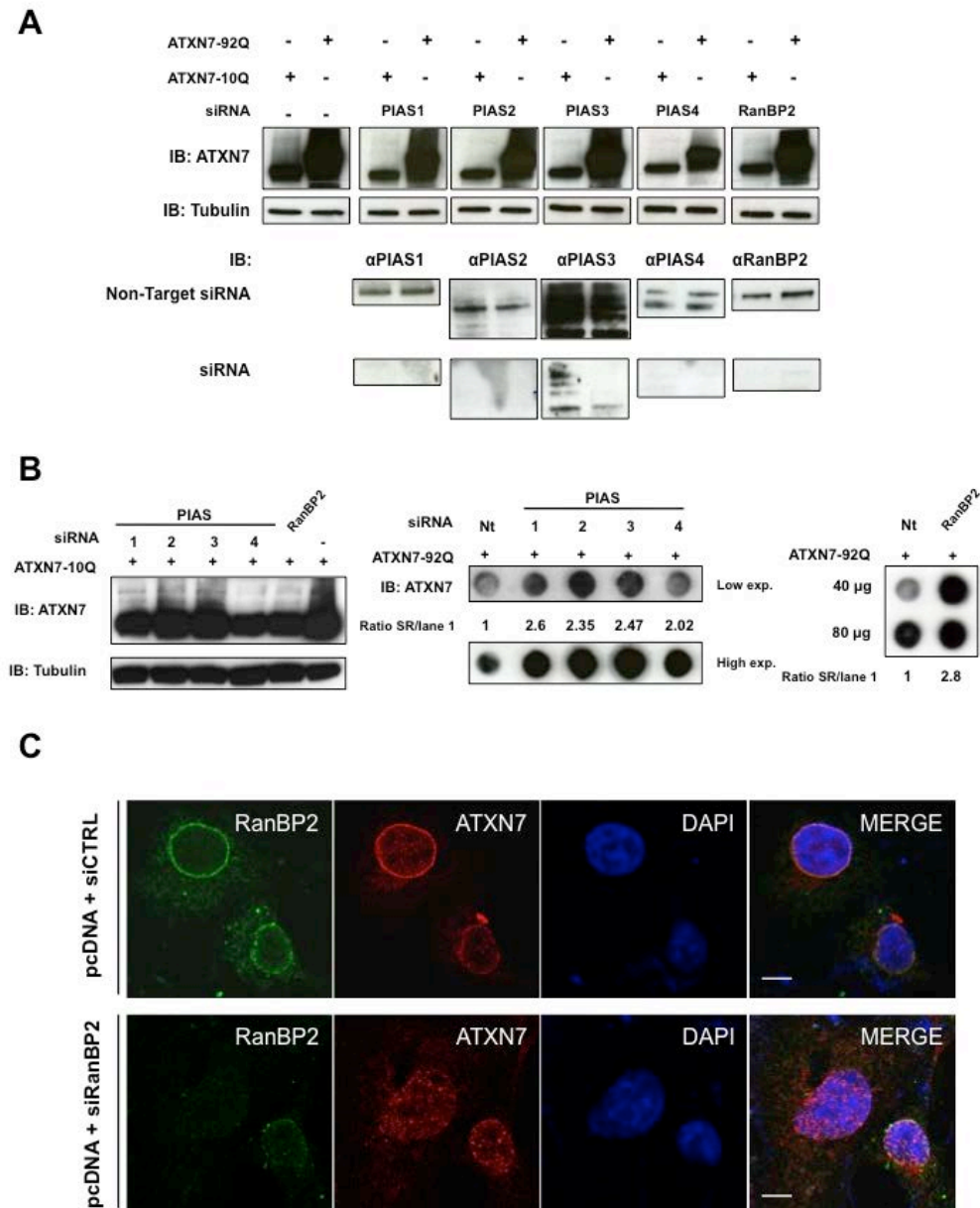


**Figure 22 - PIAS and RanBP2 silencing enhance mutant ataxin-7 aggregation**

(A) Western blot analysis. Expression of normal ATXN7-10Q or expanded ATXN7-92Q was performed in HeLa cells treated with siRNA that target PIAS1, PIAS2, PIAS3, PIAS4 or RanBP2. 60 hours after siRNA addition, extracts were analysed by SDS-PAGE. The upper panel shows ATXN7-10Q and -92Q expression and modification. The bottom panel shows the efficiency of PIAS and RanBP2 silencing. Antibodies specific for each PIAS isoform and RanBP2 were used (see table in Material and Methods) as indicated above the gels. Non-target siRNA did not affect the signal of each PIAS. SMART Pool siRNA specific for each PIAS prevented their expression. (B) Samples of overexpressed ATXN7-10Q were reanalysed to improve detection of the RNA interference on soluble ataxin-7. SiRNAs against the PIAS and RanBP2 are indicated above the gels. PIAS4 silencing had the greatest effect, but RanBP2 silencing also robustly decreased modified ataxin-7 levels. Tubulin was the loading control. (C) Filter retardation assay of ATXN7-92Q after silencing of the PIAS and RanBP2. Aggregation of mutant ATXN7 was increased by PIAS (until up to 230%) and RanBP2 silencing (280%). The filter was probed with an anti-ataxin-7 antibody. Nt, non-target. Relative ratios of SR ataxin-7 versus ATXN7-92Q overexpression alone lane are indicated. (C) Confocal images of immunofluorescence in HeLa cells treated with non-target or RanBP2 siRNA. Endogenous RanBP2 and ataxin-7 were observed at the nuclear rim with non-target siRNA; RanBP2 and ataxin-7 staining at the nuclear rim were prevented by siRanBP2. In these conditions ataxin-7 staining at the nuclear membrane was no more detected. Scale bar 8  $\mu$ m.

### 3.1.6. Ataxin-7 is SUMOylated by RanBP2 *in vitro*: a validation that it is a candidate ataxin-7 SUMO E3 ligase.

SUMOylation of proteins *in vitro* is an indispensable tool for the functional analysis of this post-translational modification. In collaboration with Andreas Werner in Frauke Melchior's laboratory, we tested whether ataxin-7 could be SUMOylated *in vitro* by addition of recombinant RanBP2. To perform the assay we used a truncated form of GST-ATXN7 (aa 90-406), incubated with E1, E2 enzymes, ATP, SUMO-1 and two different E3 ligases, PIAS1 or RanBP2. As for RanBP2, either free RanBP2, corresponding to the fragment between amino acids 2304-3062, or a RanBP2 complex, consisting of RanBP2/RanGAP SUMOylated by SUMO-1/Ubc9 (Werner et al, 2012), were incubated with GST-ATXN7 and E1, E2, ATP, SUMO-1.

SUMOylation of the GST-ATXN7 fragment (aa 90-406) was remarkable with the RanBP2 complex: a strong band corresponding to addition of one SUMO-1 residue to GST-ATXN7 was detected by immunoblot revealed with anti-GST antibody (Figure 23-A). A less intense band corresponding to two SUMO residues conjugated to GST-ATXN7 was also observed. When incubated with the free form of RanBP2, GST-ATXN7 was poly-SUMOylated with SUMO-1 (Figure 23-A). It is not yet known, whether this poly-SUMOylation is of physiological relevance, since poly-SUMO-1 chains have not yet been described so far *in vivo*. GST-PIAS1 was able to mono-SUMOylate ataxin-7 (Figure 23-A); it is to be noted that the background in this lane is due to GST-PIAS1, as seen in the GST control lane (Figure 23-A).

These results show that the ataxin-7 fragment 90-406 containing the previously identified Lysine 257 is an excellent substrate for *in vitro* SUMOylation by the RanBP2 complex. We conclude that RanBP2 acts, *in vitro*, as the major SUMO E3 ligase for ataxin-7.

### 3.1.7. Ataxin-7 contains motifs for non-covalent binding to SUMO

SUMOylation regulates the molecular interactions of the modified proteins leading to changes in the localization, activity, solubility, or stability of respective target proteins. In addition to covalent attachment of SUMO to target proteins, specific non-covalent SUMO Interaction Motifs (SIMs), which are generally short hydrophobic peptide motifs, have been identified. It has become clear that there is

also some flexibility in the precise sequence of the hydrophobic core of the SIMs: as shown by NMR studies, the hydrophobic core interacts with a groove of SUMO formed by a  $\beta$  sheet and part of the  $\alpha$  helix (Song et al., 2004) (Hecker et al., 2006). Interestingly, consensus SIMs are found in several components of the SUMOylation machinery, including members of the PIAS E3 family and RanBP2. Additionally, SIMs are found in some SUMO substrates. This clearly raises the possibility that components of the modification pathway interact non-covalently with SUMO to facilitate its transfer to substrates.

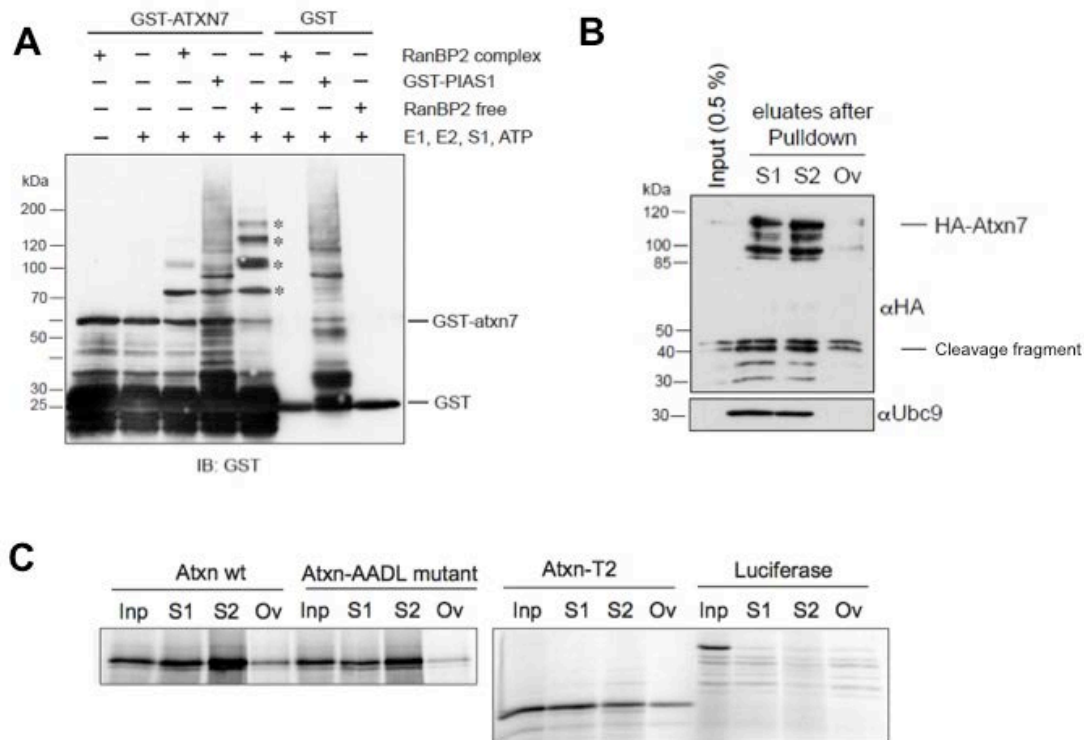


**Figure 23 - Ataxin-7 is efficiently SUMOylated *in vitro* by free RanBP2 and by the RanBP2/RanGAP1\*SUMO1/Ubc9 complex. Ataxin-7 also interacts with SUMO-1 and SUMO-2.** (A) GST-ATXN7 (aa 90-406) was incubated with E1, E2 enzymes, ATP, SUMO-1 and two E3 ligases, PIAS1 or RanBP2. Free RanBP2 is the fragment between amino acids 2304-3062. Complex is RanBP2/RanGAP SUMOylated by SUMO-1/Ubc9. SUMOylation of the GST-ATXN7 fragment (aa 90-406) was remarkable with the RanBP2 complex. SUMOylation of GST-ATXN7 with the free form of RanBP2 gave poly-SUMO-1 modified bands. Asterisks represent (\*) SUMO residues added onto GST-ATXN7. GST-PIAS1 was able to mono-SUMOylate ataxin-7. The background in this lane is due to GST-PIAS1, as seen in the GST control lane. (B) Extracts of HEK-293 cells transfected with ATXN7-10Q HA were incubated with SUMO-1 beads (S1), SUMO-2 beads (S2) or ovalbumin beads (Ov) as control. Pull down with the SUMO-1 or-2 beads demonstrated that ATXN7-10Q interacts with SUMO-1 and with SUMO-2. Ubc9 was used as a positive control; (C) Radioactive-labelled ATXN7-10Q produced by *in vitro* transcription/translation was incubated with SUMO-1 beads (S1), SUMO-2 beads (S2) or ovalbumin beads (Ov) as control. The eluates were analyzed by SDS-PAGE and autoradiography; 10% Input (Inp). Luciferase, used as control protein, did not bind to SUMO beads.

To investigate whether ataxin-7 interacts non-covalently with SUMO-1 or SUMO-2, we transiently transfected HA-tagged ATXN7-10Q into HEK293 cells and incubated the lysate with immobilized SUMO-1, SUMO-2 or ovalbumin as the control. Pull-down was performed by a 4h incubation on rotator, at 4°C, followed by a centrifugation to precipitate beads. Beads were washed and subsequently boiled in Laemmli buffer to release the proteins bound to SUMO-1 or SUMO-2 or ovalbumin. The samples were analyzed by SDS-PAGE. Ubc9 blot is the positive control for the pull-down: Ubc9 is known to interact non-covalently with SUMO and we show here that it is highly enriched with pull-down using SUMO beads (but not ovalbumin control). Using a HA-tag antibody to detect ataxin-7, we were able to visualize efficient protein pull-down. As shown in Figure 23-B, ataxin-7 seems to interact more efficiently with SUMO-2 compared to SUMO-1.

To define which residues of ataxin-7 are involved in the interaction with SUMO, we looked at the protein sequence to identify a possible candidate sequence, which must have the characteristic hydrophobic core (V/I-V/I-X-V/I) followed or preceded by a negatively charged cluster of amino acids. Based on sequence analysis, we found a candidate sequence located between amino acids 349 to 352 (VIDL). To confirm a potential interaction between this candidate SIM on ataxin-7 and SUMO, we mutated this sequence by replacing valine and isoleucine with two alanine residues in consecutive hydrophobic cores (VIDL→AADL). We also used a plasmid coding for a truncated human wild-type form of ataxin-7 (ATXN7-T2) containing amino acids 1-232; it has been shown that ataxin-7 is cleaved by caspase 7 at position 266 and 344 (Young et al., 2007) and the truncated N-terminal form of ataxin-7 that we used is close to the shortest natural fragment observed and should therefore be relevant to the study of SCA7 pathology. Another way to test a non-covalent interaction is to incubate beads covalently coupled to recombinant His-SUMO1, His-SUMO2 or ovalbumin to target protein produced by *in vitro* transcription-translation. SUMO beads were incubated with *in vitro* transcribed-translated (<sup>35</sup>S labelled) full-length wild type ataxin-7, AADL-mutant ataxin-7, and ataxin-7-T2 or luciferase as control. As shown above in pull-down assay, wild type ataxin-7 preferentially bound SUMO-2 (Figure 23-C). The AADL-mutant ataxin-7 was still able to bind SUMO-1 and SUMO-2, with a preference for the latter, but to a lesser degree than wild-type ataxin-7.

This means that additional SIMs are to be found in the ataxin-7 sequence. Finally ataxin-7-T2 only weakly bound SUMO, if at all, and did not show a preference for SUMO-2. We conclude that this N-terminal sequence does not play an active role in a direct interaction between SUMO and ataxin-7. Taken together, these findings demonstrate that the interaction between ataxin-7 and SUMO-1, -2 could also involve a SUMO-SIM interface. Further investigation will be necessary to confirm VIDL (aa 349-352) as an ataxin-7 SIM motif and identify other potential SIMs. In fact, proteins containing multiples SIM were identified.

### 3.2. Does PML SUMOylation affect mutant ataxin-7 aggregation or degradation?

In 2006, our team discovered that a subgroup of PML bodies, called clastosomes, prevent nuclear accumulation of mutant ataxin-7 and other polyglutamine proteins. In particular, expression of PML isoform IV leads to the formation of distinct nuclear bodies enriched in components of the ubiquitin-proteasome system. SUMOylation plays an important role in the scaffold function of PML and permits assembly of mature nuclear bodies. SUMO-3 attachment has been reported to be responsible for the correct nuclear localization of PML (Fu et al., 2005), and without SUMO-1 modification several protein partners are not recruited to the PML-NB (Lallemand-Breitenbach et al., 2008). However, a non SUMOylable mutant of PML (3K mutated into 3R) still shows the typical speckled nuclear pattern, indicating that other factors also play a role in PML-NB formation (Lallemand-Breitenbach et al., 2001). Keeping in mind the relevance of SUMOylation also for PML body formation, we decided to investigate the effects on mutant ataxin-7 localisation and aggregation of various mutants of PML isoform IV, which were described to affect PML SUMOylation (Shen et al, 2006). We obtained four PML IV plasmids (kind gift from P. Pandolfi) harbouring either mutations of SUMOylated lysines or mutations/a deletion of the SIM motif, and a combination of both (Figure 24-A). We performed an immunofluorescence analysis to study the effect of PML mutations on subcellular localization of ataxin-7. In COS7 cells, we coexpressed ATXN7-92Q with wild type and mutant PML isoform IV for 48 hours and analysed the localisation of both proteins.

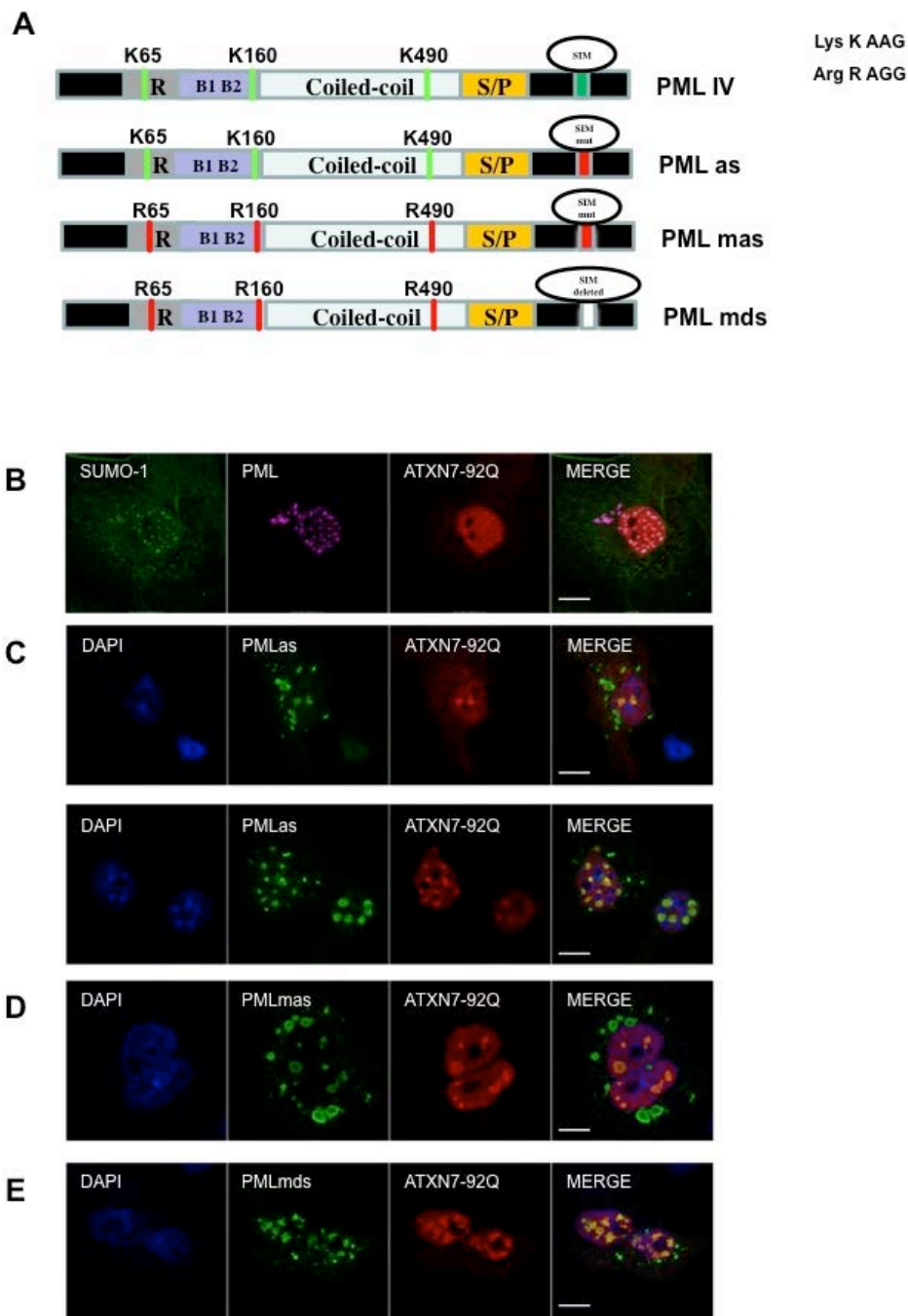


**Figure 24 - SUMO-deficient PML is still able to partially colocalize with mutant ataxin-7**

(A) Schematic representation of PML mutants. Wild type PML IV, SUMO binding motif mutant (PMLas), SUMOylation-deficient and SUMO binding motif mutant (PML3mas), SUMOylation-deficient and SUMO binding motif deletion mutant (PML3mds) PML constructs. (B) In COS-7 cells, full-length mutant ATXN7-92Q colocalized with PML IV in round, regular PML bodies (C). Upper panel: colocalization of ATXN7-92Q and PMLas; note the abnormal irregular shape of the nuclear bodies. Lower panel: one cell contains irregular rod-like PML bodies, which partially colocalize with ataxin-7; the other cell contains enlarged round PML bodies, reminiscent of PML IV (wt), which colocalize with less intense ataxin-7 staining. (D) Co-transfected ATXN7-92Q and PMLmas co-localized, but the nuclear bodies lost their usual staining pattern: intensity was low in the nucleus and abnormally intense outside the nucleus. (E) In cells overexpressing PMLmds, ATXN7-92Q aggregates were not homogeneously stained, but still colocalized with disrupted PML bodies, confirming an effort to degrade nuclear inclusions. Antibodies used were anti-ataxin-7 (1C1) and polyclonal anti-PML. Representative confocal images are presented. Scale bar 8  $\mu$ m.

In cells expressing wild type PML IV and ATXN7-92Q, ataxin-7 staining was typically nuclear in a subset of cells; the presence of multiple round dots corresponded to the mutant protein in aggregates (Figure 24-B). As expected, these aggregates colocalized perfectly with PML IV nuclear bodies, confirming our previously published results. Moreover, staining with an anti SUMO-1 antibody confirmed the colocalization between this protein and the known SUMOylation targets ataxin-7 and PML (Figure 24-B).

This result provides evidence supporting the hypothesis that PML NBs are a (de)SUMOylation platform where SUMO is coupled or detached to/from its target protein. To determine whether there is a difference in the subcellular localization of ataxin-7 or PML when the latter cannot either be SUMOylated, or interact with other SUMO-modified proteins, we transfected ATXN7-92Q with different SUMO/SIM mutant PML constructs. In Figure 24-C, we present immunofluorescence from cells overexpressing ATXN7-92Q and PML SUMO binding motif (SIM) mutant (PMLas). Ataxin-7 staining is always nuclear but, compared to the image above (Figure 24-B), the dots seem to be less numerous and the shape of the aggregates is not homogenous. We found a similar change in nuclear staining for PML: PMLas formed fewer and aberrant structures compared to those formed by PML IV in the nucleus, but still colocalized with ATXN7-92Q. This pattern is still in agreement with the notion that PMLas can still be SUMOylated and is probably still able to be a platform for the proteasome-component implicated in the degradation of mutant ataxin-7. The study of Shen and co-authors (Shen et al., 2006) showed that PML, in which 3K is mutated to R (named PMLm), also formed fewer and aberrant compact structures compared to those formed by wild-type PML in the nucleus and still colocalized with GFP-SUMO-1, in agreement with the notion that it retains the SUMO binding motif. Mutagenesis or removal of the SUMO binding motif in PMLm (PMLmas and PMLmids, respectively) completely abrogated colocalization with GFP-SUMO-1 (Shen et al., 2006). In our experiments, ataxin-7 staining was nuclear and the colocalization with PML mutants, PMLmas and PMLmids, although not totally abolished, was highly reduced. In some cells, PMLmas showed no colocalisation with ATXN7-92Q dots (not shown); in other cells, partial colocalization was observed (Figure 24-D). In the cell presented in Figure 24-D, the presence of PMLmas in large

cytoplasmic dots may be due to aberrant overexpression of PML. Finally PMLmids completely lost their regular round shape. Either we observed no colocalization at all (rare event, not shown) between PMLmids and ATXN7-92Q, or we observe colocalized proteins in non-homogenous nuclear inclusions (Figure 24-E). The aspect of these inclusions is reminiscent of the previously described non-homogenous inclusions of mutant ataxin-7 (Janer et al, 2006). These non-homogenous inclusions were less SUMO-1- and SUMO-2-positive than the homogenous inclusions, and less associated with endogenous clastosomes, but rather with no nuclear bodies (Janer et al., 2006). We propose here that PMLmids may not be able to recruit or interact, as its SIM is missing, with mutant ataxin-7. Nevertheless, the proteins colocalize.

To better compare the effect on mutant ataxin-7 aggregation of wild type PML IV to the SUMO-deficient PML expression, we cotransfected COS7 cells with ATXN7-92Q and SUMO-mutant PML and analyzed cell extracts by western blot (Figure 25-A) and filter retardation assay (Figure 25-B). Since aberrant patterns of PML NB formation were observed by immunofluorescence when PMLmas and PMLmids were overexpressed, including the loss of perfect colocalization with mutant ataxin-7, we expected that these PML mutants would not actively degrade ataxin-7. Surprisingly, SUMO-deficient PML co-transfected with ATXN7-92Q was still able to reduce mutant protein aggregation, as shown by filter retardation assay (Figure 25-B). A question thus emerged: could the observed effect be linked to endogenous levels of PML? We then used transformed *Pml*<sup>-/-</sup> MEFs to determine whether we would obtain different results, or reproduce those obtained in COS7 cells. We transfected ATXN7-92Q with one of each SUMO-deficient PML plasmid in *Pml*<sup>-/-</sup> MEFs, and after 48h of expression we analyzed cell extracts by western blot (Figure 25-C) and filter retardation assay (Figure 25-D). As in COS7 cells, wild type and SUMO-deficient PML overexpression in *Pml*<sup>-/-</sup> MEFs cells led to a strong decrease in aggregated mutant ataxin-7 (Figure 25-D). As a control, PML III, an isoform that we previously demonstrated to be unable to degrade mutant ataxin-7, was included (Figure 25-D). The results confirm the specificity of ataxin-7 degradation by PML isoform IV. Why do PMLmas and PMLmids still degrade mutant ataxin-7 efficiently? Is the SUMOylation of PML and interaction via the SIM not required for recruitment of

ataxin-7 and its subsequent proteasomal degradation? Very recently, analysis of PML3KR  $\Delta$  SIM demonstrates that SUMO-SIM interactions are not responsible for the initial nucleation of the spherical mesh (Sahin et al., 2014), in opposition to what was previously thought (Shen et al., 2006). This structure is triggered by a complex polymerization scheme involving PML coiled-coil and disulfide bonds (Sahin et al., 2014). Consequently, a second hypothesis is that proteasome components can still be recruited in the inner matrix core of these pre-mature PML NBs, inducing degradation of mutant ataxin-7.

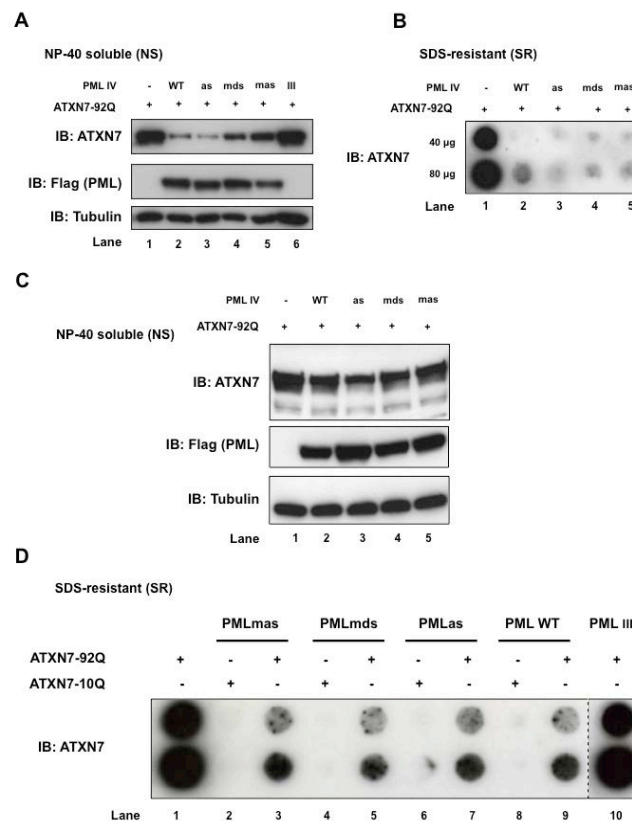


**Figure 25 - SUMO-deficient PML degrades mutant ataxin-7 aggregates**

(A) Western blot analysis. ATXN7-92Q and either wild type or PML SUMO-deficient variants were expressed in COS7 cells. Western blot was revealed using anti ataxin-7 antibody. The expression of PML SUMO-deficient variants was detected by anti-Flag. Ataxin-7 levels strongly decreased in the presence of PML IV, as expected (lane 2), but slightly less when co-expression was performed with SUMO-deficient mutant PML plasmids (lane 3-6). PML III was tested to assess the specificity of PML IV on ataxin-7 degradation. (B) Filter retardation assay. Coexpression of wild type and mutant PML led to the disappearance of SDS-resistant (SR) aggregates of mutant ataxin-7 (lane 2-5). (C) Western blot of *Pml*<sup>-/-</sup> MEFs cells co-expressing ATXN7-92Q and wild-type (lane 2) or SUMO-deficient variants of PML plasmids (lanes 3-5). All PML constructs slightly decreased NP-40-soluble ataxin-7 (same antibodies as in A). (D) Filter retardation assay on *Pml*<sup>-/-</sup> MEFs. Cells were transfected with ATXN7-10Q or 92Q in the presence of wild type and SUMO-deficient PML (lane 1-10). ATXN7-10Q does not aggregate (lane 2, 4, 6, 8), as opposed to ATXN7-92Q. Co-expression of wild type or SUMO-deficient PML with ATXN7-92Q led to the decrease of SDS-resistant (SR) aggregates of mutant ataxin-7 (lane 3, 5, 7, 9). PML III co-expressed with ATXN7-92Q did not degrade soluble mutant ataxin-7 and had no effect on aggregation (lane 10).

### 3.2.1. RNF4 attenuates the propensity of ataxin-7 to aggregate

Proteins conjugated with a poly-SUMO-2/3 chain can be recognized and ubiquitinated by RNF4, a RING domain ubiquitin ligase. Since we have shown that ataxin-7 is modified by SUMO-2, we inferred that poly-SUMOylated ataxin-7 might be a target for RNF4. RNF4 would thus recognize ataxin-7, mediate its ubiquitination and facilitate its degradation by the proteasome. We tested our hypothesis in a cellular overexpression system. Jacob Seeler (Institut Pasteur) kindly gave us three constructs for expression of human RNF4: the first containing the wild-type sequence (RNF4 WT), the second with mutations at the 4 SIMs in the N-terminal domain to prevent binding to SUMO-2 chains (RNF4  $\Delta$  SIM), and the third with a mutation in the RING domain that abolishes ubiquitin E3 ligase activity (RNF4 dHC). In COS7 cells, we overexpressed ATXN7-92Q with either one of the three plasmids encoding RNF4 (Figure 26-A lane 1 compared to lanes 3, 5, 7). In this case, the cells contained endogenous SUMO-2 levels. We also overexpressed each RNF4 construct in the presence of a SUMO-2 construct to make sure to be in conditions appropriate for ataxin-7 recruitment by RNF4, and did not limit SUMO-2 levels (Figure 26-A lane 2 compared to lanes 4, 6, 8). The idea was to test ataxin-7 recognition by RNF4 via SUMO-2 chains.

We analyzed and confirmed by western blot the overexpression of ATXN7-92Q, SUMO-2 and RNF4 (Figure 26-A). More specifically, we observed that wild type RNF4 expression affected soluble mutant ataxin-7 when coexpressed with SUMO-2 (Figure 26-A lane 4): ataxin-7 levels were decreased compared to the condition in which only wild type RNF4 was overexpressed (Figure 26-A, lane 4 compared to lane 3). In COS7 cells transfected with ATXN7-92Q and RNF4  $\Delta$  SIM, we did not detect any change in the band of soluble ataxin-7, also in presence of SUMO-2 (Figure 26-A lane 5-6 compared to lane 1-2). Intriguingly, coexpression of ATXN7-92Q with the RING mutant RNF4 dHC improved SUMOylation of ataxin-7 (Figure 26-A lane 7). This effect was potentiated by cotransfection of SUMO-2, as we observe even higher molecular weight bands above ataxin-7 (Figure 26-A lane 8). These could correspond to either poly-SUMOylated or poly-ubiquitinated ataxin-7.

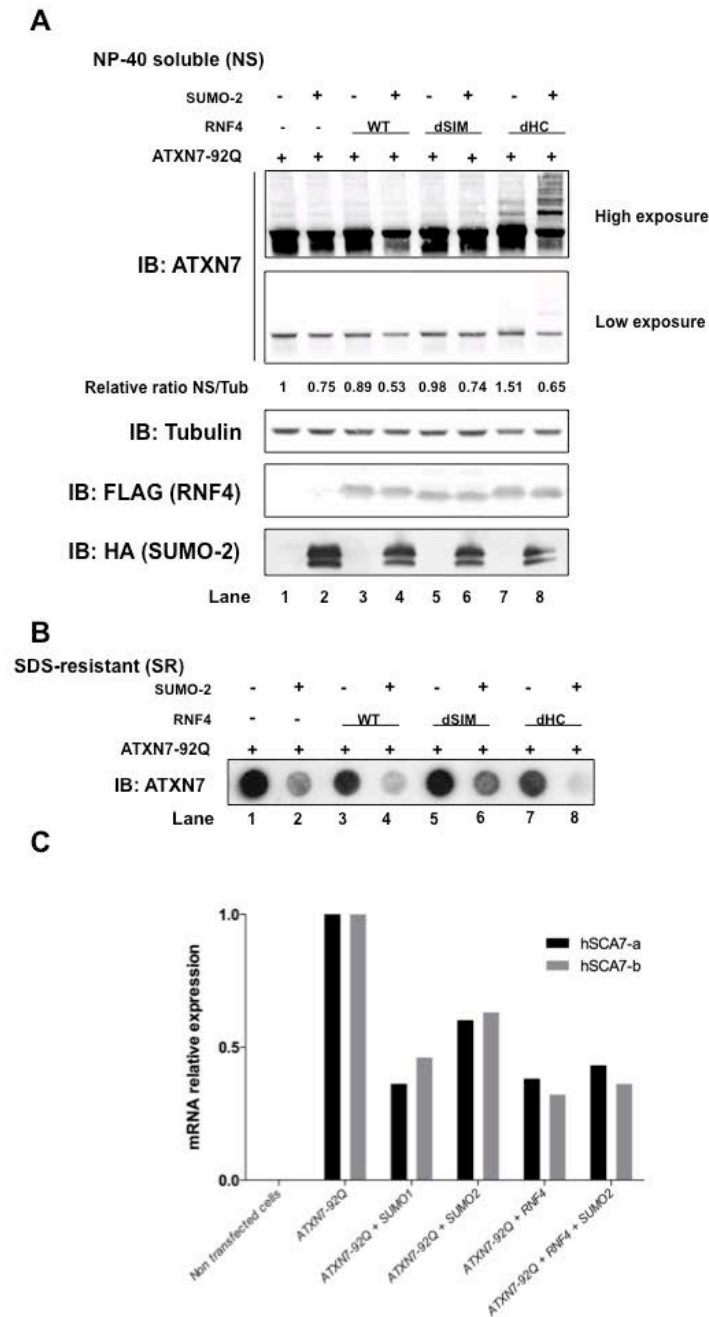


**Figure 26 - RNF4 overexpression in the presence of SUMO-2 leads to a decrease in mutant ataxin-7 aggregates**

Western blot analysis of NP-40 soluble proteins (A) and filter retardation assay of SDS-resistant aggregates (B) of ATXN7-92Q co-expressed with SUMO-2 and either wild type or mutant RNF4 in COS-7 cells. (A) Wild type RNF4 and SUMO-2 co-expression led to a greater decrease in the amount of NP-40 soluble mutant ATXN7 by 47% (lane 4) than RNF4 dSIM by 36% (lane 6). Overexpression of RNF4 dHC and SUMO-2 improved ATXN7 modification and decreased soluble protein by 35% (lane 8). Anti ataxin-7 and anti-FLAG were used, respectively, to detect mutant ataxin-7 and RNF4. Relative ratios of NS ataxin-7 versus tubulin are indicated. (B) SDS-resistant mutant ataxin-7 aggregates, in the presence of wild type RNF4 and SUMO-2 (lane 4) were reduced by 60%. Mutant RNF4 dSIM was not able to degrade ataxin-7 aggregates (lane 5 and 6). Co-expression of a RING mutant of RNF4 (RNF4 dHC) with SUMO-2 and ATXN7-92Q (lane 8) led to a greater decrease in ataxin-7 aggregation. (C) qRT-PCR. mRNAs were extracted from COS-7 cells expressing ATXN7-92Q alone or combined with SUMO-1, SUMO-2 or/and wild type RNF4. Two primers specific for the human SCA7 cDNA and a primer to GAPDH reference cDNA were used for qRT-PCR. The effect of wild type RNF4 and SUMO-2 was similar to the effect of RNF4 alone.

We then investigated the level of aggregated mutant ataxin-7, since increasing the SUMO chains on ataxin-7 and their recognition by RNF4, should lead to the degradation of soluble ataxin-7 and consequently also reduce its aggregation. We performed a filter retardation assay to test the effect of RNF4 coexpression with ATXN7-92Q. As previously described, SUMO-2 overexpression induced a decrease in ataxin-7 aggregation (Figure 26-B lane 2 compared to lane 1). The expression of wild-type RNF4 is able to slightly reduce ataxin-7 aggregates (Figure 26-B lane 3 compared to 1). Very interestingly, when wild type RNF4 and SUMO-2 were coexpressed, the decrease of aggregated mutant ataxin-7 was significantly reduced by 60% (Figure 26-B lane 4), as compared to wild type RNF4 or SUMO-2 alone. We conclude that there is an additive effect of RNF4 and SUMO-2 on mutant ataxin-7 degradation. In presence of RNF4 mutated in the SIM motifs, we did not detect a decrease in ataxin-7 aggregation (Figure 26-B lane 5), even when SUMO-2 was overexpressed (Figure 26-B lane 6). Our conclusion is that there is no cooperation between SUMO-2 and RNF4  $\Delta$ SIM, because the latter is not able to bind ataxin-7 poly-SUMO-2 chains, and cannot facilitate its degradation by the proteasome system.

Finally, we tested overexpression of RING-mutant RNF4 (RNF4 dHC) with and without cotransfection of SUMO-2 and in presence of ATXN7-92Q. With overexpression of RNF4 dHC alone, ataxin-7 aggregates are only slightly reduced, as with the other RNF4 constructs (Figure 26-B lane 7). Surprisingly, the addition of SUMO-2 induced a stronger decrease in aggregated mutant ataxin-7 (Figure 26-B lane 8). Since RNF4 dHC is mutated in the RING sequence, the protein is not supposed to ubiquitylate ataxin-7 poly-SUMO-2 chains. We may hypothesize that RNF4 dHC might form heterodimers with endogenous RNF4, such that the resultant dimer would retain catalytic ubiquitin E3 ligase activity. In that case, ataxin-7 would be poly-ubiquitinated and degraded via the proteasome. Another potential explanation may be that the C-terminal domain of RNF4 could play a role in its E3-ligase activity, in accordance with the low level of ubiquitin discharge and transfer demonstrated *in vitro* (Liew et al., 2010).

The results obtained with RNF4 on ATXN7-92Q levels raise a new question: could RNF4 also be a regulator of ataxin-7 at the transcriptional level?

The effects that we described on mutant ataxin-7 protein upon expression of RNF4 can be mediated upon the E3 ubiquitin ligase activity only and/or repression of transcription of the transfected plasmid. We thus measured the level of messenger RNA corresponding to the exogenously expressed ataxin-7 (Figure 26-C). In parallel to protein extraction, RNA was extracted from the samples, reverse transcribed and subjected to quantitative PCR. Primers were designed to specifically amplify exogenously expressed, not endogenous monkey-derived ataxin-7. We observed that RNF4 expression reduced the messenger level of overexpressed ataxin-7 by 60%, compared to mutant ataxin-7 expression with a control plasmid. We obtained a 45% reduction of ataxin-7 mRNA when only SUMO-2 was expressed, and quite similar effects were obtained (55%) when we cotransfected RNF4 in presence of SUMO-2. The effect of wild type RNF4 and SUMO-2 was similar to the effect of RNF4 alone, on overexpressed ataxin-7 messenger RNA level.

These results demonstrate that RNF4 affects the level of the overexpressed messenger encoding ataxin-7. However, it is important to note that the effects obtained at the protein level do not mirror the messenger levels. By western blot and filter retardation assay, we described an additive effect of co-expression of RNF4 with SUMO-2 on mutant ataxin-7 protein degradation, compared to RNF4 expression alone. On the contrary, ataxin-7 mRNA levels were similar in conditions where RNF4 was alone, or when RNF4 was combined to SUMO-2. This is why we conclude that a combination of SUMO-2 and RNF4 is required for the recruitment of poly-SUMOylated mutant ataxin-7 by the SUMO E3 ubiquitin ligase and promote its degradation by the proteasome.

To demonstrate that the decrease in mutant ataxin-7 is really due to proteasome degradation via RNF4 recognition, and not only mRNA reduction, we inhibited the proteasome in COS7 cells co-expressing ATXN7-92Q and wild type RNF4 plasmids. We exposed cells to 1  $\mu$ M of epoxomicin for 24 hours; epoxomicin is a cell-permeable, potent and selective irreversible inhibitor of the 20S proteasome subunit. After 24 hours of epoxomicin treatment, cells were lysed and subjected to western blot analysis and filter retardation assay.

On the western blot, we could not detect a significant increase in soluble ataxin-7 in epoxomicin-treated compared to DMSO-treated samples. In particular, we found a

decrease in the intensity of ataxin-7 when it was co-expressed with SUMO-2 and wild type RNF4, as described above (Figure 27-A). We reasonably expected, if the proteasome was inhibited, to obtain accumulation of ataxin-7, in soluble and SDS-insoluble forms. The extracts were prepared by lysis in the NP-40 0.5% buffer described in paragraph 4.7; the supernatant contained the soluble or NP-40 soluble fraction, the pellet contained the NP-40 insoluble, aggregated material, and pelleted membranes. This pellet is usually only analysed by filter retardation assay (SDS-insoluble material), but it can be further divided into SDS-soluble (SS) and SDS-resistant (SR) species after boiling for 5 min in 2% SDS-50 mM DTT. By filter retardation assay we analysed the SDS-resistant species (SR) and we observed an increase in mutant ataxin-7 aggregates in epoxomicin treated cells (Figure 27-B). Compared to DMSO treated cells, co-expression of SUMO-2 and ataxin-7 was not able to reduce protein aggregates in epoxomicin-treated cells (Figure 27-B lane 5 compared to lane 2). The same was true for RNF4 and SUMO-2 coexpression with mutant ataxin-7, attesting that SDS-resistant species accumulated in epoxomicin-treated cells (Figure 27-B lane 6 compared to lane 3). Interestingly, when we subjected the SDS-soluble (SS) species to western blot analysis, we observed a significant accumulation of ataxin-7 in epoxomicin-treated cells compared to DMSO-treated cells (Figure 27-C). In cells expressing ATXN7-92Q and SUMO-2 treated with epoxomicin, an increase in ataxin-7 levels was observed (Figure 27-C lane 5 compared to lane 2), supporting our hypothesis that SUMO-2 induces the modification and subsequent degradation of ataxin-7 via the proteasome. The co-expression of wild type RNF4 and SUMO-2 in epoxomicin treated cells was unable to activate degradation of either SDS-resistant or SDS-soluble ataxin-7 (Figure 27-B and -C lane 6 compared to lane 3). Note that on western blot of epoxomicin-treated cells, we found in the SDS-soluble fraction (Figure 27-C lane 6 compared to lane 3), an increase in RNF4 protein (Figure 27-C lane 6 compared to lane 3). Like PML (Janer et al., 2006), RNF4 might co-aggregate or be co-trapped into mutant ataxin-7, and be released after boiling in 2% SDS. These results confirm an involvement of RNF4 in mutant ataxin-7 degradation via the proteasome. Finally, we showed that epoxomicin treatment inhibited the proteasome, since we observed the accumulation of ubiquitin species. Altogether we confirmed here that mutant ataxin-7 is degraded by the proteasome, via implication of RNF4 and SUMO-2. This

effect is independent of RNF4-mediated transcriptional repression of the ataxin-7 plasmid (Figure 26-C).

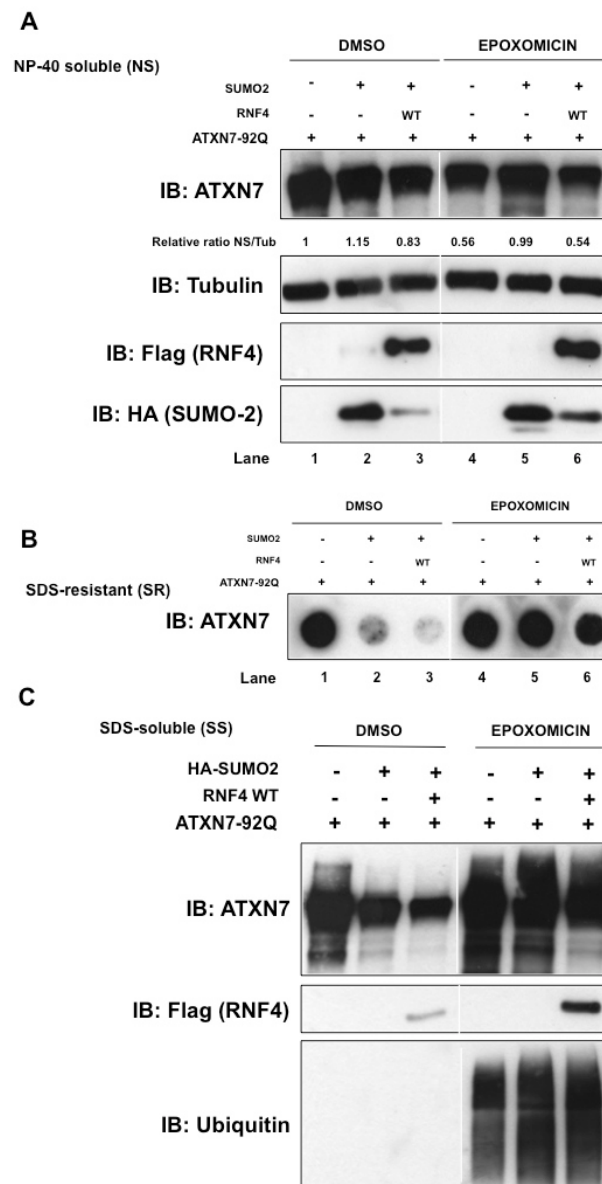


**Figure 27 - Proteasome inhibition abolishes mutant ataxin-7 degradation by RNF4**

(A) Western blot. COS-7 cells were transfected with ATXN7-92Q with or without SUMO-2 and RNF4. Inhibition of the proteasome by epoxomicin (1  $\mu$ m) treatment did not increase NP-40-soluble ataxin-7 (NS) fractions (lane 4-6 compared to 1-3). Mutant ataxin-7 was detected with an anti ataxin-7, RNF4 with anti-FLAG, SUMO-2 with anti-HA antibodies. Relative ratios of NS ataxin-7 versus tubulin are indicated. (B) Filter retardation assay. ATXN7-92Q, wild type RNF4 and SUMO-2 overexpression decreased SDS-resistant (SR) aggregates (DMSO, lane 2 and 3 compared to lane 1). Proteasome inhibition by epoxomicin treatment abolished the effect of RNF4, leading to an important accumulation of aggregated mutant ataxin-7 (lane 5 and 6 compared to 2 and 3). Anti ataxin-7 antibody detected mutant ataxin-7 aggregates. (C) Western blot analysis of the effects of overexpressed SUMO-2 and RNF-4 on the SDS-soluble ataxin-7 separated from aggregates (SS). Epoxomicin-treatment induced ataxin-7 accumulation even when SUMO-2 and RNF4 were overexpressed (lane 4-6 compared to 1-3). Thus, the degradation of mutant ataxin-7 by RNF4 occurs via the proteasome. An anti-ubiquitin antibody was used to detect non-degraded ubiquitinated proteins, confirming the efficacy of proteasome inhibition.

The above-described experiment confirmed the effect of epoxomicin. We undertook to test other proteasome inhibitors, MG132 and lactacystin. MG132 is a strong reversible inhibitor of the multiple peptidase activities of the proteasome; lactacystin is an antibiotic that hydrolyses cellular clasto-lactacystin into beta-lactone, an active inhibitor of the 20S proteasome. We transfected COS7 cells with ATXN7-92Q alone and co-expressed with SUMO-2 and wild type RNF4 (Figure 28-A). The cells were treated for 16 hours at 10  $\mu$ M MG132 or 10  $\mu$ M lactacystin before lysis. The analysis of the NP-40 soluble fractions by western blot showed no increase in soluble ataxin-7 protein in samples treated with MG132 and lactacystin. To further confirm that these components blocked the proteasome, we reprobbed the membrane with anti-ubiquitin, and detected an increase in ubiquitin species in samples treated with MG132 and lactacystin (Figure 28-A). This confirms the inhibition of the proteasome machinery.

To analyse the effects of proteasome inhibition on SDS-resistant (SR) samples, we performed a filter retardation assay (Figure 28-B). Interestingly, when we co-transfected ATXN7-92Q with SUMO-2 and wild type RNF4, we detected a decrease in mutant ataxin-7 aggregates in DMSO treated cells, but strangely also in MG132- and lactacystin-treated cells. This suggests that, under specific conditions, mutant ataxin-7 could be degraded by another pathway such as autophagy. This hypothesis is consistent with our recent publication in which we showed that autophagy, the major pathway for organelle and protein turnover, is implicated in SCA7 (Alves et al., 2014). In particular, we demonstrated in a cellular model that the autophagy flux was impaired but not completely blocked in cells overexpressing full-length mutant ataxin-7. In addition, it is known that, when the proteasome is impaired, the autophagic degradative pathway may be turned on (Ding et al., 2007) (Rideout et al., 2004). This led us to consider the activation of the autophagy pathway as a possible way to degrade ataxin-7 in presence of proteasome inhibition by MG132 or lactacystin at the concentration used (10  $\mu$ M). Further investigations will be however necessary to confirm this hypothesis.

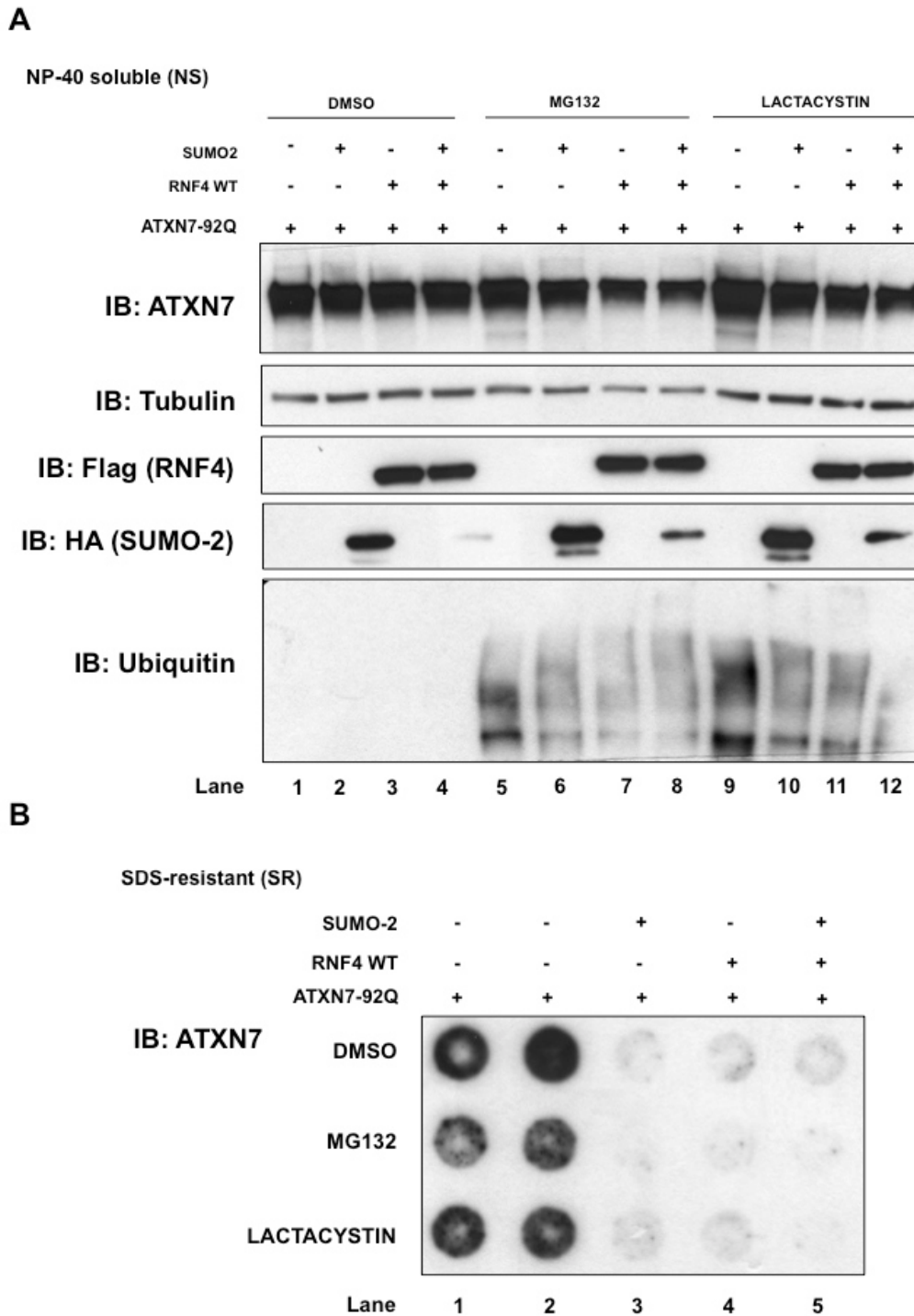


**Figure 28 - Proteasome inhibition by high concentration of MG132 and lactacystin did not impair mutant ataxin-7 degradation by overexpressed RNF4**

(A) Mutant ATXN7-92Q and SUMO-2 were co-expressed, in COS7 cells, with or without RNF4. The proteasome inhibition was inhibited by treatment with 10  $\mu$ M MG132 (lane 5-8) or 10  $\mu$ M lactacystin (lane 9-12) for 16 hours. Soluble and aggregated ataxin-7 were detected with an anti-ataxin-7 antibody, RNF4 with an anti-FLAG and SUMO-2 with anti-HA antibodies. Poly-ubiquitinated proteins were detected with an anti-ubiquitin antibody, confirming proteasome inhibition. (B) Even after strong proteasome inhibition, the filter retardation assay showed that SUMO-2 overexpression, with or without RNF4 overexpression, decreased mutant ataxin-7 aggregates (lane 3-5 compared to 1-2), suggesting that mutant ataxin-7 was degraded another cellular pathway. Mutant ataxin-7 was detected with an anti ataxin-7 antibody.

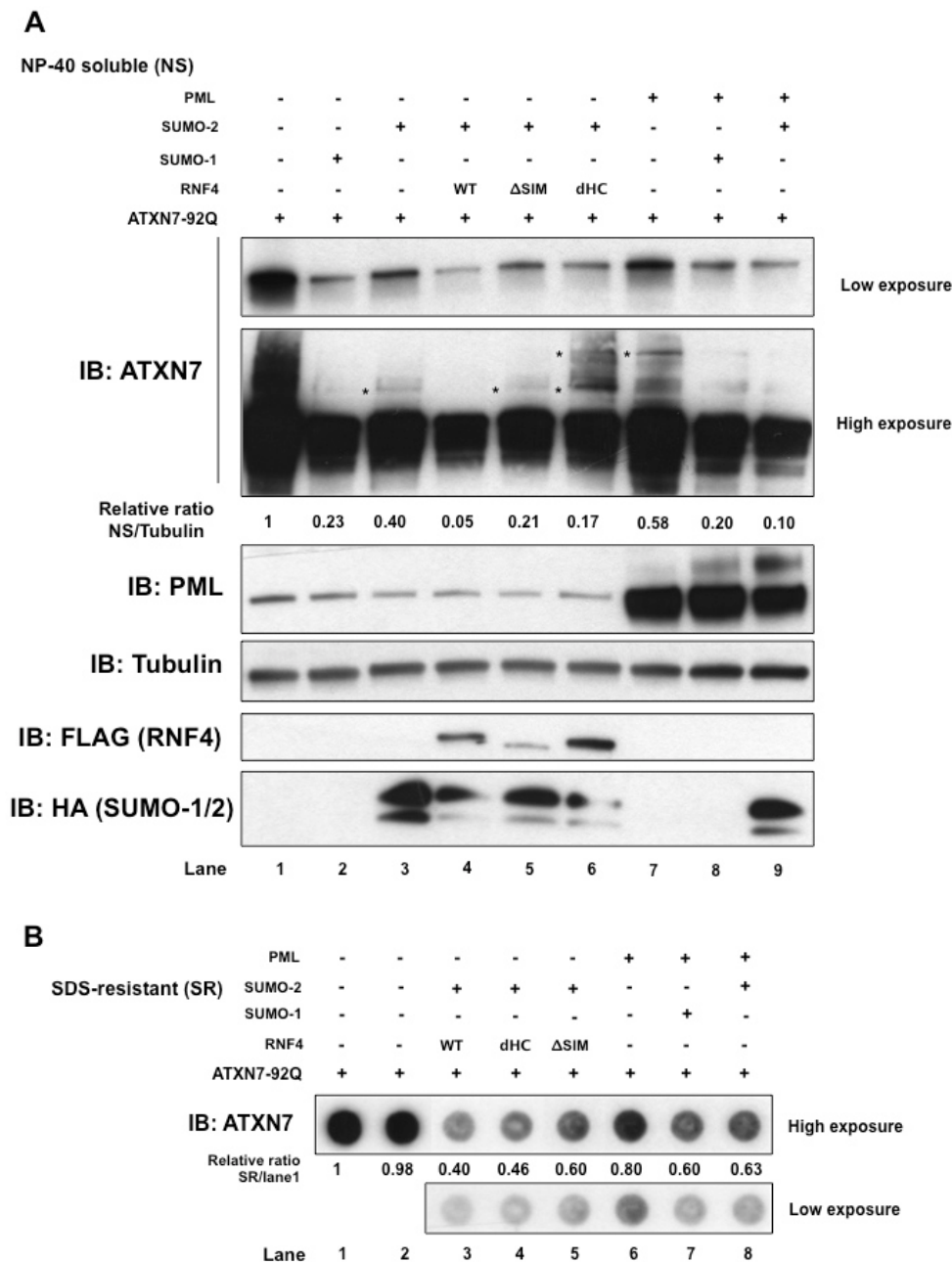


**Figure 29 - Degradation of mutant ataxin-7 in the presence of PML IV or RNF4**

(A) Western blot analysis. ATXN7-92Q and wild type or mutant RNF4 were co-expressed in COS-7 cells, with or without SUMO-2 (lane 1-6). SUMO-1 or SUMO-2 overexpression reduced NP-40 soluble mutant ataxin-7 and the higher molecular weight bands corresponding to SUMO-modified protein (lane 2 and 3 compared to 1). Overexpression of wild-type RNF4 decreased soluble ataxin-7 more than SUMO-2 (lane 4 compared to 3) or ATXN7-92Q co-expressed with a mock plasmid (lane 4 compared to 1). RNF4  $\Delta$ SIM and dHC co-expression with SUMO-2 did not reduce soluble ataxin-7 to the levels observed with wild-type RNF4 (lane 5 and 6 compared to 4). RNF4 dHC increased high molecular weight bands corresponding to ataxin-7 modified by poly-SUMO or poly-ubi (lane 6). ATXN7-92Q was also co-expressed with PML IV, in presence of SUMO-1 or SUMO-2 (lanes 7-9): PML overexpression decreased mutant ataxin-7 (lane 7 compared to 1); the effect was greater when co-expressed with SUMO-1 or SUMO-2 (lane 8 and 9 compared to 1). Anti-ataxin-7 and anti-PML were used to detect the respective proteins. Anti-FLAG detected RNF4 and anti-HA SUMO-1 and SUMO-2. \* Post-translationally modified ataxin-7. Relative ratios of NS ataxin-7 versus tubulin are indicated. (B) Filter retardation assay showing that wild type RNF-4 coexpression with SUMO-2 (lane 3-5 compared to lane 1-2) reduced mutant ataxin-7 aggregates more than PML (lane 6-8 compared to lane 1-2). Relative ratios of SR ataxin-7 versus lane 1 are indicated.

To better understand the impact of RNF4 on ataxin-7, we compared it to PML, as PML IV was shown to degrade mutant ataxin-7 in clastosomes (Janer et al., 2006). As shown in Figure 29-A, we transfected ATXN7-92Q in COS7 cells with wild type and mutant (dSIM and dHC) RNF4 and compared them to the samples transfected with ATXN7-92Q and PML IV co-expressed with SUMO-1 or -2. SUMO-1 and SUMO-2 alone induced a decrease in NP-40-soluble protein (NS) and SDS-resistant species (Figure 29-A and -B). When co-expression of wild type RNF4 and SUMO-2 was analysed, we obtained a reduction of 95% of soluble (Figure 29-A lane 4) and 60% of ataxin-7 SDS resistant protein (Figure 29-B lane 3). The effect was less important for mutant RNF4 and SUMO-2 co-expression: 40% of reduction with dSIM and 54% with dHC. We then compared wild type RNF4 expression to expression of PML IV alone or with SUMO-1/-2, and their respective effects on the amount of mutant ataxin-7. With PML overexpression we obtained a reduction of soluble ataxin-7 by 42% and by 20% for the insoluble form. The co-expression with SUMO-1 or SUMO-2 improves the decrease of both soluble (by 80 and 90%, respectively) and insoluble (by 40 and 37%, respectively) mutant ataxin-7. These results suggest that PML is able to reduce soluble and insoluble mutant ataxin-7 protein but RNF4 overexpression could be more efficient to poly-ubiquitinate and recruit ataxin-7 to the proteasome and increase its degradation.

### 3.3. SUMO pathway deregulation in SCA7 KI mice

#### 3.3.1. Deregulation of PIAS and SUMO in SCA7 mouse brain

The key to the discovery of therapeutic targets that regulate SUMOylation may be the identification of the E3 ligase that promotes SUMOylation of ataxin-7. This is why we investigated whether ataxin-7 is modified via a major SUMO E3 ligase that we identified as RanBP2 or PIAS4. In order to establish whether these enzymes are indeed *in vivo* candidates for therapeutic strategies, we investigated their expression in brain regions affected by the SCA7 disease. We obtained from Prof. Huda Zoghbi a polyQ-Atxn7 knock-in line, *Atxn7<sup>100Q/5Q</sup>*, that developed previously described symptoms of a SCA7 mouse model including weight loss, kyphosis, ataxia, ptosis, tremors and gradual loss of mobility (Yoo et al., 2003). This line named *Atxn7<sup>100Q/5Q</sup>*

was derived from the *SCA7*<sup>266Q/5Q</sup> line by spontaneous contraction of the CAG repeat (Chen et al., 2012). Wild-type *Atxn7*<sup>5Q/5Q</sup> mice have a lifespan of more than 24 months, whereas *Atxn7*<sup>100Q/5Q</sup> mice have a shorter lifespan, averaging 13 months in our colony.

To determine whether the expression of SUMO pathway-related genes was affected by mutant ataxin-7, we quantified the expression of each gene by quantitative RT-PCR, in wild-type *Atxn7*<sup>5Q/5Q</sup> and *Atxn7*<sup>100Q/5Q</sup> mouse cerebellum, striatum and retina. We performed these analyses at 6 months, before or close to symptom onset, and at 12 months, at the end of their lifespan when they had severe SCA7 symptoms. Since the most affected regions in SCA7 are the cerebellum and retina, we analysed mRNA expression in these tissues; the striatum, which is not affected by neurodegeneration in the SCA7 mouse model, was used as a control.

With quantitative RT-PCR (qRT-PCR), we detected some deregulations that began to occur as early as at 6 months of age, when the aggregates were detectable by IHC but symptoms were not yet present. At six months, we observed statistically significant reductions in *Sumo-2*, *Senp1*, *Senp2* and *PanPML* expression in SCA7 cerebellum, compared to wild type littermates (Figure 30-A), and of *Senp1*, *RanBP2* and *PanPML* expression in SCA7 striatum (Figure 31-A). At 12 months, we found a statistically significant reduction in *Sumo-1*, *Pias4*, *Senp2*, *RanBP2* and *Pml isoform 3* expression in SCA7 cerebellum (Figure 30-B), *Senp3*, *Senp6* in SCA7 striatum (Figure 31-A) and *Senp6* also in SCA7 retina (Figure 31-B).

These results strongly suggest that, *in vivo*, SUMO-modifying pathways might be perturbed in SCA7. The reductions in *Sumo-1* and *Sumo-2*, specifically in the cerebellum, the region of greatest vulnerability to neurodegeneration, were particularly noteworthy. Moreover, the significant decrease at the late stage of the disease (12 months) in mRNA levels of *RanBP2* and *Pias4* supports our hypothesis concerning the importance of these enzymes in ataxin-7 modification by the SUMO pathway, this time in an *in vivo* SCA7 model. As for Senps, we noticed a significantly reduction in *Senp1* and 2, the main role of which in the SUMOylation process is to de-conjugate SUMO-1 and SUMO-2. It is interesting to note that the reduction in *Senp1* and *Senp2* mirror those of *Sumo-1* and *Sumo-2* at 6 months. This result was particularly noteworthy for *Senp2*, the translation product of which is present at the

nuclear pore complex, the location we suppose to be the principal site of SUMOylation for ataxin-7 by RanBP2. The most consistent changes in this SCA7 mouse model was the downregulation of the SUMO pathway, strongly suggesting that it may be deregulated *in vivo*.

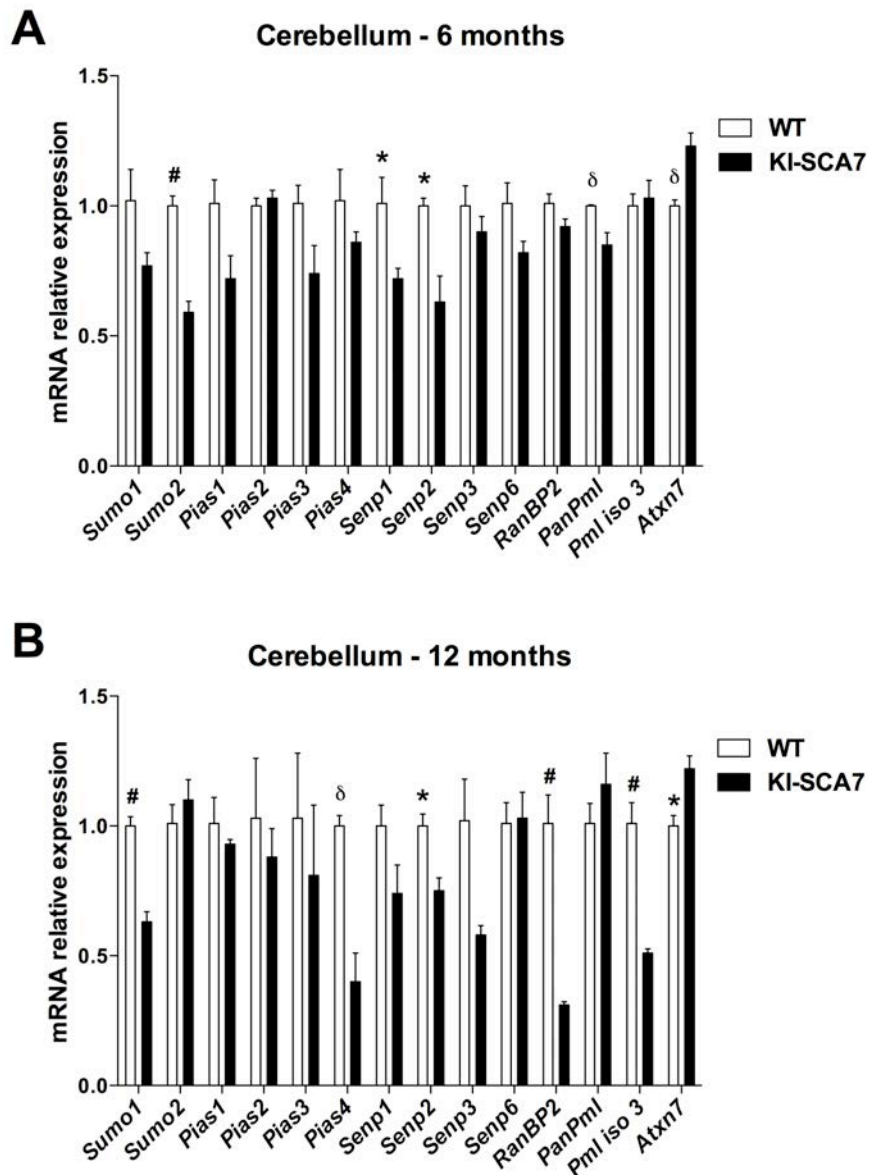


**Figure 30 - Downregulation of SUMO-1 and SUMO-2 mRNA in *Atxn7*<sup>100Q/5Q</sup> KI mice**  
qRT-PCR analysis of SUMO-modifying proteins and enzymes in cerebella of *Atxn7*<sup>100Q/5Q</sup>. (A) qRT-PCR of SUMO mRNAs from cerebella of 6-month-old SCA7 KI mice and wild-type littermates. SUMO enzymes were differentially expressed in SCA7 KI versus wild type with statistically significant decreases in *Sumo-2* ( $p = 0.003$ ), *Semp-1* ( $p = 0.03$ ), *Semp2* ( $p = 0.015$ ), *PanPML* ( $p = 0.04$ ). (B) qRT-PCR of SUMO mRNAs from cerebella of 12-month-old SCA7 KI mice and wild-type littermates. SUMO enzymes were differentially expressed in SCA7 KI versus wildtype mice with a statistically significant decrease in *Sumo-1* ( $p = 0.003$ ), *Pias4* ( $p = 0.013$ ), *Semp2* ( $p = 0.016$ ), *RanBP2* ( $p = 0.007$ ), *PML iso 3* ( $p = 0.0002$ ). Samples were analysed in triplicate and normalized to mouse *36b4*. Data are shown as SCA7 KI expression relative to wild-type levels set at 1 for each enzyme with  $\pm$  SEM ( $n=4$ ). \*  $p < 0.05$   $\delta$   $p < 0.01$  #  $p < 0.005$

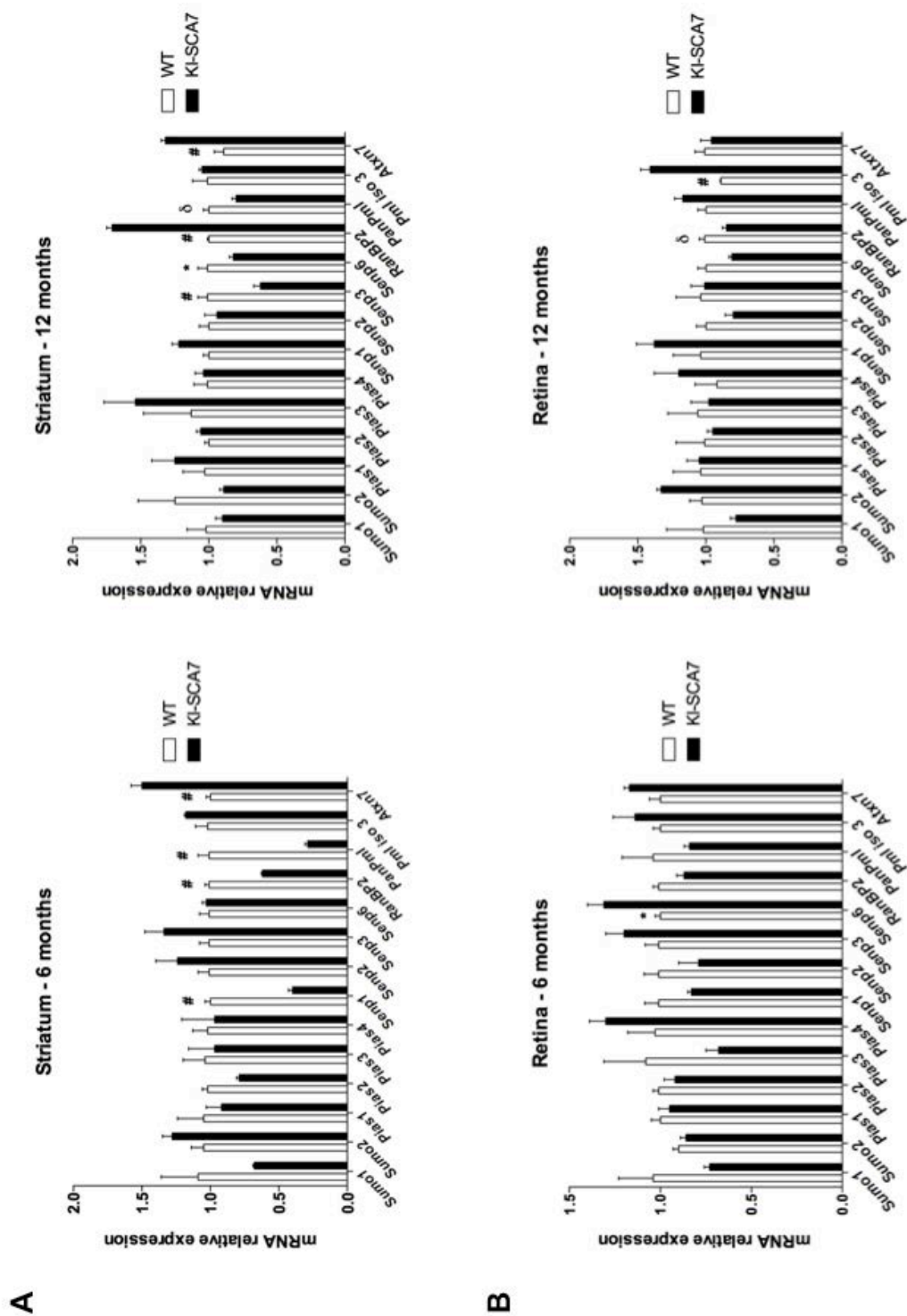


**Figure 31 - qRT-PCR analysis of SUMO-modifying proteins and enzymes in striatum and retina of wild-type compared to *Atxn7*<sup>100Q/5Q</sup> KI mice**

(A) qRT-PCR of SUMO mRNAs from striata of 6- and 12-month-old SCA7 KI mice and wild-type littermates. SUMO enzymes were differentially expressed in SCA7 KI versus wild-type mice with statistically significant decreases in *Senp1* ( $p = 0.029$ ), *RanBP2* ( $p = 0.0014$ ), *PanPml* ( $p = 0.0001$ ) in 6-month-old mice; *Senp3* ( $p = 0.005$ ), *Senp6* ( $p = 0.04$ ) and *PanPml* ( $p = 0.007$ ) for 12-month-old mice. (B) qRT-PCR of SUMO mRNAs from retina of SCA7 KI mice and wild-type littermates. SUMO enzymes were differentially expressed in SCA7 KI versus wild type with a statistically significant decrease in *Senp6* ( $p = 0.045$ ) at 12-months-old. Samples were analysed in triplicate and normalized to mouse *36b4*. Data are shown as SCA7 KI expression relative to wild-type littermate levels set at 1 for each enzyme with  $\pm$  SEM ( $n = 4$ ). \*  $p < 0.05$  #  $p < 0.01$   $\delta$   $p < 0.005$

We then focused our attention on the potential deregulation of the mRNA for murine PML isoform 3 corresponding to the human isoform IV (Figure 30-A and -B). This is especially interesting, since we previously showed that stimulation of PML transcription by interferon-beta provides a possible therapeutic strategy to counteract mutant ataxin-7 aggregation (Chort et al., 2013). This treatment is also a potential way to improve the behavioural performance of SCA7<sup>266Q/5Q</sup> KI mice. At 6 months of age, *Atxn7*<sup>100Q/5Q</sup> mice showed a small increase in the mRNA of *Pml isoform 3*; on the contrary, at 12 months, they showed a dramatic decrease of about 50%. These data are extremely important, because they suggest that the pathology might deregulate other cellular pathways in addition to SUMOylation. Since we know that PML isoform IV is the main constituent of clastosomes (Janer et al., 2006), the small increase found at 6 months might be a hint that early on the mice try to compensate for mutant ataxin-7 accumulation by upregulating *Pml 3*, and at late stage (12 months) the decrease in its mRNA level suggests that less PML protein may be present to constitute clastosomes. The negative consequence of such deregulation could be a worsening of the pathology due to the reduced presence of nuclear PML, which we demonstrated to be one of the main actors for mutant ataxin-7 degradation (Janer et al., 2006).

In order to verify whether deregulation of the expression of mRNA of elements of the SUMO pathway also induces a change in protein expression, we performed a western blot on whole cerebellar lysates. We compared four samples from *Atxn7*<sup>5Q/5Q</sup> mice against four samples from *Atxn7*<sup>100Q/5Q</sup> mice at 12 months of age. Soluble wild-type ataxin-7 levels did not change. In addition, high molecular weight insoluble mutant ataxin-7 was detected in the stacking gel for *Atxn7*<sup>100Q/5Q</sup> mice but not their wild-type littermates (Figure 32-A). This accumulation of mutant ataxin-7 observed by western blot was further confirmed by filter retardation assays of the same samples (Figure 32-C).

The main goal of the experiments described above was to verify whether a deregulation of proteins implicated in SUMOylation actually existed in *Atxn7*<sup>100Q/5Q</sup> mice. To this end, we compared SUMO-1 and SUMO-2 expression levels, and saw an increase in the soluble forms of both proteins in *Atxn7*<sup>100Q/5Q</sup> mice (Figure 32-B). This increase was consistent with the decrease of SUMO-1 and SUMO-2 detected in

modified high molecular weight proteins. This was clearly observed in the stacking gel on western blot (Figure 32-B) and filter retardation assays (Figure 32-C), which showed decreases in the insoluble proteins SUMO-1 and SUMO-2.

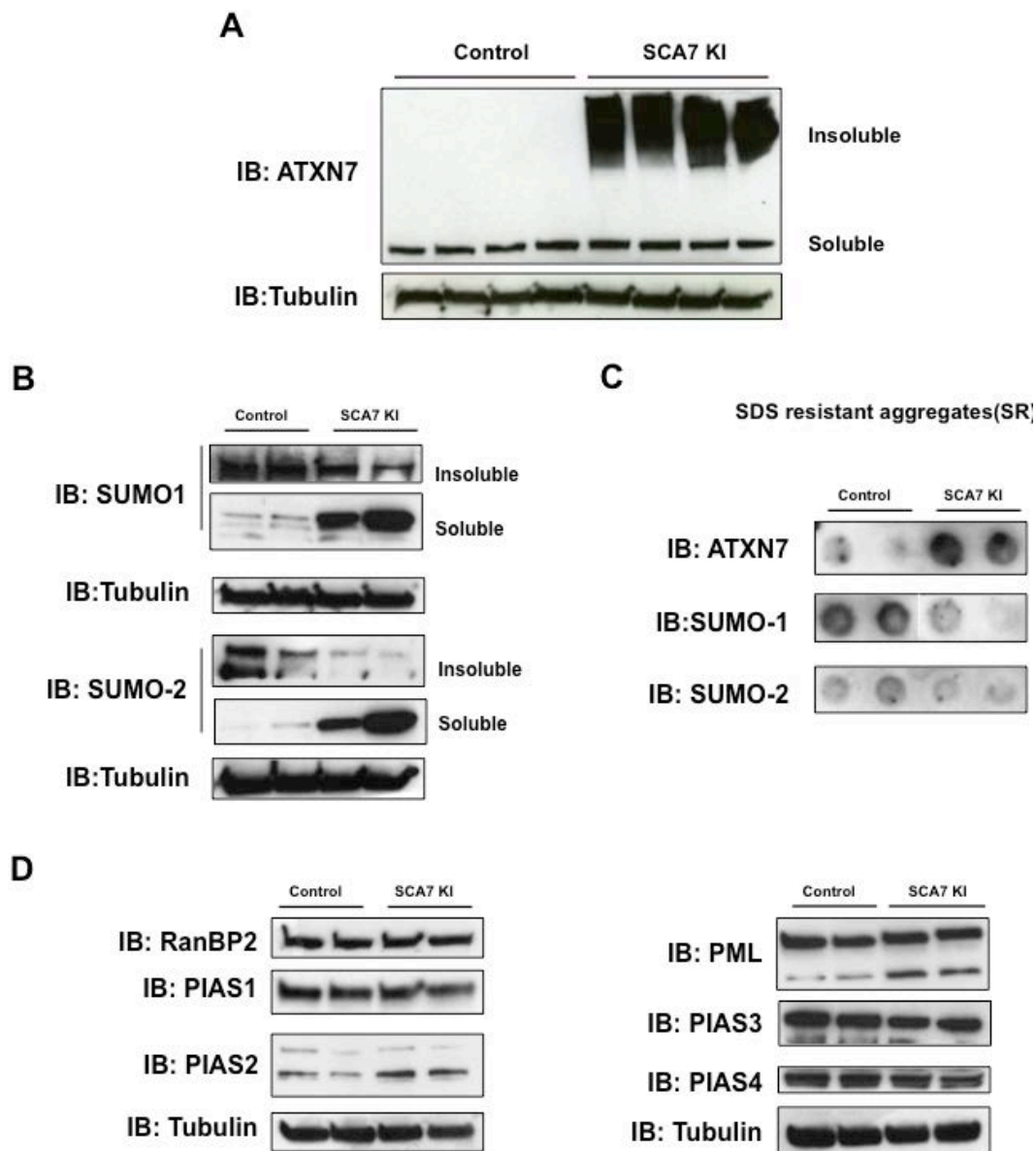


**Figure 32 - Deregulation of SUMO-modifying proteins and enzymes expression in *Atxn7<sup>100Q/5Q</sup>* KI mouse model at a late stage of disease**

(A) Representative western blot showing an accumulation of insoluble ataxin-7 protein in the stacking gel from mouse cerebella of *Atxn7<sup>100Q/5Q</sup>* at 12-months of age (n=4) compared to wild-type littermates at the same age (n=4). (B) SUMO-1 and SUMO-2 protein expression in SCA7 KI (n=2) and age-matched control mice (n=2): both proteins increased soluble ataxin-7 in SCA7 KI compared to wild-type samples, consistent with the reduction of insoluble SUMO-1 and SUMO-2 proteins in the stacking gel. Anti-ataxin-7 was used to detect mouse ataxin-7, and polyclonal anti-SUMO-1 or SUMO-2 antibodies were used to identify SUMO-1 and SUMO-2, respectively. (C) Filter retardation assay performed on *Atxn7<sup>100Q/5Q</sup>* mice at 12-months of age confirmed the increase of insoluble ataxin-7 in cerebella of SCA7 KI compared to wild type. SUMO-1-positive SDS-insoluble material was reduced in SCA7 KI mice compared to samples from wild-type mice. SUMO-2-positive proteins “aggregates” were slightly reduced in *Atxn7<sup>100Q/5Q</sup>*. Antibodies used were the same as for the western blot. (D) Expression of the SUMO-modifying enzyme PIAS1 did not change. PIAS2 expression increased in SCA7 KI compared to

wild-type mice. PIAS3 and PIAS4 decreased slightly in cerebella of *Atxn7<sup>100Q/5Q</sup>* mice compared to wild-type littermates. Two major bands corresponding to PML were detected: the upper band (presumably isoforms 1 and 2) did not change; the lower band (presumably isoforms 3 and 4) increased in SCA7 KI mice compared to wild-type littermates. Polyclonal anti-PIASn and PML were used to identify the protein.

These results suggest that the efficiency of the modification by SUMO of ataxin-7 is reduced over time. A notable decrease of SUMO-2-modified proteins in the insoluble fraction, shown on western blot, (Figure 32-B) also suggests that fewer SUMO chains are conjugated, thus impairing overall degradation.

We then determined whether other enzymes in the SUMOylation pathway were deregulated in *Atxn7<sup>100Q/5Q</sup>* mice. Expression of RanBP2 and PIAS1 did not change, whereas PIAS2 expression increased by 70% (Figure 32-D). PIAS3 and PIAS4 expression decreased by 15%, respectively: this is consistent with the reduction in *Pias3* and *Pias4* mRNA shown above (Figure 31-B).

Investigating on PML protein expression, we did not detect any change of the 100-kDa band probably corresponding to the soluble murine isoform 1 or 2 protein in *Atxn7<sup>100Q/5Q</sup>* 12 months old mice compared to wild type littermates at the same age. The 70-kDa band that might correspond to mouse isoform 3 or 4, the smallest PML isoforms, however increased (Figure 32-D).

These last results confirm deregulation of the expression the proteins involved in the SUMOylation process in SCA7 KI mice. We then determined whether the changes in expression were associated with changes in the cellular localisations of ataxin-7 and SUMO. To this end, we performed an immunohistofluorescence study on *Atxn7<sup>5Q/5Q</sup>* and *Atxn7<sup>100Q/5Q</sup>* brain slices from 12-month-old mice. In wild type mice, we detected a significant amount of ataxin-7 in the cytoplasm (Figure 33-A). Co-staining ataxin-7 with the GMP1 (SUMO-1) antibody was performed to detect the colocalization of ataxin-7 and SUMO-1 in intranuclear inclusions (Figure 33-B). In Figure 33-A, ataxin-7 and SUMO-1 are co-localized at the nuclear membrane. This corresponds to the localisation of RanBP2, the major candidate enzyme for SUMO-1 conjugation to ataxin-7. Thus, the results of this immunohistofluorescence experiment are consistent with the hypothesis concerning the role of RanBP2.

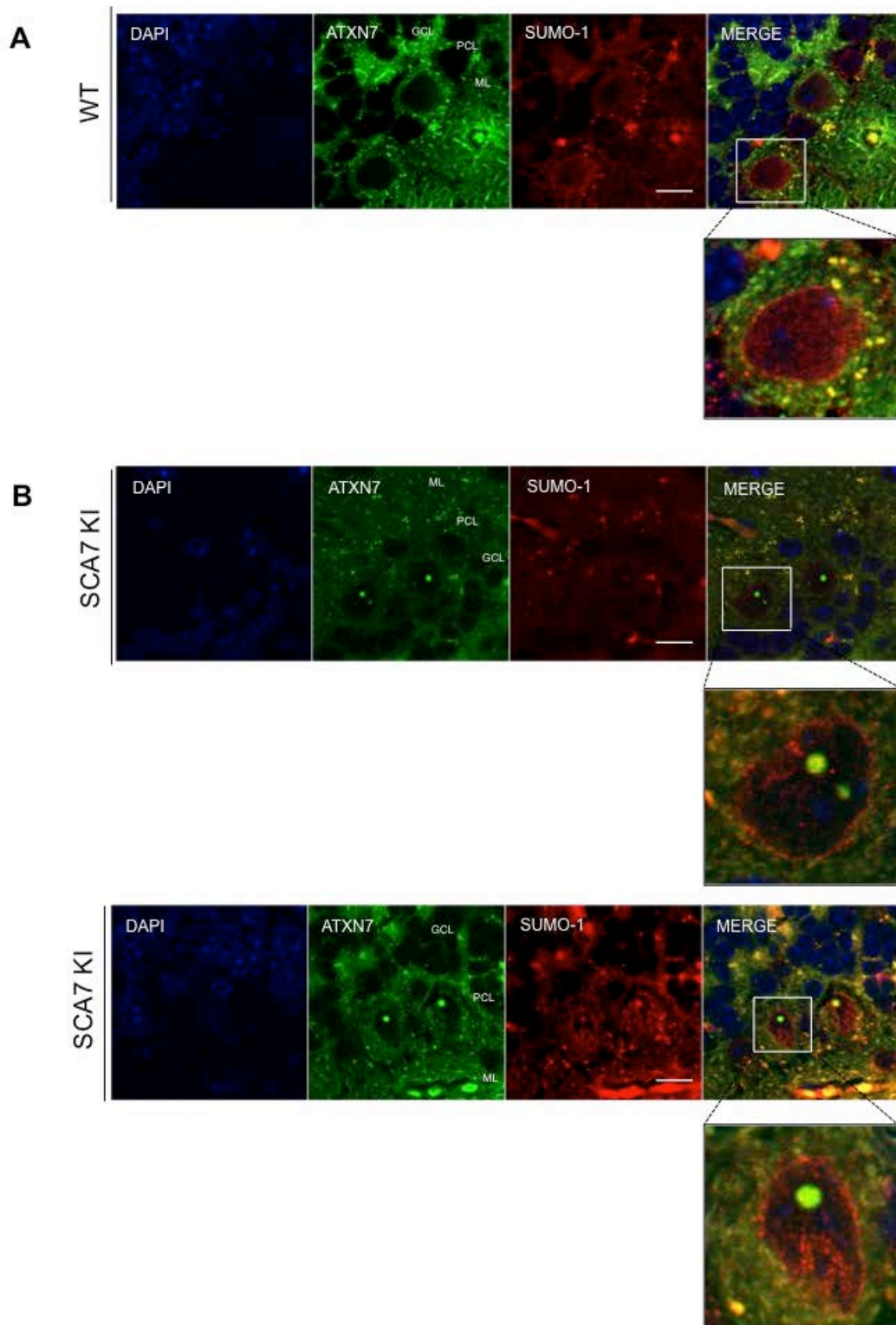


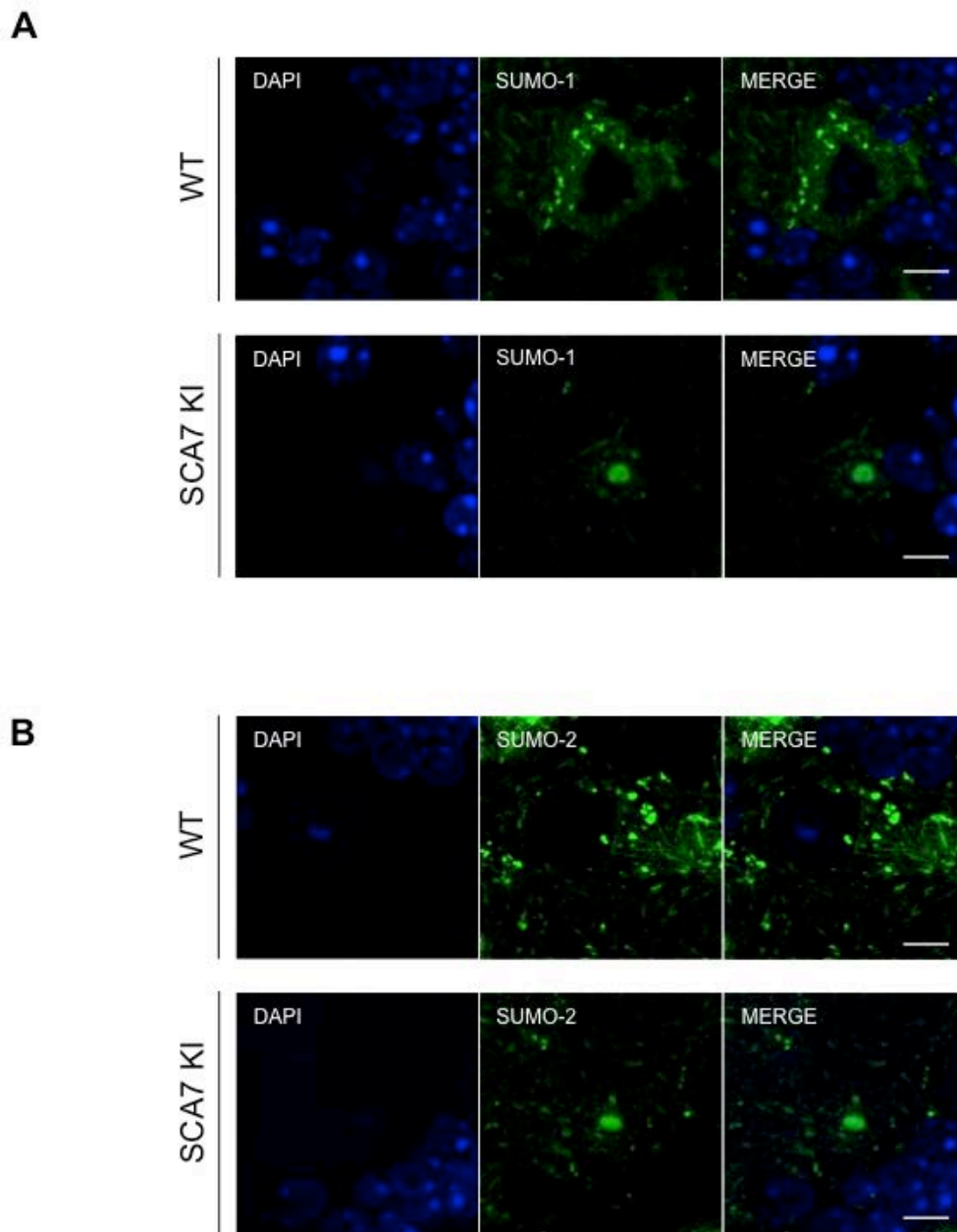
**Figure 33 - Co-localisation of SUMO-1 and ataxin-7 in the cerebellum of *Atxn7*<sup>1000/50</sup> KI mice**  
 (A) Purkinje cells in the cerebellum of a 12-month-old wild-type littermate were labelled with anti-ataxin-7 and anti-GMP1 (SUMO-1) antibodies. Ataxin-7 immunoreactivity was detected as diffuse staining in the cytoplasm, but was also present in cytoplasmic dots. SUMO-1 was present along the nuclear membrane, in granular staining in the nucleoplasm and in cytoplasmic dots. Ataxin-7 and SUMO-1 colocalized in the latter and partially co-localized along the nuclear membrane. (B) Purkinje cells from the cerebellum of a 12-month-old knock-in mouse showed partial colocalisation of SUMO-1 with intranuclear inclusions. One large size inclusion contained SUMO-1, whereas a smaller inclusion in the same Purkinje cell was ataxin-7 but not SUMO-1 positive. In the lower panel SUMO-1

immunoreactivity was detected along the nuclear membrane and in a large, round ataxin-7-positive inclusion. Co-localisation was very strong, as attested by the yellow dots in the inclusion (see enlargement). Note that, in this enlargement of a Purkinje cell, some colocalisation of ataxin-7 and SUMO-1 can be seen at the nuclear membrane, potentially corresponding to the nuclear rim. Intense yellow colocalisation within an aggregate is also detected in a second Purkinje close to the enlarged cell. GCL, Granular cell layer; PCL, Purkinje cell layer; ML, Molecular cell layer. Confocal images are shown. Scale bar 20  $\mu$ m

We also examined by immunohistofluorescence the presence of mutant ataxin-7 intranuclear inclusions in Purkinje cells in 12-month-old *Atxn7<sup>100Q/5Q</sup>* (Figure 33-B). In the cerebellum, these aggregates are usually present as one or two big ataxin-7-positive dots in Purkinje cell nuclei. SUMO-1, present at the nuclear membrane of SCA7 KI mice was also clearly co-localized with ataxin-7 aggregates inside the nucleus (Figure 33-B).

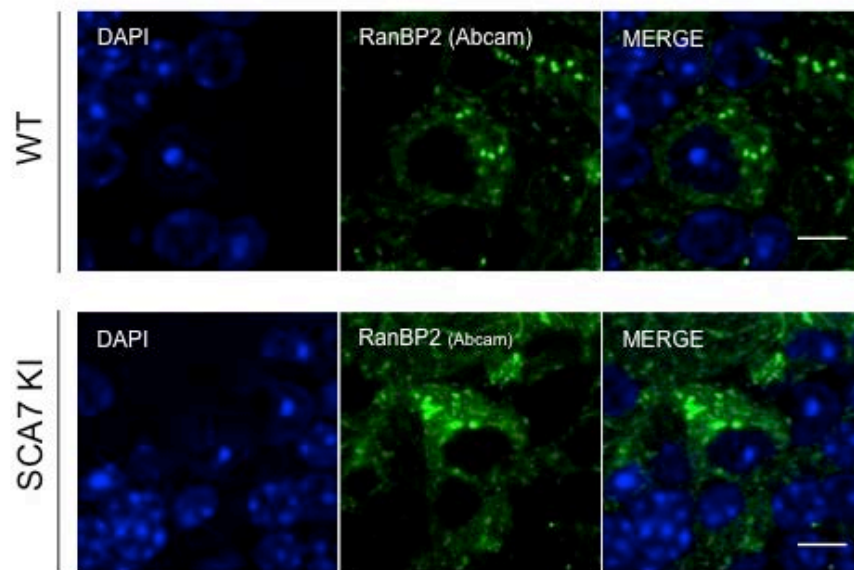
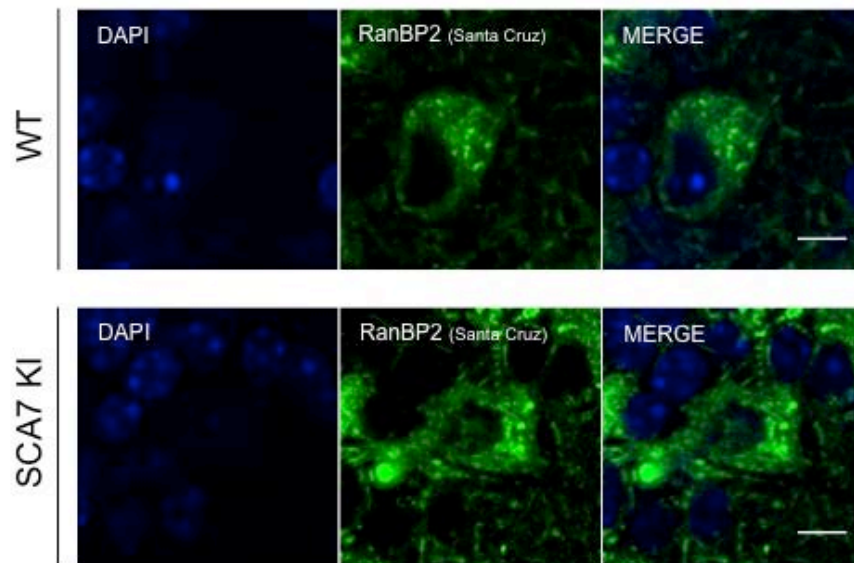
Using different antibodies SUMO-1 and SUMO-2 staining were also performed in *Atxn7<sup>100Q/5Q</sup>* mice and their wild type littermates. In wild type brain tissue, cytosolic SUMO-1 and SUMO-2 staining was stronger than in SCA7 KI brains (Figure 34). In SCA7 KI mice we observed a decrease in the general cytosolic staining (Figure 34-A and B upper panel), but an increase in nuclear immunoreactivity of SUMO-1 and SUMO-2, particularly as dots in Purkinje cell nuclei that may correspond to ataxin-7 aggregates (Figure 34-A and B bottom panel). SUMOylation seems therefore to be part of the physiopathological process in SCA7.

As for RanBP2, quantitative RT-PCR showed a statistically significantly decrease in *RanBP2* mRNA levels at 12 months in *Atxn7<sup>100Q/5Q</sup>* mice. On the contrary, by western blot, we did not detect any difference at the protein level for RanBP2 comparing two wild-type littermates to two *Atxn7<sup>100Q/5Q</sup>* mice. Immunohistological analysis on SCA7 KI mice compared to wild-type littermates showed an increase in RanBP2-positive punctate structures in the cytoplasm of Purkinje cells (Figure 35-A and B bottom panel). We confirmed, using two different anti-RanBP2 antibodies, the specificity of this staining related to SCA7 mice: both of them showed an increase of cytosolic staining in Purkinje cells from *Atxn7<sup>100Q/5Q</sup>* mice. This localisation is consistent with previous studies that described how RanBP2 is present not only at the nuclear envelope but also in the extranuclear annulate lamellae (AL), which are thought to serve as reservoirs of excess nuclear membrane components (Tirard et al., 2012).



**Figure 34 - SUMO-1 and SUMO-2 in nuclear dots in *Atxn7<sup>100Q/5Q</sup>* knock-in mice**

(A) Upper panel: confocal immunofluorescence images of Purkinje cells from a 12-month-old wild-type mouse showing diffuse, intense cytoplasmic staining of SUMO-1, and its presence in some more intense dots. Lower panel: Purkinje cells in an *Atxn7<sup>100Q/5Q</sup>* knock-in mouse showing relocation of SUMO-1 staining into big nuclear dots that could also contain ataxin-7, as previously showed with a monoclonal antibody (GMP1). (B) SUMO-2 is intensely stained in the cytoplasm of a Purkinje cell from a wild-type mouse that contains numerous intense positive dots. SUMO-2 staining was very intense in the nucleus of an *Atxn7<sup>100Q/5Q</sup>* Purkinje cell; the dot-like staining resembles that of SUMO-1. Scale bar 8  $\mu\text{m}$ .

**A****B**

**Figure 35 - RanBP2 staining increases in the *Atxn7*<sup>100Q/5Q</sup> KI mouse**

RanBP2 immunostaining in Purkinje cells from SCA7 KI mice and wild-type littermates. (A) Confocal immunofluorescence images show diffuse staining of RanBP2 in the cytoplasm of wild type Purkinje cells. Note the small dots in the cytoplasm, like those of SUMO-1 and SUMO-2. In the SCA7 KI cerebellum, RanBP2 staining was more intense than in wild type littermates, but was always cytoplasmic. Polyclonal anti-RanBP2 was used to detect RanBP2 protein. (B) RanBP2 staining was performed with a second antibody to confirm the specificity of the signal. Monoclonal anti-RanBP2 confirmed the increase in RanBP2 in the cytoplasm of *Atxn7*<sup>100Q/5Q</sup> Purkinje cells. Scale bar 8  $\mu$ m.

### 3.4. SUMO pathway components detected in the cerebellum of a SCA7 patient

In our previous study, we showed the co-localization of SUMO-1, SUMO-2 and mutant ataxin-7 intranuclear inclusions in temporal and frontal cortex of two SCA7 patients (Janer et al., 2010). Here we investigated the cerebellum of one SCA7 patient, since neuronal death is particularly important in the Purkinje cell layer. Ataxin-7 accumulated throughout the cerebellum of the SCA7 patient, and labeling with anti ataxin-7 antibody was particularly intense in the few remaining Purkinje cells, in which staining of a large nuclear inclusion was prominent (Figure 36-D). Compared to Purkinje cells in a control patient (Figure 36-A), the Purkinje cell from a diseased patient totally lost its arborisation and the cell body was shrunken with some accumulation of ataxin-7 in the cytoplasm in addition to the large intranuclear inclusion. In the control brain, ataxin-7 staining was diffuse in both the nucleus and the cytoplasm (Figure 36-A).

We then visualized SUMO-1 and RanBP2 by immunohistochemistry. Compared to the control brain (Figure 36-B and -C), SUMO-1 (Figure 36-E) and RanBP2 (Figure 36-F) both increased in the nucleus and at the nuclear rim (the expected localisation for RanBP2), as well as in the cytosol of the Purkinje cell in a SCA7 patient. The accumulation of these proteins, involved in the SUMOylation pathway of ataxin-7, suggests deregulation of this pathway during the disease.

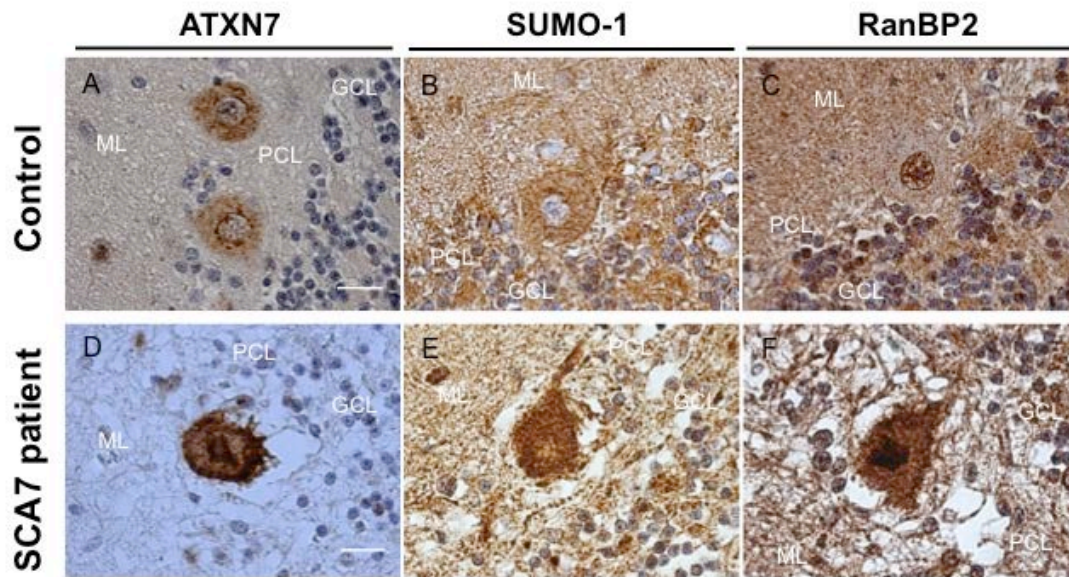


**Figure 36 - SUMO-1 and RanBP2 accumulate abnormally in the cerebellum of a SCA7 patient**  
 Cerebellae from an SCA7 patient and a control with no neurological disease were analysed. Representative sections are shown. In the cerebellum of the SCA7 patient, ataxin-7 accumulated strongly in nuclei and in other areas, such as the cytoplasm of the few surviving Purkinje cells. Ataxin-7 immunoreactivity was diffuse in the nucleus, both diffuse and granular in the cytosol and present at the nuclear membrane of control Purkinje cells. SUMO-1 immunoreactivity increased in the cytoplasm and in the nucleus of a Purkinje cell in the SCA7 patient: staining was granular. In the control Purkinje cell, staining was diffuse in the cytoplasm. No SUMO-1 immunoreactivity was detected in the nucleus of the control. Nuclear RanBP2 immunoreactivity was very strong in a Purkinje cell in the SCA7 patient: it was intense and granular in the cytoplasm; massive accumulation was detected in the nucleus. In the control, RanBP2 immunoreactivity was found in the nucleus, along the nuclear membrane and in dots in the nucleoplasm. Some granule cells show similar RanBP2 immunoreactivity in dots in the nucleoplasm, as well as in the nuclear membrane. GCL, Granular cell layer; PCL, Purkinje cell layer; ML, Molecular cell layer. Scale bar 20  $\mu$ m.

# 4. Materials & Methods

## 4.1. Plasmids and site-directed mutagenesis

The SCA7 constructs were previously described in (Zander et al., 2001). ATXN7-10Q and ATXN7-92Q, cloned in pcDNA3 vector (Invitrogen), contain the full-length wild type ATXN7 cDNA and an ATXN7 cDNA with 92 CAG repeats, as well as an HA tag at the NH<sub>2</sub> terminus and a FLAG tags at the COOH terminus. The construct ATXN7-10Q-AADL-pCS2 (VI mutated into AA at position 349/350) was obtained by site-directed mutagenesis with the QuickChange II Kit (Stratagene). The RanBP2 plasmids and HA-SUMO-1, -2 were kind gifts from A. Werner (DKFZ-ZMBH, Heidelberg) and were previously described (Werner et al., 2012). PIAS1, 3, x $\alpha$ , x $\beta$  and y were previously described (Janer et al., 2010). Plasmids coding for wild type and mutant RNF4 (dSIM: mutation in all three SIM motif; dHC: mutation to inactivate RING domain) were kindly given by J. Seeler (Pasteur Institute, Paris). Plasmid coding for myc-actin was kindly gift by Joan Steffan and already described in (O'Rourke et al., 2013). All constructs were verified by DNA sequencing.

## 4.2. RNA interference

Dharmacon On Target Plus SMARTpools (Thermo Scientific) were used for siRNA disruption of all PIAS genes: PIAS1 (L-008167), PIAS2 (L-009428), PIAS3 (L-004164), PIAS4 (L-006445) and Non-targeting siRNA (D-001810). RanBP2/Nup358 silencing was performed with a single target sequence: CACAGACAAAGCCGUUGAA (corresponding to nucleotides 351-369; accession no. NM\_006267) as described in (Hutten et al., 2008), HeLa cells were seeded in six-well dishes at a density of  $3 \times 10^5$  per well in 2 ml of DMEM complete medium. One day later cells were transfected with 75  $\mu$ mol of RNA using 4  $\mu$ l of RNAi Max in 2 ml of DMEM according to the manufacturer's instructions. After 24 h cells were transfected with 2  $\mu$ g of ATXN7-92Q using Lipofectamine 2000. After 48h incubation, cells were harvested and analysed by Western blot.

### 4.3. Primary Antibodies

Antibodies used in western blot (WB), immunofluorescence, immunohistochemical and immunoprecipitation analyses:

Primary Antibodies	Species	Source	WB	IHC	IF	IP
1C1 (ataxin-7)	Mouse	Home Made			1:1000	
Actin	Rabbit	Abcam	1:1000			
Ataxin-7	Rabbit	Thermo Scientific	1:2000	1:1000	1:1000	2,5 ug/mg of protein
c-Myc	Rabbit	Abcam	1:2000			1,5 ug/mg of protein
FLAG	Mouse	Sigma	1:500			
GMP1 (SUMO-1)	Mouse	ZYMED		1:500		
PIAS1	Rabbit	Abcam	1:2000	1:250		
PIAS2	Rabbit	Thermo Scientific	1:2000	1:500		
PIAS3	Rabbit	Abgent	1:500			
PIAS3	Rabbit	Thermo Scientific	1:2000	1:500		
PIAS4	Rabbit	Thermo Scientific	1:2000	1:500		
PIASx 1/2	Rabbit	Abgent	1:500			
PIASy/4	Rabbit	Novus Biologicals	1:500			
PML	Rabbit	Santa Cruz	1:2000		1:1000	
RanBP2	Mouse	Santa Cruz	1:2000		1:2000	
RanBP2	Rabbit	Abcam	1:2000	1:500		5 ug/mg of protein
RanGAP1	Goat	Home Made	1:2000			
SUMO-1	Rabbit	Abcam	1:2000	1:500	1:500	
SUMO-1 21C7 (coupled-beads)	Mouse	Home Made				10 ul/mg of protein
SUMO-2 8A2 (coupled-beads)	Mouse	Home Made				10 ul/mg of protein
SUMO-2+3	Rabbit	Abcam	1:2000	1:500	1:500	
Ubiquitin	Mouse	Santa Cruz	1:2000			
$\alpha$ -Tubulin	Rabbit	Abcam	1:2000			

**Table 5 - Primary antibodies**

### 4.4. Cell culture

COS7, HeLa, HEK293, MCF7 and *Pml*<sup>-/-</sup> MEF were maintained in DMEM (Invitrogen) supplemented with 10% fetal bovine serum and penicillin-streptomycin (100 UI/ml; 100  $\mu$ g/ml). Cell lines were transfected with Lipofectamine 2000 (Invitrogen) as prescribed. Depending on type of analysis to be performed, cells were either scraped in PBS containing NEM, centrifuged and lysed, or directly lysed in Laemmli 2% SDS sample buffer or in the buffer mentioned in the paragraph 3.7. Expression of different constructs (see paragraph 3.1) was usually allowed for 48h for western blot analysis. For immunofluorescence, COS-7 cells were analysed 40-45h post-transfection.

## 4.5. Animals

Heterozygous *Atxn7*<sup>100Q/5Q</sup> knock-in mice carrying 100Q CAG repeats in the mouse *Sca7* locus on the pathological allele, kindly provided by prof. H. Zoghbi (Baylor College of Medicine, USA), were housed in a temperature-controlled room and maintained on a 12 h light/dark cycle. Food and water were available ad libitum. For immunohistochemical analysis they were analysed at 12 months of age (late stage disease) and compared to 12 months old wild-type littermates. For mRNA analysis by quantitative RT-PCR, they were analysed at 6 (n=4) and 12 (n=5) months of age and compared to wild-type littermates at the same age: 6 (n=4) and 12 (n=4) months old. The experiments were carried out in accordance with the European Community Council directive (86/609/EEC) for the care and use of laboratory animals and were approved by the Commission Génie Génétique of the French Ministry for Scientific Research and Education (06/26/2010).

## 4.6. *In vitro* SUMOylation and *in vitro* binding assay

### *In vitro* SUMOylation

GST, GST-ATXN7 (90-406) and -PIAS1 were expressed in BL21DE3 *E.coli* cells and purified according to standard procedures. RanBP2 complex and recombinant free RanBP2 were prepared as described in (Werner et al., 2012). 1.3  $\mu$ M GST-ATXN7 (aa 90-406) or GST were incubated with 90 nM E1, 111 nM E2, 16  $\mu$ M SUMO-1, 5 mM ATP and different E3 ligases: 25 nM free RanBP2 (aa 2304-3062), 25 nM RanBP2/RanGAP1\*SUMO1/Ubc9 complex or 75 nM GST-PIAS1, for 90 min at 30 °C. Reaction was stopped by addition of SDS sample buffer. The *in vitro* reaction products were directly analysed by Western blot, using anti-GST antibody.

### *In vitro* binding assay

Equal amounts of recombinants SUMO-1, SUMO-2 or ovalbumin were covalently coupled to Cyanogen-bromide-activated sepharose (Sigma-Aldrich) in 0.2 M Carbonate buffer pH 8.9 at a concentration of 1 mg protein per ml beads. Ataxin-7 was produced by overexpression of construct HA-ATXN7-pCS2 in HEK293 cells for 48hr. Cells from two 10-cm dishes were lysed in 1 ml TB buffer (20 mM Hepes pH 7.3, 110 mM potassium acetate, 2 mM magnesium acetate, 1 mM EGTA, 1 mM DTT, 1  $\mu$ g/ $\mu$ l of each aprotinin, leupeptin, pepstatin) by incubation on ice for 20 min,

followed by three freeze/thawing steps (using liquid nitrogen and 37 °C heating block). The samples were centrifuged at 4 °C for 60 min at 20000 g. The supernatant was used as cell lysate for the pulldown. 1% of input sample was taken for control on western blot. 300 µl of the cell lysate was added to the beads and incubated for 3 h at 4 °C on rotator. Beads were centrifuged at 600g and supernatant was removed, beads were washed 3 times with 1 ml of TB buffer. Bound proteins were eluted by adding 60 µl of SDS sample buffer and boiling. The entire sample was loaded on the gel for western blot analysis.

## 4.7. Protein extraction and western blot analysis

### *Protein extraction from cell lines*

Cells were washed and harvested in PBS supplemented with 20 mM of freshly dissolved NEM (N-Ethylmaleimide is used to inhibit de-sumoylation of proteins; Sigma), pelleted, and lysed 30 min on ice in lysis buffer containing 50 mM Tris, pH 8.8, 100 mM NaCl, 5 mM MgCl<sub>2</sub>, 0.5% NP-40, 1 mM EDTA, 20 mM NEM and 250 IU/ml benzonase (Merck) supplemented with a cocktail of protease inhibitors (Complete and Pefabloc; Roche). Total extracts were centrifuged at 13,000 rpm for 15 min at 4°C to separate soluble proteins from aggregates and membranes. Supernatants (30 µg protein) were analyzed by Western blot (NP-40 soluble fraction, NS). Pellets were further incubated 30 min on ice in a pellet buffer containing 20 mM Tris, pH 8.0, 15 mM MgCl<sub>2</sub>, and 250 IU/ml benzonase. Protein concentrations (supernatant and pellet) were determined by Bradford assay (Bio-Rad Laboratories). The pellet was analysed in a filter retardation assay (SDS-resistant fraction, SR), but was also loaded, after boiling in Laemmli buffer on gels for western blot analysis (SDS-soluble fraction, SS).

### *Protein extraction from mouse tissue*

Mouse cerebella, striatum and retina were collected and frozen at -80 °C. Cerebella were lysed in radioimmunoprecipitation assay-buffer solution (RIPA buffer: 50 mM Tris HCl, pH 8.0, 150 mM NaCl, 1% NP-40, 0,5% sodium deoxycholate, 0,1% sodium dodecyl sulphate) containing protease inhibitors (Roche diagnostics GmbH) and 250 IU/ml benzonase (Merck). Samples were sonicated by a 4 seconds ultra-sound chase (1 pulse/sec). Total protein lysates were stored at -80 °C and protein concentration

was determined with the Bradford protein assay (Bio-Rad laboratories).

#### *Western blot analysis*

Depending on the analysis and the sample, 25 µg (COS-7, HeLa, *Pml*<sup>-/-</sup> MEF cell lines) or 100 µg (mouse cerebellae) were resolved on precast gel 4-12 % (Invitrogen) and 4-20% (Bio-Rad), respectively. Samples were transferred onto a nitrocellulose membrane (Protran, Whatman) by liquid transfer for 1.5 hr. Ponceau staining of the nitrocellulose membrane was performed, followed by blocking in 5% dry non-fat milk. Selected primary antibodies were incubated over night at 4 °C (see Table 5) followed by three washes with PBS/Tween20 0.1%; secondary antibodies were applied for 2 hr at room temperature. Membranes were incubated with enhanced chemiluminescence substrate (Pierce) and chemiluminescence or fluorescence signals were revealed on a film (ECL, Amersham Hyperfilm), or captured with Odyssey Imaging (Li-COR, U.S.A) systems. Densitometric analysis was carried out using ImageJ software (NIH).

#### 4.8. Immunoprecipitation

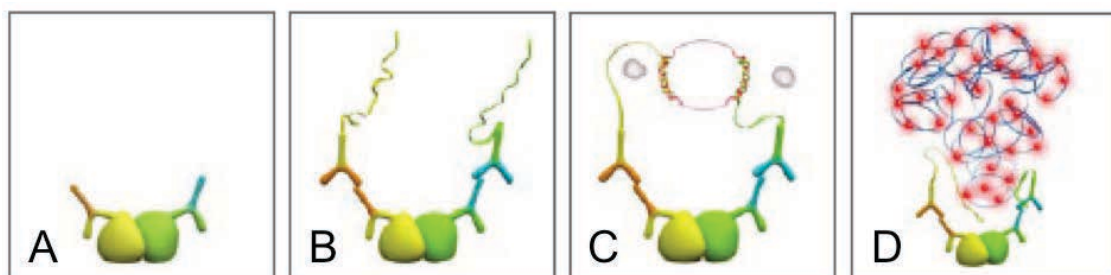
SUMO immunoprecipitation (SUMO-IP) to detect endogenous ataxin-7 as a target of both SUMO-1 and -2 was performed as described (Becker et al., 2013) (Barysch et al., 2014). Briefly, the day before IP we plated MCF7 cells in 9 15-cm plates and let them grow to confluence. At least 3 plates were used for each IP condition (Control, SUMO-1, SUMO-2). The day of the experiment, the culture medium was removed and the plates washed with 15 ml of cold wash buffer (10 mM NEM in PBS). 250 µl of 2x lysis buffer (1x PBS, 2% (wt/vol) SDS, 10 mM EDTA, 10 mM EGTA, 20 mM NEM, 2 mM Pefabloc and 2 µg/ml each of aprotinin, leupeptin and pepstatin) was then added to each plate and the cells collected with a cell scraper.

For immunoprecipitation of ataxin-7 and RanBP2, 1 mg of total MCF7 lysate was diluted in two buffers differing in their detergent composition (50 mM Tris pH 7,4; 100 mM NaCl; 2 mM MgCl<sub>2</sub>; 1mM EGTA; 0,1% Triton or 0,5% NP-40). The lysates were added to G-Sepharose beads (Fast Flow, Sigma) complexed with antibodies against ataxin-7 (Thermo Scientific), RanBP2 (Abcam) or c-myc (Abcam). Following overnight incubation at 4 °C on rotator, beads were collected by centrifugation at 600g. Beads were then washed three times in lysis buffer. Bound proteins were

eluted into 80  $\mu$ l of Laemmli buffer by heating to 95 °C for 5 minutes, followed by centrifugation to pellet the beads and 40  $\mu$ l was loaded on a gel for western blot analysis.

#### 4.9. Proximity ligation assay (PLA) – Duolink® in situ

COS-7 cells plated on glass coverslips were fixed for 20 min with 4% paraformaldehyde. Three washes of 5 min were performed with PBS, followed by a permeabilization step with PBS/TritonX-100 0.1% for 15 min at room temperature. After three subsequent washes with PBS, blocking buffer, composed of 5% bovine serum albumin diluted in PBS, was added and incubated for 1 hour at room temperature. We then added diluted ataxin-7 (1:1000) and SUMO-1 (1:500) antibody in blocking buffer overnight at 4 °C (A).



PLA PROBES STEP (day 2)- We prepared a mix of two PLA probes (one anti-mouse to link ATXN7 antibody, the other anti-rabbit to link SUMO-1 antibody) diluted 1:5 in blocking buffer and allowed the mixture was kept for 20 min at room temperature. During this time, the primary antibody solution was removed and each coverslip was transferred into a 6-well and twenty washes were performed for each well using Wash Buffer A prepared according to the manufacturer's instructions. In a pre-heated humidified chamber, we placed the coverslips on glass slides and added the diluted PLA probes (anti-rabbit and anti-mouse for ataxin-7 and SUMO-1 detection, respectively) probes solution. Incubation of the PLA probes was for 1ht at 37 °C (B). LIGATION STEP - After two washes of 5 min each with Wash Buffer A under gentle agitation, we added Ligation-Ligase solution to each sample followed by an incubation in a humidified chamber for 30 min at 37 °C (C). AMPLIFICATION STEP – After removal of the Ligation-Ligase solution, two washes of 2 min under gentle agitation were performed with Wash Buffer A. The Amplification-Polymerase

solution was added prepared according to the manufacturer's instruction followed by an incubation for 100 min at 37 °C in a pre-heated humidity chamber (D).

FINAL STEP – After removal of the Amplification-Polymerase solution from the coverslips, two washes of 10 min with 1x Wash Buffer B (prepared according manufacturer's instruction) were performed.

The last wash was made with 0.01x of Wash Buffer B for 1 min. Glass coverslip were mounted onto a glass slide using a mounting medium with DAPI.

**Wash buffer A:** dissolve 8.8 g NaCl, 1.2 g Tris base and 0.5 ml Tween 20 in 800 ml high purity water. Adjusted pH to 7.4 using HCl. Added high purity water to 1000 ml (final concentrations 0.01 M Tris, 0.15 M NaCl and 0.05% Tween 20). Filter the solution through a 0.22 µm filter and store at +4 °C. Bring the solutions to room temperature before use.

**Wash buffer B:** Dissolve 5.84 g NaCl, 4.24 g Tris base and 26.0 g Tris-HCl in 500 ml high purity water. Adjust pH to 7.5 using HCl. Add high purity water to 1000 ml (final concentrations 0.2 M Tris and 0.1 M NaCl). Filter the solution through a 0.22 µm filter and store at +4 °C. Bring the solutions to room temperature before use.

#### 4.10. Filter Retardation Assay

This assay is based on the finding that the polyglutamine-containing protein aggregates are insoluble in SDS and are retained on a cellulose acetate filter (Wanker et al., 1999). Whole cells, the pellet fraction or tissue extracts (40 µg of protein for COS7, HeLa and *Pml*<sup>-/-</sup> MEF cells; 100 µg of protein for mouse cerebellar extracts) were diluted in 100 µl of 2% SDS and 50 mM DTT in phosphate-buffered saline (PBS), boiled at 95° for 5 minutes. Samples were filtered on a BRL dot-blot filtration unit through a cellulose acetate membrane (Schleicher and Schuell, NH, 0.2 µm pore size) that was pre-equilibrated with 0.1% SDS. Wells were washed twice with 200 µl 0.1% SDS and membrane blocked in PBS-Tween20 0.1% containing 5% non-fat dried milk, followed by incubation with desired antibody overnight at 4 °C. Membrane was washed three times in PBS-Tween20 0.1% then incubated for two hours at room temperature with a secondary anti-rabbit antibody conjugated to horseradish

peroxidase (Jackson laboratories) followed by ECL detection (Pierce). Densitometric analysis was carried out using ImageJ software (NIH).

#### 4.11. RNA Purification and Real-Time Quantitative PCR

Cerebellum, striatum and retina were dissected from 6 and 12 months old *Atxn7<sup>100Q/5Q</sup>* and wild type littermates mice. Tissues were homogenized using an electric pestle (Sigma) in QIAzol (Qiagen), and total RNA was isolated using RNeasy® Lipid Tissue Mini kit (Qiagen) including an RNase-free DNase step to remove residual DNA. RNA from whole-cell lysate of transfected or untransfected COS7 cells was extracted using the RNeasy® kit (QIAGEN). Total RNA was controlled for RNA quality (Bioanalyser 2100, Agilent®). Biological replicate samples of 1 µg of total RNA were reverse transcribed using iScript cDNA synthesis kit (Bio-Rad) according to the manufacturer's instructions. Quantification of mRNAs was performed by real time RT-PCR using a Roche LightCycler LC480 sequence detection system (Roche, France). Oligonucleotide primer pairs were obtained from mwg/operon (France), designed with Oligo Explorer 1.0 and verified for specificity with the NCBI Blast engine ([www.ncbi.nlm.nih.gov/BLAST](http://www.ncbi.nlm.nih.gov/BLAST)) using the “nearly exact short match” program (Table 6). The end point PCR (35 cycles) was performed with LightCycler 480 SYBER Green I master (Roche, France) on 20 ng of RT product. After amplification, PCR products were analyzed by the melting curve to confirm the amplification specificity. The relative levels of mRNA were standardized using 36b4 ribosomal RNA as the non-variant RNA species: primer forward 5'-TACACCTTCCCCTTGCTG-3' and primer reverse 5'-TCTGATTCCTCCGACTCTTC-3'. The quantitative RT-PCR on each sample was performed in triplicate. Expression values were determined using the  $\Delta\Delta CT$  method.

#### 4.12. Immunofluorescence

COS-7 or HeLa cells plated on glass coverslips coated with poly-lysine (Sigma) were fixed for 20 min with 4% paraformaldehyde. Cells were incubated for 30 min with gentle agitation, washed two times for 5 min at room temperature with PBS. Cells were permeabilized in 0.1% Triton in PBS for 15 min, washed 2 x 5 min in PBS, and blocked in 4% fetal bovine serum (FBS) in PBS for 1 hour. Primary antibodies were diluted in 4% FBS in PBS and incubated with cells over night at 4 °C. Cells were then

washed 3 x 10 min in PBS, secondary antibodies diluted in 4 % FBS in PBS was applied for 2 h at room temperature (RT) and washed. Finally cells were incubated with DAPI diluted in 1x PBS for 15 min at room temperature and washed 3 x 5 min with PBS. Cells were mounted with Fluorescent Mounting Medium (Dako). Slides were stored at 4 °C. Confocal images were acquired with an Olympus BX 61 microscope equipped with x60/1.35 lens and a Fluoview FV-1000 image acquisition system.

Oligonucleotides	Sequence
mAtxn7-F	5'-GGCATGCCGCTCTATGACCTT-3'
mAtxn7-R	5'-GTGGGTCTGCCTACCAACTC-3'
Pan Pml-F	5'-GATCTCCGCGACAATTCAGT-3'
Pan Pml-R	5'-TCACCAATATCGCAATGGAG-3'
Pias1-F	5'-GTCTCCTACGTCACCACTAAG-3'
Pias1-R	5'-GCATAGGCGTCATGTGGAAG-3'
Pias2-F	5'-CCGTGCAGTGACTTGTACAC-3'
Pias2-R	5'-CTCATCCACATCAGAACAGTC-3'
Pias3-F	5'-GGTGAGGCAATTGACTGCAG-3'
Pias3-R	5'-GTAGTAGCCACTTCACTGTCCG-3'
Pias4-F	5'-GACGCTAGTGCCAAGATGG-3'
Pias4-R	5'-GTCACCAGTTCGTGCTTCAG-3'
Pml Iso3-F	5'-GATGAGAGCCTCGCCGAAC-3'
Pml Iso3-R	5'-TTGGGAAACCCACTTTCATTG-3'
RanBP2-F	5'-ATTGCCTGTTCCCTTGAGT-3'
RanBP2-R	5'-CGAGGTGGTGTCTTTGGAG-3'
SCA7a-F	5'-GCTCAGGAAAGAAACGCAAA-3'
SCA7a-R	5'-CCGATGCTATGGGAAGATGT-3'
SCA7b-F	5'-CCAGTACCACCTCACCCATC-3'
SCA7b-R	3'-CGATTTGCTATTTGGGAAGA-3'
Senp1-F	5'-GCTGACTGACAGTGAAGACG-3'
Senp1-R	5'-GAGTCTGAATGTCTTTGCGTG-3'
Senp2-F	5'-GAAGGTGCTCATGGAAGCACG-3'
Senp2-R	5'-CTGACGCCATGATTCTGCTC-3'
Senp3-F	5'-CAGGCAACGCTATGGTAAGG-3'
Senp3-R	5'-CTGTGTCCATGACCAGATCTC-3'
Senp6-F	5'-CCTCCTTATGGACTCACTCAG-3'
Senp6-R	5'-CTACATACTGCAGCACATAGAC-3'
Sumo1-F	5'-GTGAATCCACGTCACCATGTC-3'
Sumo1-R	5'-GTATCTCACTGCTATCCTGTC-3'
Sumo2-F	5'-GTCAATGAGGCAGATCAGATTC-3'
Sumo2-R	5'-CACATCAATCGTATCTTCATCC-3'

Table 6 - Oligonucleotides sequences

### 4.13. Human post-mortem brain

Formalin-fixed, paraffin-embedded cerebellar tissue from SCA7 patients, with morphologically and genetically confirmed SCA7 (10 years of age at death, with 85 CAG repeats on the mutant allele), and a control individual with no evidence of neurological disease, were obtained from the Brain Bank of the Pitié-Salpêtrière (Cancel et al., 2000). The European Institute for Bioethics approved the use of this material (12/30/2008).

### 4.14. Immunohistochemical analysis

#### *Mouse brain tissues*

The mice were given an overdose of sodium pentobarbital and were perfused transcardially with 4% paraformaldehyde in 0.1 M PBS. The brains were post-fixed in 4% paraformaldehyde for 24h and cryoprotected in 30% sucrose-PBS for 48 h at 4 °C. Immunostaining were performed on 12 µm-thick frozen tissue sections collected from a cryostat.

Antigens were retrieved by boiling the sections in 1 mM citrate buffer pH 6.0, in a microwave oven at 350 W. Sections were permeabilized and non-specific epitopes were blocked by incubation for 2 h at room temperature in PBS containing 3% bovine serum albumin, 4% normal goat serum, 0.1% Triton™ X-100. Section were incubated for 48 h at 4° with primary antibodies (see Table 5) followed by appropriate Alexa Fluor® dye-conjugated secondary antibodies (1:1000). Sections were mounted with Fluorescence Mounting Medium (S3023, Dako). Fluorochromes are indicated in the figure legends. Confocal images were acquired with an Olympus BX 61 microscope equipped with x60/1.35 lens and a Fluoview FV-1000 image acquisition system.

#### *Human brain tissue*

Five micrometre sections were cut from paraffin-embedded brains and stained with anti ataxin-7, SUMO-1 and RanBP2 antibodies. Secondary antibodies for DAB staining were biotinylated goat anti-rabbit or goat anti-mouse antibodies (BA-9200, BA-1000, respectively; Vector) 1:250. 3,3'-Diaminobenzidine (DAB) staining was carried out with the Vectastain ABC kit (Pierce). Images of immunostained sections

were acquired with LAS V3.8 (Leica) software, at room temperature, with a bright-field Leica DM 4000B microscope equipped with x40/0.75 and x100/1.35 lenses and a Leica DFC500 digital camera.



## 5. Discussion

The main goal of this study was to contribute to the identification of new potential targets for SCA7 therapeutic intervention. In order to achieve this objective, I focused on gaining a better understanding of the mechanisms regulating ataxin-7 degradation by the SUMOylation pathway, including the modifying and demodifying enzymes.

In the introduction, I illustrated how previous studies identified several polyQ proteins as targets for SUMO modification. In 2010, my team showed that ataxin-7 is also modified by SUMO-1 and identified the major acceptor site as lysine 257. In addition, SUMOylation was observed to attenuate the propensity of polyglutamine-expanded ataxin-7 to aggregate and its cellular toxicity (Janer et al., 2010). The observation that SUMOylation plays an important role in SCA7 by modifying the aggregation of polyQ-expanded ataxin-7 suggests that cellular mechanisms modulating the SUMOylation pathway might be involved in ataxin-7 pathogenesis.

Given this scientific background, the first step was to investigate the role of RanBP2 in the transfer of the SUMO-1 protein to the ataxin-7 substrate, then to compare effects of overexpression of different known SUMO E3 ligases on mutant ataxin-7 aggregation. We thus identified RanPB2 as the major modifying enzyme and PIAS4 as a minor modifier.

To further confirm that ataxin-7 was a target of SUMOylation at the physiological level, we established a collaboration with F. Melchior's team at Heidelberg University. Thanks to their lab competences and infrastructure, I was able to identify ataxin-7 as an endogenous SUMO-1 and SUMO-2 modification target.

As an additional confirmation of these findings, I proceeded with experiments on a SCA7 mouse model to quantify expression of the mRNA SUMO modifying enzymes to determine whether the SUMO pathway was deregulated in the central nervous system in tissues affected by the pathology. Finally, by immunohistochemical

analysis of human brain samples from SCA7 cerebellum, I observed an accumulation of SUMO1 and RanBP2 in Purkinje cells - a further indication that SUMOylation deregulation goes hand in hand with the worsening of the pathology.

In the following sections, I will discuss each major result in relation with the state of the art and its impact and significance in the global context of spinocerebellar ataxia type 7. Where appropriate, I will also highlight possible future research directions to build on the obtained results.

## 5.1. SUMOylation as regulator of toxic ATXN7 protein in SCA7 disease

In this section, I will illustrate how I gained experimental evidence that SUMOylation is a regulator agent of mutant ataxin-7. For the past few years, SUMOylation has attracted increasing attention as a versatile regulator of toxic proteins in neurodegenerative diseases such as SCA7.

### 5.1.1. Scientific background

The yeast SUMO (small ubiquitin-like modifier) orthologue SMT3 was initially discovered in a genetic suppressor screen for the centromeric protein Mif2 (Meluh and Koshland, 1995). It later emerged that the homologous mammalian proteins SUMO-1 to SUMO-4 are reversible protein modifiers that can form isopeptide bonds with lysine residues of target proteins (Mahajan et al., 1997). This was the discovery of a post-translational modification called SUMOylation, which enzymatically resembles ubiquitination (Krumova and Weishaupt, 2013).

Whereas the contribution of other post-translational modifications, especially phosphorylation and ubiquitination, to neuronal function and dysfunction have been investigated for a long time, SUMOylation of neuron-specific targets remained unknown until recently (Hudson et al., 2012). In fact, most assays identifying SUMO conjugated proteins were carried out in non-neuronal cell lines. In addition, covalent SUMO modifications, in general, escaped discovery until 1996, partly due to the unstable nature of this protein modification, which is hard to detect.

SUMOylation has been implicated in repair of DNA single-strand breaks in neurons. DNA single-strand breaks, which occur continuously and are an inherent feature of chromosome metabolism to overcome torsion barriers, are resealed by tyrosyl DNA

phosphodiesterase 1 (TDP1) (Takashima et al., 2002). In 2002, it was shown that mutations in TDP1 and subsequent loss of TDP1 DNA repair activity are the cause of a familial form of ataxia (spinocerebellar ataxia with axonal neuropathy; SCAN1). Deficiency of this DNA repair pathway affects primarily the post-mitotic, terminally differentiated, large neuronal cells (e.g., cerebellar pyramidal cells) (Takashima et al., 2002). Very recently, it was shown that SUMO modification of TDP1 is necessary for proper subnuclear TDP1 targeting in neurons guaranteeing that sufficiently high local concentrations of TDP1 protein are reached at sites of DNA damage (Hudson et al., 2012). Of note, topoisomerase 1, which is responsible for a large proportion of protein-linked single-strand DNA breaks, is itself a SUMO target and rapidly modified upon cellular stress (Mao et al., 2000).

In 2004, Steffan et al. (Steffan et al., 2004) showed for the first time that a protein involved in neurodegeneration is SUMO conjugated. SUMO-1 modified a pathogenic fragment of Huntingtin (Httex1p) at the N-terminal lysines 6, 10, and 15. It was demonstrated that a SUMO-Htt97QP fusion protein reduces Htt inclusion formation when SUMO is N-terminally fused to Htt. On the contrary, Huntingtin's cytotoxicity is reduced in flies heterozygous for SUMO and in transgenic *Drosophila*, expressing SUMO-deficient Htt. This indicates that SUMOylation of Htt contributes to the disease pathology possibly by stabilizing toxic Htt species (Steffan et al., 2004). This is also an example of how SUMO-dependent reductions in aggregation are not always associated with a reduction in toxicity, and how SUMO effects on toxicity can be both positive and negative (Krumova and Weishaupt, 2013).

Altered solubility is related to a pathological propensity to form intracellular protein aggregates. In addition, several aggregation-prone proteins implicated in neurodegeneration were found to be SUMOylated (Riley et al., 2005) (Steffan et al., 2004) (Krumova et al., 2011). Based on the presumed function of SUMO attachments as a "protein solubility enhancer", it seems plausible that regulation of protein aggregation is another way by which SUMOylation may influence neurodegenerative diseases. This makes SUMOylation in principle an important candidate regulator in disease conditions characterized by reduced protein solubility and pathological aggregation, as in the neurodegenerative diseases. However, only in a few instances the direct impact of SUMO on protein solubility has been

documented, among which: alpha-synuclein, DJ-1, huntingtin and STAT1 (Krumova and Weishaupt, 2013).

Our team has linked SUMOylation to SCA7, since SUMO-1 and -2 co-localized with ataxin-7 in intranuclear inclusions in a SCA7 cell culture model and in the cortex of a patient. Furthermore, a SUMOylation-deficient mutant ataxin-7 showed increased inclusion formation, implying that SUMO plays a role in the regulation of ataxin-7 aggregation (Janer et al., 2010).

### 5.1.2. Contribution and contextualisation of this work

In order to identify potential factors responsible for ataxin-7 SUMOylation and their effects on normal and mutant ataxin-7, I expressed proteins implicated in this pathway.

Overexpression of SUMO-1 with wild type (10Q) and mutant (92Q) ataxin-7 led to the appearance of a modified western blot band corresponding to ataxin-7 with the addition of 20 kDa corresponding to SUMO-1. In presence of SUMO isoform 2, I detected a faint band in addition to the previous one, corresponding to the conjugation of two SUMO-2 residues. When SUMO-2 was co-expressed with mutant (92Q) ataxin-7, a smear was sometimes observed, indicating that the substrate was poly-SUMOylated. I compared the consequences of SUMO-1 and SUMO-2 overexpression in the SCA7 cell model, analysing the levels of both soluble and the SDS-insoluble ataxin-7. As we previously showed that SUMOylation attenuated aggregation of mutant ataxin-7, I compared here the effect of SUMO-1 and SUMO-2 by filter retardation assay: a stronger decrease was observed in the presence of SUMO-2. **This result supports the hypothesis that ataxin-7 is also a target for modification by SUMO-2. This is particularly noteworthy because we know from the literature that SUMO-2 conjugation is usually stimulated in a stress-dependent manner (Saitoh and Hinchey, 2000).**

To contextualise the importance of the correlation above, it should be noted that oxidative stress represents one of the most direct links between neurodegenerative diseases and impaired SUMOylation. In general, the activity of key enzymes of the SUMO pathway responds to a number of different external stimuli. More interestingly, the enzymatic centre of the E1 and E2 enzymes of the SUMOylation

cascade is reversibly oxidized and thereby efficiently inhibited by low levels of oxidative stress (Bossis and Melchior, 2006). High levels of reactive oxygen species (ROS), which damage cellular components and trigger apoptosis, is observed in the neurons of HD patients and an HD-like animal model (Browne and Beal, 2006). The same happens in a stable, inducible SCA7 cell model, in which polyQ expanded ataxin-7 results in a concomitant increase in ROS levels and aggregation of the disease protein, and later in cellular toxicity (Ajayi et al., 2012).

From the references above, we know that oxidative stress is a typical reaction to neurodegenerative diseases such as SCA7. Since we showed in this study that ataxin-7 is a target for SUMOylation by SUMO-2, we may postulate that polyQ ataxin-7 triggers an increase in ROS levels; this in turn would lead to activation of endogenous SUMO-2. This cellular response is triggered to cope with aggregation of mutant ataxin-7, in an attempt to degrade it. Overexpression of SUMO-2 mimics and amplifies the cellular response, and aggregates of mutant ataxin-7 are degraded as attested by filter assay analysis.

Above I stated that overexpressed SUMO-2 modifies ataxin-7. However, the interplay among SUMO-conjugation, SUMO-deconjugation and SUMO-mediated interactions requires tight regulation, both at the level of the individual targets and of the proteome (Flotho and Melchior, 2013) (Watts, 2013). This fragile balance can easily be disturbed by overexpressing SUMO, which is rate-limiting for the modification of targets *in vivo*, or by overexpressing enzymes that in high concentrations might override regulatory mechanisms. As a consequence, full insight into the regulation and role of SUMOylation requires analysis in the absence of protein overexpression.

Very recently, Frauke Melchior and her collaborators developed a method for specific enrichment of endogenous SUMO-1 and SUMO2/3-modified proteins. Thanks to the collaboration with this team, we performed the experiments required to understand whether ataxin-7 is a target for SUMO modification at endogenous levels. Although SUMOylated ataxin-7 is not abundant, this technique allowed us to show that the protein is a SUMO-1 and -2 target. In particular, immunoprecipitation with monoclonal antibodies recognizing SUMO-1 and SUMO2/3 showed that ataxin-7 was preferentially modified by isoform 2.

To confirm the novelty of this finding, we carefully checked the literature to see if previous studies already described endogenous ataxin-7 as a SUMO target. In 2006, the Lamond team used quantitative proteomics to investigate the target protein preferences of SUMO-1 and SUMO-2 in HeLa cells stably expressing His-SUMO-1 or His-SUMO-2. One third of the identified proteins were transcriptional regulators: this functional group included 10 preferential SUMO-1 targets, six preferential SUMO-2 targets and one protein that was possibly conjugated to both SUMOs, showing that both SUMO family members play a role in transcription (Vertegaal et al., 2006). Ataxin-7 is a member of the TFTC/STAGA complex, which is implicated in several steps of transcriptional regulation: but ataxin-7 was not present in their list. More recently, colleagues from the Melchior group analysed elution from SUMO-1 and 2/3 immunoprecipitation in HeLa cells by mass spectrometry (unpublished data): ataxin-7 was not detected in this case either.

As HeLa did not appear to contain SUMO-modified ataxin-7, we compared various cell lines for their content in endogenous ataxin-7. By western blot we found that MCF7 cells contained higher levels of ataxin-7 than COS7, HEK293 and HeLa cells. Thus, I performed the immunoprecipitation experiments in MCF7 cells to increase the probability of detecting endogenous SUMO-modified ataxin-7. As previously described, SUMOylation is a very fast and instable modification. Moreover, not all proteins are modified by SUMO. We realized the immunoprecipitation with monoclonal anti-SUMO-1 and anti-SUMO-2 antibodies, starting from 9 plates (or 15 mg of protein/condition) of MCF7 cells; a large amount of starting material is needed since only 1 or 2% of the protein is SUMOylated.

Since SUMO-modified ataxin-7 would be present in low quantities if at all, we concentrated the eluted proteins by TCA precipitation. This allowed us to detect ataxin-7 as an endogenous target in the SUMOylation pathway. Ataxin-7 was found to be modified both by SUMO-1 and by SUMO-2, to a higher extent, in MCF7 cells. Even if the amount of modified ataxin-7 was low, we demonstrated that endogenous ataxin-7 is indeed a SUMO target. To confirm that endogenous ataxin-7 is modified, I investigated the interaction between ataxin-7 and SUMO-1. A proximity ligation assay (PLA) in COS7 cells revealed the proximity of the two proteins by the presence

of red fluorescent spots, further confirming the results obtained by immunoprecipitation.

We conclude **that ataxin-7 is in the growing list of proteins endogenously modified by SUMO.**

## 5.2. RanBP2 as a major SUMO E3 ligase of ataxin-7 for SUMO-1 conjugation.

In this section, we focus on the role of RanBP2 as a SUMO E3 ligase. Since SUMO E3 ligases provide specificity in targeting proteins, identification of the E3 ligase(s) that promotes ataxin-7 SUMOylation may be a key to the discovery of therapeutic targets that regulate this modification.

### 5.2.1. Scientific background

RanBP2 was identified as a candidate for ataxin-7 SUMO-modification by *in vitro* SUMOylation (Janer et al., 2010). For this reason, I evaluated whether this protein, or other known ligases, could function as ataxin-7 E3 SUMO ligases.

During interphase, RanBP2 is localized at the cytoplasmic face of the Nuclear Pore Complex, where it forms a stable subcomplex with Ran GTPase-activating protein 1 (RanGAP1) and the SUMO E2-conjugating enzyme Ubc9. At the onset of mitosis when the nuclear envelope (NE) disintegrates and Nuclear Pore Complexes disassemble, RanBP2-RanGAP1-SUMO1-Ubc9 subcomplexes disperse into the mitotic cytosol and accumulate at the spindle microtubules and at kinetochores of chromosomes.

Since its discovery as a SUMO E3 ligase, numerous proteins have been SUMO-modified with the help of catalytic RanBP2 fragments *in vitro*. However, no major evidence of SUMOylation by RanBP2 was found *in vivo* until 2008. The critical biological functions of the mammalian RanBP2 protein were not elucidated. Since depletion of RanBP2 caused various mitotic abnormalities in HeLa cells, including misalignment of chromosomes in metaphase, the authors generated mutant mice in which the dose of RanBP2 was reduced in a graded fashion (Dawlaty et al., 2008). Complete loss of the protein is embryonic lethal. Mitotic defects, such as anaphase-bridge formation were observed in mice that were hypomorphic for RanBP2. The

observation that RanBP2 hypomorphism led to decreased SUMOylation of Topoisomerase II $\alpha$  in mitosis suggested that Topo II $\alpha$  was an *in vivo* substrate of RanBP2 during this cell-cycle stage (Dawlaty et al., 2008). A SUMO1-Topo II $\alpha$ -EGFP fusion protein encoding a non-hydrolyzable SUMO-1 restored a correct mitotic spindle in MEF cells from the mutant RanBP2 mice, allowing efficient separation of sister chromatids. This was the first direct evidence that RanBP2 was a SUMO E3 ligase. To date the known targets of RanBP2 in cells are topoisomerase II and borealin, both of which are involved in binding to complexes associated with chromosomal segregation during mitosis (Dawlaty et al., 2008) (Klein et al., 2009). Thus, the SUMOylation properties of RanBP2 have been demonstrated *in vivo* during mitosis.

### 5.2.2. Contribution and contextualisation of this work

One of my objectives was to verify whether ataxin-7 is a target for SUMOylation by RanBP2 *in vivo*. This hypothesis emerged from the results of an *in vitro* experiment where PIAS were tested for their E3 ligase activity. Unexpectedly RanBP2 modified ataxin-7 to a greater extent than other SUMO E3 ligases (Janer et al., 2010 - supp data).

**My first contribution was then to show that overexpression of RanBP2 and SUMO-1 influenced the level of aggregated expanded ataxin-7 in a cellular SCA7 model.** In addition to RanBP2 expression, SUMO-1 co-expression significantly improved degradation of mutant aggregates. This is consistent with previous finding that state that RanBP2 has a major affinity for isoform 1 of SUMO (Hecker et al., 2006). I also confirmed by filter retardation assay the beneficial effect of RanBP2 co-expressed with SUMO-1, which emerged as its preferential partner in the SUMOylation of ataxin-7.

Mirroring the approach pursued in the previous section, I proceeded with additional immunoprecipitation experiments to confirm that the interaction between ataxin-7 and RanBP2 also occurs endogenously. The main difficulty to face when approaching this specific problem is the important size of RanBP2, along with its stable integration into one of the largest complex in the cell. In mitotic extracts, RanBP2 is soluble but remains associated with SUMOylated RanGAP1 (Swaminathan et al.,

2004). This information helped us to immunoprecipitate RanBP2 after cell synchronisation by nocodazole treatment to ensure that the majority of the cells were in mitosis. These conditions favour RanBP2 immunoprecipitation along with its interaction partners because RanBP2 is soluble and not bound to the nuclear membrane. Technically speaking, the protocol proved to work, because I was able to co-immunoprecipitate RanGAP1, but I did not co-immunoprecipitate ataxin-7 with RanBP2 (not presented in this manuscript). In my opinion, this was due to the following reasons: I conducted this experiment during mitosis, which is characterised by the absence of the nuclear membrane; RanBP2 and ataxin-7 might not interact during mitosis, but only in interphase. In addition, HeLa cells express a lower level of ataxin-7 than MCF7 cells. Thus, the experimental conditions were sub-optimal for studying possible interactions between the two proteins, especially if interaction is transient during the cell cycle. This is consistent with my hypothesis that ataxin-7 modification by RanBP2 at the nuclear pores complex might take place during ataxin-7 shuttling from the cytoplasm to the nucleus. To circumvent this issue, I used an alternative immunoprecipitation protocol.

This protocol is in the “Materials and Methods” chapter. We used MCF7 cells and tested, in a pilot experiment, different percentages of non-ionic detergents in the extraction buffer: the aim was to increase the probability of extracting RanBP2 from the nuclear membrane along with its interaction partners during the SUMOylation process. We identified two buffers that extracted RanBP2 efficiently from the membrane, as well as extracting ataxin-7. The next step was to perform an immunoprecipitation under non-denaturing conditions.

**Co-immunoprecipitation of endogenous ataxin-7 and RanBP2 in MCF7 cells was the first step in the demonstration that RanBP2 and ataxin-7 may interact endogenously.**

To further support the hypothesis that RanBP2 and ataxin-7 interact endogenously, I verified by immunofluorescence that, in some cells, ataxin-7 staining was present at the nuclear membrane, exactly where RanBP2 is located. The percentage of cells in which colocalization was observed was low, however, mostly because SUMOylation is a rapid and reversible “unstable” process, and thus difficult to detect by immunofluorescence. Nevertheless, using a recently developed technique, PLA

(Proximity Ligation Assay), I was able to detect the physical proximity (less than 40 nm) of SUMO-1 and ataxin-7 at the cell nuclear rim. By attentive visual inspection of Figure 17-C, it is possible to see red fluorescent dots in both the cytoplasm and close to the nucleus. This zone could be the cytoplasmic filament at the nuclear pore complex, where RanBP2 is located. **This observation contributes to the validation of our hypothesis that ataxin-7 is SUMO-1-modified by RanBP2.** The reason why I focused on SUMO-1, and not SUMO-2, is because, as demonstrated in the previous section, it is the preferential partner for ataxin-7 modification by RanBP2.

To summarize, we suggested that RanBP2 might SUMOylate ataxin-7 in interphase, at the nuclear pore complex. Our results are in line with the work of Saitoh and collaborators, who also suggested that RanBP2 could act as a SUMO E3 ligase of PML in interphase. When the RanBP2 was invalidated, an anti-SUMO-1 antibody detected fewer PML bodies and nuclear foci. Based on the fact that RanBP2 acts as SUMO E3 ligase for PML *in vitro* (Tatham et al., 2005) and that SUMOylation of PML is required for proper formation for PML bodies, the results suggested that RanBP2 might be involved in the formation of PML bodies, probably through its SUMO E3 ligase activity (Saitoh et al., 2006).

An alternative approach for demonstrating that ataxin-7 SUMOylation is important to prevent aggregation of the mutant protein was to show that aggregation in the nucleus is influenced by the absence of the SUMO E3 ligase. To this end, I chose to selectively silence each SUMO E3 ligase in a cellular SCA7 model. By western blot, I was able to confirm the silencing of each target protein. The western blot of wild type ataxin-7 shows that in absence of either PIAS4 or RanBP2, there was a decrease in the presence of high molecular bands compared non-target control siRNA condition. This result gained in significance when the filter retardation assay showed that the absence of RanBP2 induced an increase in the aggregation of mutated ataxin-7. Although the selective silencing of each SUMO E3 ligase led to an increase in aggregation, the most significant aggregation was obtained in the absence of RanBP2.

In our above-described *in vitro* experiments, we demonstrated that PIAS4 and RanBP2 silencing reduced ataxin-7 modification, and by filter assay that RanBP2

silencing had the greatest effect. We then wanted to compare these *in vitro* results to the SCA7 KI mouse model *in vivo*. By comparing the mRNA of SCA7 KI mice (aged 12 months) and their wild-type littermates, we observed that RanBP2 and PIAS4 were deregulated compared to the other SUMO E3 ligases tested. **This result supports previous evidence that RanBP2 is the main actor in ataxin-7 SUMO modifications, whereas PIAS4 plays a secondary role.**

Co-expression of PIAS4 and SUMO-2 led to the appearance of high molecular weight bands that were more intensely labelled than those seen with other SUMO E3 ligases (Figure 18-B). **These results are consistent with the hypothesis that RanBP2 SUMOylates ataxin-7 by SUMO-1 conjugation, whereas PIAS4 conjugates ataxin-7 to SUMO-2.** Our findings are in line with the literature. In 2006, Hecker and co-authors showed in a yeast two hybrid screen that PIAS4 preferentially coupled SUMO-2 (Hecker et al., 2006). Topoisomerase II also is a target of SUMOylation by RanBP2 and PIAS4 *in vivo*, much like ataxin-7 (Dawlaty et al., 2008). Finally, PIAS4 was shown to mediate SUMO-2 conjugation of topoisomerase II on mitotic chromosomes in (Azuma et al., 2005).

### 5.2.3. Future research perspectives

Starting from this base, it would be extremely interesting to determine whether the mRNA deregulation observed in SCA7 mice can also be seen in SCA7 patients. However, brain tissue from SCA7 patients is very rare. This hypothesis will, therefore, be very difficult to test.

It would also be interesting to confirm the deregulation of the SUMOylation machinery observed in SCA7 mice by microarray analysis. To this end, we recently started collaboration with David Housman's team at MIT in Boston to analyse samples from SCA7 mice by microarray. In the coming months, we hope to confirm deregulation of the SUMO pathway in SCA7 mice.

### 5.3. PML IV SUMOylation: a role in expanded ataxin-7 degradation?

In this section we focus on the role of PML IV SUMOylation and nuclear bodies in the degradation of mutant ataxin-7.

#### 5.3.1. Scientific background

In 2006, our team demonstrated that subcategories of PML bodies, the clastosomes, recruit ataxin-7 to degrade the mutant protein via the proteasome components (Janer et al., 2006). One point of major interest is that PML, the main component of clastosomes, requires SUMOylation to form structurally correct nuclear bodies. In the same year, Shen demonstrated that the simple presence of different mutations within lysines involved in PML SUMOylation, prevents the correct formation of PML bodies (Shen et al., 2006). From the above, we understand the importance of the role played by SUMOylation in PML body formation. To further increase our understanding of the role of SUMOylation in ataxin-7 degradation, I investigated whether PML that is not modified by SUMO can still prevent ataxin-7 degradation.

#### 5.3.2. Contribution and contextualisation of this work

Based on the literature, we expected that degradation of mutant ataxin-7 would be inversely proportional to the severity of PML mutation affecting the SUMO interacting motif (SIM) and the three lysines (K65, 160, 490) to which SUMO can be attached (Shen et al., 2006). We tested this hypothesis with three SUMO-deficient PML constructs: PMLs mutated in the SIM; PMLs with a mutation in the three lysines and in the SIM sequence; PMLs, harbouring a mutation in the three lysine and deletion of the SIM. However, regardless of the PML mutation, a significant reduction in mutant ataxin-7 was detected.

To determine whether this was due to the presence of endogenous PML, we overexpressed SUMO-deficient PML in *Pml*<sup>-/-</sup>MEF cells. The results confirmed the previous experiments on COS7 cells, suggesting that even abnormal PML bodies can degrade ataxin-7. As we will see in the next paragraph, this hypothesis is consistent with the most recent data in the literature.

To confirm that mutated PML formed structurally abnormal PML bodies, I investigated the morphology of the bodies by immunofluorescence. The increase in

the number of PML mutations was correlated with a structural change in the nuclear bodies, as also reported by others (Shen et al., 2006). PML in which the three lysines are mutated and SIM-deleted (PML<sub>mds</sub>) colocalized with mutant ataxin-7, but the inclusions resembled those described, in 2010, as non homogeneous (Janer et al., 2010). At that time, the non-homogeneous inclusions were observed to co-localize mostly with Hsp70, the 19s proteasome subunit and caspase 3, confirming the effort of the cell to degrade nuclear inclusions. These inclusions, which have a star-like structure, were detected in my immunofluorescence experiment as well.

Taken together, these results suggest that non-conventional PML-positive structures are still able to degrade mutant ataxin-7 in the nucleus. SUMO-deficient PML mutated on the three lysine and in the SIM motif still have a functional RING sequence that might be responsible for another activity, as ubiquitin E3 ligase, attributed to TRIM family member who PML belongs to (Ikeda and Inoue, 2012) (Bell et al., 2012).

In addition, very recent results, (Guo et al., 2014), reported the discovery of two substrate recognition regions in PML thanks to *in vitro* binding experiments. The first of these regions, SRS1, preferentially recognizes the pathogenic variants of Htt, and corresponds to the coiled-coil domain (CC) of PML. The CC domain of PML thus serves as an interaction platform for CC structures typically found in long polyQ stretches. The second is SRS2 that specifically binds to short peptides in denatured luciferase, which was used as a misfolded model substrate.

Given this evidence, it is possible that a SUMO-deficient PML might still be able to interact with poly Q proteins, such as ataxin-7, via the SRS1 region due to its preference for polyQ stretches, or via SRS2 domain. With respect to SRS2, it is important to note that this region is encoded by a part of exon 8a and exon 8b, both of which are present in PML IV (Gärtner and Muller, 2014), responsible for ataxin-7 degradation. The CC domain that contains SRS1, or the SRS2 at the C-terminal domain, could affect the potential ubiquitin E3 ligase activity of PML, as suggested by the presence of a RING sequence. Moreover, in SUMO-deficient PML, the RING domain identified as responsible for the E3 ligase activity in other proteins is still active and, in collaboration with the SRS1 or SRS2 sequence, could convert PML into an ubiquitin E3 ligase. This would explain the reduction of ataxin-7 aggregates

during SUMO-deficient PML overexpression in a SCA7 cell model.

### 5.3.3. Future research perspectives

It would be interesting to express PML isoform IV, mutant/deleted or not in the coiled-coil (aa 223-360) or C-terminal (aa 571-633) domain to determine whether ataxin-7 and PML still co-localise. This would be a significant contribution, because it would help to show whether PML actually has ubiquitin E3 ligase activity.

## 5.4. The role of RNF4 in ATXN7 degradation

### 5.4.1. Scientific background

Proteins conjugated with poly-SUMO2/3 chains are recognized and ubiquitinated by RNF4, a RING domain ubiquitin ligase with four tandem SUMO-interacting motifs (SIMs) (Sun et al., 2007). However the role of RNF4 in degrading misfolded proteins remains to be investigated.

### 5.4.2. Contribution and contextualisation of this work

In the previous sections, we provided evidence that both exogenous and endogenous ataxin-7 is a target for modification by SUMO-1 and SUMO-2. The experiments discussed above suggest a non-negligible preference of ataxin-7 for SUMO-2, which implies that ataxin-7 may be poly-SUMOylated. Protein degradation is mediated by the recruitment of ataxin-7 to the proteasome via SUMO-2 modifications (see epoxomicin-based treatment reported in Figure 27). It was unclear, however, whether RNF4 would contribute to the degradation of ataxin-7, even if this mechanism of degradation was first demonstrated for PML (Geoffroy et al., 2010) and very recently for another polyQ-containing protein ATXN1 (Guo et al., 2014). This is important because RNF4 recognizes proteins as a target for the proteasome via their poly-SUMO chains, and could thus contribute to the degradation of polySUMOylated ataxin-7. RNF4 is able to act as an ubiquitin E3 ligase when it binds to polySUMO chains by its SIMs domains. At this point, via the RING, catalytic addition of ubiquitin residues to the target protein finally leads to its degradation by the proteasome (Plechanovová et al., 2012).

As demonstrated also for ATXN1 (Guo et al., 2014), the co-expression of wild-type RNF4 and SUMO-2 in the cellular SCA7 model led to a significant decrease in ataxin-7 aggregation. When the proteasome was inhibited, there was a strong accumulation of mutant ataxin-7, even in the presence of RNF4. This suggested that RNF4 could recruit ataxin-7 via the poly-SUMO chain to catalyse its ubiquitination and re-direct the protein to the proteasome. To confirm these results, we performed the same experiment with a SIM-mutated form of RNF4 (RNF4 dSIM). Overexpression of RNF4 dSIM in the SCA7 cell model was unable to induce a decrease of either soluble ataxin-7 or its aggregated form, as expected if the dSIM mutant is defective for binding to any SUMO target – ataxin-7, in our case. We also tested another mutant form of RNF4 (dHC), which is unable to catalyse the ubiquitin transfer to the protein target due to a mutation in the RING sequence. Dimerization is an essential feature of many RING-containing proteins. In RNF4, dimerization confers ubiquitin E3 ligase activity (Plechanovová et al., 2011)(Liew et al., 2010). Surprisingly, even when the zinc finger motif was mutated, RNF4 was nevertheless able to degrade mutant ataxin-7 and possibly to conjugate ubiquitin protein to ataxin-7.

To explain this unexpected result, I hypothesise that the mutated RNF4 could create a heterodimer with endogenous RNF4 and still maintain ubiquitin E3 ligase activity due to the RING sequence in the wild type protein. This hypothesis is supported by previous studies that demonstrated that PML with a mutation in its RING sequence was still able to recruit endogenous PML (fig. 5 in Shen et al., 2006).

In addition to the unexpected property described above, mutated RNF4 dHC co-expressed with SUMO-2 increased high molecular weight (HMW) modified ataxin-7 bands on western blots. We could not confirm whether these modified bands corresponded to a poly-ubiquitin or to a poly-SUMOylated protein. Additional experiments are necessary to investigate the nature of these modifications; for example, immunoprecipitation under denaturing conditions to precipitate SUMO-2 or ubiquitin, and verification of the presence of ataxin-7 in the immunoprecipitated material.

The results discussed above suggest that RNF4 recruits mutant ataxin-7 to the proteasome via its SUMO-2 chains for degradation. However, RNF4 has been described as a transcriptional regulator: it behaves as a co-repressor when associated

with a novel POZ-AT hook-zinc finger (PATZ) (Fedele et al., 2000). To investigate the possibility that RNF4 negatively regulated ataxin-7 by acting as a transcription co-repressor, we quantified ataxin-7 mRNA during RNF4 overexpression with and without co-expression of SUMO-2. By qRT-PCR, we observed a reduction in ataxin-7 mRNA in cells overexpressing ATXN7-92Q, RNF4 wild type and SUMO-2. A similar reduction was detected in cells overexpressing ATXN7-92Q and RNF4, but not SUMO-2. The reduction in mRNA levels did not, however, mirror the decrease in ataxin-7 protein observed when SUMO-2 and RNF4 were overexpressed which had additive effects. **This was the final confirmation that the effects observed in a SCA7 cellular model were actually related to RNF4 activity on protein degradation and not to mRNA transcription repression. This confirms that RNF4 recruits mutant ataxin-7 to the proteasome via its SUMO-2 chains for degradation.**

## 5.5. SUMO enzymes and proteins deregulation in SCA7 KI mouse model

### 5.5.1. Scientific background

Joan Steffan's team showed for the first time, in 2013, that deregulation of SUMOylation affects the Huntington mouse model R6/2: this mouse contains N-terminally truncated mutant Htt (mHtt) with CAG repeat expansion (125 repeats) within the huntingtin gene exon 1 (Mangiarini et al., 1996). In this model, both *Sumo-1* and *Sumo-2* mRNA increases in the mice at a late stage of their disease; the same pattern is observed in the expression of the enzymes involved in this pathway, such as *Senp2*, *Senp3* and *Senp6*. These alterations suggested that SUMO disregulation depends on the huntingtin gene triplet expansion, suggesting that the same might be true in a SCA7 mouse model.

### 5.5.2. Contribution and contextualisation of this work

In the previous sections, we demonstrated that endogenous ataxin-7 is a target for SUMOylation and that this pathway is important for the cellular response to mutant ataxin-7 aggregation. We now focus on the *in vivo* evidence for SUMOylation deregulation in a SCA7 mouse model, to determine whether a reduction in

SUMOylation prevents the cell from coping efficiently with the accumulation of aggregated ataxin-7 in the cerebellum.

Quantification of mRNA by qRT-PCR showed a decrease in the transcription of key genes, such as *Sumo-1* and *Sumo-2*, starting at 6 months, just before the onset of symptoms in this mouse model of SCA7. This deregulation increased during the following months, along with the worsening of the disease: *Sumo-1* mRNA decreased whereas *Sumo-2* mRNA increased. This is consistent with the activation of SUMO-2 in response to stress described in the literature for other neurodegenerative diseases. The SUMO-2 response to neuronal stressors has recently been observed in several systems, including APP overexpression in AD mice (McMillan et al., 2011) and transient ischemia in cells (Yang et al., 2012). In some cases, this promotes a neuroprotective response to ischemic stress (Datwyler et al., 2011). As for SCA7, we have *in vitro* evidence that the expression of expanded polyQ in a stable, inducible cell model results in a concomitant increase of ROS levels, cellular toxicity and aggregation of the disease-causing protein. The increase in ROS could be completely prevented by inhibition of NADPH oxidase (NOX) complexes, suggesting that ataxin-7 directly or indirectly causes oxidative stress by increasing superoxide anion production from these complexes (Ajayi et al., 2012). **From the literature and our results above, we can deduce that the presence of polyQ-expanded ataxin-7 leads to a cellular reaction, which can in turn induce an increase in SUMO-2 mRNA.**

In addition to the cerebellum, we considered retina, which we know being a tissue particularly affected by the disease – a unique feature of SCA7 among all other spinocerebellar ataxias. Since SUMO E3 ligases has been confirmed to be expressed in the retina and to regulate SUMOylation of the metabotropic glutamate receptor 8b (Dütting et al., 2011), we pursued our investigation on this specific tissue.

*Sumo-1* and *Sumo-2* mRNA was also reduced at 6 months in the retina. At 12 months, the decrease in *Sumo-1* mRNA and the increase of *Sumo-2* mRNA was observed in the retina as well as in the cerebellum. **This recurrent pattern confirms that SUMO pathway deregulation is present in the tissues most affected by the disease.**

We identified, in *in vitro* experiments, RanBP2 as the major SUMO E3 ligase for ataxin-7. *In vivo*, a significant decrease in the mRNA for this enzyme was observed, along with *Pias4*, in SCA7 KI mice compared to wild type littermates. **This result validates our hypothesis that these enzymes are involved in SUMO modification of ataxin-7. Their deregulation could negatively affect degradation of mutant ataxin-7.** The reduction is less evident in the retina, however: this may imply that the SUMO E3 ligases catalysing this process in the retina are different from those in the cerebellum. For example, PIAS3-regulated SUMOylation of transcription factors has been described in photoreceptors, demonstrating additional functions for SUMO proteins in the CNS, such as the development of rods (Onishi et al., 2010). **This result is particularly noteworthy from a therapeutic point of view, because it suggests that different targets for regulation should be chosen depending on the affected tissue.**

Our results suggest that chronic expression of ataxin-7 with expanded CAG repeats produces a misfolded protein that activate stress response pathways inducing SUMO-2 modification of ataxin-7. This response is, nevertheless, not sufficient to cope with the accumulation of insoluble and HMW species that reflect on-going pathogenesis. By western blot, we showed an increase in the non-conjugated form of SUMO-1 and SUMO-2 from SCA7 KI cerebellae samples and a decrease in the HMW species that we observed in the stacking gel from the same samples. We deduce neither isoform is conjugated with either mutant ataxin-7 or other SUMOylation targets.

The above observations could be explained by a modification of the three-dimensional structure of ataxin-7 that would hide the SUMO acceptor site. In the cellular SCA7 model, in which ataxin-7 aggregates (Figure 16-C and Figure 24-B) are smaller in size than in the SCA7 KI mice (Figure 33-B), SUMO-1 and SUMO-2 overexpression induced the degradation of the mutant protein. In the Purkinje cells of the mouse model, we detected one or at most two large inclusions that were circular in shape. These structural characteristics might result from a protein conformation that prevents SUMO from reaching its site of attachment. We also demonstrated by immunofluorescence that mutant ataxin-7 aggregates and SUMO-1 are co-localized, although this does not prove that they interact. PML, another

protein involved in ataxin-7 degradation, is also a SUMOylation target. It is possible that SUMO-1 conjugates with PML in the nucleus. Likewise, we cannot ignore that ataxin-7 and SUMO-1 co-localized in the nuclear rim and cytoplasm of wild-type mice but also in the knock-in mice. As previously reported, RanBP2 is present in both cell compartments, and RanBP2 is a major SUMO E3 ligase. **This confirms that the co-localization of ataxin-7 and SUMO-1 is compatible with SUMO-1-modification of ataxin-7 by RanBP2 *in vivo*.**

### 5.5.3. Future perspective

To confirm that SUMOylation is impaired in SCA7 mice, and that SUMO conjugation is defective, it would be interesting to perform a SUMO-immunoprecipitation on samples of mouse cerebellum. This could be done with the protocol developed in Melchior's laboratory (Barysch et al., 2014) (Becker et al., 2013), as it was used successfully for the detection of SUMOylated proteins in mouse liver tissues.

This is encouraging for its use on mouse brain samples, but will require collecting a large number of cerebellae to be able to detect the low levels of SUMO-modified ataxin-7. Using this protocol in MCF7 cells, SUMO-2 and SUMO-1 modified ataxin-7 was detectable only with "super-sensitive" ECL detection kit. It will thus be a challenge to detect SUMO-ataxin-7 in cerebella. Immunoprecipitation could tell us whether ataxin-7 is also a target for SUMO modification *in vivo* and whether SUMO-1 and SUMO-2 conjugation is affected in SCA7 KI mice.

## 5.6. SUMO-1 and RanBP2 accumulation in the brain of SCA7 patients

### 5.6.1. Scientific background

SUMO proteins have been detected in inclusions in various neurodegenerative diseases, such as multiple system atrophy (Terashima et al., 2002), Huntington's disease and other polyglutamine disorders (Ueda et al., 2002). In addition, several proteins specifically involved in these neurological diseases have been identified as SUMO targets. An example is ataxin-7, which we demonstrated to be a target for SUMOylation both *in vitro* and *in vivo*.

### 5.6.2. Contribution and contextualisation of this work

After confirming the expression of SUMO-related proteins in SCA7 KI mice, we targeted tissues from SCA7 patients. We previously showed that SUMO-1 and SUMO-2 co-localized with ataxin-7 in the cortex of SCA7 patients (Janer et al., 2010). Here, I demonstrated by IHC in the cerebellum of a SCA7 patient that Purkinje cells contained much more SUMO-1 than the control cerebellum. This accumulation suggests that SUMO-1 expression might be deregulated during the course of the disease.

SUMO-1 staining is nuclear but also cytoplasmic, and increases specifically in the cytoplasm in SCA7 brain tissue. An increase in the cytoplasmic staining for SUMO-1 was already shown in other neurodegenerative diseases, such as multiple system atrophy (MSA) (Poutney et al., 2005). Fluorescence immunohistochemistry showed that SUMO-1 sub-domains were frequent within and around inclusion bodies in MSA disease and co-localized with the lysosomal marker, cathepsin D, in affected brain regions. This suggests that SUMO-1 plays a role in lysosome function (Wong et al., 2013), and would explain the increase in cytoplasmic SUMO-1 in Purkinje cells in a human SCA7 brain. Moreover, we very recently published that autophagy-lysosomal degradation pathway contributes to SCA7, as shown by the increase in cathepsin-D expression in the SCA7<sup>266Q/5Q</sup> knock-in mouse model and in brain tissue from SCA7 patients (Alves et al., 2014). **These results suggest that molecular markers of SUMOylation accumulate in the brain of SCA7 patients.** It might also imply that there could be a connection between SUMO-1 and the autophagy-lysosome system in this disease. These results confirm the importance of this pathway in SCA7 disease and indicate that proteins involved in the SUMOylation or deSUMOylation of ataxin-7 might represent target for therapeutic strategies, as already identified for cancer therapy.

### 5.6.3. Future perspective

At present, there is no *in vivo* evidence in other neurodegenerative diseases, except for Huntington disease and SCA1, of mutations affecting or deregulating SUMOylation.

It would be of interest to determine whether the expression of genes related to the SUMOylation pathway is correlated with the progression and severity of SCA7 pathology. Potentially, this could be investigated in blood cells from patients, although expression of the relevant messenger RNA in blood may differ from their expression in neurons. In the animal model of SCA7, one could perform a laser dissection of Purkinje cells in order to investigate deregulation of mRNA expression; this is a feasible approach.

The obtained results could help us determine whether SUMOylation, and notably the enzymes involved in this pathway, are potential targets for therapeutic intervention. These results could contribute to a better understanding of the basic cell mechanisms triggered by the disease.



## 6. Conclusions

The overall scientific goal of this work was to advance the understanding of the fundamental molecular processes that regulate the interaction of ataxin-7 with other proteins involved in the SUMOylation pathway. In the longer term, this study could contribute to the identification of a therapeutic strategy for spinocerebellar ataxia type 7 (SCA7), a polyQ neurodegenerative disease mostly affecting Purkinje cells in the cerebellum and photoreceptor cells in the retina.

Our first main result indicates a correlation between the SCA7 pathology and a deregulation in SUMO-related mRNA levels *in vivo*. This correlation is supported by additional evidence that we collected; in particular that ataxin-7 is an endogenous SUMO target with a preference for SUMO-2 over SUMO-1.

Moreover, we identified RanBP2 as the major SUMO E3 ligase of ataxin-7: the overexpression of RanBP2 and SUMO-1 decreases the level of aggregated and mutant ataxin-7 in a SCA7 cellular model. We also observed the same phenomenon for PIAS4, which however induces ataxin-7 SUMOylation via SUMO-2 instead of SUMO-1. RanBP2 and PIAS4 mRNA reduction in a SCA7 mouse model validates our hypothesis that these enzymes are involved in SUMO modification of mutant ataxin-7.

We also showed that “non-conventional” PML-positive structures are still able to degrade mutant ataxin-7 in the nucleus. Being a member of the TRIM family and having a RING sequence, PML could possess an ubiquitin E3 ligase activity that could explain our results in the degradation of mutant ataxin-7, even when PML is SUMO deficient.

Finally, we demonstrated that molecular markers of SUMOylation accumulate in the brain of SCA7 patients, both in the cytoplasm and the nucleus. Increase in cytoplasmic staining of SUMO-1 could represent a connection between the SUMO pathway and the autophagy-lysosome system in SCA7.



# Bibliography

Abou-Sleymane, G., Chalmel, F., Helmlinger, D., Lardenois, A., Thibault, C., Weber, C., Mérienne, K., Mandel, J.-L., Poch, O., Devys, D., et al. (2006). Polyglutamine expansion causes neurodegeneration by altering the neuronal differentiation program. *Hum. Mol. Genet.* *15*, 691–703.

Adachi, H., Waza, M., Tokui, K., Katsuno, M., Minamiyama, M., Tanaka, F., Doyu, M., and Sobue, G. (2007). CHIP Overexpression Reduces Mutant Androgen Receptor Protein and Ameliorates Phenotypes of the Spinal and Bulbar Muscular Atrophy Transgenic Mouse Model. *J. Neurosci.* *27*, 5115–5126.

Ajayi, A., Yu, X., Lindberg, S., Langel, Ü., and Ström, A.-L. (2012). Expanded ataxin-7 cause toxicity by inducing ROS production from NADPH oxidase complexes in a stable inducible Spinocerebellar ataxia type 7 (SCA7) model. *BMC Neurosci.* *13*, 86.

Alexandre Janer, Werner, A., Takahashi-Fujigasaki, J., Daret, A., Fujigasaki, H., Takada, K., Duyckaerts, C., Brice, A., Dejean, A., and Sittler, A. (2010). SUMOylation attenuates the aggregation propensity and cellular toxicity of the polyglutamine expanded ataxin-7. *Hum. Mol. Genet.* *19*, 181–195.

Allingham-Hawkins, D.J., and Ray, P.N. (1995). FRAXE expansion is not a common etiological factor among developmentally delayed males. *Am. J. Hum. Genet.* *57*, 72.

Alves, S., Cormier-Dequaire, F., Marinello, M., Marais, T., Muriel, M.-P., Beaumatin, F., Charbonnier-Beaupel, F., Tahiri, K., Seilhean, D., Hachimi, K.E., et al. (2014). The autophagy/lysosome pathway is impaired in SCA7 patients and SCA7 knock-in mice. *Acta Neuropathol. (Berl.)* 1–18.

Andrews, E.A., Palecek, J., Sergeant, J., Taylor, E., Lehmann, A.R., and Watts, F.Z. (2005). Nse2, a component of the Smc5-6 complex, is a SUMO ligase required for the response to DNA damage. *Mol. Cell. Biol.* *25*, 185–196.

Arrasate, M., Mitra, S., Schweitzer, E.S., Segal, M.R., and Finkbeiner, S. (2004). Inclusion body formation reduces levels of mutant huntingtin and the risk of neuronal death. *Nature* *431*, 805–810.

Azuma, Y., Arnautov, A., Anan, T., and Dasso, M. (2005). PIASy mediates SUMO-2 conjugation of Topoisomerase-II on mitotic chromosomes. *EMBO J.* *24*, 2172–2182.

Barysch, S.V., Dittner, C., Flotho, A., Becker, J., and Melchior, F. (2014).

Identification and analysis of endogenous SUMO1 and SUMO2/3 targets in mammalian cells and tissues using monoclonal antibodies. *Nat. Protoc.* *9*, 896–909.

Becker, J., Barysch, S.V., Karaca, S., Dittner, C., Hsiao, H.-H., Diaz, M.B., Herzig, S., Urlaub, H., and Melchior, F. (2013). Detecting endogenous SUMO targets in mammalian cells and tissues. *Nat. Struct. Mol. Biol.* *20*, 525–531.

Bell, J.L., Malyukova, A., Holien, J.K., Koach, J., Parker, M.W., Kavallaris, M., Marshall, G.M., and Cheung, B.B. (2012). TRIM16 Acts as an E3 Ubiquitin Ligase and Can Heterodimerize with Other TRIM Family Members. *PLoS ONE* *7*, e37470.

Bennett, E.J., Bence, N.F., Jayakumar, R., and Kopito, R.R. (2005). Global Impairment of the Ubiquitin-Proteasome System by Nuclear or Cytoplasmic Protein Aggregates Precedes Inclusion Body Formation. *Mol. Cell* *17*, 351–365.

Benomar, A., Le Guern, E., Dürr, A., Ouhabi, H., Stevanin, G., Yahyaoui, M., Chkili, T., Agid, Y., and Brice, A. (1994). Autosomal-dominant cerebellar ataxia with retinal degeneration (ADCA type II) is genetically different from ADCA type I. *Ann. Neurol.* *35*, 439–444.

Benton, C.S., de Silva, R., Rutledge, S.L., Bohlega, S., Ashizawa, T., and Zoghbi, H.Y. (1998). Molecular and clinical studies in SCA-7 define a broad clinical spectrum and the infantile phenotype. *Neurol. Oct. 1998* *51*, 1081–1086.

Bett, J.S., Goellner, G.M., Woodman, B., Pratt, G., Rechsteiner, M., and Bates, G.P. (2006). Proteasome impairment does not contribute to pathogenesis in R6/2 Huntington's disease mice: exclusion of proteasome activator REG $\gamma$  as a therapeutic target. *Hum. Mol. Genet.* *15*, 33–44.

Bjørkøy, G., Lamark, T., Brech, A., Outzen, H., Perander, M., Øvervatn, A., Stenmark, H., and Johansen, T. (2005). p62/SQSTM1 forms protein aggregates degraded by autophagy and has a protective effect on huntingtin-induced cell death. *J. Cell Biol.* *171*, 603–614.

Blazek, E., Mittler, G., and Meisterernst, M. (2005). The Mediator of RNA polymerase II. *Chromosoma* *113*, 399–408.

Boddy, M.N., Howe, K., Etkin, L.D., Solomon, E., and Freemont, P.S. (1996). PIC 1, a novel ubiquitin-like protein which interacts with the PML component of a multiprotein complex that is disrupted in acute promyelocytic leukaemia. *Oncogene* *13*, 971–982.

Bondareff, W., Mountjoy, C.Q., Roth, M., and Hauser, D.L. (1989). Neurofibrillary degeneration and neuronal loss in Alzheimer's disease. *Neurobiol. Aging* *10*, 709–715.

Bossis, G., and Melchior, F. (2006). Regulation of SUMOylation by Reversible Oxidation of SUMO Conjugating Enzymes. *Mol. Cell* *21*, 349–357.

Bowman, A.B., Yoo, S.-Y., Dantuma, N.P., and Zoghbi, H.Y. (2005). Neuronal

dysfunction in a polyglutamine disease model occurs in the absence of ubiquitin–proteasome system impairment and inversely correlates with the degree of nuclear inclusion formation. *Hum. Mol. Genet.* *14*, 679–691.

Browne, S.E., and Beal, M.F. (2006). Oxidative Damage in Huntington's Disease Pathogenesis. *Antioxid. Redox Signal.* *8*, 2061–2073.

Bucciantini, M., Giannoni, E., Chiti, F., Baroni, F., Formigli, L., Zurdo, J., Taddei, N., Ramponi, G., Dobson, C.M., and Stefani, M. (2002). Inherent toxicity of aggregates implies a common mechanism for protein misfolding diseases. *Nature* *416*, 507–511.

Bunday, S., Carter, C.O., and Soothill, J.F. (1970). Early recognition of heterozygotes for the gene for dystrophia myotonica. *J. Neurol. Neurosurg. Psychiatry* *33*, 279–293.

Campuzano, V., Montermini, L., Moltò, M.D., Pianese, L., Cossée, M., Cavalcanti, F., Monros, E., Rodius, F., Duclos, F., Monticelli, A., et al. (1996). Friedreich's ataxia: autosomal recessive disease caused by an intronic GAA triplet repeat expansion. *Science* *271*, 1423–1427.

Cancel, G., Duyckaerts, C., Holmberg, M., Zander, C., Yvert, G., Lebre, A.S., Ruberg, M., Faucheux, B., Agid, Y., Hirsch, E., et al. (2000). Distribution of ataxin-7 in normal human brain and retina. *Brain J. Neurol.* *123 Pt 12*, 2519–2530.

Caughey, B., and Lansbury, P.T. (2003). PROTOFIBRILS, PORES, FIBRILS, AND NEURODEGENERATION: Separating the Responsible Protein Aggregates from The Innocent Bystanders.

Caviston, J.P., Ross, J.L., Antony, S.M., Tokito, M., and Holzbaur, E.L.F. (2007). Huntingtin facilitates dynein/dynactin-mediated vesicle transport. *Proc. Natl. Acad. Sci. U. S. A.* *104*, 10045–10050.

Chai, Y., Koppenhafer, S.L., Shoesmith, S.J., Perez, M.K., and Paulson, H.L. (1999). Evidence for Proteasome Involvement in Polyglutamine Disease: Localization to Nuclear Inclusions in SCA3/MJD and Suppression of Polyglutamine Aggregation in vitro. *Hum. Mol. Genet.* *8*, 673–682.

Chan, H.Y.E., Warrick, J.M., Gray-Board, G.L., Paulson, H.L., and Bonini, N.M. (2000). Mechanisms of chaperone suppression of polyglutamine disease: selectivity, synergy and modulation of protein solubility in *Drosophila*. *Hum. Mol. Genet.* *9*, 2811–2820.

Chan, H.Y.E., Warrick, J.M., Andriola, I., Merry, D., and Bonini, N.M. (2002). Genetic modulation of polyglutamine toxicity by protein conjugation pathways in *Drosophila*. *Hum. Mol. Genet.* *11*, 2895–2904.

Chen, H.-K., Fernandez-Funez, P., Acevedo, S.F., Lam, Y.C., Kaytor, M.D., Fernandez, M.H., Aitken, A., Skoulakis, E.M.C., Orr, H.T., Botas, J., et al. (2003). Interaction of Akt-Phosphorylated Ataxin-1 with 14-3-3 Mediates Neurodegeneration in Spinocerebellar Ataxia Type 1. *Cell* *113*, 457–468.

- Chen, S., Peng, G.-H., Wang, X., Smith, A.C., Grote, S.K., Sopher, B.L., and Spada, A.R.L. (2004). Interference of Crx-dependent transcription by ataxin-7 involves interaction between the glutamine regions and requires the ataxin-7 carboxy-terminal region for nuclear localization. *Hum. Mol. Genet.* *13*, 53–67.
- Chen, Y.C., Gatchel, J.R., Lewis, R.W., Mao, C.-A., Grant, P.A., Zoghbi, H.Y., and Dent, S.Y.R. (2012). Gcn5 loss-of-function accelerates cerebellar and retinal degeneration in a SCA7 mouse model. *Hum. Mol. Genet.* *21*, 394–405.
- Cho, G., Lim, Y., and Golden, J.A. (2009). SUMO Interaction Motifs in Sizn1 Are Required for Promyelocytic Leukemia Protein Nuclear Body Localization and for Transcriptional Activation. *J. Biol. Chem.* *284*, 19592–19600.
- Choi, J.Y., Ryu, J.H., Kim, H.-S., Park, S.G., Bae, K.-H., Kang, S., Myung, P.K., Cho, S., Park, B.C., and Lee, D.H. (2007). Co-chaperone CHIP promotes aggregation of ataxin-1. *Mol. Cell. Neurosci.* *34*, 69–79.
- Chort, A., Alves, S., Marinello, M., Dufresnois, B., Dornbierer, J.-G., Tesson, C., Latouche, M., Baker, D.P., Barkats, M., Hachimi, K.H.E., et al. (2013). Interferon beta induces clearance of mutant ataxin 7 and improves locomotion in SCA7 knock-in mice. *Brain* *136*, 1732–1745.
- Chou, A.-H., Chen, C.-Y., Chen, S.-Y., Chen, W.-J., Chen, Y.-L., Weng, Y.-S., and Wang, H.-L. (2010). Polyglutamine-expanded ataxin-7 causes cerebellar dysfunction by inducing transcriptional dysregulation. *Neurochem. Int.* *56*, 329–339.
- Christie, N.T.M., Lee, A.L., Fay, H.G., Gray, A.A., and Kikis, E.A. (2014). Novel Polyglutamine Model Uncouples Proteotoxicity from Aging. *PLoS ONE* *9*, e96835.
- Colin, E., Régulier, E., Perrin, V., Dürr, A., Brice, A., Aebischer, P., Déglon, N., Humbert, S., and Saudou, F. (2005). Akt is altered in an animal model of Huntington's disease and in patients. *Eur. J. Neurosci.* *21*, 1478–1488.
- Cummings, C.J., Sun, Y., Opal, P., Antalffy, B., Mestril, R., Orr, H.T., Dillmann, W.H., and Zoghbi, H.Y. (2001). Over-expression of inducible HSP70 chaperone suppresses neuropathology and improves motor function in SCA1 mice. *Hum. Mol. Genet.* *10*, 1511–1518.
- Van Damme, E., Laukens, K., Dang, T.H., and Van Ostade, X. (2010). A manually curated network of the PML nuclear body interactome reveals an important role for PML-NBs in SUMOylation dynamics. *Int. J. Biol. Sci.* *6*, 51–67.
- Danielsen, J.R., Povlsen, L.K., Villumsen, B.H., Streicher, W., Nilsson, J., Wikstrom, M., Bekker-Jensen, S., and Mailand, N. (2012). DNA damage-inducible SUMOylation of HERC2 promotes RNF8 binding via a novel SUMO-binding Zinc finger. *J. Cell Biol.* *197*, 179–187.
- Datwyler, A.L., Lättig-Tünnemann, G., Yang, W., Paschen, W., Lee, S.L.L., Dirnagl, U., Endres, M., and Harms, C. (2011). SUMO2/3 conjugation is an endogenous

- neuroprotective mechanism. *J. Cereb. Blood Flow Metab.* *31*, 2152–2159.
- David, G., Abbas, N., Stevanin, G., Dürr, A., Yvert, G., Cancel, G., Weber, C., Imbert, G., Saudou, F., Antoniou, E., et al. (1997). Cloning of the SCA7 gene reveals a highly unstable CAG repeat expansion. *Nat. Genet.* *17*, 65–70.
- David, G., Dürr, A., Stevanin, G., Cancel, G., Abbas, N., Benomar, A., Belal, S., Lebre, A.-S., Abada-Bendib, M., Grid, D., et al. (1998). Molecular and Clinical Correlations in Autosomal Dominant Cerebellar Ataxia with Progressive Macular Dystrophy (SCA7). *Hum. Mol. Genet.* *7*, 165–170.
- Dawlaty, M.M., Malureanu, L., Jeganathan, K.B., Kao, E., Sustmann, C., Tahk, S., Shuai, K., Grosschedl, R., and van Deursen, J.M. (2008). Resolution of Sister Centromeres Requires RanBP2-Mediated SUMOylation of Topoisomerase II $\alpha$ . *Cell* *133*, 103–115.
- Deshaies, R.J., and Joazeiro, C.A.P. (2009). RING domain E3 ubiquitin ligases. *Annu. Rev. Biochem.* *78*, 399–434.
- Desterro, J.M., Rodriguez, M.S., Kemp, G.D., and Hay, R.T. (1999). Identification of the enzyme required for activation of the small ubiquitin-like protein SUMO-1. *J. Biol. Chem.* *274*, 10618–10624.
- Díaz-Hernández, M., Hernández, F., Martín-Aparicio, E., Gómez-Ramos, P., Morán, M.A., Castaño, J.G., Ferrer, I., Avila, J., and Lucas, J.J. (2003). Neuronal Induction of the Immunoproteasome in Huntington's Disease. *J. Neurosci.* *23*, 11653–11661.
- Díaz-Hernández, M., Valera, A.G., Morán, M.A., Gómez-Ramos, P., Alvarez-Castelao, B., Castaño, J.G., Hernández, F., and Lucas, J.J. (2006). Inhibition of 26S proteasome activity by huntingtin filaments but not inclusion bodies isolated from mouse and human brain. *J. Neurochem.* *98*, 1585–1596.
- Ding, Q., Dimayuga, E., Martin, S., Bruce-Keller, A.J., Nukala, V., Cuervo, A.M., and Keller, J.N. (2003). Characterization of chronic low-level proteasome inhibition on neural homeostasis. *J. Neurochem.* *86*, 489–497.
- Ding, W.-X., Ni, H.-M., Gao, W., Yoshimori, T., Stolz, D.B., Ron, D., and Yin, X.-M. (2007). Linking of Autophagy to Ubiquitin-Proteasome System Is Important for the Regulation of Endoplasmic Reticulum Stress and Cell Viability. *Am. J. Pathol.* *171*, 513–524.
- Dobson, C.M. (2002). Protein-misfolding diseases: Getting out of shape. *Nature* *418*, 729–730.
- Dobson, C.M. (2003a). Protein folding and misfolding. *Nature* *426*, 884–890.
- Dobson, C.M. (2003b). Protein folding and misfolding. *Nature* *426*, 884–890.
- Dobson, C.M., Šali, A., and Karplus, M. (1998). Protein Folding: A Perspective from Theory and Experiment. *Angew. Chem. Int. Ed.* *37*, 868–893.

Dovey, C.L., Varadaraj, A., Wyllie, A.H., and Rich, T. (2004). Stress responses of PML nuclear domains are ablated by ataxin-1 and other nucleoprotein inclusions. *J. Pathol.* *203*, 877–883.

Drag, M., and Salvesen, G.S. (2008). DeSUMOylating enzymes—SENPs. *IUBMB Life* *60*, 734–742.

Duncan, C.E., An, M.C., Papanikolaou, T., Rugani, C., Vitelli, C., and Ellerby, L.M. (2013). Histone deacetylase-3 interacts with ataxin-7 and is altered in a spinocerebellar ataxia type 7 mouse model. *Mol. Neurodegener.* *8*, 42.

Duprez, E., Saurin, A.J., Desterro, J.M., Lallemand-Breitenbach, V., Howe, K., Boddy, M.N., Solomon, E., The, H. de, Hay, R.T., and Freemont, P.S. (1999). SUMO-1 modification of the acute promyelocytic leukaemia protein PML: implications for nuclear localisation. *J. Cell Sci.* *112*, 381–393.

Dütting, E., Schröder-Kress, N., Sticht, H., and Enz, R. (2011). SUMO E3 ligases are expressed in the retina and regulate SUMOylation of the metabotropic glutamate receptor 8b. *Biochem. J.* *435*, 365–371.

Emamian, E.S., Kaytor, M.D., Duvick, L.A., Zu, T., Tousey, S.K., Zoghbi, H.Y., Clark, H.B., and Orr, H.T. (2003). Serine 776 of Ataxin-1 Is Critical for Polyglutamine-Induced Disease in SCA1 Transgenic Mice. *Neuron* *38*, 375–387.

Enevoldson, T.P., Sanders, M.D., and Harding, A.E. (1994). Autosomal dominant cerebellar ataxia with pigmentary macular dystrophy. A clinical and genetic study of eight families. *Brain* *117*, 445–460.

Everett, R.D., Lomonte, P., Sternsdorf, T., Driel, R. van, and Orr, A. (1999). Cell cycle regulation of PML modification and ND10 composition. *J. Cell Sci.* *112*, 4581–4588.

Evert, B.O., Araujo, J., Vieira-Saecker, A.M., Vos, R.A.I. de, Harendza, S., Klockgether, T., and Wüllner, U. (2006). Ataxin-3 Represses Transcription via Chromatin Binding, Interaction with Histone Deacetylase 3, and Histone Deacetylation. *J. Neurosci.* *26*, 11474–11486.

Del-Favero, J., Krols, L., Michalik, A., Theuns, J., Löfgren, A., Goossens, D., Wehnert, A., Bossche, D.V. den, Zand, K.V., Backhovens, H., et al. (1998). Molecular Genetic Analysis of Autosomal Dominant Cerebellar Ataxia with Retinal Degeneration (ADCA Type II) Caused by CAG Triplet Repeat Expansion. *Hum. Mol. Genet.* *7*, 177–186.

Fedele, M., Benvenuto, G., Pero, R., Majello, B., Battista, S., Lembo, F., Vollono, E., Day, P.M., Santoro, M., Lania, L., et al. (2000). A Novel Member of the BTB/POZ Family, PATZ, Associates with the RNF4 RING Finger Protein and Acts as a Transcriptional Repressor. *J. Biol. Chem.* *275*, 7894–7901.

Fersht, A.R. (2000). Transition-state structure as a unifying basis in protein-folding mechanisms: contact order, chain topology, stability, and the extended nucleus

- mechanism. *Proc. Natl. Acad. Sci. U. S. A.* *97*, 1525–1529.
- Flotho, A., and Melchior, F. (2013). Sumoylation: A Regulatory Protein Modification in Health and Disease. *Annu. Rev. Biochem.* *82*, 357–385.
- Fu, C., Ahmed, K., Ding, H., Ding, X., Lan, J., Yang, Z., Miao, Y., Zhu, Y., Shi, Y., Zhu, J., et al. (2005). Stabilization of PML nuclear localization by conjugation and oligomerization of SUMO-3. *Oncogene* *24*, 5401–5413.
- Fuertes, G., Villarroya, A., and Knecht, E. (2003a). Role of proteasomes in the degradation of short-lived proteins in human fibroblasts under various growth conditions. *Int. J. Biochem. Cell Biol.* *35*, 651–664.
- Fuertes, G., Martin De Llano, J.J., Villarroya, A., Rivett, A.J., and Knecht, E. (2003b). Changes in the proteolytic activities of proteasomes and lysosomes in human fibroblasts produced by serum withdrawal, amino-acid deprivation and confluent conditions. *Biochem. J.* *375*, 75–86.
- Garden, G.A., Libby, R.T., Fu, Y.-H., Kinoshita, Y., Huang, J., Possin, D.E., Smith, A.C., Martinez, R.A., Fine, G.C., Grote, S.K., et al. (2002). Polyglutamine-expanded ataxin-7 promotes non-cell-autonomous purkinje cell degeneration and displays proteolytic cleavage in ataxic transgenic mice. *J. Neurosci. Off. J. Soc. Neurosci.* *22*, 4897–4905.
- Gareau, J.R., and Lima, C.D. (2010). The SUMO pathway: emerging mechanisms that shape specificity, conjugation and recognition. *Nat. Rev. Mol. Cell Biol.* *11*, 861–871.
- Gärtner, A., and Muller, S. (2014). PML, SUMO, and RNF4: Guardians of Nuclear Protein Quality. *Mol. Cell* *55*, 1–3.
- Geiss-Friedlander, R., and Melchior, F. (2007). Concepts in sumoylation: a decade on. *Nat. Rev. Mol. Cell Biol.* *8*, 947–956.
- Geoffroy, M.-C., Jaffray, E.G., Walker, K.J., and Hay, R.T. (2010). Arsenic-Induced SUMO-Dependent Recruitment of RNF4 into PML Nuclear Bodies. *Mol. Biol. Cell* *21*, 4227–4239.
- Glabe, C.G., and Kaye, R. (2006). Common structure and toxic function of amyloid oligomers implies a common mechanism of pathogenesis. *Neurol. Incl.-Body Myositis Clin. Pathol. Asp. Basic Res. Potential. Relev. Treat.* *66*.
- Glenner, G.G., and Wong, C.W. (2012). Alzheimer's disease: initial report of the purification and characterization of a novel cerebrovascular amyloid protein. 1984. *Biochem. Biophys. Res. Commun.* *425*, 534–539.
- Glickman, M.H., and Ciechanover, A. (2002). The Ubiquitin-Proteasome Proteolytic Pathway: Destruction for the Sake of Construction. *Physiol. Rev.* *82*, 373–428.
- Goldberg, A.L. (2003). Protein degradation and protection against misfolded or damaged proteins. *Nature* *426*, 895–899.

- Goldberg, Y.P., Andrew, S.E., Theilmann, J., Kremer, B., Squitieri, F., Telenius, H., Brown, J.D., and Hayden, M.R. (1993). Familial predisposition to recurrent mutations causing Huntington's disease: genetic risk to sibs of sporadic cases. *J. Med. Genet.* *30*, 987.
- Gouw, L.G., Castañeda, M.A., McKenna, C.K., Digre, K.B., Pulst, S.M., Perlman, S., Lee, M.S., Gomez, C., Fischbeck, K., Gagnon, D., et al. (1998). Analysis of the Dynamic Mutation in the SCA7 Gene Shows Marked Parental Effects on CAG Repeat Transmission. *Hum. Mol. Genet.* *7*, 525–532.
- Gray, P.A., Fu, H., Luo, P., Zhao, Q., Yu, J., Ferrari, A., Tenzen, T., Yuk, D., Tsung, E.F., Cai, Z., et al. (2004). Mouse Brain Organization Revealed Through Direct Genome-Scale TF Expression Analysis. *Science* *306*, 2255–2257.
- Grundke-Iqbal, I., Iqbal, K., Quinlan, M., Tung, Y.C., Zaidi, M.S., and Wisniewski, H.M. (1986). Microtubule-associated protein tau. A component of Alzheimer paired helical filaments. *J. Biol. Chem.* *261*, 6084–6089.
- Guo, D., Li, M., Zhang, Y., Yang, P., Eckenrode, S., Hopkins, D., Zheng, W., Purohit, S., Podolsky, R.H., Muir, A., et al. (2004). A functional variant of SUMO4, a new I $\kappa$ B $\alpha$  modifier, is associated with type 1 diabetes. *Nat. Genet.* *36*, 837–841.
- Guo, L., Giasson, B.I., Glavis-Bloom, A., Brewer, M.D., Shorter, J., Gitler, A.D., and Yang, X. (2014). A Cellular System that Degrades Misfolded Proteins and Protects against Neurodegeneration. *Mol. Cell*.
- Gusella, J.F., and MacDonald, M.E. (2000). Molecular genetics: unmasking polyglutamine triggers in neurodegenerative disease. *Nat. Rev. Neurosci.* *1*, 109–115.
- Gutkunst, C.-A., Li, S.-H., Yi, H., Mulroy, J.S., Kuemmerle, S., Jones, R., Rye, D., Ferrante, R.J., Hersch, S.M., and Li, X.-J. (1999). Nuclear and Neuropil Aggregates in Huntington's Disease: Relationship to Neuropathology. *J. Neurosci.* *19*, 2522–2534.
- Haass, C., and Selkoe, D.J. (2007). Soluble protein oligomers in neurodegeneration: lessons from the Alzheimer's amyloid  $\beta$ -peptide. *Nat. Rev. Mol. Cell Biol.* *8*, 101–112.
- Hamada, M., Haeger, A., Jeganathan, K.B., Ree, J.H. van, Malureanu, L., Wälde, S., Joseph, J., Kehlenbach, R.H., and Deursen, J.M. van (2011). Ran-dependent docking of importin- $\beta$  to RanBP2/Nup358 filaments is essential for protein import and cell viability. *J. Cell Biol.* *194*, 597–612.
- Hardy, J., and Orr, H. (2006). The genetics of neurodegenerative diseases. *J. Neurochem.* *97*, 1690–1699.
- Hay, R.T. (2005). SUMO: A History of Modification. *Mol. Cell* *18*, 1–12.
- Hecker, C.-M., Rabiller, M., Haglund, K., Bayer, P., and Dikic, I. (2006). Specification of SUMO1- and SUMO2-interacting Motifs. *J. Biol. Chem.* *281*, 16117–16127.

- Helmlinger, D., Bonnet, J., Mandel, J.-L., Trottier, Y., and Devys, D. (2004a). Hsp70 and Hsp40 Chaperones Do Not Modulate Retinal Phenotype in SCA7 Mice. *J. Biol. Chem.* *279*, 55969–55977.
- Helmlinger, D., Hardy, S., Sasorith, S., Klein, F., Robert, F., Weber, C., Miguet, L., Potier, N., Van-Dorselaer, A., Wurtz, J.-M., et al. (2004b). Ataxin-7 is a subunit of GCN5 histone acetyltransferase-containing complexes. *Hum. Mol. Genet.* *13*, 1257–1265.
- Helmlinger, D., Hardy, S., Abou-Sleymane, G., Eberlin, A., Bowman, A.B., Gansmüller, A., Picaud, S., Zoghbi, H.Y., Trottier, Y., Tora, L., et al. (2006). Glutamine-Expanded Ataxin-7 Alters TFTC/STAGA Recruitment and Chromatin Structure Leading to Photoreceptor Dysfunction. *PLoS Biol* *4*, e67.
- Heng, M.Y., Detloff, P.J., Paulson, H.L., and Albin, R.L. (2010). Early alterations of autophagy in Huntington disease-like mice. *Autophagy* *6*, 1206–1208.
- Hickey, C.M., Wilson, N.R., and Hochstrasser, M. (2012). Function and regulation of SUMO proteases. *Nat. Rev. Mol. Cell Biol.* *13*, 755–766.
- Ho, T.H., Charlet-B, N., Poulos, M.G., Singh, G., Swanson, M.S., and Cooper, T.A. (2004). Muscleblind proteins regulate alternative splicing. *EMBO J.* *23*, 3103–3112.
- Holmberg, M., Duyckaerts, C., Dürr, A., Cancel, G., Gourfinkel-An, I., Damier, P., Faucheux, B., Trottier, Y., Hirsch, E.C., Agid, Y., et al. (1998). Spinocerebellar Ataxia Type 7 (SCA7): A Neurodegenerative Disorder With Neuronal Intranuclear Inclusions. *Hum. Mol. Genet.* *7*, 913–918.
- Hudson, J.J.R., Chiang, S.-C., Wells, O.S., Rookyard, C., and El-Khamisy, S.F. (2012). SUMO modification of the neuroprotective protein TDP1 facilitates chromosomal single-strand break repair. *Nat. Commun.* *3*, 733.
- Humbert, S., Bryson, E.A., Cordelières, F.P., Connors, N.C., Datta, S.R., Finkbeiner, S., Greenberg, M.E., and Saudou, F. (2002). The IGF-1/Akt Pathway Is Neuroprotective in Huntington’s Disease and Involves Huntingtin Phosphorylation by Akt. *Dev. Cell* *2*, 831–837.
- Hutten, S., Flotho, A., Melchior, F., and Kehlenbach, R.H. (2008). The Nup358-RanGAP complex is required for efficient importin alpha/beta-dependent nuclear import. *Mol. Biol. Cell* *19*, 2300–2310.
- Ignatova, Z., Thakur, A.K., Wetzell, R., and Gierasch, L.M. (2007). In-cell Aggregation of a Polyglutamine-containing Chimera Is a Multistep Process Initiated by the Flanking Sequence. *J. Biol. Chem.* *282*, 36736–36743.
- Ikeda, K., and Inoue, S. (2012). Trim Proteins as Ring Finger E3 Ubiquitin Ligases. In *TRIM/RBCC Proteins*, G.M. Phd, ed. (Springer New York), pp. 27–37.
- Imarisio, S., Carmichael, J., Korolchuk, V., Chen, C.-W., Saiki, S., Rose, C., Krishna, G., Davies, J.E., Ttofi, E., Underwood, B.R., et al. (2008). Huntington’s disease: from

pathology and genetics to potential therapies. *Biochem. J.* 412, 191.

Ishov, A.M., Sotnikov, A.G., Negorev, D., Vladimirova, O.V., Neff, N., Kamitani, T., Yeh, E.T.H., Strauss, J.F., and Maul, G.G. (1999). Pml Is Critical for Nd10 Formation and Recruits the Pml-Interacting Protein Daxx to This Nuclear Structure When Modified by Sumo-1. *J. Cell Biol.* 147, 221–234.

Jacquemont, S., Hagerman, R.J., Leehey, M., Grigsby, J., Zhang, L., Brunberg, J.A., Greco, C., Des Portes, V., Jardini, T., Levine, R., et al. (2003). Fragile X premutation tremor/ataxia syndrome: molecular, clinical, and neuroimaging correlates. *Am. J. Hum. Genet.* 72, 869–878.

Jana, N.R., Zemskov, E.A., Wang, G., and Nukina, N. (2001). Altered proteasomal function due to the expression of polyglutamine-expanded truncated N-terminal huntingtin induces apoptosis by caspase activation through mitochondrial cytochrome c release. *Hum. Mol. Genet.* 10, 1049–1059.

Janer, A., Martin, E., Muriel, M.-P., Latouche, M., Fujigasaki, H., Ruberg, M., Brice, A., Trottier, Y., and Sittler, A. (2006). PML clastosomes prevent nuclear accumulation of mutant ataxin-7 and other polyglutamine proteins. *J. Cell Biol.* 174, 65–76.

Janer, A., Werner, A., Takahashi-Fujigasaki, J., Daret, A., Fujigasaki, H., Takada, K., Duyckaerts, C., Brice, A., Dejean, A., and Sittler, A. (2010). SUMOylation attenuates the aggregation propensity and cellular toxicity of the polyglutamine expanded ataxin-7. *Hum. Mol. Genet.* 19, 181–195.

Jeanne, M., Lallemand-Breitenbach, V., Ferhi, O., Koken, M., Le Bras, M., Duffort, S., Peres, L., Berthier, C., Soilihi, H., Raught, B., et al. (2010). PML/RARA Oxidation and Arsenic Binding Initiate the Antileukemia Response of As<sub>2</sub>O<sub>3</sub>. *Cancer Cell* 18, 88–98.

Jensen, K., Shiels, C., and Freemont, P.S. (2001). PML protein isoforms and the RBCC/TRIM motif. *Oncogene* 20, 7223–7233.

Jiang, H., Nucifora, F.C., Ross, C.A., and DeFranco, D.B. (2003). Cell death triggered by polyglutamine-expanded huntingtin in a neuronal cell line is associated with degradation of CREB-binding protein. *Hum. Mol. Genet.* 12, 1–12.

Jin, P., Alisch, R.S., and Warren, S.T. (2004). RNA and microRNAs in fragile X mental retardation. *Nat. Cell Biol.* 6, 1048–1053.

Johansson, J., Forsgren, L., Sandgren, O., Brice, A., Holmgren, G., and Holmberg, M. (1998). Expanded CAG Repeats in Swedish Spinocerebellar Ataxia Type 7 (SCA7) Patients: Effect of CAG Repeat Length on the Clinical Manifestation. *Hum. Mol. Genet.* 7, 171–176.

Johnson, E.S., and Blobel, G. (1997). Ubc9p Is the Conjugating Enzyme for the Ubiquitin-like Protein Smt3p. *J. Biol. Chem.* 272, 26799–26802.

- Kagey, M.H., Melhuish, T.A., and Wotton, D. (2003). The Polycomb Protein Pc2 Is a SUMO E3. *Cell* 113, 127–137.
- Kahyo, T., Nishida, T., and Yasuda, H. (2001). Involvement of PIAS1 in the Sumoylation of Tumor Suppressor p53. *Mol. Cell* 8, 713–718.
- Kaytor, M.D., Duvick, L.A., Skinner, P.J., Koob, M.D., Ranum, L.P.W., and Orr, H.T. (1999). Nuclear Localization of the Spinocerebellar Ataxia Type 7 Protein, Ataxin-7. *Hum. Mol. Genet.* 8, 1657–1664.
- Kerscher, O. (2007). SUMO junction-what's your function? New insights through SUMO-interacting motifs. *EMBO Rep.* 8, 550–555.
- Keusekotten, K., Bade, V.N., Meyer-Teschendorf, K., Sriramachandran, A.M., Fischer-Schrader, K., Krause, A., Horst, C., Schwarz, G., Hofmann, K., Dohmen, R.J., et al. (2014). Multivalent interactions of the SUMO-interaction motifs in RING finger protein 4 determine the specificity for chains of the SUMO. *Biochem. J.* 457, 207–214.
- Kim, P.K., Hailey, D.W., Mullen, R.T., and Lippincott-Schwartz, J. (2008). Ubiquitin signals autophagic degradation of cytosolic proteins and peroxisomes. *Proc. Natl. Acad. Sci.* 105, 20567–20574.
- Kirsh, O., Seeler, J.-S., Pichler, A., Gast, A., Muller, S., Miska, E., Mathieu, M., Harel-Bellan, A., Kouzarides, T., Melchior, F., et al. (2002). The SUMO E3 ligase RanBP2 promotes modification of the HDAC4 deacetylase. *EMBO J.* 21, 2682–2691.
- Klein, U.R., Haindl, M., Nigg, E.A., and Muller, S. (2009). RanBP2 and SENP3 Function in a Mitotic SUMO2/3 Conjugation-Deconjugation Cycle on Borealin. *Mol. Biol. Cell* 20, 410–418.
- Klement, I.A., Skinner, P.J., Kaytor, M.D., Yi, H., Hersch, S.M., Clark, H.B., Zoghbi, H.Y., and Orr, H.T. (1998a). Ataxin-1 Nuclear Localization and Aggregation: Role in Polyglutamine-Induced Disease in SCA1 Transgenic Mice. *Cell* 95, 41–53.
- Klement, I.A., Skinner, P.J., Kaytor, M.D., Yi, H., Hersch, S.M., Clark, H.B., Zoghbi, H.Y., and Orr, H.T. (1998b). Ataxin-1 Nuclear Localization and Aggregation: Role in Polyglutamine-Induced Disease in SCA1 Transgenic Mice. *Cell* 95, 41–53.
- Koegl, M., Hoppe, T., Schlenker, S., Ulrich, H.D., Mayer, T.U., and Jentsch, S. (1999). A Novel Ubiquitination Factor, E4, Is Involved in Multiubiquitin Chain Assembly. *Cell* 96, 635–644.
- Komander, D., and Rape, M. (2012). The ubiquitin code. *Annu. Rev. Biochem.* 81, 203–229.
- Komatsu, M., Waguri, S., Koike, M., Sou, Y., Ueno, T., Hara, T., Mizushima, N., Iwata, J., Ezaki, J., Murata, S., et al. (2007). Homeostatic Levels of p62 Control Cytoplasmic Inclusion Body Formation in Autophagy-Deficient Mice. *Cell* 131, 1149–1163.
- Korolchuk, V.I., Mansilla, A., Menzies, F.M., and Rubinsztein, D.C. (2009).

Autophagy Inhibition Compromises Degradation of Ubiquitin-Proteasome Pathway Substrates. *Mol. Cell* **33**, 517–527.

Krumova, P., and Weishaupt, J.H. (2013). Sumoylation in neurodegenerative diseases. *Cell. Mol. Life Sci.* **70**, 2123–2138.

Krumova, P., Meulmeester, E., Garrido, M., Tirard, M., Hsiao, H.-H., Bossis, G., Urlaub, H., Zweckstetter, M., Kügler, S., Melchior, F., et al. (2011). Sumoylation inhibits alpha-synuclein aggregation and toxicity. *J. Cell Biol.* **194**, 49–60.

Kuemmerle, S., Gutekunst, C.-A., Klein, A.M., Li, X.-J., Li, S.-H., Beal, M.F., Hersch, S.M., and Ferrante, R.J. (1999). Huntingtin aggregates may not predict neuronal death in Huntington's disease. *Ann. Neurol.* **46**, 842–849.

Kumada, S., Uchihara, T., Hayashi, M., Nakamura, A., Kikuchi, E., Mizutani, T., and Oda, M. (2002). Promyelocytic leukemia protein is redistributed during the formation of intranuclear inclusions independent of polyglutamine expansion: an immunohistochemical study on Marinesco bodies. *J. Neuropathol. Exp. Neurol.* **61**, 984–991.

Kuusisto, E., Salminen, A., and Alafuzoff, I. 1, 2 (2001). Ubiquitin-binding protein p62 is present in neuronal and glial inclusions in human tauopathies and synucleinopathies. [Miscellaneous Article]. *Neuroreport* July 20 2001 **12**, 2085–2090.

Lafarga, M., Berciano, M.T., Pena, E., Mayo, I., Castaño, J.G., Bohmann, D., Rodrigues, J.P., Tavanez, J.P., and Carmo-Fonseca, M. (2002). Clastosome: A Subtype of Nuclear Body Enriched in 19S and 20S Proteasomes, Ubiquitin, and Protein Substrates of Proteasome. *Mol. Biol. Cell* **13**, 2771–2782.

Lallemand-Breitenbach, V., Zhu, J., Puvion, F., Koken, M., Honoré, N., Doubeikovsky, A., Duprez, E., Pandolfi, P.P., Puvion, E., Freemont, P., et al. (2001). Role of Promyelocytic Leukemia (Pml) Sumoylation in Nuclear Body Formation, 11s Proteasome Recruitment, and as2O3-Induced Pml or Pml/Retinoic Acid Receptor  $\alpha$  Degradation. *J. Exp. Med.* **193**, 1361–1372.

Lallemand-Breitenbach, V., Jeanne, M., Benhenda, S., Nasr, R., Lei, M., Peres, L., Zhou, J., Zhu, J., Raught, B., and de Thé, H. (2008). Arsenic degrades PML or PML-RAR $\alpha$  through a SUMO-triggered RNF4/ubiquitin-mediated pathway. *Nat. Cell Biol.* **10**, 547–555.

Lang, G., Bonnet, J., Umlauf, D., Karmodiya, K., Koffler, J., Stierle, M., Devys, D., and Tora, L. (2011). The Tightly Controlled Deubiquitination Activity of the Human SAGA Complex Differentially Modifies Distinct Gene Regulatory Elements. *Mol. Cell. Biol.* **31**, 3734–3744.

Lansbury, P.T., and Lashuel, H.A. (2006). A century-old debate on protein aggregation and neurodegeneration enters the clinic. *Nature* **443**, 774–779.

Lehesjoki, A.-E. (2002). Clinical features and genetics of Unverricht-Lundborg

- disease. *Adv. Neurol.* 89, 193–197.
- Li, D. (2006). Selective degradation of the I $\kappa$ B kinase (IKK) by autophagy. *Cell Res.* 16, 855–856.
- Li, L.-B., Yu, Z., Teng, X., and Bonini, N.M. (2008). RNA toxicity is a component of ataxin-3 degeneration in *Drosophila*. *Nature* 453, 1107–1111.
- Liew, C.W., Sun, H., Hunter, T., and Day, C.L. (2010). RING domain dimerization is essential for RNF4 function. *Biochem. J.* 431, 23–29.
- Lin, M.T., and Beal, M.F. (2006). Mitochondrial dysfunction and oxidative stress in neurodegenerative diseases. *Nature* 443, 787–795.
- Lin, D.-Y., Huang, Y.-S., Jeng, J.-C., Kuo, H.-Y., Chang, C.-C., Chao, T.-T., Ho, C.-C., Chen, Y.-C., Lin, T.-P., Fang, H.-I., et al. (2006). Role of SUMO-Interacting Motif in Daxx SUMO Modification, Subnuclear Localization, and Repression of Sumoylated Transcription Factors. *Mol. Cell* 24, 341–354.
- Lindorff-Larsen, K., Vendruscolo, M., Paci, E., and Dobson, C.M. (2004). Transition states for protein folding have native topologies despite high structural variability. *Nat. Struct. Mol. Biol.* 11, 443–449.
- Mackenzie, I.R., Baker, M., West, G., Woulfe, J., Qadi, N., Gass, J., Cannon, A., Adamson, J., Feldman, H., Lindholm, C., et al. (2006). A family with tau-negative frontotemporal dementia and neuronal intranuclear inclusions linked to chromosome 17. *Brain* 129, 853–867.
- MacLaren, A.. (2001). p53-dependent apoptosis induced by proteasome inhibition in mammary epithelial cells. *Publ. Online* 22 March 2001 Doi101038sjcdd4400801 8.
- Mahajan, R., Delphin, C., Guan, T., Gerace, L., and Melchior, F. (1997). A Small Ubiquitin-Related Polypeptide Involved in Targeting RanGAP1 to Nuclear Pore Complex Protein RanBP2. *Cell* 88, 97–107.
- Mangiarini, L., Sathasivam, K., Seller, M., Cozens, B., Harper, A., Hetherington, C., Lawton, M., Trottier, Y., Lehrach, H., Davies, S.W., et al. (1996). Exon 1 of the HD Gene with an Expanded CAG Repeat Is Sufficient to Cause a Progressive Neurological Phenotype in Transgenic Mice. *Cell* 87, 493–506.
- Mangiarini, L., Sathasivam, K., Mahal, A., Mott, R., Seller, M., and Bates, G.P. (1997). Instability of highly expanded CAG repeats in mice transgenic for the Huntington's disease mutation. *Nat. Genet.* 15, 197–200.
- Mao, Y., Sun, M., Desai, S.D., and Liu, L.F. (2000). SUMO-1 conjugation to topoisomerase I: A possible repair response to topoisomerase-mediated DNA damage. *Proc. Natl. Acad. Sci. U. S. A.* 97, 4046–4051.
- Margolis, R.L., O'Hearn, E., Rosenblatt, A., Willour, V., Holmes, S.E., Franz, M.L., Callahan, C., Hwang, H.S., Troncoso, J.C., and Ross, C.A. (2001). A disorder similar to Huntington's disease is associated with a novel CAG repeat expansion. *Ann. Neurol.*

50, 373–380.

Marquis Gacy, A., Goellner, G., Juranić, N., Macura, S., and McMurray, C.T. (1995). Trinucleotide repeats that expand in human disease form hairpin structures in vitro. *Cell* 81, 533–540.

Martin, J.-J., Van Regemorter, N., Del-Favero, J., Löfgren, A., and Van Broeckhoven, C. (1999). Spinocerebellar ataxia type 7 (SCA7) – correlations between phenotype and genotype in one large Belgian family. *J. Neurol. Sci.* 168, 37–46.

Martin, J.J., Van Regemorter, N., Krols, L., Brucher, J.M., de Barsy, T., Szliwowski, H., Evrard, P., Ceuterick, C., Tassignon, M.J., and Smet-Dieleman, H. (1994). On an autosomal dominant form of retinal-cerebellar degeneration: an autopsy study of five patients in one family. *Acta Neuropathol. (Berl.)* 88, 277–286.

Masclé, X.H., Lussier-Price, M., Cappadocia, L., Estéphan, P., Raiola, L., Omichinski, J.G., and Aubry, M. (2013). Identification of a Non-covalent Ternary Complex Formed by PIAS1, SUMO1, and UBC9 Proteins Involved in Transcriptional Regulation. *J. Biol. Chem.* 288, 36312–36327.

Matilla, A., Gorbea, C., Einum, D.D., Townsend, J., Michalik, A., Broeckhoven, C. van, Jensen, C.C., Murphy, K.J., Ptáček, L.J., and Fu, Y.-H. (2001). Association of ataxin-7 with the proteasome subunit S4 of the 19S regulatory complex. *Hum. Mol. Genet.* 10, 2821–2831.

Matsumoto, M., Yada, M., Hatakeyama, S., Ishimoto, H., Tanimura, T., Tsuji, S., Kakizuka, A., Kitagawa, M., and Nakayama, K.I. (2004). Molecular clearance of ataxin-3 is regulated by a mammalian E4. *EMBO J.* 23, 659–669.

Maynard, C.J., Böttcher, C., Ortega, Z., Smith, R., Florea, B.I., Díaz-Hernández, M., Brundin, P., Overkleeft, H.S., Li, J.-Y., Lucas, J.J., et al. (2009). Accumulation of ubiquitin conjugates in a polyglutamine disease model occurs without global ubiquitin/proteasome system impairment. *Proc. Natl. Acad. Sci.* 106, 13986–13991.

McBride, J.L., Pitzer, M.R., Boudreau, R.L., Dufour, B., Hobbs, T., Ojeda, S.R., and Davidson, B.L. (2011). Preclinical Safety of RNAi-Mediated HTT Suppression in the Rhesus Macaque as a Potential Therapy for Huntington’s Disease. *Mol. Ther.*

McC Campbell, A., Taylor, J.P., Taye, A.A., Robitschek, J., Li, M., Walcott, J., Merry, D., Chai, Y., Paulson, H., Sobue, G., et al. (2000). CREB-binding protein sequestration by expanded polyglutamine. *Hum. Mol. Genet.* 9, 2197–2202.

McClellan, A.J., and Frydman, J. (2001). Molecular chaperones and the art of recognizing a lost cause. *Nat. Cell Biol.* 3, E51–E53.

McCullough, S.D., and Grant, P.A. (2010). Histone Acetylation, Acetyltransferases, and Ataxia—Alteration of Histone Acetylation and Chromatin Dynamics is Implicated in the Pathogenesis of Polyglutamine-Expansion Disorders. In *Advances in Protein Chemistry and Structural Biology*, (Elsevier), pp. 165–203.

- McMahon, S.J., Pray-Grant, M.G., Schieltz, D., Yates, J.R., and Grant, P.A. (2005). Polyglutamine-expanded spinocerebellar ataxia-7 protein disrupts normal SAGA and SLIK histone acetyltransferase activity. *Proc. Natl. Acad. Sci.* *102*, 8478–8482.
- McMillan, L.E., Brown, J.T., Henley, J.M., and Cimarosti, H. (2011). Profiles of SUMO and ubiquitin conjugation in an Alzheimer's disease model. *Neurosci. Lett.* *502*, 201–208.
- Meluh, P.B., and Koshland, D. (1995). Evidence that the MIF2 gene of *Saccharomyces cerevisiae* encodes a centromere protein with homology to the mammalian centromere protein CENP-C. *Mol. Biol. Cell* *6*, 793–807.
- Menzies, F.M., Huebener, J., Renna, M., Bonin, M., Riess, O., and Rubinsztein, D.C. (2010). Autophagy induction reduces mutant ataxin-3 levels and toxicity in a mouse model of spinocerebellar ataxia type 3. *Brain* *133*, 93–104.
- Meroni, G., and Diez-Roux, G. (2005). TRIM/RBCC, a novel class of “single protein RING finger” E3 ubiquitin ligases. *BioEssays News Rev. Mol. Cell. Dev. Biol.* *27*, 1147–1157.
- Michalik, A., Martin, J.-J., and Van Broeckhoven, C. (2003). Spinocerebellar ataxia type 7 associated with pigmentary retinal dystrophy. *Eur. J. Hum. Genet.* *12*, 2–15.
- Miller, J.W., Urbinati, C.R., Teng-umnuay, P., Stenberg, M.G., Byrne, B.J., Thornton, C.A., and Swanson, M.S. (2000). Recruitment of human muscleblind proteins to (CUG)<sub>n</sub> expansions associated with myotonic dystrophy. *EMBO J.* *19*, 4439–4448.
- Miller, V.M., Nelson, R.F., Gouvion, C.M., Williams, A., Rodriguez-Lebron, E., Harper, S.Q., Davidson, B.L., Rebagliati, M.R., and Paulson, H.L. (2005). CHIP Suppresses Polyglutamine Aggregation and Toxicity In Vitro and In Vivo. *J. Neurosci.* *25*, 9152–9161.
- Mitra, S., Tsvetkov, A.S., and Finkbeiner, S. (2009). Single Neuron Ubiquitin-Proteasome Dynamics Accompanying Inclusion Body Formation in Huntington Disease. *J. Biol. Chem.* *284*, 4398–4403.
- Moechars, D., Dewachter, I., Lorent, K., Reversé, D., Baekelandt, V., Naidu, A., Tesseur, I., Spittaels, K., Haute, C.V.D., Checler, F., et al. (1999). Early Phenotypic Changes in Transgenic Mice That Overexpress Different Mutants of Amyloid Precursor Protein in Brain. *J. Biol. Chem.* *274*, 6483–6492.
- Monckton, D.G., Cayuela, M.L., Gould, F.K., Brock, G.J.R., Silva, R. de, and Ashizawa, T. (1999). Very Large (CAG)<sub>n</sub> DNA Repeat Expansions in the Sperm of Two Spinocerebellar Ataxia Type 7 Males. *Hum. Mol. Genet.* *8*, 2473–2478.
- Mookerjee, S., Papanikolaou, T., Guyenet, S.J., Sampath, V., Lin, A., Vitelli, C., DeGiacomo, F., Sopher, B.L., Chen, S.F., Spada, A.R.L., et al. (2009). Posttranslational Modification of Ataxin-7 at Lysine 257 Prevents Autophagy-Mediated Turnover of an N-Terminal Caspase-7 Cleavage Fragment. *J. Neurosci.* *29*,

15134–15144.

Moseley, M.L., Benzow, K.A., Schut, L.J., Bird, T.D., Gomez, C.M., Barkhaus, P.E., Blindauer, K.A., Labuda, M., Pandolfo, M., Koob, M.D., et al. (1998). Incidence of dominant spinocerebellar and Friedreich triplet repeats among 361 ataxia families. *Neurol. Dec.* 1998 *51*, 1666–1671.

Muchowski, P.J., Schaffar, G., Sittler, A., Wanker, E.E., Hayer-Hartl, M.K., and Hartl, F.U. (2000). Hsp70 and Hsp40 chaperones can inhibit self-assembly of polyglutamine proteins into amyloid-like fibrils. *Proc. Natl. Acad. Sci.* *97*, 7841–7846.

Mukhopadhyay, D., and Dasso, M. (2007). Modification in reverse: the SUMO proteases. *Trends Biochem. Sci.* *32*, 286–295.

Nagaoka, U., Kim, K., Jana, N.R., Doi, H., Maruyama, M., Mitsui, K., Oyama, F., and Nukina, N. (2004). Increased expression of p62 in expanded polyglutamine-expressing cells and its association with polyglutamine inclusions. *J. Neurochem.* *91*, 57–68.

Nakamura, Y., Tagawa, K., Oka, T., Sasabe, T., Ito, H., Shiwaku, H., Spada, A.R.L., and Okazawa, H. (2012). Ataxin-7 associates with microtubules and stabilizes the cytoskeletal network. *Hum. Mol. Genet.* *21*, 1099–1110.

Namanja, A.T., Li, Y.-J., Su, Y., Wong, S., Lu, J., Colson, L.T., Wu, C., Li, S.S.C., and Chen, Y. (2012). Insights into High Affinity Small Ubiquitin-like Modifier (SUMO) Recognition by SUMO-interacting Motifs (SIMs) Revealed by a Combination of NMR and Peptide Array Analysis. *J. Biol. Chem.* *287*, 3231–3240.

Nascimento-Ferreira, I., Santos-Ferreira, T., Sousa-Ferreira, L., Auregan, G., Onofre, I., Alves, S., Dufour, N., Colomer Gould, V.F., Koeppen, A., Déglon, N., et al. (2011). Overexpression of the autophagic beclin-1 protein clears mutant ataxin-3 and alleviates Machado-Joseph disease. *Brain J. Neurol.* *134*, 1400–1415.

Nucifora, F.C., Sasaki, M., Peters, M.F., Huang, H., Cooper, J.K., Yamada, M., Takahashi, H., Tsuji, S., Troncoso, J., Dawson, V.L., et al. (2001). Interference by Huntingtin and Atrophin-1 with CBP-Mediated Transcription Leading to Cellular Toxicity. *Science* *291*, 2423–2428.

O'Rourke, J.G., Gareau, J.R., Ochaba, J., Song, W., Raskó, T., Reverter, D., Lee, J., Monteys, A.M., Pallos, J., Mee, L., et al. (2013). SUMO-2 and PIAS1 Modulate Insoluble Mutant Huntingtin Protein Accumulation. *Cell Rep.* *4*, 362–375.

Okuma, T., Honda, R., Ichikawa, G., Tsumagari, N., and Yasuda, H. (1999). In Vitro SUMO-1 Modification Requires Two Enzymatic Steps, E1 and E2. *Biochem. Biophys. Res. Commun.* *254*, 693–698.

Onishi, A., Peng, G.-H., Chen, S., and Blackshaw, S. (2010). Pias3-dependent SUMOylation controls mammalian cone photoreceptor differentiation. *Nat. Neurosci.* *13*, 1059–1065.

- Orr, H.T. (2001). Beyond the Qs in the polyglutamine diseases. *Genes Dev.* *15*, 925–932.
- Palhan, V.B., Chen, S., Peng, G.-H., Tjernberg, A., Gamper, A.M., Fan, Y., Chait, B.T., La Spada, A.R., and Roeder, R.G. (2005). Polyglutamine-expanded ataxin-7 inhibits STAGA histone acetyltransferase activity to produce retinal degeneration. *Proc. Natl. Acad. Sci. U. S. A.* *102*, 8472–8477.
- Pankiv, S., Clausen, T.H., Lamark, T., Brech, A., Bruun, J.-A., Outzen, H., Øvervatn, A., Bjørkøy, G., and Johansen, T. (2007). p62/SQSTM1 Binds Directly to Atg8/LC3 to Facilitate Degradation of Ubiquitinated Protein Aggregates by Autophagy. *J. Biol. Chem.* *282*, 24131–24145.
- Pardo, R., Colin, E., Régulier, E., Aebischer, P., Déglon, N., Humbert, S., and Saudou, F. (2006). Inhibition of Calcineurin by FK506 Protects against Polyglutamine-Huntingtin Toxicity through an Increase of Huntingtin Phosphorylation at S421. *J. Neurosci.* *26*, 1635–1645.
- Pearson, C.E., Edamura, K.N., and Cleary, J.D. (2005). Repeat instability: mechanisms of dynamic mutations. *Nat. Rev. Genet.* *6*, 729–742.
- Perry, J.J.P., Tainer, J.A., and Boddy, M.N. (2008). A SIM-ultaneous role for SUMO and ubiquitin. *Trends Biochem. Sci.* *33*, 201–208.
- Pichler, A., Gast, A., Seeler, J.S., Dejean, A., and Melchior, F. (2002). The nucleoporin RanBP2 has SUMO1 E3 ligase activity. *Cell* *108*, 109–120.
- Pickart, C.M. (2001). Ubiquitin Enters the New Millennium. *Mol. Cell* *8*, 499–504.
- Plechanovová, A., Jaffray, E.G., McMahon, S.A., Johnson, K.A., Navrátilová, I., Naismith, J.H., and Hay, R.T. (2011). Mechanism of ubiquitylation by dimeric RING ligase RNF4. *Nat. Struct. Mol. Biol.* *18*, 1052–1059.
- Plechanovová, A., Jaffray, E.G., Tatham, M.H., Naismith, J.H., and Hay, R.T. (2012a). Structure of a RING E3 ligase and ubiquitin-loaded E2 primed for catalysis. *Nature* *489*, 115–120.
- Plechanovová, A., Jaffray, E.G., Tatham, M.H., Naismith, J.H., and Hay, R.T. (2012b). Structure of a RING E3 ligase and ubiquitin-loaded E2 primed for catalysis. *Nature* *489*, 115–120.
- Poukka, H., Karvonen, U., Jänne, O.A., and Palvimo, J.J. (2000). Covalent modification of the androgen receptor by small ubiquitin-like modifier 1 (SUMO-1). *Proc. Natl. Acad. Sci.* *97*, 14145–14150.
- Price, D.L., Wong, P.C., Markowska, A.L., Lee, M.K., Thinakaran, G., Cleveland, D.W., Sisodia, S.S., and Borchelt, D.R. (2000). The Value of Transgenic Models for the Study of Neurodegenerative Diseases. *Ann. N. Y. Acad. Sci.* *920*, 179–191.
- De Pril, R., Fischer, D.F., Roos, R.A.C., and van Leeuwen, F.W. (2007). Ubiquitin-conjugating enzyme E2-25K increases aggregate formation and cell death in

- polyglutamine diseases. *Mol. Cell. Neurosci.* *34*, 10–19.
- Quimby, B.B., Yong-Gonzalez, V., Anan, T., Strunnikov, A.V., and Dasso, M. (2006). The promyelocytic leukemia protein stimulates SUMO conjugation in yeast. *Oncogene* *25*, 2999–3005.
- Ramachandran, P.S., Bhattarai, S., Singh, P., Boudreau, R.L., Thompson, S., LaSpada, A.R., Drack, A.V., and Davidson, B.L. (2014). RNA Interference-Based Therapy for Spinocerebellar Ataxia Type 7 Retinal Degeneration. *PLoS ONE* *9*, e95362.
- Al-Ramahi, I., Lam, Y.C., Chen, H.-K., Gouyon, B. de, Zhang, M., Pérez, A.M., Branco, J., Haro, M. de, Patterson, C., Zoghbi, H.Y., et al. (2006). CHIP Protects from the Neurotoxicity of Expanded and Wild-type Ataxin-1 and Promotes Their Ubiquitination and Degradation. *J. Biol. Chem.* *281*, 26714–26724.
- Ravikumar, B., Sarkar, S., Berger, Z., and Rubinsztein, D.C. (2003). The roles of the ubiquitin-proteasome and autophagy-lysosome pathways in Huntington's disease and related conditions. *Clin. Neurosci. Res.* *3*, 141–148.
- Regad, T., and Chelbi-Alix, M.K. (2001). Role and fate of PML nuclear bodies in response to interferon and viral infections. *Publ. Online* 29 Oct. 2001 Doi101038sjonc1204854 20.
- Regad, T., Bellodi, C., Nicotera, P., and Salomoni, P. (2009). The tumor suppressor Pml regulates cell fate in the developing neocortex. *Nat. Neurosci.* *12*, 132–140.
- Reverter, D., and Lima, C.D. (2005). Insights into E3 ligase activity revealed by a SUMO-RanGAP1-Ubc9-Nup358 complex. *Nature* *435*, 687–692.
- Reymond, A., Meroni, G., Fantozzi, A., Merla, G., Cairo, S., Luzi, L., Riganelli, D., Zanaria, E., Messali, S., Cainarca, S., et al. (2001). The tripartite motif family identifies cell compartments. *EMBO J.* *20*, 2140–2151.
- Rideout, H.J., Lang-Rollin, I., and Stefanis, L. (2004). Involvement of macroautophagy in the dissolution of neuronal inclusions. *Int. J. Biochem. Cell Biol.* *36*, 2551–2562.
- Riley, B.E., Zoghbi, H.Y., and Orr, H.T. (2005). SUMOylation of the polyglutamine repeat protein, ataxin-1, is dependent on a functional nuclear localization signal. *J. Biol. Chem.* *280*, 21942–21948.
- Rodriguez, M.S., Dargemont, C., and Hay, R.T. (2001). SUMO-1 Conjugation in Vivo Requires Both a Consensus Modification Motif and Nuclear Targeting. *J. Biol. Chem.* *276*, 12654–12659.
- Rojas-Fernandez, A., Plechanovová, A., Hattersley, N., Jaffray, E., Tatham, M.H., and Hay, R.T. (2014). SUMO Chain-Induced Dimerization Activates RNF4. *Mol. Cell* *53*, 880–892.
- Ross, C.A., and Poirier, M.A. (2004). Protein aggregation and neurodegenerative disease. *Publ. Online* 01 July 2004 Doi101038nm1066 10, S10–S17.

- Ross, C.A., and Poirier, M.A. (2005). What is the role of protein aggregation in neurodegeneration? *Nat. Rev. Mol. Cell Biol.* *6*, 891–898.
- Rubinsztein, D.C., Amos, W., Leggo, J., Goodburn, S., Jain, S., Li, S.-H., Margolis, R.L., Ross, C.A., and Ferguson-Smith, M.A. (1995). Microsatellite evolution — evidence for directionality and variation in rate between species. *Nat. Genet.* *10*, 337–343.
- Rudnicki, D.D., Holmes, S.E., Lin, M.W., Thornton, C.A., Ross, C.A., and Margolis, R.L. (2007). Huntington’s disease-like 2 is associated with CUG repeat-containing RNA foci. *Ann. Neurol.* *61*, 272–282.
- Rytinki, M.M., Kaikkonen, S., Pehkonen, P., Jääskeläinen, T., and Palvimo, J.J. (2009). PIAS proteins: pleiotropic interactors associated with SUMO. *Cell. Mol. Life Sci.* *66*, 3029–3041.
- Sadri-Vakili, G., Bouzou, B., Benn, C.L., Kim, M.-O., Chawla, P., Overland, R.P., Glajch, K.E., Xia, E., Qiu, Z., Hersch, S.M., et al. (2007). Histones associated with downregulated genes are hypo-acetylated in Huntington’s disease models. *Hum. Mol. Genet.* *16*, 1293–1306.
- Sahin, U., Ferhi, O., Jeanne, M., Benhenda, S., Berthier, C., Jollivet, F., Niwa-Kawakita, M., Faklaris, O., Setterblad, N., Thé, H. de, et al. (2014). Oxidative stress-induced assembly of PML nuclear bodies controls sumoylation of partner proteins. *J. Cell Biol.* *204*, 931–945.
- Saitoh, H., and Hinchey, J. (2000). Functional Heterogeneity of Small Ubiquitin-related Protein Modifiers SUMO-1 versus SUMO-2/3. *J. Biol. Chem.* *275*, 6252–6258.
- Saitoh, N., Uchimura, Y., Tachibana, T., Sugahara, S., Saitoh, H., and Nakao, M. (2006). In situ SUMOylation analysis reveals a modulatory role of RanBP2 in the nuclear rim and PML bodies. *Exp. Cell Res.* *312*, 1418–1430.
- Salinas, S., Briançon-Marjollet, A., Bossis, G., Lopez, M.-A., Piechaczyk, M., Jariel-Encontre, I., Debant, A., and Hipskind, R.A. (2004). SUMOylation regulates nucleocytoplasmic shuttling of Elk-1. *J. Cell Biol.* *165*, 767–773.
- Saudou, F., Finkbeiner, S., Devys, D., and Greenberg, M.E. (1998). Huntingtin Acts in the Nucleus to Induce Apoptosis but Death Does Not Correlate with the Formation of Intranuclear Inclusions. *Cell* *95*, 55–66.
- Savouret, C. (2003). CTG repeat instability and size variation timing in DNA repair-deficient mice. *EMBO J.* *22*, 2264–2273.
- Scheel, H., Tomiuk, S., and Hofmann, K. (2003). Elucidation of ataxin-3 and ataxin-7 function by integrative bioinformatics. *Hum. Mol. Genet.* *12*, 2845–2852.
- Schipper-Krom, S., Juenemann, K., and Reits, E.A.J. (2012). The Ubiquitin-Proteasome System in Huntington’s Disease: Are Proteasomes Impaired, Initiators of Disease, or Coming to the Rescue? *Biochem. Res. Int.* *2012*, e837015.

- Seeler, J.-S., and Dejean, A. (2003). Nuclear and unclear functions of SUMO. *Nat. Rev. Mol. Cell Biol.* *4*, 690–699.
- Seo, H., Sonntag, K.-C., and Isacson, O. (2004). Generalized brain and skin proteasome inhibition in Huntington's disease. *Ann. Neurol.* *56*, 319–328.
- Shen, T.H., Lin, H.-K., Scaglioni, P.P., Yung, T.M., and Pandolfi, P.P. (2006). The Mechanisms of PML-Nuclear Body Formation. *Mol. Cell* *24*, 331–339.
- Sittler, A., Lurz, R., Lueder, G., Priller, J., Hayer-Hartl, M.K., Hartl, F.U., Lehrach, H., and Wanker, E.E. (2001). Geldanamycin activates a heat shock response and inhibits huntingtin aggregation in a cell culture model of Huntington's disease. *Hum. Mol. Genet.* *10*, 1307–1315.
- Song, J., Durrin, L.K., Wilkinson, T.A., Krontiris, T.G., and Chen, Y. (2004). Identification of a SUMO-binding motif that recognizes SUMO-modified proteins. *Proc. Natl. Acad. Sci. U. S. A.* *101*, 14373–14378.
- Song, J., Zhang, Z., Hu, W., and Chen, Y. (2005). Small Ubiquitin-like Modifier (SUMO) Recognition of a SUMO Binding Motif A REVERSAL OF THE BOUND ORIENTATION. *J. Biol. Chem.* *280*, 40122–40129.
- Sopher, B.L., Thomas Jr., P.S., LaFevre-Bernt, M.A., Holm, I.E., Wilke, S.A., Ware, C.B., Jin, L.-W., Libby, R.T., Ellerby, L.M., and La Spada, A.R. (2004). Androgen Receptor YAC Transgenic Mice Recapitulate SBMA Motor Neuronopathy and Implicate VEGF164 in the Motor Neuron Degeneration. *Neuron* *41*, 687–699.
- Soto, C. (2003). Unfolding the role of protein misfolding in neurodegenerative diseases. *Nat. Rev. Neurosci.* *4*, 49–60.
- Spada, A.R.L., Wilson, E.M., Lubahn, D.B., Harding, A.E., and Fischbeck, K.H. (1991). Androgen receptor gene mutations in X-linked spinal and bulbar muscular atrophy. *Nature* *352*, 77–79.
- La Spada, A.R., and Taylor, J.P. (2003). Polyglutamines Placed into Context. *Neuron* *38*, 681–684.
- La Spada, A.R., Paulson, H.L., and Fischbeck, K.H. (1994). Trinucleotide repeat expansion in neurological disease. *Ann. Neurol.* *36*, 814–822.
- Steffan, J.S., Agrawal, N., Pallos, J., Rockabrand, E., Trotman, L.C., Slepko, N., Illes, K., Lukacsovich, T., Zhu, Y.-Z., Cattaneo, E., et al. (2004). SUMO modification of Huntingtin and Huntington's disease pathology. *Science* *304*, 100–104.
- Stevanin, G., Giunti, P., David, G., Belal, S., Dürr, A., Ruberg, M., Wood, N., and Brice, A. (1998). De Novo Expansion of Intermediate Alleles in Spinocerebellar Ataxia 7. *Hum. Mol. Genet.* *7*, 1809–1813.
- Stevanin, G., Durr, A., and Brice, A. (2000). Clinical and molecular advances in autosomal dominant cerebellar ataxias: from genotype to phenotype and physiopathology. *Publ. Online* 15 Febr. 2000 Doi101038sjejhg5200403 8.

- Stevanin, G., Fujigasaki, H., Lebre, A.-S., Camuzat, A., Jeannequin, C., Dodé, C., Takahashi, J., Sâh, C., Bellance, R., Brice, A., et al. (2003). Huntington's disease-like phenotype due to trinucleotide repeat expansions in the TBP and JPH3 genes. *Brain* *126*, 1599–1603.
- Sun, H., Leverson, J.D., and Hunter, T. (2007). Conserved function of RNF4 family proteins in eukaryotes: targeting a ubiquitin ligase to SUMOylated proteins. *EMBO J.* *26*, 4102–4112.
- Sutherland, G.R., and Baker, E. (1992). Characterisation of a new rare fragile site easily confused with the fragile X. *Hum. Mol. Genet.* *1*, 111–113.
- Swaminathan, S., Kiendl, F., Körner, R., Lupetti, R., Hengst, L., and Melchior, F. (2004). RanGAP1\*SUMO1 is phosphorylated at the onset of mitosis and remains associated with RanBP2 upon NPC disassembly. *J. Cell Biol.* *164*, 965–971.
- Takahashi, J., Fujigasaki, H., Zander, C., Hachimi, K.H.E., Stevanin, G., Dürr, A., Lebre, A.-S., Yvert, G., Trottier, Y., Thé, H. de, et al. (2002). Two populations of neuronal intranuclear inclusions in SCA7 differ in size and promyelocytic leukaemia protein content. *Brain* *125*, 1534–1543.
- Takahashi, J., Fujigasaki, H., Iwabuchi, K., Bruni, A.C., Uchihara, T., El Hachimi, K.H., Stevanin, G., Dürr, A., Lebre, A.-S., Trottier, Y., et al. (2003). PML nuclear bodies and neuronal intranuclear inclusion in polyglutamine diseases. *Neurobiol. Dis.* *13*, 230–237.
- Takahashi, Y., Kahyo, T., Toh-e, A., Yasuda, H., and Kikuchi, Y. (2001). Yeast Ull1/Siz1 Is a Novel SUMO1/Smt3 Ligase for Septin Components and Functions as an Adaptor between Conjugating Enzyme and Substrates. *J. Biol. Chem.* *276*, 48973–48977.
- Takashima, H., Boerkoel, C.F., John, J., Saifi, G.M., Salih, M.A.M., Armstrong, D., Mao, Y., Quioco, F.A., Roa, B.B., Nakagawa, M., et al. (2002). Mutation of TDP1, encoding a topoisomerase I-dependent DNA damage repair enzyme, in spinocerebellar ataxia with axonal neuropathy. *Nat. Genet.* *32*, 267–272.
- Tang, T.-S., Slow, E., Lupu, V., Stavrovskaya, I.G., Sugimori, M., Llinas, R., Kristal, B.S., Hayden, M.R., and Bezprozvanny, I. (2005). Disturbed Ca<sup>2+</sup> signaling and apoptosis of medium spiny neurons in Huntington's disease. *Proc. Natl. Acad. Sci. U. S. A.* *102*, 2602–2607.
- Tatham, M.H., Kim, S., Jaffray, E., Song, J., Chen, Y., and Hay, R.T. (2005). Unique binding interactions among Ubc9, SUMO and RanBP2 reveal a mechanism for SUMO paralog selection. *Nat. Struct. Mol. Biol.* *12*, 67–74.
- Tatham, M.H., Geoffroy, M.-C., Shen, L., Plechanovova, A., Hattersley, N., Jaffray, E.G., Palvimo, J.J., and Hay, R.T. (2008). RNF4 is a poly-SUMO-specific E3 ubiquitin ligase required for arsenic-induced PML degradation. *Nat. Cell Biol.* *10*, 538–546.

Taylor, J., Grote, S.K., Xia, J., Vandelft, M., Graczyk, J., Ellerby, L.M., Spada, A.R.L., and Truant, R. (2006). Ataxin-7 Can Export from the Nucleus via a Conserved Exportin-dependent Signal. *J. Biol. Chem.* *281*, 2730–2739.

Taylor, J.P., Taye, A.A., Campbell, C., Kazemi-Esfarjani, P., Fischbeck, K.H., and Min, K.-T. (2003). Aberrant histone acetylation, altered transcription, and retinal degeneration in a *Drosophila* model of polyglutamine disease are rescued by CREB-binding protein. *Genes Dev.* *17*, 1463–1468.

Terashima, T., Kawai, H., Fujitani, M., Maeda, K., and Yasuda, H. (2002). SUMO-1 co-localized with mutant atrophin-1 with expanded polyglutamines accelerates intranuclear aggregation and cell death. *Neuroreport* *13*, 2359–2364.

Thompson, L.M., Aiken, C.T., Kaltenbach, L.S., Agrawal, N., Illes, K., Khoshnan, A., Martinez-Vincente, M., Arrasate, M., O'Rourke, J.G., Khashwji, H., et al. (2009). IKK phosphorylates Huntingtin and targets it for degradation by the proteasome and lysosome. *J. Cell Biol.* *187*, 1083–1099.

Timmers, H.T.M., and Tora, L. (2005). SAGA unveiled. *Trends Biochem. Sci.* *30*, 7–10.

Tirard, M., Hsiao, H.-H., Nikolov, M., Urlaub, H., Melchior, F., and Brose, N. (2012). In vivo localization and identification of SUMOylated proteins in the brain of His6-HA-SUMO1 knock-in mice. *Proc. Natl. Acad. Sci.* *109*, 21122–21127.

Todi, S.V., Laco, M.N., Winborn, B.J., Travis, S.M., Wen, H.M., and Paulson, H.L. (2007). Cellular Turnover of the Polyglutamine Disease Protein Ataxin-3 Is Regulated by Its Catalytic Activity. *J. Biol. Chem.* *282*, 29348–29358.

Trejo, J.L., Carro, E., Garcia-Galloway, E., and Torres-Aleman, I. (2004). Role of insulin-like growth factor I signaling in neurodegenerative diseases. *J. Mol. Med.* *82*, 156–162.

Tsai, C.-C., Kao, H.-Y., Mitzutani, A., Banayo, E., Rajan, H., McKeown, M., and Evans, R.M. (2004). Ataxin 1, a SCA1 neurodegenerative disorder protein, is functionally linked to the silencing mediator of retinoid and thyroid hormone receptors. *Proc. Natl. Acad. Sci.* *101*, 4047–4052.

Tsai, Y.C., Fishman, P.S., Thakor, N.V., and Oyler, G.A. (2003). Parkin Facilitates the Elimination of Expanded Polyglutamine Proteins and Leads to Preservation of Proteasome Function. *J. Biol. Chem.* *278*, 22044–22055.

Udd, B., Meola, G., Krahe, R., Thornton, C., Ranum, L., Day, J., Bassez, G., and Ricker, K. (2003). Report of the 115th ENMC workshop: DM2/PROMM and other myotonic dystrophies. 3rd Workshop, 14-16 February 2003, Naarden, The Netherlands. *Neuromuscul. Disord. NMD* *13*, 589–596.

Ueda, H., Goto, J., Hashida, H., Lin, X., Oyanagi, K., Kawano, H., Zoghbi, H.Y., Kanazawa, I., and Okazawa, H. (2002). Enhanced SUMOylation in polyglutamine

- diseases. *Biochem. Biophys. Res. Commun.* *293*, 307–313.
- Uldrijan, S., Pannekoek, W.-J., and Vousden, K.H. (2007). An essential function of the extreme C-terminus of MDM2 can be provided by MDMX. *EMBO J.* *26*, 102–112.
- Uzunova, K., Götttsche, K., Miteva, M., Weisshaar, S.R., Glanemann, C., Schnellhardt, M., Niessen, M., Scheel, H., Hofmann, K., Johnson, E.S., et al. (2007). Ubiquitin-dependent Proteolytic Control of SUMO Conjugates. *J. Biol. Chem.* *282*, 34167–34175.
- Vendruscolo, M., Zurdo, J., MacPhee, C.E., and Dobson, C.M. (2003). Protein folding and misfolding: a paradigm of self-assembly and regulation in complex biological systems. *Philos. Transact. A Math. Phys. Eng. Sci.* *361*, 1205–1222.
- Verkerk, A.J.M.H., Pieretti, M., Sutcliffe, J.S., Fu, Y.-H., Kuhl, D.P.A., Pizzuti, A., Reiner, O., Richards, S., Victoria, M.F., Zhang, F., et al. (1991). Identification of a gene (FMR-1) containing a CGG repeat coincident with a breakpoint cluster region exhibiting length variation in fragile X syndrome. *Cell* *65*, 905–914.
- Vertegaal, A.C.O., Andersen, J.S., Ogg, S.C., Hay, R.T., Mann, M., and Lamond, A.I. (2006). Distinct and Overlapping Sets of SUMO-1 and SUMO-2 Target Proteins Revealed by Quantitative Proteomics. *Mol. Cell. Proteomics* *5*, 2298–2310.
- Villagra, N.T., Navascues, J., Casafont, I., Val-Bernal, J.F., Lafarga, M., and Berciano, M.T. (2006). The PML-nuclear inclusion of human supraoptic neurons: a new compartment with SUMO-1- and ubiquitin–proteasome-associated domains. *Neurobiol. Dis.* *21*, 181–193.
- Villagr a, N.T., Berciano, J., Altable, M., Navascu es, J., Casafont, I., Lafarga, M., and Berciano, M.T. (2004). PML bodies in reactive sensory ganglion neurons of the Guillain–Barr e syndrome. *Neurobiol. Dis.* *16*, 158–168.
- Wanker, E.E., Scherzinger, E., Heiser, V., Sittler, A., Eickhoff, H., and Lehrach, H. (1999). [24] Membrane filter assay for detection of amyloid-like polyglutamine-containing protein aggregates. In *Methods in Enzymology*, Ronald Wetzel, ed. (Academic Press), pp. 375–386.
- Warby, S.C., Chan, E.Y., Metzler, M., Gan, L., Singaraja, R.R., Crocker, S.F., Robertson, H.A., and Hayden, M.R. (2005). Huntingtin phosphorylation on serine 421 is significantly reduced in the striatum and by polyglutamine expansion in vivo. *Hum. Mol. Genet.* *14*, 1569–1577.
- Warrick, J.M., Morabito, L.M., Bilen, J., Gordesky-Gold, B., Faust, L.Z., Paulson, H.L., and Bonini, N.M. (2005). Ataxin-3 Suppresses Polyglutamine Neurodegeneration in *Drosophila* by a Ubiquitin-Associated Mechanism. *Mol. Cell* *18*, 37–48.
- Watts, F.Z. (2013). Starting and stopping SUMOylation. *Chromosoma* *122*, 451–463.
- Webb, J.L., Ravikumar, B., Atkins, J., Skepper, J.N., and Rubinsztein, D.C. (2003).  $\alpha$ -Synuclein Is Degraded by Both Autophagy and the Proteasome. *J. Biol. Chem.* *278*,

25009–25013.

Weisshaar, S.R., Keusekotten, K., Krause, A., Horst, C., Springer, H.M., Götttsche, K., Dohmen, R.J., and Praefcke, G.J.K. (2008). Arsenic trioxide stimulates SUMO-2/3 modification leading to RNF4-dependent proteolytic targeting of PML. *FEBS Lett.* *582*, 3174–3178.

Werner, A., Flotho, A., and Melchior, F. (2012a). The RanBP2/RanGAP1\*SUMO1/Ubc9 complex is a multisubunit SUMO E3 ligase. *Mol. Cell* *46*, 287–298.

Werner, A., Flotho, A., and Melchior, F. (2012b). The RanBP2/RanGAP1\*SUMO1/Ubc9 Complex Is a Multisubunit SUMO E3 Ligase. *Mol. Cell* *46*, 287–298.

Whitney, A., Lim, M., Kanabar, D., and Lin, J.-P. (2007). Massive SCA7 expansion detected in a 7-month-old male with hypotonia, cardiomegaly, and renal compromise. *Dev. Med. Child Neurol.* *49*, 140–143.

Wolynes, P.G., Onuchic, J.N., and Thirumalai, D. (1995). Navigating the folding routes. *Science* *267*, 1619–1620.

Wong, E., and Cuervo, A.M. (2010). Integration of Clearance Mechanisms: The Proteasome and Autophagy. *Cold Spring Harb. Perspect. Biol.* *2*.

Wong, M.B., Goodwin, J., Norazit, A., Meedeniya, A.C.B., Richter-Landsberg, C., Gai, W.P., and Pountney, D.L. (2013). SUMO-1 is Associated with a Subset of Lysosomes in Glial Protein Aggregate Diseases. *Neurotox. Res.* *23*, 1–21.

Woulfe, J., Gray, D., Prichett-Pejic, W., Munoz, D.G., and Chretien, M. (2004). Intranuclear rodlets in the substantia nigra: interactions with marinesco bodies, ubiquitin, and promyelocytic leukemia protein. *J. Neuropathol. Exp. Neurol.* *63*, 1200–1207.

Woulfe, J.M., Prichett-Pejic, W., Rippstein, P., and Munoz, D.G. (2007). Promyelocytic leukaemia-immunoreactive neuronal intranuclear rodlets in the human brain. *Neuropathol. Appl. Neurobiol.* *33*, 56–66.

Yang, W., Thompson, J.W., Wang, Z., Wang, L., Sheng, H., Foster, M.W., Moseley, M.A., and Paschen, W. (2012). Analysis of Oxygen/Glucose-Deprivation-Induced Changes in SUMO3 Conjugation Using SILAC-Based Quantitative Proteomics. *J. Proteome Res.* *11*, 1108–1117.

Yeh, E.T.H. (2009). SUMOylation and De-SUMOylation: Wrestling with Life's Processes. *J. Biol. Chem.* *284*, 8223–8227.

Yoo, S.-Y., Pennesi, M.E., Weeber, E.J., Xu, B., Atkinson, R., Chen, S., Armstrong, D.L., Wu, S.M., Sweatt, J.D., and Zoghbi, H.Y. (2003). SCA7 Knockin Mice Model Human SCA7 and Reveal Gradual Accumulation of Mutant Ataxin-7 in Neurons and Abnormalities in Short-Term Plasticity. *Neuron* *37*, 383–401.

- Young, J.E., Gouw, L., Propp, S., Sopher, B.L., Taylor, J., Lin, A., Hermel, E., Logvinova, A., Chen, S.F., Chen, S., et al. (2007). Proteolytic Cleavage of Ataxin-7 by Caspase-7 Modulates Cellular Toxicity and Transcriptional Dysregulation. *J. Biol. Chem.* *282*, 30150–30160.
- Yu, X., Ajayi, A., Boga, N.R., and Ström, A.-L. (2012). Differential Degradation of Full-length and Cleaved Ataxin-7 Fragments in a Novel Stable Inducible SCA7 Model. *J. Mol. Neurosci.* *47*, 219–233.
- Yu, X., Muñoz-Alarcón, A., Ajayi, A., Webling, K.E., Steinhof, A., Langel, Ü., and Ström, A.-L. (2013). Inhibition of Autophagy via p53-Mediated Disruption of ULK1 in a SCA7 Polyglutamine Disease Model. *J. Mol. Neurosci.* *50*, 586–599.
- Yvert, G., Lindenberg, K.S., Picaud, S., Landwehrmeyer, G.B., Sahel, J.A., and Mandel, J.L. (2000). Expanded polyglutamines induce neurodegeneration and trans-neuronal alterations in cerebellum and retina of SCA7 transgenic mice. *Hum. Mol. Genet.* *9*, 2491–2506.
- Zander, C., Takahashi, J., Hachimi, K.H.E., Fujigasaki, H., Albanese, V., Lebre, A.S., Stevanin, G., Duyckaerts, C., and Brice, A. (2001). Similarities between spinocerebellar ataxia type 7 (SCA7) cell models and human brain: proteins recruited in inclusions and activation of caspase-3. *Hum. Mol. Genet.* *10*, 2569–2579.
- Zhang, X.-W., Yan, X.-J., Zhou, Z.-R., Yang, F.-F., Wu, Z.-Y., Sun, H.-B., Liang, W.-X., Song, A.-X., Lallemand-Breitenbach, V., Jeanne, M., et al. (2010). Arsenic Trioxide Controls the Fate of the PML-RAR $\alpha$  Oncoprotein by Directly Binding PML. *Science* *328*, 240–243.
- Zhao, J. (2007). Sumoylation regulates diverse biological processes. *Cell. Mol. Life Sci.* *64*, 3017–3033.



